

***In vitro* anti-diabetic and anti-obesity activities of compounds
from the Cuban medicinal plant, *Allophylus cominia* (L.) Sw.**

A thesis submitted in accordance with the regulations governing the award of the
Degree of Doctor of Philosophy

By

Dima Semaan

2014



Strathclyde Institute of Pharmacy and Biomedical Sciences

The John Arbuthnott Building

University of Strathclyde

27 Taylor Street

Glasgow, G4 0NR

Copyright

The copyright of this thesis belongs to the author under the terms of the United Kingdom Copyright Acts, as qualified by University of Strathclyde regulation 3.50.

Acknowledgement must always be made of the use of any material contained in, or derived from, this thesis.

Dedication

This thesis is dedicated to my parents, my husband Mohamed and my son Adam in appreciation of their support and sacrifice in the accomplishment and for funding my project.

Acknowledgements

My gratitude goes to my supervisors, Dr. Edward Rowan and Prof. Alexander Gray, for being wise mentors, for their guidance, support and advice. Dr Edward Rowan has influenced me greatly and his wide and creative knowledge and thoughts have been of great value for this project. In addition, Prof. Alexander Gray supported my work, ideas, my knowledge and phytochemical work, in addition to being a caring friend.

Particular thanks go to Prof. Alan Harvey, Ms. Louise Young and Ms. Grainne Abbott for their support at the beginning of this project, for the use of their facilities in the SIDR laboratory and for their detailed and constructive comments and organised working style throughout the project. Special thanks go to Ms. Louise Young for sharing her optimised methods and enzyme assays, most of which were adapted in this project.

My profound thanks to Dr. John Igoli for his support and advice during the Phytochemistry Laboratory. His expertise and time were greatly appreciated.

I am very thankful to Prof. Brian Furman for his support and advise in the diabetes experiments.

In addition, I appreciate the help and support of Dr. Tong Zhang in the mass spectrometry.

Sincere thanks are also due to Dr. Ibrahim Khadra for his collaboration and support in the high performance liquid chromatography separation. And thanks to Martin Werno for his help in the western blot.

I am also deeply grateful to Dr. Eva Marrero and Janet Sanchez from La Habana, Cuba for introducing the Cuban plant and its important activity in diabetes, for their help in the collection of the plant and for sending it to the University of Strathclyde, Glasgow.

Further, I am very thankful to all my friends and colleagues in the laboratory and the office for their friendship and support on all occasions.

Abstract

Based on ethnobotanical information collected from Cuban diabetic patients in Cuba, medicinal plants such as *Allophylus cominia* (L.) Sw. (*A. cominia*) was identified as a possible source of new drugs that could be used for the treatment of type 2 diabetes mellitus.

Type 2 diabetes mellitus or non-insulin dependent diabetes mellitus (T2-DM) is a chronic disease, and when associated with obesity (a condition known as diabetes) leads to an increase in the risk of a number of comorbidities, e.g. cardiovascular, kidney and liver diseases. *A. cominia* is a Cuban plant used traditionally by diabetic patients for the treatment of their diabetes symptoms. Preliminary studies of its leaves (Veliz *et al.*, 2003; Veliz *et al.*, 2005 Sanchez *et al.*, 2014) have shown potential anti-diabetic activity and it is therefore being further investigated in the search for a novel, nontoxic, and efficacious anti-diabetic agent.

The present project investigated the *in vitro* hypo-glycaemic activity of *A. cominia* extracts. Chemical characterisation of the extracts was carried out using different phytochemical methods. Fatty acids, tannins, pheophytins (A and B), and a mixture of flavonoids were detected. The identified flavonoids (42.1 mg) were mearnsitrin, quercitrin, quercetin-3-alloside, and naringenin-7-glucoside. Some of these compounds have been reported in the literature as potent hypo-glycaemic agents. Separation of the mixture of quercitrin and mearnsitrin was carried out by high performance liquid chromatography using an amino column.

Extracts from *A. cominia* were tested for their ability to inhibit the activity of four enzymes. DPPIV plays an essential role in glucose metabolism. PTP1B is important in inhibiting downstream signalling of the insulin and leptin receptors. Alpha-glucosidase is one of the enzymes responsible for the breakdown of carbohydrates into monosaccharides, and alpha-amylase breaks down large, insoluble starch molecules into soluble starches, producing successively smaller starches and ultimately, maltose.

The flavonoids produced a concentration-dependent inhibition against DPPIV with a K_i value of $2.6 \pm 0.2 \mu\text{g/ml}$. The flavonoids fraction from *A. cominia* revealed a competitive inhibition using DPPIV substrate comparable to the inhibition by the commercial (P32/98) inhibitor. In addition, PTP1B enzyme was $100 \pm 5\%$ inhibited by the flavonoid mixture and $65 \pm 2\%$ inhibited by pheophytin A and $61 \pm 1\%$ inhibition by pheophytin B at $30 \mu\text{g/ml}$ respectively. The flavonoid mixture elicited a significant concentration-dependent inhibition against PTP1B with a K_i value of $3.2 \pm 0.09 \mu\text{g/ml}$, as well as with pheophytin A with a K_i value of $0.64 \pm 0.05 \mu\text{g/ml}$ and pheophytin B with a K_i value of $0.88 \pm 0.03 \mu\text{g/ml}$; both were lower than that of TFMS inhibitor, with a K_i value of $1.1 \pm 0.03 \mu\text{g/ml}$. Both flavonoid and pheophytin A extracts from *A. cominia* revealed a competitive inhibition of PTP1B enzyme using DiFMUP as substrate. Competitive inhibition was also shown with TFMS inhibitor. On α -glucosidase enzyme, a $79 \pm 1\%$ inhibition was produced by the flavonoid mixture at $30 \mu\text{g/ml}$. The flavonoid fraction from *A. cominia* showed a concentration-dependent pattern against α -glucosidase, with a K_i value of $1.7 \pm 0.5 \mu\text{g/ml}$ that was lower than that of acarbose inhibitor ($190 \pm 0.5 \mu\text{g/ml}$). These extracts have shown a competitive inhibition using 4-nitrophenyl-glucopyranoside as substrate. Acarbose also produced a competitive inhibition against α -glucosidase. No significant effect was found with any of the extracts from *A. cominia* at $30 \mu\text{g/ml}$ against α -amylase enzyme. After separation of the flavonoids, mearnsitrin and quercitrin did not produce any effect (at $30 \mu\text{g/ml}$) on any of the enzyme activities (DPPIV, PTP1B, α -glucosidase and α -amylase). Quercitrin and mearnsitrin were active only in synergy.

On a glucose uptake assay using HepG2 cells, the crude methanolic extract from *A. cominia* enhanced insulin activity by increasing 2-NBDG uptake by two-fold (2-NBDG is a fluorescently-tagged glucose derivative).

The 2-deoxy-D-glucose uptake by differentiated 3T3-L1 cell line showed an increase of the glucose uptake in the presence of $100 \mu\text{g/ml}$ of flavonoids by enhancing insulin activity (100 nM), whereas the uptake was increased in the presence of $100 \mu\text{g/ml}$ of pheophytin A without enhancing insulin activity. The effect of different compounds from *A. cominia* on 3T3-L1 cell differentiation was also confirmed by

quantifying GLUT4 transporters in the pre-treated cells with flavonoids and pheophytin A. GLUT4 transporters in the pre-treated cells were similar to those of the differentiated normal 3T3-L1 adipocytes.

2-NBDG glucose uptake assay was also performed using L6 myotubes. The uptake was significantly increased by two-fold in the presence of 100 nM insulin, and by four-fold in the presence of both 100 nM insulin and 100 µg/ml flavonoids. A significant increase was also shown in the presence of 100 µg/ml pheophytin A and 100 nM insulin with a 10-fold increase ($P<0.05$) of glucose uptake by L6 cells. An increase of 2-NBDG uptake by L6 cells was shown in the presence of flavonoids and pheophytin A in addition to 100 nM insulin.

Both flavonoid and pheophytin extracts (100 µg/ml) blocked the differentiation of 3T3-L1 fibroblasts into adipocytes by decreasing the fat accumulation by two-fold (more than the TNF- α inhibition at 10 ng/ml). A significant difference was shown ($P<0.05$) compared to the control. Troglitazone significantly enhanced 3T3-L1 differentiation by two-fold. Exposing 3T3-L1 cells to both extracts from the third day of the differentiation induction did not alter the adipogenesis. Exposing 3T3-L1 adipocytes to the extracts from *A. cominia* containing flavonoids and pheophytin A showed a significant decrease in the fat accumulation after five days of incubation with the extracts ($P<0.05$). However, no fat accumulation was observed after withdrawal of the extracts from the cell growth medium.

These compounds may be responsible for the pharmacological effects observed in experimental diabetic models in Cuba. Therefore, all these results strongly suggest that this plant could be a new and promising candidate for treating diabetes with natural sources.

Abbreviations

¹H NMR: Hydrogen-1 NMR

2-NBDG: 2-deoxy-2-[(7-nitro-2,1,3-benzoxadiazol-4-yl)amino]-D-glucose

2-DG: 2-Deoxy-D-glucose

3T3-L1: Isolated clonal cell line derived from cultures of mouse fibroblast 3T3 line

ADH: Antidiuretic hormone

AVP: Arginine vasopressin

Brd: Broad doublet

Brm: broad multiplet

Brq: broad quartet

Brs: broad singlet

BSA: bovine serum albumin

CC: column chromatography

CDCl₃: chloroform

COSY: Correlation spectroscopy

D: doublet

Dd: doublet of doublet

Ddd: doublet of doublet of doublet

DI: diabetes insipidus

DiFMUP: 6,8-Difluoro-4-Methylumbelliferyl Phosphate

DM: diabetes mellitus

DMEM: Dulbecco's Modified Eagle Medium

DMSO: Dimethyl sulfoxide

DPPIV: Dipeptidyl peptidase-4

Dt: doublet of triplet

DTT: Dithiothreitol

EDTA: Ethylenediaminetetraacetic acid

FBS: foetal bovine serum

FCS: foetal calf serum

Flav: flavonoids

G-DM: gestational diabetes mellitus

GIP: Gastric inhibitory polypeptide

GLP-1: Glucagon-like peptide-1

Gly-pro: Gly-pro-7-amido-4-methylcoumarin hydrobromide

GSK: Glycogen synthetase kinase

HepG2: human liver hepatocellular carcinoma cell line

HPLC: high performance liquid chromatography

Ki: constant inhibitor

LC: liquid chromatography

M: multiplet

MS: mass spectrometry

MW: molecular weight

NBS: new born serum

NMR: Nuclear magnetic resonance

P32-98: 3-N-[[[(2S,3S)-2-Amino-3-methylpentanoyl]-1,3-thiazolidine . hemi-fumarate

Pheo: pheophytins

PI3K: Phosphatidylinositol 3-kinases

PKB: Protein Kinase B

PTP1B: Tyrosine-protein phosphatase non-receptor type 1

PTPs: Protein tyrosine phosphatases

PVP: Polyvinylpyrrolidone

Q: quartet

S: singlet

T: triplet

T1-DM: type 1 diabetes mellitus

T2-DM: type 2 diabetes mellitus

TFMS: Trifluoromethyl sulfonamido

TLC: Thin Layer Chromatography

TNF- α : tumour necrosis factor alpha

Tris-HCl: Tris(hydroxymethyl)amine hydrochloride

TZD: Thiazolidinedione

UV: ultraviolet light

VLC: Vacuum liquid chromatography

α -Glucosidase: alpha glucosidase

B-cells: pancreatic beta cells

Contents

Title	I
Copyright	II
Dedication	III
Acknowledgements	IV
Abstract	V
Abbreviation	VIII
Contents	XI
List of Tables	XIX
List of Figures	XX
List of Appendices	XXV

Chapter 1

Introduction	2
1 Overview of diabetes	2
1.1.1 Causes of diabetes mellitus	3
1.2 Types of diabetes	4
1.2.1 Type 1 diabetes mellitus	4
1.2.2 Type 2 diabetes mellitus	5
1.2.3 Gestational diabetes mellitus	7
1.2.4 Other types of diabetes	7
1.3 Diabesity: definition	7
1.4 Treatment of type 2 diabetes	8
1.5 Mechanism of action of drugs	12
1.5.1 Metformin	12
1.5.2 Sulfonylureas	12
1.5.3 Thiazolidinediones	13
1.5.4 The incretins	14
1.5.5 Alpha-glucosidase inhibitors	14
1.5.6 Alpha-amylase inhibitors	17
1.5.7 Glinides	17
1.5.8 DPPIV inhibitors	17
1.5.9 Exenatide	18
1.6 Insulin	18
1.6.1 Insulin secretion	19
1.6.2 Mechanism of action of insulin	21

1.7	Traditional treatment of T2-DM	22
1.7.1	History of traditional treatment	22
1.7.2	Treatment using natural products with hypo-glycaemic activity	23
1.7.3	“Hypo-glycaemic activities” of anti-diabetic plant extracts.....	27
	A. <i>Enhancement of insulin release</i>	28
	B. <i>Repair of β-cells</i>	28
	C. <i>Increase of glucose uptake (PTP1B-deficiency)</i>	29
	D. <i>Prolongation the action of insulin-like hormones (e.g. DPPIV)</i>	30
1.8	Problems of developing plant therapies as new oral anti-diabetics drugs.....	31
1.9	Phenol-containing plants with hypo-glycaemic activity	31
1.10	Cuban medicinal plants used in the treatment of type 2 diabetes mellitus.....	32
1.11	Phytochemistry of anti-diabetic medicinal plants	33
1.12	Plant extraction.....	34
1.12.1	Plant analysis.....	34
1.12.2	Methods of extraction and isolation.....	35
1.12.3	Methods of separation.....	35
1.12.4	Methods of identification	39
1.12.5	Nuclear magnetic resonance spectroscopy (NMR).....	40
1.12.6	Analysis of results.....	41
1.13	Aims and Objectives.....	42
2	Phytochemical separation and identification of compounds from <i>Allophylus cominia</i>	45
2.1	Introduction	45
2.2	Materials and Methods.....	46
2.2.1	Solvents, reagents and chemicals	46
2.2.2	Plant material.....	46
2.2.3	Maceration.....	47
2.2.4	Chromatographic techniques.....	48
	A. <i>Thin layer chromatography (TLC)</i>	48
	B. <i>Vacuum liquid chromatography (VLC)</i>	49
	E. <i>Sephadex column chromatography</i>	51
	F. <i>Silica gel column chromatography</i>	52
	G. <i>Preparative thin layer chromatography (prep-TLC)</i>	53
2.2.5	Structural elucidation.....	54

2.2.6	Nuclear magnetic resonance spectroscopy (NMR).....	54
2.2.7	Mass spectrometry (MS).....	54
2.2.8	Liquid chromatography-Mass spectrometry (LC-MS).....	55
2.2.9	High performance liquid chromatography (HPLC).....	55
2.2.10	Separation of pheophytins by silica gel column chromatography.....	56
2.2.11	Isolation of the flavonoids from fatty acids by Sephadex.....	56
2.2.12	Separation of flavonoids by HPLC	56
2.3	Results.....	57
2.3.1	Characterisation of the compounds in <i>A. cominia</i>	57
2.3.2	Characterisation of HEC solid as a mixture of flavonoids	57
2.3.2.1	Purification of the flavonoids.....	65
2.3.2.2	Separation of quercetin and mearnsitrin.....	69
2.3.3	Characterisation of MeOH fraction D as a mixture of pheophytins	71
2.3.3.1	Purification of pheophytins.....	72
2.3.3.2	Prep-TLC	73
2.3.3.3	Silica gel column chromatography	75
2.4	Conclusion and discussion	79
3	<i>In vitro</i> determination of the effect of <i>A. cominia</i> on the glucose uptake in HepG2, L6 and 3T3-L1 cells.....	81
3.1	Introduction	81
3.2	Material and Methods	82
3.2.1	Preparation of <i>Allophylus cominia</i> extracts	82
3.2.2	HepG2 liver cells.....	82
A.	HepG2 seeding	83
B.	HepG2 culture	84
C.	HepG2 storage	84
3.2.3	3T3-L1 cell culture and adipocyte differentiation.....	84
A.	Cell growth	84
B.	Cell storage.....	85
C.	3T3-L1 cell differentiation.....	85
3.2.4	Oil Red-O staining of 3T3-L1 adipocytes	86
3.2.5	L6 muscle cells.....	87
A.	Cell growth	87

B.	Cell storage.....	87
C.	L6 cell differentiation	88
3.2.6	Cytotoxicity assays	88
3.2.6.1	Alamar blue assay	89
3.2.6.2	MTT assay.....	89
3.2.7	2-NBDG uptake assay.....	91
3.2.8	2-Deoxy-D-glucose uptake assay.....	93
3.2.8.1	2-Deoxy-D-glucose uptake by 3T3-L1 adipocytes.....	93
3.2.8.2	Metabolite extraction	94
3.2.8.3	Mass spectrometry	94
3.2.9	Statistical Analysis.....	95
3.3	Results.....	96
3.3.1	Cell culture	96
3.3.1.1	3T3-L1 adipocytes morphology.....	96
3.3.1.2	Oil Red-O staining for 3T3-L1 cells	97
3.3.1.3	L6 cells morphology	98
3.3.2	Effects of extracts from <i>A. cominia</i> on cell viability.....	99
3.3.2.1	Effects of extracts from <i>A. cominia</i> on HepG2 cell viability.....	99
3.3.2.2	Effects of extracts from <i>A. cominia</i> on 3T3-L1 fibroblasts and adipocytes cell viability101	
A.	Effect of crude AC extract on fibroblast viability	101
B.	Effect of the crude methanolic extract from <i>A. cominia</i> on 3T3-L1 fibroblasts using Alamar blue and MTT assays	102
C.	Effect of extracts from <i>A. cominia</i> on 3T3-L1 fibroblasts viability	103
D.	Effect of extracts from <i>A. cominia</i> on 3T3-L1 adipocytes viability.....	104
3.3.2.3	Effects of extracts from <i>A. cominia</i> on L6 myoblast viability	106
3.3.2.4	Conclusion and discussion	107
3.3.3	Effect of extracts from <i>A. cominia</i> on 2-NBDG glucose uptake	108
3.3.3.1	Effect of extracts from <i>A. cominia</i> on 2-NBDG glucose uptake by HepG2 cells.....	108
3.3.4	Effect of extracts from <i>A. cominia</i> on 2-NBDG glucose uptake by 3T3-L1 fibroblasts	110
3.3.5	Effect of insulin, 2-NBDG and cell density on the glucose uptake by 3T3-L1 adipocyte cells.....	113

3.3.6	Effect of extracts from <i>A. cominia</i> on 2-NBDG glucose uptake by 3T3-L1 adipocytes.....	115
3.3.7	Effect of extracts from <i>A. cominia</i> on 2-NBDG glucose uptake by L6 cells..	117
3.4	Conclusion and discussion	121
3.5	Effect of extracts from <i>A. cominia</i> on 2-deoxy-D-glucose uptake by 3T3-L1 by MS.....	123
3.5.1	Effect of wortmannin on insulin activity.....	123
3.5.2	Effect of pheophytins on 2-DG uptake analysed by MS	126
3.5.3	Effect of flavonoids on 2-DG uptake analysed by MS.....	128
3.5.4	Effect of differentiation on 2-deoxy-D-glucose uptake analysed by MS	130
3.6	Conclusion and discussion	134
3.7	Summary of <i>in vitro</i> studies involving the <i>A. cominia</i> extracts in the glucose uptake.....	135
4	<i>In vitro</i> determination of lipid accumulation in 3T3-L1 adipocytes	137
4.1	Introduction.....	137
4.2	Methods.....	138
4.2.1	Adipogenesis.....	138
4.2.2	Lipid accumulation.....	138
4.2.3	Caspase-3 assay	139
4.2.4	Protein assay.....	141
4.2.5	Western blot	142
4.3	Results	143
4.3.1	Effect of extracts from <i>A. cominia</i> on 3T3-L1 adipogenesis on the first day of differentiation.....	143
4.3.2	Effect of extracts from <i>A. cominia</i> on 3T3-L1 adipogenesis on the third day of differentiation.....	146
4.3.3	Apoptotic effect of extracts from <i>A. cominia</i> in 3T3-L1 adipocytes.....	147
4.3.4	Effect of addition of extracts from <i>A. cominia</i> on the accumulation of lipid in 3T3-L1 cells	151
4.3.5	Effect of withdrawal of extracts from <i>A. cominia</i> on the accumulation of lipid in 3T3-L1 cells.....	153
4.3.6	Effect of the extracts from <i>A. cominia</i> on protein concentrations in 3T3-L1 adipocytes	155
4.3.7	Effect of the extracts from <i>A. cominia</i> on insulin-mediated GLUT4 transporters.....	158

4.3.8	Conclusion and discussion.....	160
4.3.9	Summary of <i>in vitro</i> studies involving the <i>A. cominia</i> extracts in adipogenesis	162
5	Effect of the extracts from <i>A. cominia</i> on the activities of PTP1B, DPPIV, α -glucosidase and α -amylase enzymes	164
5.1	Introduction.....	164
5.2	Material and Methods	165
5.2.1	Z-factor	165
5.2.2	Plant sample preparation	166
5.2.3	DPPIV assay	167
5.2.3.1	Buffer preparation.....	167
5.2.3.2	Enzyme preparation.....	167
5.2.3.3	Substrate preparation	167
5.2.3.4	Inhibitor preparation	167
5.2.3.5	Assay method.....	167
5.2.3.6	Z-factor method	168
5.2.3.7	Kinetics of the inhibition of DPPIV enzyme by <i>A. cominia</i>	168
5.2.4	PTP1B assay.....	169
5.2.4.1	Buffer preparation.....	169
5.2.4.2	Enzyme preparation.....	169
5.2.4.3	Substrate preparation	169
5.2.4.4	Inhibitor preparation	169
5.2.4.5	Assay method.....	169
5.2.4.6	Kinetics of the inhibition of PTP1B enzyme by <i>A. cominia</i>	170
5.2.5	α -glucosidase assay.....	171
5.2.5.1	Buffer preparation.....	171
5.2.5.2	Enzyme preparation.....	171
5.2.5.3	Substrate preparation	171
5.2.5.4	Inhibitor preparation	172
5.2.5.5	Assay method.....	172
5.2.5.6	Kinetics of the inhibition of α -glucosidase by <i>A. cominia</i>	172
5.2.6	α -amylase assay.....	173
5.2.6.1	Buffer preparation.....	173

5.2.6.2	Enzyme preparation.....	173
5.2.6.3	Substrate preparation	173
5.2.6.4	Inhibitor preparation	173
5.2.6.5	Assay method.....	173
5.2.6.6	Results analysis	174
5.3	Results	175
5.3.1	DPPIV enzyme.....	175
5.3.1.1	Z-factor of DPPIV assay	175
5.3.1.2	Effect of extracts from <i>A. cominia</i> on DPPIV enzyme.....	176
5.3.1.3	Concentration dependent inhibition of the flavonoids from <i>A. cominia</i>	179
5.3.1.4	Kinetics of the inhibition of DPPIV by the flavonoids from <i>A. cominia</i>	180
5.3.1.5	Conclusion and discussion.....	183
5.3.2	PTP1B enzyme.....	184
5.3.2.1	Z-factor of PTP1B assay	184
5.3.2.2	Effect of extracts of <i>A. cominia</i> on the PTP1B enzyme.....	185
5.3.2.3	Effect of compounds isolated from AC-HEC on PTP1B enzyme	185
5.3.2.3.1	Effect of compounds isolated from AC-MC on PTP1B enzyme.....	187
5.3.2.3.2	Effect of compounds isolated from AC-MC-D on PTP1B enzyme...	191
5.3.2.3.3	Concentration dependent inhibition of the flavonoids and pheophytins	192
5.3.2.4	Kinetics of the inhibition of PTP1B by the flavonoids and pheophytin A from <i>A. cominia</i>	196
5.3.2.5	Conclusion and discussion.....	200
5.3.3	α -Glucosidase enzyme.....	201
5.3.3.1	Z-factor of α -glucosidase assay	201
5.3.3.2	Effect of extracts from <i>A. cominia</i> on the α -glucosidase enzyme....	202
5.3.3.2.1	Effect of crude extracts from <i>A. cominia</i> on α -glucosidase	203
5.3.3.2.2	Effect of extracts from HEC on α -glucosidase.....	204
5.3.3.2.3	Effect of the methanolic extracts from MC on α -glucosidase	205
5.3.3.2.4	Effect of extracts from AC-MC-KLMN on α -glucosidase.....	206
5.3.3.2.5	Effect of extracts from AC-MC-KLMN-91-175 on α -glucosidase	207
5.3.3.2.6	Effect of extracts from AC-MC-D on α -glucosidase.....	209

5.3.3.3	Concentration-dependent inhibition of the flavonoids.....	210
5.3.3.4	Kinetics of the inhibition of α -glucosidase by the flavonoids from <i>A. cominia</i>	213
5.3.3.5	Conclusion and discussion.....	216
5.3.4	α -Amylase enzyme	217
5.3.4.1	Z-factor of α -amylase assay	217
5.3.4.2	Effect of extracts from <i>A. cominia</i> on the α -amylase enzyme.....	218
5.3.4.3	Conclusion and discussion.....	219
5.3.5	Summary of inhibition studies involving the <i>A. cominia</i> extracts	220
6	General conclusions and suggestions for future work	222
7	References	228

List of tables

Chapter 1

Table 1.1 Drugs used for the treatment of T2-DM, their mode of action, daily injections and their side effects	11
Table 1.2 Examples of anti-diabetic compounds.....	27
Table 1.3 Methods of separation and their specific compounds.....	37

Chapter 2

Table 2.1 A step gradient elution technique used for separation of the methanol crude extract of the maceration extraction.....	50
Table 2.2 The gradient method followed in the mass spectrometry.	55
Table 2.3 ¹ H and ¹³ C NMR for quercitrin and mearnsitrin (in DMSO-d6) including rhamnose moiety by comparison to quercitrin.	60
Table 2.4 Selected HMBC correlations of quercitrin and mearnsitrin.....	62
Table 2.5 ¹ H NMR spectral assignments for pheophytin A and B.....	77
Table 2.6 Selected HMBC correlations of pheophytin A and B.....	78

Chapter 3

Table 3.1 Mass spectrometry gradient method used for the quantification of 2-deoxy-D-glucose in the 3T3-L1 adipocytes metabolite extracts.....	95
Table 3.2 Concentration of 2-deoxy-D-glucose uptake uptake by 3T3-L1 cells of different pre-treated cells in the presence or absence of insulin 100 nM (Ins) and 10 nM of wortmannin (Inh)..	125
Table 3.3 Concentration of 2-deoxy-D-glucose uptake by 3T3-L1 cells of different pre-treated cells in the presence or absence of insulin 100 nM (Ins) and 10 or 100 µg/ml of pheophytins (phea).....	127
Table 3.4 Concentration of 2-deoxy-D-glucose uptake by 3T3-L1 cells of different pre-treated cells in the presence or absence of insulin 100 nM (Ins) and 10 or 100 µg/ml of flavonoids (flav).....	129
Table 3.5 Concentration of 2-deoxy-D-glucose uptake by 3T3-L1 cells of different pre-treated cells with TNF-α, flavonoids and pheophytins..	133

Chapter 4

Table 4.1 Guideline table presenting the amount of p-nitroaniline (p-NA) in µmol produced per 100 µl per well and their relative concentration in µM of p-NA.	141
Table 4.2 Caspase-3 activity of different cell lysate of pre-treated cells with staurosporine, TNF-α, flavonoids (flav) and pheophytin A (phea).	150
Table 4.3 Protein concentration in pre-treated 3T3-L1 cells. Protein concentration was calculated using BSA standard curve.....	157

Chapter 5

Table 0.1 High-throughput screening assay fitness table.....	168
--	-----

List of figures

Chapter 1

Figure 1.1 Chemical structure of metformin.....	12
Figure 1.2 General chemical structure of sulfonylureas.	13
Figure 1.3 Chemical structure of two TZDs	14
Figure 1.4 Effect of α -glucosidase inhibitors on the enzymatic hydrolysis of polysaccharides by α -glucosidase in the small intestine.	16
Figure 1.5 Chemical structures for two alpha-glucosidase inhibitors.....	16
Figure 1.6 Chemical structure of glinide.	17
Figure 1.7 Example of chemical structure of a DPPIV inhibitor.....	18
Figure 1.8 The fuel hypothesis and the secretion of insulin by β -cells and mechanisms of the glucose-dependent insulin secretion.	20
Figure 1.9 Effect of incretins and DPPIV on pancreatic cells and the glucose homeostasis..	20
Figure 1.10 The general insulin pathway.....	21
Figure 1.11 Physiological role of PTP1B in glucose homeostasis.....	30
Figure 1.12 Examples of some chemical structures of certain flavonoids, which are phenol-containing compounds with anti-diabetic activity.	32
Figure 1.13 Schematic representation of an HPLC.....	38
Figure 1.14 Various possible extract tests for T2-DM.....	43

Chapter 2

Figure 2.1 Extraction scheme for the leaves of <i>Allophylus cominia</i>	47
Figure 2.2 Fractionation scheme for the crude methanol extract of <i>Allophylus cominia</i> obtained from maceration.	51
Figure 2.3 Fractionation scheme for the crude hexane and ethyl acetate extracts of <i>Allophylus cominia</i> from maceration.	53
Figure 2.4 Separation of compounds by LC-MS from HEC solid of <i>A. cominia</i>	62
Figure 2.5 Identification of compounds by LC-MS for HEC solid of <i>A. cominia</i>	63
Figure 2.6 LC-MS spectrum of HEC solid of <i>A. cominia</i> showing the retention times of different compounds and the method followed for the separation.....	64
Figure 2.7 Photomycographs illustrating the effect of crude extracts of AC-MC-KLMN-91-175 (mixture of flavonoids and fats) on the 3T3-L1 differentiation (before and after differentiation process)..	66
Figure 2.8 Chemical structures of the different compounds in <i>A. cominia</i> extracts from HEC and MeOH-D extracts.	68
Figure 2.9 HPLC chromatogram showing different peaks for the flavonoids.	69
Figure 2.10 MS for fraction 1 collected at 8.5-9.5 minutes.	70
Figure 2.11 MS of fraction 2 collected at 9.5-11 minutes..	70
Figure 2.12 Chemical structures of pheophytins A and B.	72
Figure 2.13 TLC plate for MeOH-D dissolved in chloroform in 70:30 hexane:EtOAc.	73
Figure 2.14 Prep-TLC for MeOH-D sample of <i>A. cominia</i> in TLC solvent 70:30 hexane:EtOAc.....	73

Figure 2.15 TLC plate for fractions separated by prep-TLC from the crude MeOH-D extracts of <i>A. cominia</i>	74
Figure 2.16 TLC plate for fractions separated by silica gel column chromatography from the crude MeOH-D extract of <i>A. cominia</i>	75

Chapter 3

Figure 3.1 Alamar blue reaction that occurs in the mitochondria of the living cells leading to the change in the colour of the Alamar blue from blue to pink.	89
Figure 3.2 MTT reaction mechanism that occurs in the mitochondria of the living cells leading to a change in the colour of the MTT from yellow to purple (Formazan).	90
Figure 3.3 Chemical structure of the 2-N-7-(nitrobenz-2-oxa-1,3-diazol-4-yl)amino-2-deoxy-D-glucose (2-NBDG).....	91
Figure 3.4 Chemical structure for 2-deoxy-D-glucose.	93
Figure 3.5 Series of images depicting the 3T3-L1 fibroblast differentiation.....	96
Figure 3.6 Microscopy of mature 3T3-L1 cells adipocytes before and after Oil Red-O staining.....	97
Figure 3.7 Images depicting the growth of L6 cells over a period of five days following seeding in 75 cm ² flask at 1x10 ⁶ cells/ml in DMEM supplemented with 10% FBS at 37°C in an atmosphere containing 95% air and 5% CO ₂ (x10).	98
Figure 3.8 Images depicting the differentiation of L6 cells over a period of five days following differentiation in a 96-well black clear bottom plate (x40).	98
Figure 3.9 A lack of cytotoxic effect of the crude methanolic extract from <i>A. cominia</i> on HepG2 cell viability by Alamar blue test.....	100
Figure 3.10 Cytotoxic effect of the methanolic crude extract from <i>A. cominia</i> on 3T3-L1 fibroblast viability by Alamar blue test.....	101
Figure 3.11 The methanolic crude extract from <i>A. cominia</i> cytotoxicity effect on 3T3-L1 fibroblast viability using Alamar blue test and MTT assays.....	102
Figure 3.12 A lack of cytotoxic effect of different extracts from <i>A. cominia</i> on 3T3-L1 fibroblast viability by MTT test.....	103
Figure 3.13 Lack of cytotoxic effect of different extracts of <i>A. cominia</i> (100 µg/ml) on 3T3-L1 fibroblasts (A) and 3T3-L1 adipocytes (B) viability by Alamar blue test.....	105
Figure 3.14 No cytotoxic effect of a range of concentration of flavonoids (A) and pheophytin A (B) from <i>A. cominia</i> on L6 cell viability by MTT assay.....	106
Figure 3.15 Concentration-dependent increase of 2-NBDG uptake by HepG2 produced by insulin.....	108
Figure 3.16 The methanolic crude extract of <i>A. cominia</i> (AC) produces an insulin concentration- dependent increase of 2-NBDG uptake by HepG2 cells.....	109
Figure 3.17 The methanolic extract from <i>A. cominia</i> increases 2-NBDG uptake by HepG2 liver cells in the presence or absence of 100 nM insulin.	110
Figure 3.18 No effect of AC on insulin activity on 2-NBDG glucose uptake by non-differentiated 3T3-L1 fibroblasts.....	111
Figure 3.19 The crude extracts from <i>A. cominia</i> produce a concentration-dependent uptake of 2-NBDG in non-differentiated fibroblasts via insulin concentration.....	112

Figure 3.20 Insulin produces a concentration-dependent increase of 2-NBDG glucose uptake in fully differentiated adipocytes in the absence of crude extracts of <i>A. cominia</i>	113
Figure 3.21 2-NBDG produces a concentration-dependent uptake by fully-differentiated 3T3-L1 cells in the absence of <i>A. cominia</i>	114
Figure 3.22 Increased fibroblast seeding density increases 2-NBDG glucose uptake in fully-differentiated adipocytes.....	114
Figure 3.23 Effect of <i>A. cominia</i> on 2-NBDG uptake by fully-differentiated adipocytes in the presence or absence of 100 nM insulin.....	115
Figure 3.24 Effect of <i>A. cominia</i> crude extract on 2-NBDG uptake by differentiated 3T3-L1 fibroblasts in the presence or absence of 100 nM insulin.	116
Figure 3.25 Insulin produces an increase in 2-NBDG uptake by L6 cells in the absence of <i>A. cominia</i>	118
Figure 3.26 Insulin produces a concentration-dependent uptake of 2-NBDG by L6 cells in the presence of 100 µg/ml of flavonoids from <i>A. cominia</i>	118
Figure 3.27 Insulin produces a concentration-dependent uptake of 2-NBDG by L6 cells in the presence of 100 µg/ml of pheophytin A from <i>A. cominia</i>	119
Figure 3.28 Flavonoid extract from <i>A. cominia</i> produces a concentration-dependent uptake of 2-NBDG by L6 cells in the presence of 100 nM insulin.....	119
Figure 3.29 Pheophytin A extract from <i>A. cominia</i> produces a concentration-dependent uptake of 2-NBDG by L6 cells in the presence of 100 nM insulin.....	120
Figure 3.30 Flavonoids and pheophytin A from <i>A. cominia</i> enhance insulin activity in 2-NBDG uptake by L6 cells.....	120
Figure 3.31 2-Deoxy-D-glucose standard curve.	124
Figure 3.32 100 nM insulin increases 2-deoxy-D-glucose (2-DG) uptake by differentiated 3T3-L1 (metabolites), whereas Inh is the inhibitor which is wortmannin (10 nM) inhibits insulin activity.....	125
Figure 3.33 Pheophytin A increases 2-deoxy-D-glucose uptake by differentiated 3T3-L1 adipocytes.	127
Figure 3.34 Flavonoid extract from <i>A. cominia</i> enhances insulin activity in 2-deoxy-D-glucose uptake by differentiated 3T3-L1 (metabolites).	129
Figure 3.35 MS spectrum representing the 2-deoxy-D-glucose uptake by differentiated 3T3-L1 in 25cm ² flasks following different treatments (metabolite extracts) in the presence of 100 nM insulin.	132
Figure 3.36 2-Deoxy-D-glucose uptake by differentiated 3T3-L1 (metabolite extracts) in the presence of 100 nM insulin and the effect of different treatments on the glucose uptake assay after differentiation.	132

Chapter 4

Figure 4.1 Inhibitory effects of <i>A. cominia</i> extracts on 3T3-L1 differentiation starting from day 1 of the differentiation.....	144
Figure 4.2 Morphological examination of adipocyte differentiation influenced by extracts of <i>A. cominia</i> and drugs treatments.	145
Figure 4.3 Inhibitory effects of <i>A. cominia</i> extracts on 3T3-L1 differentiation starting from day 3 of the differentiation.....	146

Figure 4.4 Series of pictures of 3T3-L1 cells depicting the effect of TNF- α , flavonoids, pheophytin A and staurosporine effect on the morphology of 3T3-L1 at day 8 of differentiation by comparison to the undifferentiated cells.	148
Figure 4.5 p-Nitroaniline concentration dependent curve.....	149
Figure 4.6 TNF- α , flavonoids and pheophytins extracts from <i>A. cominia</i> do not induce apoptosis in 3T3-L1 adipocytes.....	150
Figure 4.7 Inhibitory effects of <i>A. cominia</i> extracts on lipid accumulation in adipocytes for 72 hours.....	152
Figure 4.8 12-Well plate representing the inhibitory effects of <i>A. cominia</i> extracts on lipid accumulation in adipocytes for 72 hours.	152
Figure 4.9 The inhibitory effect of <i>A. cominia</i> extracts on lipid accumulation in adipocytes over 5 days and the withdrawal effect of the extracts on the adipocytes over 6 days.....	154
Figure 4.10 Morphological examination of 3T3-L1 adipocytes influenced by the extracts of <i>A. cominia</i>	154
Figure 4.11 Protein determination of the pre-treated 3T3-L1 cells with TNF- α , flavonoids and pheophytin A.....	156
Figure 4.12 Western blot showing the effect of TNF- α , flav and phoe extracts of <i>A. cominia</i> on GLUT4 protein in plasma membranes in 3T3-L1 adipocytes.....	159

Chapter 5

Figure 5.1 High-throughput screening fitness for DPPIV assay using gly-pro-7-amido-4-methylcoumarin hydrobromide as substrate and DPPIV enzyme.....	175
Figure 5.2 Effect of various <i>A. cominia</i> extracts on DPPIV enzyme in the presence of Gly-pro substrate.....	176
Figure 5.3 Effect of various extracts of AC-MC on DPPIV enzyme at two different concentrations (3 μ g/ml and 30 μ g/ml) in the presence of Gly-pro substrate.....	177
Figure 5.4 Effect of various extracts of AC-KLMN-91-175 on DPPIV enzyme.	178
Figure 5.5 Effect of each fraction KLMN(91-175)66-72 (mixture of flavonoids) from <i>A. cominia</i> extracts on DPPIV enzyme.....	179
Figure 5.6 Michaelis-Menten plot of the inhibitory effect of the flavonoid fraction of <i>A. cominia</i> on DPPIV-catalysis hydrolysis of the enzyme.....	181
Figure 5.7 Michaelis-Menten plot of the inhibitory effect of P32/98 inhibitor on DPPIV-catalysis hydrolysis of the enzyme.....	182
Figure 5.8 High-throughput screening fitness for PTP1B assay using TFMS as substrate and PTP1B enzyme.....	184
Figure 5.9 Effect of various AC-HEC fractions (separated by silica gel column chromatography) on PTP1B enzyme in the presence of DiFMUP substrate.....	186
Figure 5.10 Effect of various AC-MC fractions (separated by VLC) on PTP1B enzyme in the presence of DiFMUP substrate.....	187
Figure 5.11 Effect of various AC-MC-KLMN fractions (separated by sephadex column chromatography) on PTP1B enzyme in the presence of DiFMUP substrate.....	188
Figure 5.12 Effect of various AC-MC-KLMN-91-175 Fractions (separated by sephadex column chromatography) on PTP1B enzyme in the presence of DiFMUP substrate.....	189

Figure 5.13 Effect of various fractions from AC-KLMN-(91-175)-66-72 (separated by HPLC) on PTP1B enzyme in the presence of DiFMUP substrate.....	190
Figure 5.14 Effect of various AC-MC-D fractions (separated by silica gel column chromatography) on PTP1B enzyme in the presence of DiFMUP substrate.....	191
Figure 5.15 Effect of TFMS inhibitor on PTP1B enzyme in the presence of DiFMUP substrate.....	192
Figure 5.16 Series of graphs showing the effect of various fractions of AC-HEC extracts (AC-HEC, AC-HEC-35-38 and AC-HEC-48) on the PTP1B enzyme.....	193
Figure 5.17 Series of graphs showing the effect of various fractions of AC-MC extracts (AC-MC, AC-MC-D, AC-MC-D-5-13 and AC-MC-D-24-44) on the PTP1B enzyme.	194
Figure 5.18 Series of graphs showing the effect of various fractions of AC-MC-KLMN extracts (AC-MC-KLMN, AC-MC-KLMN-91-175 and AC-MC-KLMN-(91-175)66-72) on the PTP1B enzyme.....	195
Figure 5.19 Michaelis-Menten plot of the inhibitory effect of the flavonoid fractions of <i>A. cominia</i> on PTP1B-catalysis hydrolysis of the enzyme.	197
Figure 5.20 Michaelis-Menten plot of the inhibitory effect of the pheophytin A fraction of <i>A. cominia</i> on PTP1B-catalysis hydrolysis of the enzyme.	198
Figure 5.21 Michaelis-Menten plot of the inhibitory effect of the TFMS on PTP1B-catalysis hydrolysis of the enzyme.	199
Figure 5.22 High-throughput screening fitness for α -glucosidase assay using 4-nitrophenyl- α -D-glucopyranoside as substrate and α -glucosidase enzyme.	201
Figure 5.23 Effect of acarbose on the α -glucosidase assay in the presence of 4-nitrophenyl-glucopyranoside (substrate).	202
Figure 5.24 Effect of various crude extracts of <i>A. cominia</i> from maceration extraction on the α -glucosidase assay in the presence of 4-nitrophenyl-glucopyranoside (substrate).	203
Figure 5.25 Effect of various extracts of <i>A. cominia</i> from hexane and ethyl acetate crude extract separated by silica gel column chromatography on the α -glucosidase enzyme.	204
Figure 5.26 Effect of various methanolic extracts of <i>A. cominia</i> from vacuum liquid chromatography separation on the α -glucosidase enzyme.....	205
Figure 5.27 Effect of various methanolic extracts of <i>A. cominia</i> from KLMN extract fraction separated by sephadex column chromatography on the α -glucosidase enzyme.	206
Figure 5.28 Effect of various methanolic extracts of <i>A. cominia</i> from fraction KLMN-91-175 separated by sephadex column chromatography on the α -glucosidase enzyme.	208
Figure 5.29 Effect of separated flavonoids of <i>A. cominia</i> by HPLC (fractions 1 and 2) on α -glucosidase enzyme.	208
Figure 5.30 Effect of various methanolic extracts of <i>A. cominia</i> from fraction D separated by silica gel column chromatography on the α -glucosidase enzyme.	209
Figure 5.31 Effect of acarbose on the α -glucosidase assay in the presence of 4-nitrophenyl-glucopyranoside (substrate).	210
Figure 5.32 The effect of some fractions of AC-MC extracts (AC-MC, AC-MC-I and AC-MC-KLMN) on α -glucosidase enzyme..	211
Figure 5.33 The effect of the flavonoids mixture of AC (AC-MC-KLMN-91-175 and AC-MC- KLMN-(91-175)-66-72) on α -glucosidase enzyme.....	212

Figure 5.34 Michaelis-Menten plot of the inhibitory effect of flavonoids mixture on α -glucosidase-catalysis hydrolysis of the enzyme.....	214
Figure 5.35 Michaelis-Menten plot of the inhibitory effect of the acarbose inhibitor on α -glucosidase-catalysis hydrolysis of the enzyme.....	215
Figure 5.36 High-throughput screening fitness for α -amylase assay using 4-nitrophenyl- α -D-maltohexaside as substrate and α -amylase enzyme.	217
Figure 5.37 Effect of various AC fractions on α -amylase enzyme in the presence of 4-nitrophenyl- α -D-maltohexaside substrate.....	218

List of Appendices

Appendix 1. ^1H NMR spectrum (400 MHz) of the flavonoid mixture from AC-MC-KLMN-91-175 in DMSO- d_6	247
Appendix 2. ^1H NMR spectrum (400 MHz) of MeOH-D (crude) in CDCl_3	248
Appendix 3. ^1H NMR spectrum (400 MHz) of pheophytin A (fraction 5-13) in DMSO- d_6	249
Appendix 4. ^1H NMR spectrum (400 MHz) of pheophytin B (fraction 14-24) in DMSO- d_6	250
Appendix 5. A. ^1H NMR spectrum (400 MHz) of HEC solid of <i>A. cominia</i> in DMSO- d_6	251
Appendix 5. B. ^1H NMR expanded spectrum for the aromatic region (400 MHz) of HEC solid of <i>A. cominia</i> in DMSO- d_6	252
Appendix 5. C. ^1H NMR expanded spectrum for the sugar region (400 MHz) of HEC solid of <i>A. cominia</i> in DMSO- d_6	253
Appendix 5. D. ^1H NMR expanded spectrum for the aliphatic region (400 MHz) of HEC solid of <i>A. cominia</i> in DMSO- d_6	254
Appendix 5. E. ^1H NMR expanded spectrum for the hydroxyl group (400 MHz) of HEC solid of <i>A. cominia</i> in DMSO- d_6	255
Appendix 6. ^{13}C NMR spectrum (100 MHz) of HEC solid from <i>A. cominia</i> in DMSO- d_6	256
Appendix 7. HMBC spectrum (600 MHz) of HEC solid from <i>A. cominia</i> in DMSO- d_6	257
Appendix 8. HSQC spectrum (400 MHz) of HEC solid from <i>A. cominia</i> in DMSO- d_6	258
Appendix 9. ^1H NMR spectrum (400 MHz) of MeOH-D from <i>A. cominia</i> in CDCl_3	259
Appendix 10. ^{13}C NMR spectrum (100 MHz) of MeOH-D from <i>A. cominia</i> in CDCl_3	260
Appendix 11. HMBC NMR spectrum (400 MHz) of MeOH-D from <i>A. cominia</i> in CDCl_3	261
Appendix 12. HSQC NMR spectrum (400 MHz) of MeOH-D from <i>A. cominia</i> in CDCl_3	262
Appendix 13. ^1H NMR spectrum (400 MHz) for fraction 2 in DMSO- d_6	263
Appendix 14. ^1H NMR spectrum (400 MHz) of fraction 1 in DMSO- d_6	264
Appendix 15. Comparison between ^1H NMR spectrum (400 MHz) of fractions 1 and 2... ..	265

Chapter 1

Introduction

1 Overview of diabetes

The name “diabetes” has its origin in the Greek word for “siphon”, which suggests in this case that a considerable quantity of urine is produced. This feature of the disease (production of large volumes of urine) is common to all forms of diabetes and suggests a common end point although not a common origin.

Diabetes mellitus (DM) is a group of diseases characterised by abnormally high levels of blood glucose, resulting in glucose being excreted into the urine (glycosuria) (Cooke and Plotnick, 2008). Generally, in a healthy person, when the pre-prandial (fasting) concentration of blood glucose is raised above normal (4.0 - 5.9 mM), several hormones, including insulin, which is released from the pancreatic cells (β -cells), act to regulate the blood glucose concentrations. Insulin promotes glucose uptake into liver, muscle, and fat cells. In people suffering from DM, glucose levels remain high (> 6.9 mM). The high glucose levels are due to either a reduction in the production of insulin by β -cells or the cells becoming insensitive to circulating insulin. In both cases, glucose is not transported to cells and therefore concentrates in the blood, which is not only harmful for cells but also harmful to certain organs and tissues exposed to the high glucose levels causing tissue dehydration and damage to the kidneys (Torpy and Golub, 2011). High glucose levels stimulating insulin secretion by the pancreatic β -cells causing β -cell glucose toxicity is observed typically in diabetic patients (Kaneto *et al.*, 2010).

Diabetes insipidus (DI) is also characterised by excessive thirst and an increase in passing urine. The name refers to the inability to retain fluid but is characterise by the lack of sugar in the urine. Although DM and DI have some common symptoms, they are two different conditions with unrelated mechanisms. DI is either an abnormal production or a deficiency of the anti-diuretic hormone (ADH) also known as arginine vasopressin (AVP); this type of DI is called cranial diabetes insipidus

(Babey *et al.*, 2011). DI can also be the result of insensitivity in the kidney's response to the ADH; this type of diabetes is called nephrogenic diabetes insipidus.

Chronic hyperglycaemia is largely responsible for the development and progression of long term diabetes-specific macro-vascular and micro-vascular complications. Narrowing of the major arteries to the heart, brain and lower limbs occurs alongside damage leading to a reduction in the function of the endothelium, the small blood vessels in the eyes (retinopathy), nerves (neuropathy), kidney (nephropathy), and heart (coronary vascular diseases), resulting in peripheral vascular diseases, ulceration and amputation of the feet in poorly-managed patients (Nathan *et al.*, 2009).

Pre-diabetes is a common condition related to DM. Patients with pre-diabetes have blood sugar levels higher than the normal levels, but not high enough to be termed diabetic. If uncontrolled, pre-diabetes could be a risk of developing T2-DM. It can disappear without the need of insulin or medical treatments, by losing weight or by diet and physical activities.

1.1.1 Causes of diabetes mellitus

Differences in the two types of DM (types 1 and 2), in terms of causes are well established. Type 1 DM (T1-DM) is partially inherited and its risks can be increased by certain viral infections such as the Coxsackie virus family or rubella. However, there is also a genetic element where mutations in HLA genes may increase the risk of developing T1-DM (Dean and McEntyre, 2004).

The risk factors for developing type 2 DM (T2-DM) include high blood pressure, and high triglyceride and fat levels. Gestational diabetes may transform into (T2-DM) when the new-born weighs more than 5 kilograms. In addition, a high alcohol intake or a high-fat diet can accelerate the development of T2-DM, particularly in cases of obesity. A sedentary lifestyle may also be factor of T2-DM. Moreover, genetics plays an important role in increasing the risk of developing T2-DM, particularly when at least one parent has a close relative who has had T2-DM. Finally, aging is considered

to be the most significant risk factor for T2-DM. Risk begins to rise significantly at the age of 45, and rises considerably after the age of 65.

1.2 Types of diabetes

DM is classified into categories: Type 1 DM, Type 2 DM, gestational DM and other cases of diabetes.

1.2.1 Type 1 diabetes mellitus

Type 1 diabetes mellitus (T1-DM), used to be known as insulin-dependent diabetes or juvenile diabetes, and is immune-mediated diabetes, which is an organ-specific autoimmune disease that results in the autoimmune destruction of pancreatic β -cells (Atkinson and Maclaren, 1994). This results in the body's failure to produce insulin and may have a sudden onset (Agabegi *et al.*, 2008). It is considered to be one of the most frequently diagnosed severe chronic illnesses, affecting around 1 in 300 children in addition to a high proportion of adults (Wucherpfennig and Eisenbarth, 2001). T1-DM is slightly more common in men than in women. T1-DM accounts for about 5 to 10% of all types of diabetes; however, the incidence of T1-DM is increasing in many developed countries, where its treatment and associated morbidities account for significant health costs to these countries (Daneman *et al.*, 2006).

The cause for this increase in the incidence of T1-DM is poorly understood but both environmental and genetic factors are thought to play a role in the susceptibility of individuals. The genetic influence on disease incidence is complex and involves the genes encoding the major histo-compatibility complex (MHC). In humans, MHC is known as the human leukocyte antigen (HLA) and this gene encodes for proteins associated with the immune system. The HLA complex is further subdivided into class I, class II and class III. The genes encoding class II region in particular, a gene called HLA-DR and individuals expressing the allele DR3 and DR4 are particularly susceptible to T1-DM, as HLA-DR is found in 95% of T1-DM patients (Woo *et al.*, 2000). Type 1 diabetes is treated by insulin replacement over the life of the individual. Blood glucose monitoring, diet planning, and screening for the complications related to the diabetes (e.g. micro- and macro-vascular diseases which

can be severe and cause mortality in the patient) is also carried out by the patient and by health professionals. Patients who maintain a close control of their glycaemic levels are at a reduced risk of disease complications, i.e. 30% less risk of kidney disease; 60% less risk of peripheral neuropathy; 99% less risk of retinopathy; and four times less risk of heart disease or stroke (Daneman *et al.*, 2006).

1.2.2 Type 2 diabetes mellitus

Type 2 diabetes mellitus (T2-DM) is known as adult-onset diabetes mellitus, or non-insulin-dependent diabetes mellitus (Arredondo *et al.*, 2005). Usually, in people with T2-DM, the pancreas secretes insulin, but the insulin is unable to stimulate the uptake of glucose. As a consequence of the high blood glucose levels, insulin secretion is elevated (Balkrishnan *et al.*, 2003). When the pancreas is unable to produce enough insulin to deal with the higher demands for insulin, T2-DM (insulin-resistant diabetes) develops. This type of DM has also been considered one of the most severe chronic diseases, and is one of the most widely known metabolic illnesses (Alonso-Castro *et al.*, 2008). It represents a serious public health problem since it accounts for a substantial proportion of “national health expenditures worldwide” (Balkrishnan *et al.*, 2003; and Arredondo *et al.*, 2005). T2-DM affects at least 90% of patients with diabetes and appears gradually (Agabegi *et al.*, 2008). It typically affects adults, usually aged over 45; it can also affect younger people. It is considered to be the leading cause of death in females and the second highest in males (Aguilar-Salinas *et al.*, 2003) and also has expensive consequences for the health systems in many countries (Arredondo and Zuiniga, 2004). It is a growing global health problem, particularly in Asian countries (Wild *et al.*, 2004) for example, in Japan; there are 8.9 million diabetics in addition to 13.2 million individuals with impaired glucose tolerance (NNS, 2007). T2-DM frequency has risen rapidly in recent decades. In year 2000, this frequency was estimated at around 180 million patients globally, and this number is expected to increase to as much as twice that number by the year 2030 (WHO, 2005). Many factors affect the prevalence of T2-DM, such as economic development; changes in diet and available foods, technology and culture also play an important role (Chan *et al.*, 2009).

T2-DM can also be one of the risk factors for many diseases including various cardiovascular diseases (Grundy *et al.*, 1999). In addition, diabetic patients are at high risk of surgical-site infections, which may cause increased mortality.

T2-DM pathogenesis is known by a decline in pancreatic β -cell function which begins at early stages of the diseases (around 12 years before diagnosis) and continues declining throughout the progress of the disease. In addition, T2-DM is also identified when normal β -cells are adapted to insulin resistance, which can occur through increased insulin secretion from each β -cell with or without an increase in β -cell mass (Kulkarni *et al.*, 1999; Matsuzawa *et al.*, 1999; Bulter *et al.*, 2003). However, T2-DM is mainly due to genetics and lifestyle factors (Risérus *et al.*, 2009). The main genetic cause is also related to β -cell function, including mutations of the mitochondrial DNA. Other factors related to insulin progression or the role of insulin, including defects in pro-insulin conversion, insulin gene or receptors mutations may also lead to T2-DM.

Pancreatic β -cells are susceptible to the harmful effects of reactive oxygen species (ROS). In diabetic patients, ROS are produced in many tissues through a number of pathways, such as during the non-enzymatic glycosylation reaction, and the electron transport chain in mitochondria. NADPH oxidase (nicotinamide adenine dinucleotide phosphate oxidase, a membrane-bound enzyme) is also an important source of ROS. NADPH oxidase is activated by various stimuli such as AGEs (advanced glycation end-products), insulin, and angiotensin II. Affected by the high insulin secretion, NADPH is highly activated, resulting in an increase in the production of ROS which in turn damage the pancreatic β -cells (Kaneto *et al.*, 2010) causing the induction of apoptosis and suppression of insulin biosynthesis (El-Alfy *et al.*, 2005 and Vijayakumar *et al.*, 2006), ultimately leading to T2-DM.

1.2.3 Gestational diabetes mellitus

Gestational diabetes mellitus (GDM) is also called impaired glucose tolerance. It affects pregnant women who have never had diabetes before. It is identified as a form of diabetes that appears at the end of pregnancy and normally the mother recovers from it after the delivery of the baby, which is likely to be large (ADA, 2000). It affects around 14% of pregnancies and women who have had GDM are more likely than other women to develop T2-DM later in life (Jovanovic and Pettitt, 2001). Although the levels of the risk vary, it is unclear how much of the variation is explained by variations in ethnicity (Kim *et al.*, 2002).

1.2.4 Other types of diabetes

DM exists in other forms worldwide, resulting from genetic faults and environmental factors. The most know reasons of such types are linked to genetic modifications.

These other forms of DM include:

- Congenital diabetes, which is due to genetic faults of insulin secretion
- Cystic fibrosis-related diabetes
- Steroid diabetes induced by high doses of glucocorticoids
- Several forms of monogenic diabetes

1.3 Diabesity: definition

In general, diabesity is a blend of diabetes and obesity, which sums up both problems. Most people with high BMI have a very high risk of contracting diabetes; so high that the two conditions are very closely connected. Furthermore, treatment of this type of disease becomes more complex, as diabesity causes many complications and co-morbidities which affects both diabetes and obesity (Chan *et al.*, 1994).

Recent research on obesity has presented evidence that adipose tissue may play a critical role in the increase of insulin resistance, causing T2-DM (Hotta *et al.*, 2001). However, some individuals who are obese (associated with insulin resistance) do not have T2-DM but have higher than normal levels of circulating insulin.

Adipose tissue is an important endocrine organ that produces cytokines and hormones such as tumour necrosis factor α (TNF- α), interleukins, plasminogen-activator inhibitor type 1, leptin, adiponectin, and resistin (Wolf *et al.*, 2004). Adiponectin is secreted from adipose tissue and its secretion in adults is related to the percentage of fat in the body. Obese patients with T2-DM have reported to have considerably lower levels of plasma adiponectin than normal. Adiponectin is an adipose-specific plasma protein, and plasma levels are reduced in obese patients (Yokota *et al.*, 2000). This protein controls the glucose regulation and fatty acid oxidation. Adiponectin enhances adipocytes differentiation and increases energy expenditure leading to metabolic derangements that may result in T2-DM.

In adipose tissue, TNF- α is also overproduced causing insulin resistance by decreasing the tyrosine kinase activity of the insulin receptor. TNF- α , secreted by the macrophages and adipocytes cells, is a cytokine overproduced in case of chronic inflammation (Liu *et al.*, 2011). It regulates many biological pathways such as apoptosis, energy uptake, cell differentiation and proliferation and lipid metabolism (Chen *et al.*, 2009). Furthermore, adiponectin plays an important role in the high secretion of TNF- α (Yokota *et al.*, 2000), which in turn causes insulin resistance leading to a hyperinsulinaemia.

There are other proteins such as leptin, a hormone secreted from human monocyte-macrophages, which plays an important role in regulating food intake and energy expenditure, therefore controlling the appetite and hunger. Due to the presence of severe insulin resistance, even a small decline in insulin secretion can lead to the development of diabetes mellitus.

1.4 Treatment of type 2 diabetes

In 1921, insulin became available and all forms of diabetes became treatable. T2-DM is a chronic disease that normally cannot be completely cured but can be controlled by medication. Management of T2-DM can be easily followed by diet and exercises. In severe T2-DM, gastric bypass surgery has been successfully used and helpful, particularly when T2-DM is associated with obesity. However, the treatment of T2-

DM remains complex and medication was always needed for the management of T2-DM (Yach, 2004).

Several orally-acting hypo-glycaemic drugs used clinically act by increasing the release of insulin from pancreatic β -cells. Such drugs include biguanides (metformin as a first line treatment for T2-DM), the classical sulphonylureas, thiazolidinediones (TZD), glucagon [such as peptide 1 (GLP-1) agonist], α -glucosidase inhibitors, glinide, and DPPIV inhibitor. In addition to other drugs, which have been used for the treatment of T2-DM. Each drug acts differently and the mechanisms of action of these drugs are presented in section 1.2.1.2.

Biguanides (e.g. metformin), are usually prescribed as the first-line anti-diabetic drug (DeFronzo *et al.*, 2005). Other drugs currently available for the treatment of T2-DM include sulphonylurea derivatives that stimulate the release of insulin from the pancreas, and thiazolidinediones (TZD) that restore insulin sensitivity to target tissues (Laville and Andreelli, 2000). Gluco-regulatory peptides, such as incretins are also being considered as a potential treatment (Drucker, 2003). Exenatide (exendin-4) which is a 39-amino acid peptide incretin also demonstrates a gluco-regulatory activity similar to the human incretin hormone glucagon such as peptide 1 (GLP-1) (Kolterman *et al.*, 2003; and Holst *et al.*, 2004). Combination therapies also exist for the management of diabetes. The most familiar combination of oral therapies used for people with T2-DM is metformin with a sulphonylurea (Kirpichnikov *et al.*, 2002). Both drugs can be used as monotherapy or in combination as they are safe and effective (Nathan *et al.*, 2002). The combination of exenatide with metformin-sulphonylurea therapy had good effect on weight loss by patients with T2-DM (Kendall *et al.*, 2005).

Other drug treatments have also been used such as α -glucosidase inhibitors (acarbose, miglitol and voglibose) which have an important role in the management of weight, GLP-1 agonist (such as exenatide and liraglutide) also have effects in the weight loss in diabetic patients. Other treatments such as DPPIV inhibitor, pramlintide, and glinide where all of these increases weight loss, are fast effective and hyperglycaemic (Nathan *et al.*, 2002).

However, all of these agents have unexpected treatment-limiting side effects (as shown in Table 1.1), such as weight gain, hypoglycaemia gastrointestinal intolerance, and peripheral oedema (Inzucchi, 2002) and, finally, all of these side effects fail to establish an adequate glycaemic control (Laville and Andreelli, 2000). In particular, TZD inhibits hepatic renewal (Turmelle *et al.*, 2006), induces obesity (De Souza *et al.*, 2001), and causes osteoporosis (Rzonca *et al.*, 2004). Therefore, it is preferable to find more new anti-diabetic substances that may stimulate glucose uptake by hepatic or muscle cells but, not unlike TZD (De Souza *et al.*, 2001) or insulin injection (Laville and Andreelli, 2000) and some other medications, do not induce obesity or other side effects.

Medicines name	Mode of action	Daily dosage	Side effects
Metformin (biguanide). See Fig 1.1.	Suppressing hepatic glucose production, increasing insulin sensitivity and enhancing peripheral glucose uptake	500 mg twice (oral treatment)	Renal insufficient, GI side effects
Phenformin and Butformin (biguanide)	Reversion of the cytosolic glycolysis characteristic of cancer cells to normal oxidation of pyruvate by the mitochondria	200-400 mg twice	High toxicity (withdrawn from most markets)
Sulfonylurea derivatives (such as tolbutamide and chlorpropamide). See Fig 1.2.	Acting by increasing insulin release from the pancreatic beta cells	Two to three times (30 min before meals)	Weight gain, hypoglycaemia
Insulin (additional)	Same role as the body's insulin by promoting the glucose uptake by muscle and fat tissues	One to four injection	Weight gain, hypoglycaemia
Thiazolidinediones (TZD) (such as Rosiglitazone, Pioglitazone and Troglitazone). See Fig 1.3.	Binding to PPARs which decreases insulin resistance, modifies adipocyte differentiation decrease leptin levels and raises adiponectin levels	Twice	Bone fractures (osteoporosis), inhibits hepatic renewal, weight gain, fluid retention and CHF
GLP-1 agonist	Inducing glucose-dependent stimulation of insulin secretion while suppressing glucagon secretion	Two injections	GI side effects, long-term safety not established
Alpha-glucosidase inhibitors. See Fig 1.5.	Preventing the digestion of carbohydrates	Three times	GI side effects, long-term safety not established
Glinide See Fig 1.6.	Binding to K_{ATP} channel, which increases fusion of insulin granulae with the β -cell membrane, and therefore increases secretion of (pro) insulin.	Three times	Weight gain, hypoglycaemia
Pramlintide		Three injections	GI side effects, long term safety not established
DPPIV inhibitor See Fig 1.7.	Increasing incretin levels (GLP-1 and GIP), which inhibit glucagon release, and in turn increases insulin secretion	Oral dosage depending on the patient	GI side effects, long term safety not established
Incretin	Similar to the human incretin hormone glucagon such as peptide 1 (GLP-1)	5 μ g twice	Nausea and diarrhoea
Exanatide	Advancing β -cell function and increasing insulin secretion	5 μ g twice	Gastrointestinal, including sour stomach, belching, diarrhoea, heartburn, indigestion, nausea, and vomiting

Table 1.1 Drugs used for the treatment of T2-DM, their mode of action, daily injections and their side effects

1.5 Mechanism of action of drugs

1.5.1 Metformin

Metformin (Fig 1.1) reduces hyperglycaemia essentially by reducing glucose production by the liver (hepatic gluconeogenesis). It activates AMP-activated protein kinase (AMPK), which is an enzyme that has a significant role in insulin signalling, body energy stability, glucose metabolism and fat degradation (Hundal *et al.*, 2000; Zhou *et al.*, 2001). Studies carried out in 2008 show the mechanism of action of the metformin in activating the AMPK, which is required for an augmentation in the expression of SHP (small heterodimer partner), which in turn inhibits the expression of the hepatic gluconeogenic genes PEPCK and Glc-6-Pase (Kim *et al.*, 2008). In addition, metformin enhances insulin sensitivity, augments peripheral glucose uptake (by phosphorylating the glucose transporter type 4 GLUT4 enhancer factor), increases fatty acid oxidation (Collier *et al.*, 2006), and decreases the absorption of glucose from the gastrointestinal tract (Bailey and Turner, 1996). After metformin administration, there is an increase of AMPK activity in skeletal muscle that causes GLUT4 translocation to the plasma membrane, ensuring insulin-independent glucose uptake (Musi *et al.*, 2002).

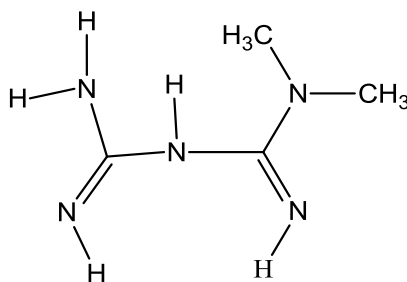


Figure 1.1 Chemical structure of metformin.

1.5.2 Sulfonylureas

Sulfonylureas (Fig 1.2) act on pancreatic β -cell plasma membranes by binding to the sulfonylurea receptor causing the closure of the ATP-dependent K^+ (K_{ATP}) channel

(the receptor binding site for hypo-glycaemic drugs is located at the cytoplasmic face of the plasma membrane). Binding of sulfonylureas to the receptors leads to a depolarisation in the β -cell plasma membrane and the voltage-gated Ca^{2+} channels open (Panten *et al.*, 1996). The rise in intracellular calcium leads to increased fusion of insulin granulae with the cell membrane, and thus to a rise in the secretion of pro-insulin hormone, thereby stimulating of insulin release (Panten *et al.*, 1996).

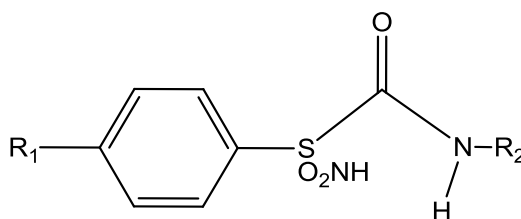
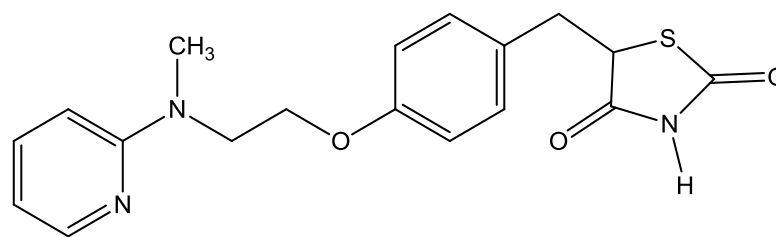


Figure 1.2 General chemical structure of sulfonylureas. Examples such as tolbutamide ($\text{R}_1 = \text{CH}_3$ and $\text{R}_2 = \text{CH}_2 \text{CH}_2 \text{CH}_2 \text{CH}_3$) and chloropropamide ($\text{R}_1 = \text{Cl}$ and $\text{R}_2 = \text{CH}_2 \text{CH}_2 \text{CH}_3$).

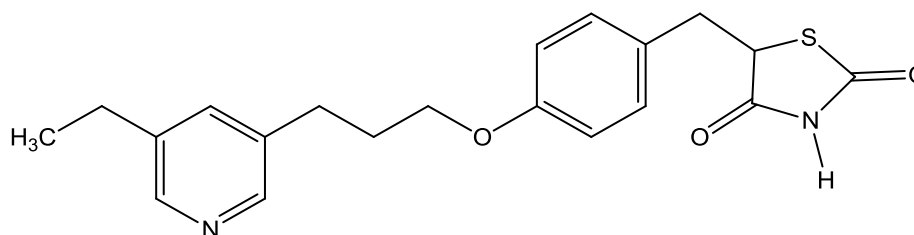
1.5.3 Thiazolidinediones

Thiazolidinediones or TZDs play an important role by binding to the intra-nuclear hormone receptor and peroxisome proliferator-activated receptors inside the cell nucleus (PPARs), particularly $\text{PPAR}\gamma$ (gamma). By activating $\text{PPAR}\gamma$, TZDs decrease insulin resistance by modifying adipocyte differentiation (Waki *et al.*, 2010), decreasing leptin levels (which leads to an increase in appetite) and increasing adiponectin levels that is involved in regulating glucose levels as well as fatty acid breakdown (Panigrahy *et al.*, 2002). Only rosiglitazone and pioglitazone (Fig 1.3) are currently on the market as the hepatoxicity of the TZDs is a clinical concern (Kendal, 2006).

Troglitazone is a member of the thiazolidinedione class of compounds, and is used as an anti-diabetic and anti-inflammatory drug (more information about troglitazone are included in chapter 4, section 4.1).



Rosiglitazone



Pioglitazone

Figure 1.3 Chemical structure of two TZDs

1.5.4 The incretins

Incretins, including glucose-dependent insulinotropic polypeptide (GIP) and glucagon-like peptide-1, are hormones secreted by the gut cells in response to food intake. GLP-1 agonists play many roles in insulin resistance (Meier *et al.*, 2004); they may increase insulin secretion from the pancreatic β -cells in a glucose-dependent manner and they augment insulin-sensitivity in both alpha cells and beta cells (Fig 1.9), reduce glucagon secretion by binding to a specific G protein-coupled receptor, and raise β -cells mass and insulin gene expression.

1.5.5 Alpha-glucosidase inhibitors

Glucosidases are glucose hydrolase enzymes that cleave the glucosidic bond between two glucose residues from glucosides; they are specified by the particular substrate and by alpha or beta configurations. Glucosidases are classified as α -, β - and α -1,3-glucosidase; α -glucosidase (maltase), and β -glucosidase (cellobiase) in the kidney, liver and intestinal mucosa.

Among T2-DM medications, oral therapy using α -glucosidase inhibitors (AGIs) such as acarbose and miglitol have been used to lower plasma glucose levels towards normo-glycaemia and preventing later complications (Andrade-Cetto *et al.*, 2007). Therapeutic approaches aim to delay the absorption of ingested carbohydrates (such as starch) by inhibiting carbohydrate hydrolysing enzymes such as α -glucosidase enzyme (El-Beshbishy and Bahashwan, 2012). Carbohydrates are normally cleaved into glucose and absorbable mono-saccharides (Samantha *et al.*, 2009) by the intestinal α -glucosidase located in the brush border of the small intestine (microvilli), which can be absorbed through the small intestine. The inhibition of these enzymes by AGIs does not prevent the absorption of ingested carbohydrates but reduces the rate of carbohydrates digestion and reduces insulin peaks; therefore less glucose is absorbed (Fig 1.4) preventing postprandial hyper-glycaemia and subsequent hyper-insulinaemia (Sindhu *et al.*, 2013).

Recently, synthetic enzyme inhibitors drugs have been used. By affecting the carbohydrate absorption in the small intestine, AGIs have side effects such as diarrhoea, abdominal bloating, flatulence and nausea. It is known that these side effects can be minimised by starting therapy with a small dose and slowly working up to the effective and required dose (Bray and Greenway, 1999). AGIs are currently a potential target in the development of lead compounds from natural products and plant resources for the treatment of T2-DM, and aim to reduce side effects caused by the known synthetic AGIs (Yuhao *et al.*, 2005).

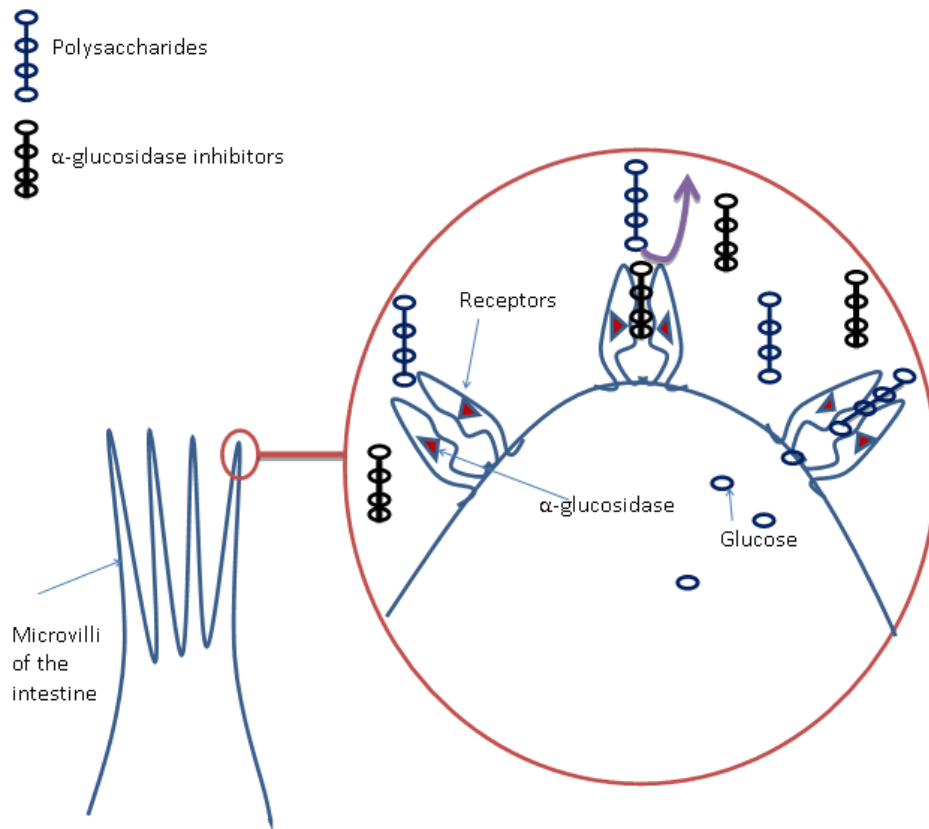


Figure 1.4 Effect of α -glucosidase inhibitors on the enzymatic hydrolysis of polysaccharides by α -glucosidase in the small intestine. (Adapted from Bischoff, 1994).

Alpha-glucosidase which hydrolyse polysaccharides into glucose in the intestinal brush borders are similar to acarbose and miglitol (Fig 1.5).

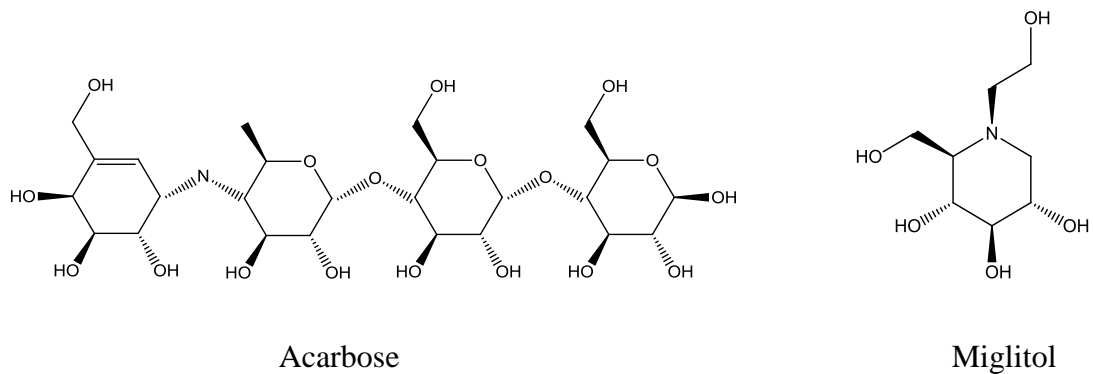


Figure 1.5 Chemical structures for two alpha-glucosidase inhibitors.

1.5.6 Alpha-amylase inhibitors

α -Amylase, one of the carbohydrate hydrolysing enzymes, breaks down the alpha bonds of large, alpha-linked polysaccharides such as starch and glycogen into glucose or maltose (Ali *et al.*, 2006). α -Amylase inhibitors such as acarbose (Fig 1.5) were expanded in section 5.1 (chapter 5).

1.5.7 Glinides

Glinides (Fig 1.6) act in a similar manner to sulfonylureas but at a separate binding site (insulinotrope). They act by closing the ATP-sensitive K (KATP) channel in pancreatic β -cells, thereby inducing depolarization, Ca^{2+} entry, and insulin secretion (Winkler *et al.*, 2007).

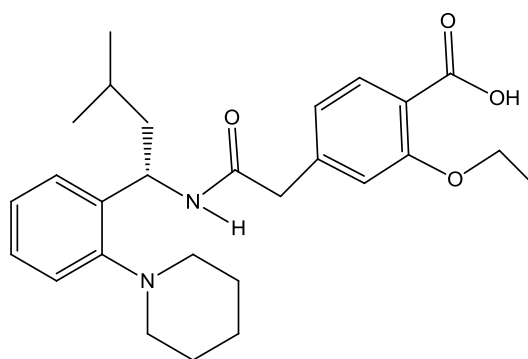


Figure 1.6 Chemical structure of glinide.

1.5.8 DPPIV inhibitors

DPPIV inhibitors (example in Fig 1.7) block the activity of dipeptidyl peptidase IV (DPPIV) which plays a major role in glucose metabolism, and is responsible for the degradation of incretins such as glucagon-like peptide 1 (GLP-1) (Shivanna and Koteshwara, 2010). Therefore, DPPIV inhibitors increase incretin levels (GLP-1 and gastric inhibitory peptide, GIP), which inhibits glucagon release, in turn improving glucose tolerance and increasing insulin secretion in response to oral glucose. Recent

research on T2-DM has shown the importance of DPPIV inhibitors in the treatment of T2-DM (Ahrén, 2005).

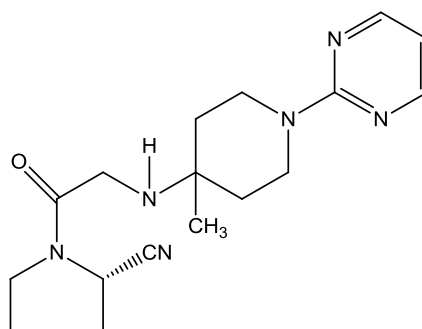


Figure 1.7 Example of chemical structure of a DPPIV inhibitor

1.5.9 Exenatide

Exenatide improves β -cell function by augmenting the expression of the genes involved in the secretion and biosynthesis of insulin, and by increasing the mass of pancreatic cells; it has a considerable influence on reducing food intake and plays a role in weight loss (DeFronzo *et al.*, 2005).

1.6 Insulin

Patients with T2-DM may require exogenous insulin for the management of their disease in order to achieve an adequate glycaemic control, and insulin injections have improved the quality of life for patients with all types of DM (Korytkowski *et al.*, 2003). Insulin is given to the patients intravenously because as a protein, the GI tract digests the insulin if taken orally. Insulin increases the uptake and metabolism of glucose by liver, muscle and fatty cells and decreases the endogenous production of glucose by the liver in both types of diabetes. Insulin also has an important role in the stimulation of the uptake of other nutrients such as fatty and amino acids and their transformation into protein, fat and glycogen (Brunton *et al.*, 2005).

In T2-DM, insulin resistance is a condition in which normal insulin levels do not result in glucose entry into the cell. Higher levels of insulin in the blood occur in

insulin resistance, resulting in most of the organs being insulin resistant. Most patients with insulin resistance are overweight or obese.

1.6.1 Insulin secretion

The pancreas, both endocrine and exocrine glands, is responsible for the secretion of various important hormones. The islets of Langerhans in the endocrine pancreas contain four different cell types: α (alpha), and β (beta) cells, secreting glucagon and insulin respectively and δ (delta), responsible for the somatostatin production which regulates acid secretion by the intestinal gut and insulin release (Hesse *et al.*, 2001), and PP cells, which produce pancreatic polypeptides, responsible for the regulation of the food intake. These pancreatic hormones all influence each other's secretion and play a complementary role in glucose homeostasis.

After food intake, the incretins (GLP-1 and GIP) are secreted by the endocrine cells that are located in the epithelium of the small intestine (Kim and Egan, 2008). However, glucose in the blood is the direct stimulus and regulator of the function of the β -cells in modulating the secretion of insulin, a peptide hormone composed of 51 amino acids. GLP-1 and GIP, when activated, lead to an increase in the secretion of insulin by β -cells and decrease of the secretion of glucagon by α -cells (Fig 1.9). Released insulin reduces glucose production by liver cells and increases glucose consumption by muscle and fat cells. Any dysfunction in the β -cells has profound effects on the glucose homeostasis, which in turn can result in increasing insulin release, causing insulin resistance, a reduction in the suppression of gluconeogenesis and impaired glucose tolerance.

The mechanism of insulin secretion by β -cells in normal subjects is shown in Fig 1.8. Glucose is transported into β -cells through facilitated diffusion via activation of GLUT2 glucose transporters. Once the intracellular glucose is metabolised to ATP, the increase in the ATP/ADP ratio induces closure of cell-surface ATP-sensitive K^+ (K_{ATP}) channels, leading to cell membrane depolarisation. In turn, the cell-surface voltage-dependent Ca^{2+} channels are opened, facilitating extracellular Ca^{2+} influx

into the cytoplasm of the β -cell. This free cytosolic Ca^{2+} triggers the exocytosis of insulin (Benninger *et al.*, 2011).

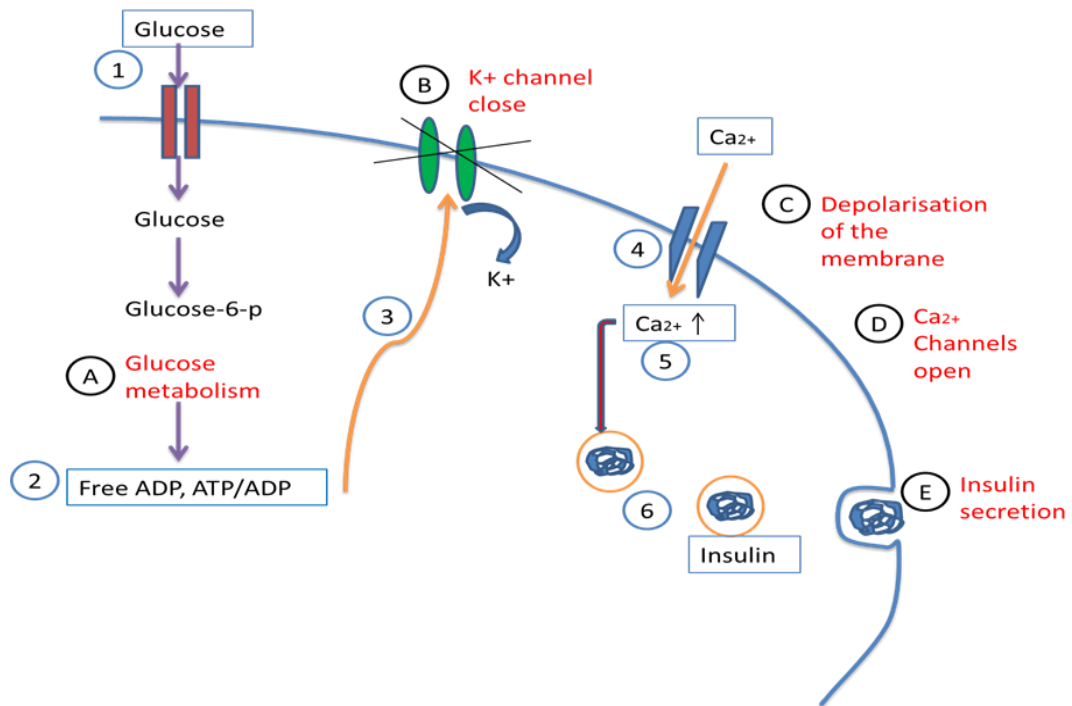


Figure 1.8 The fuel hypothesis and the secretion of insulin by β -cells and mechanisms of the glucose-dependent insulin secretion. (Adapted from Banzal and Wand, 2008).

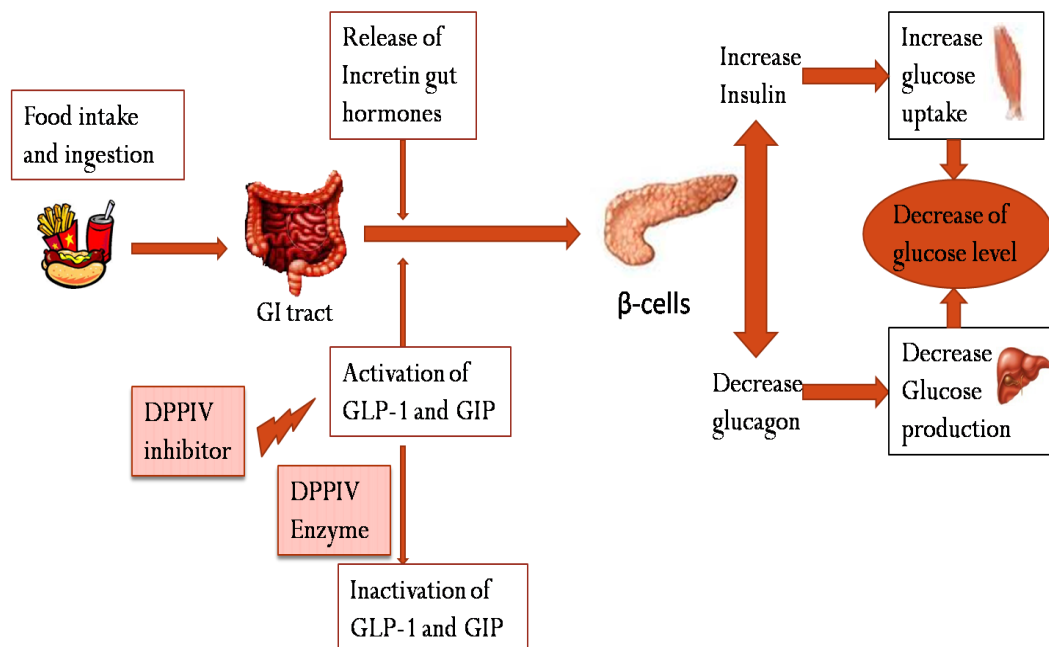


Figure 1.9 Effect of incretins and DPPIV on pancreatic cells and the glucose homeostasis. (Adapted from Baggio and Drucker, 2004).

1.7 Traditional treatment of T2-DM

1.7.1 History of traditional treatment

For thousands of years, humankind has known about the benefit of drugs from nature. The treatment used by ancient civilisations for the signs and symptoms of diabetes mellitus were extracts of plants or animal products (Dallas, 2011). However, they sought a way to cure the disease, and among the things that were tried were oil of roses, dates, raw quinces, gruel, jelly of viper's flesh, broken red coral, sweet almonds, and fresh flowers of blind nettles. Many people used dietary manipulation and medicinal plants to treat their illness. Over the years, patients continue to use natural products as alternatives or complements to manage T2-DM. The search for drugs from these medicinal plants has been almost exclusively in indigenous communities. Some ancient peoples found that after eating or drinking a tincture of one or mixture of some plants such as lupine, trigonella (fenugreek), and zedoary seed, their excessive thirst disappeared, but they were unaware of the precise mechanism of action and effects of these plants.

1.7.2 Treatment using natural products with hypo-glycaemic activity

The treatment of T2-DM with current drugs has many undesirable side effects (Cheng and Fantus, 2005). Furthermore, in low-income countries, there is a restricted access to public health systems which encourages people with T2-DM to use unconventional treatments. Plant-based medicinal products have been known since ancient times. Medicinal extracts constitute a common choice for the treatment and control of T2-DM in many countries and cultures worldwide (Pagán and Tanguma, 2007; Mentreddy 2007). Many plants have been used for many years and been found to have anti-diabetic effects in animal models and in clinical studies using human patients, particularly in Asia (e.g. China and India), Africa and South America (Mentreddy, 2007). Many plant species are also known in folk medicine of different cultures and used for their hypo-glycaemic properties to treat T2-DM (Abdel-Barry *et al.*, 1997). To date, dietary measures and traditional plant therapies prescribed by native systems of medicine have been widely used in many countries such as India (Warier, 1995).

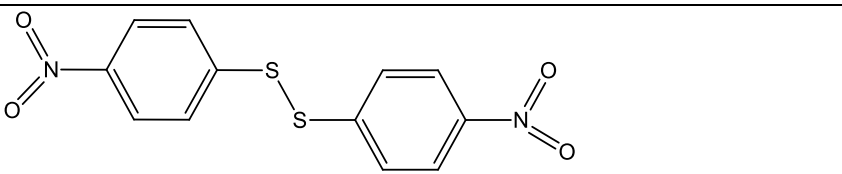
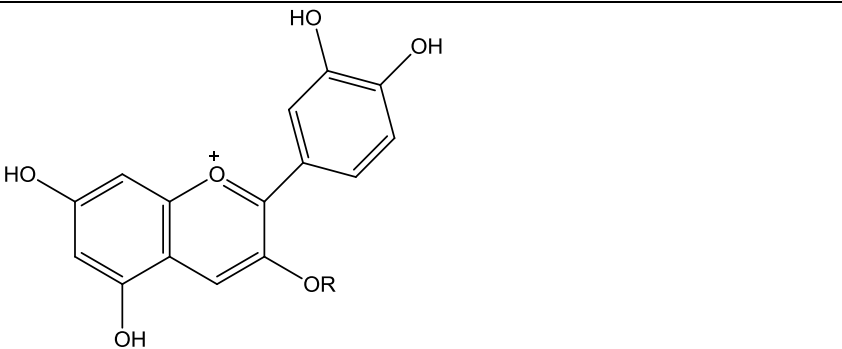
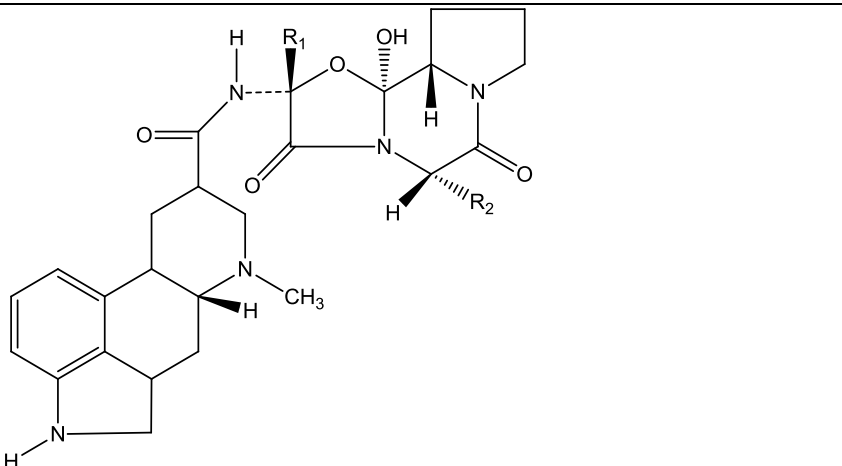
In Mexico, *Cecropia obtusifolia* Bertol. and *Guazuma ulmifolia* Lam. (Alonso-Castro *et al.*, 2008), are plants widely used as traditional medicine for the treatment of T2-DM. Many *in vitro* experiments and clinical trials have been carried out to establish the hypoglycemic properties of these plants (Andrade-Cetto and Wiedenfeld, 2001; Herrera-Arellano *et al.*, 2004; and Andrade-Cetto *et al.*, 2008). It has been discovered that the compounds found in *Cecropia obtusifolia* Bertol., such as chlorogenic acid (CGA) and iso-orientin, also found in other plants, have been shown to have anti-diabetic activities (Andrade-Cetto and Wiedenfeld, 2001). Fenugreek, onion and garlic have also been reported to have a hypo-glycaemic effect (Jelodar *et al.*, 2005). The mechanism of action of the garlic on the number of β -cells is thought to be due to the role of substances such as allyl propyl disulphide or diallyl disulphide (Table 1.2).

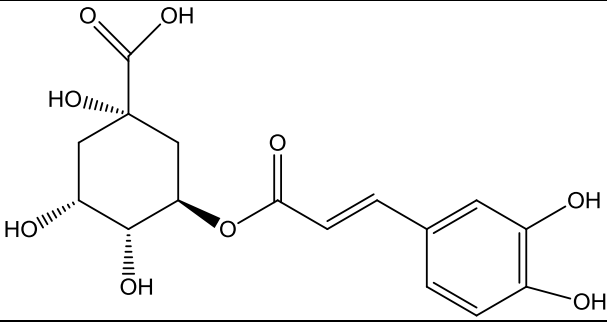
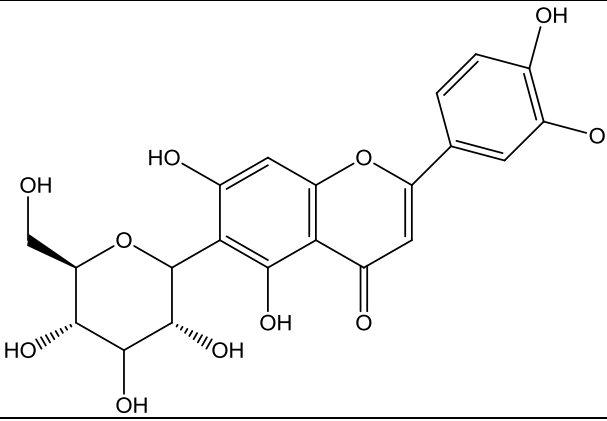
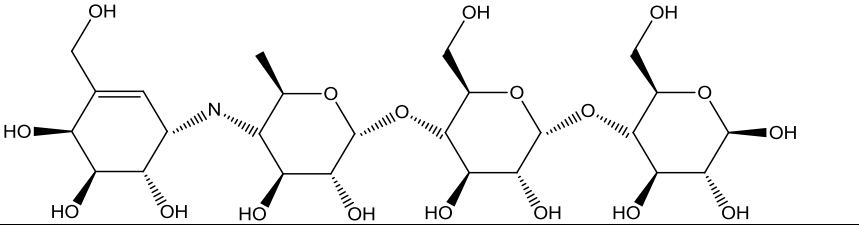
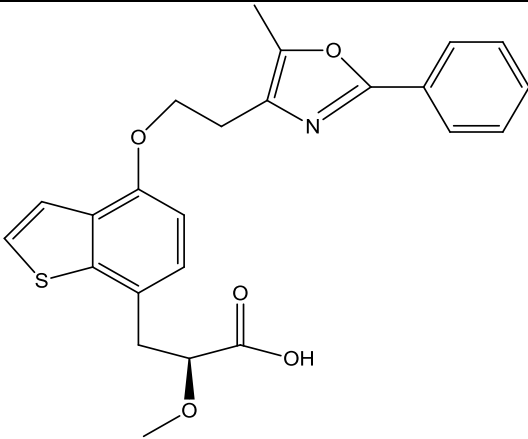
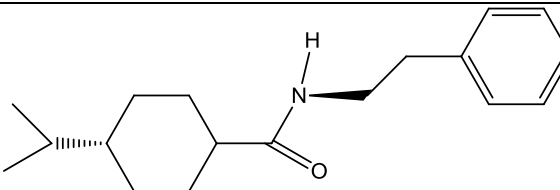
Tecoma stans and *Teucrium cubense* have been used for the treatment and management of T2-DM, and their hypo-glycaemic mechanisms have been evaluated on the glucose uptake in adipose cells (Alonso-Castro *et al.*, 2010).

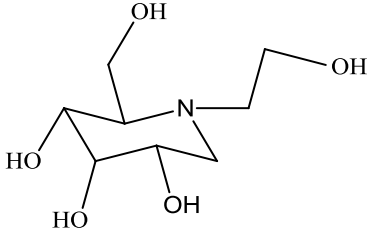
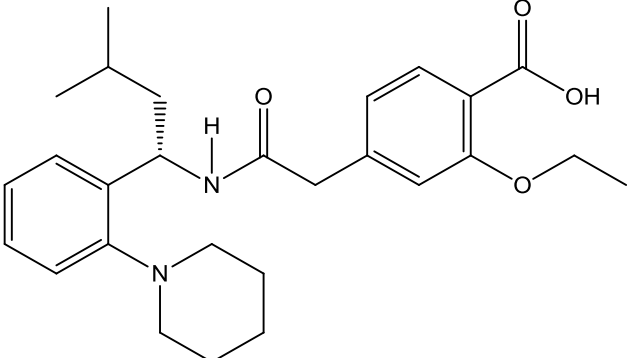
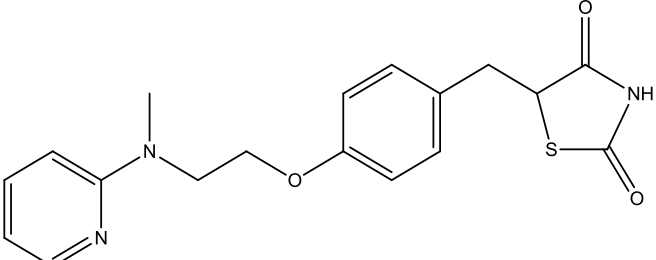
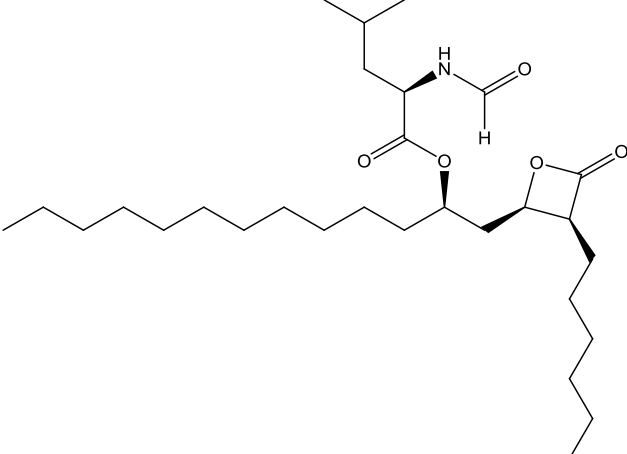
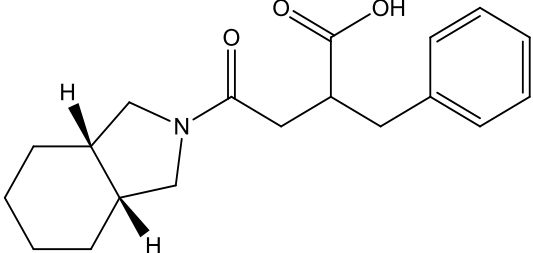
In South Africa, *Aloe ferox* is a plant frequently used as a traditional treatment for T2-DM (Loots *et al.*, 2007), due to the significant action of the flavonoids it contains.

Equisetum arvense has been found in use in the Middle East as an anti-diabetic medicinal plant, due to its alkaloid content (Shamsa *et al.*, 2008).

Further, rosemary, *Rosmarinus officinalis*, is an evergreen perennial shrub grown in many countries worldwide (Porte *et al.*, 2000), particularly in Turkey (Bakirel *et al.*, 2008). It has been used for the treatment of a wide range of diseases including T2-DM, respiratory and stomach problems, and inflammatory diseases (Kültür, 2007). Many other plant species have been discovered to have anti-diabetic effects related to their active constituents.

Anti-diabetic agents	Structures
Allylpropyl disulphide or diallyldisulfide	
Polyphenols flavonoids	
Alkaloids	

Chlorogenic acid	
Isoorientin	
Acarbose	
Aleglitazar	
Nateglinide	

Miglitol	
Repaglinide	
Rosiglitazone	
Orlistat	
Mitiglinide	

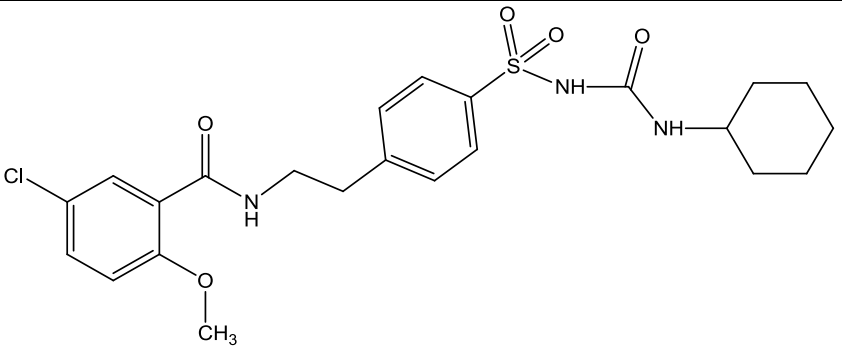
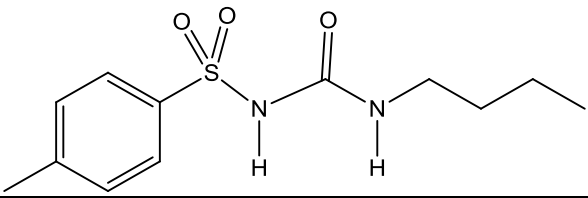
Glibenclamide	
Tolbutamide	

Table 1.2 Examples of anti-diabetic compounds. (Jelodar *et al.*, 2005; Harvey, 2010).

1.7.3 “Hypo-glycaemic activities” of anti-diabetic plant extracts

Oral hypo-glycaemic drugs (for example sulfonylurea derivatives, biguanides, thiazolidinediones (TZD), or injectable insulin) has been used for the treatment of T2-DM. However, because of their unwanted side effects (as shown in Table 1.1) and due to their failure to regulate the blood sugar level adequately (Spiller and Sawyer, 2006), many scientists have recommended medicinal plants. These medicinal plants stimulate glucose uptake by adipocytes or muscle cells, have fewer side effects on patients with diabetes and do not induce obesity.

In addition to the treatment of hypoglycaemia, some plants have been used to reduce oxidative damage in T2-DM, and interest has grown in the use of natural antioxidants. It has been assumed that many of the negative effects of oxidative stress are reduced by supplementation with certain dietary antioxidants such as vitamins E and C, in addition to other non-nutrient antioxidant such as flavonoids (Rahimi *et al.*, 2005; Al-Azzawie and Alhamdani, 2006).

In 2009, the World Health Organisation (WHO) estimated that 25% of modern drugs are obtained from plants and the global market for herbal medicines generally rose to over 60 billion dollars annually (WHO, 2009). Over 1200 plants have been used

throughout the world for the practical treatment of T2-DM, but only around 350 of them have been documented as having hypo-glycaemia activity (Abdel-Barry *et al.*, 1997; Alarcon-Aguilar *et al.*, 2002; Pushparaj *et al.*, 2000). To date, in Mexico, around 306 plants species have been identified to have anti-diabetic properties (Andrade-Cetto and Heinrich, 2005). The precise mechanism of action of many plants remains vague. Plants may act on blood glucose through different mechanisms; some plants may have insulin-like materials, while others could inhibit the activity of insulin, and others could augment pancreatic β -cells mass by triggering the renewal of these cells. A number of these plants contain fibres which may obstruct the carbohydrate absorption, thus affecting the blood glucose level (Jelodar *et al.*, 2005).

A. Enhancement of insulin release

Many people suffering from T2-DM ultimately require supplementation with additional insulin, as the ability of the pancreatic β -cells to produce their own insulin decreases dramatically (Hamaty, 2011). Numerous exogenous insulin preparations have been developed with the goal of matching, as closely as possible, endogenous insulin release (Qayyum and Greene, 2011). Agents for the enhancement of insulin release have been used to promote the generation of β -cells and to stop the decline in the function of β -cells (Bailey and Day 2002). The most stimulating agents affecting the mechanism of glucose-induced insulin secretion are incretins.

B. Repair of β -cells

Elevations in glucose, referred to as “glucotoxicity”, and in lipids as “lipotoxicity”, are both implicated in β -cell failure. Normal insulin secretion from islets relates to a communication network for managing the activity of individual insulin-producing cells. Therefore, single β -cell, which is not connected by connexin channels to others, show poor expression of the insulin gene and release low amounts of the

hormone after stimulation, whereas restoration of β -cell contacts rapidly improves both insulin biosynthesis and release (Calabrese *et al.*, 2004). Studies on plant compounds have been carried out on the repair of the β -cells and particularly on the connexion channels (Cx36 channels). Other researchers have shown that increased apoptosis also leads to reduced β -cell mass in T2-DM. In this light, many plants may work to inhibit cell apoptosis and reverse this disease (Butler *et al.*, 2003 and Jiang *et al.*, 2011).

C. Increase of glucose uptake (PTP1B-deficiency)

The liver is the main organ involved in the uptake, regulation and metabolism of glucose, while adipose tissues also play an important role in glucose homeostasis (Wang *et al.*, 2011). T2-DM is defined as an insulin resistance disease characterised by a decrease in the ability of the cells or tissues to respond to physiological levels of insulin (Heness, 2007). In patients with T2-DM (where insulin resistance is the condition), the majority of the body's organs such as muscle and the liver become resistant to the action of the insulin. Insulin resistance leads to increased glucose output from the liver and reduced uptake and metabolism of glucose by other organs (Hardie, 2008), which may be the result of an increase in the PTP1B enzyme (non-receptor Protein Tyrosine Phosphate type 1B).

Moreover, plant extracts have been shown to enhance the binding of insulin to its receptor, which induces activation of a complex network of downstream molecules, including phosphatidylinositol 3-kinase (PI3K) (Khan and Pessin, 2002; Watson *et al.*, 2004). Activation of Akt/PKB stimulates membrane translocation of the glucose transporter GLUT4 (Wang *et al.*, 1999), leading to enhanced glucose uptake. Thus, both Akt and PKB activation are required for glucose uptake (more information about PTP1B is introduced in chapter 5, section 5.1).

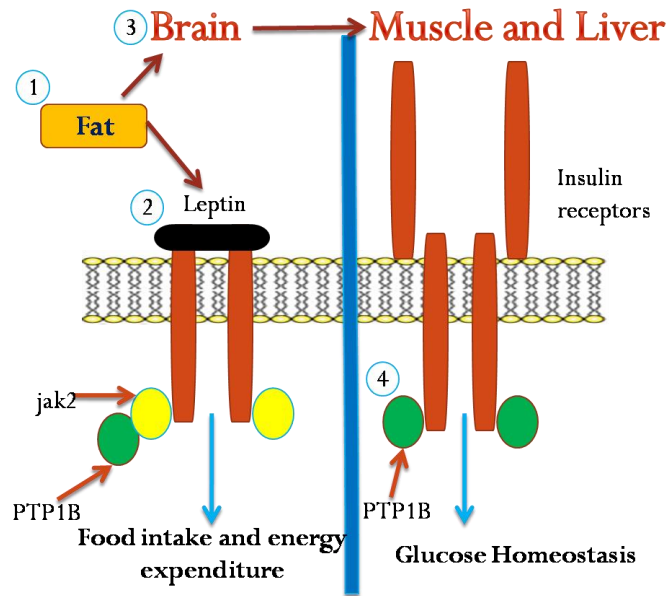


Figure 1.11 Physiological role of PTP1B in glucose homeostasis. (Adapted from Liu, 2004).

D. Prolongation the action of insulin-like hormones (e.g. DPPIV)

DPPIV inhibitors act by reducing glucagon and blood glucose levels; their mode of action is to increase incretin levels, which in turn inhibit glucagon release and increase insulin secretion. DPPIV breaks down the incretin levels (GLP-1 and GIP) particularly GLP-1 (Glucagon-like peptide 1). GLP-1 is a hormone secreted from the intestine and its role is related to enhancing insulin release, and promoting pancreatic β -cell growth and differentiation. The use of certain plant extracts may affect the role of DPPIV, and could increase the release of GLP-1 hormones, which in turn inhibits glucagon release, increases insulin secretion, and prolongs the action of insulin-like hormones. For example, Berberine, a plant extract, was used by Al-Masri *et al.* (2009) to inhibit DPPIV activity and shows a comparable activity to the DPPIV inhibitor (Fig 1.9).

1.8 Problems of developing plant therapies as new oral anti-diabetics drugs

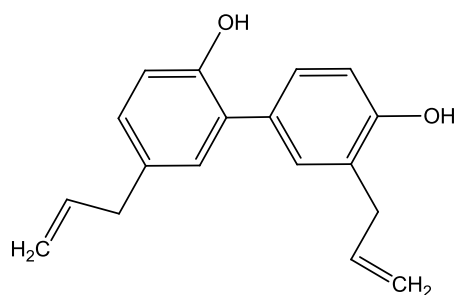
Despite the importance of many plants, and the progress in finding different medicinal compounds for the treatment of T2-DM, the search for new oral anti-diabetic drugs from natural products has difficulties. The search for newer drugs continues as the drugs in the market have a number of undesirable side effects (Kavishankar *et al.*, 2011). Plants are a potential source of hypo-glycaemic drugs, but because of the technical difficulties involved in the isolation and elucidation of their active compounds, studying their mechanism of action is time consuming and costly.

Various plants and compounds have been used for treatment (Table 1.2) all over the world, but only a few of them been tested in biological assays.

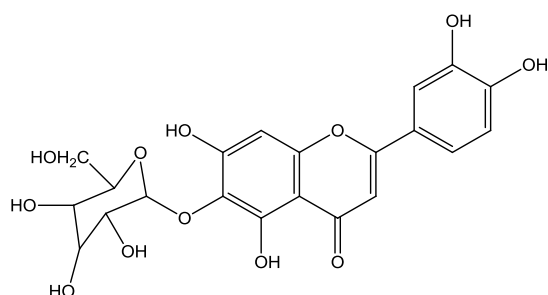
1.9 Phenol-containing plants with hypo-glycaemic activity

Phenolic compounds are aromatic compounds, including simple phenols, polyphenols, phenylpropanoids, flavonoids and tannins.

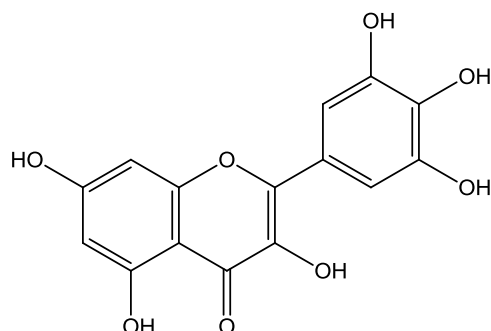
Major flavonoids have characteristic structures and no defined mechanism of action and include flavans, flavanones, flavones, flavanols, flavanonols, catechins, anthocyanidins and isoflavones. Bio-flavonoids have been studied in terms of their multi-functional biological efficacies, including anti-diabetic activity. A number of studies have been carried out to discover their potential function in the treatment of T2-DM (Brahmachari, 2011). Most of these studies have demonstrated the hypo-glycaemic effects of most of the flavonoids using different assays and *in vivo/in vitro* studies (Brahmachari, 2011). The flavonoids also play an important role in regulating the activity of some enzymes such as alpha-glucosidase and alpha-amylase that are involved in carbohydrate metabolism. As a result, flavonoids (Fig 1.12) have recently been proposed as a novel and promising natural therapy for the treatment of T2-DM.



Honokiol (Alonso-Castro *et al.*, 2011)



Isoorientin (Sezik *et al.*, 2005)



Myricetin (Liu *et al.*, 2005)

Figure 1.12 Examples of some chemical structures of certain flavonoids, which are phenol-containing compounds with anti-diabetic activity.

1.10 Cuban medicinal plants used in the treatment of type 2 diabetes mellitus

In Cuba, there are many herbal supplements, which are among the oldest and the most diverse of the medicinal systems used for the treatment of T2-DM. For a long time, oral treatment for DM with medicinal plants was based on traditional information (Marrero, 2007). Most of the plants were grown in the Western and central regions of Cuba. However, investigation, chemical characterisation and studies on the constituents and the mechanism of action of these plants have been the aim of most recent studies.

Five Cuban medicinal plants *Tamarindus indica* L., *Lippia alba* L., *Pimenta dioica* (L.) Merr, *Rheedia aristata* Griseb and *Curcuma longa* L. have been shown to have an antioxidant activity, and a hypo-glycaemic activity (Ramos *et al.*, 2003). Over the

years, the number of Cuban medicinal plants being tested for hypo-glycaemic activity has increased and continues to increase.

Allophylus cominia (L.) Sw. (Sapindaceae), also known as *Rhus cominia* (L) or *Schmideli A. cominia* Sw., which in Cuba is commonly called *palo de caja*, *caja* or *caja común*, is one of the best-known medicinal plants in Cuba. It was initially used as a remedy for gastrointestinal disorders, but was subsequently employed as a remedy for diabetes. It has also been reported in the treatment of tuberculosis and catarrhal diseases in general. In addition, medicinal properties against toothache and in venereal diseases have also been attributed to this plant (Sanchez *et al.*, 2014). More information about this plant is presented in chapter 2.

1.11 Phytochemistry of anti-diabetic medicinal plants

Phytochemistry deals with plant life and the chemical compounds biosynthesised by them. Anti-diabetic medicinal plants can generally be used in two different forms: mixtures contain constituents such as essential oils or extracts, infusions, and tinctures (alcoholic extract of plant or animal material). Pure compounds (or active principles) are generally used when a specific component from a medicinal plant has strong effects or definite activities. In a pure form, it can be used in therapeutic application in a precise dose.

A phytomedicine, or phytopharmaceutical, is a complex mixture derived from plant sources that is used as a medicine or drug. The phytopharmaceutical preparations of plants and their products were previously widely used in all countries with a strong tradition of herbal medicine. However, the development of phytopharmaceutical products, which might partially substitute some of the conventional medications demanding, imported raw materials, and which could be produced by pharmaceutical industries (Grover and Patni, 2013). The increase in the importance of plants as sources for new drugs reflects the necessity of phytochemical studies. Plants may contain a very large number of metabolites. Further studies need to be undertaken to screen and isolate the bioactive compounds, evaluate the bioactive potential and phytochemically characterize them.

1.12 Plant extraction

1.12.1 Plant analysis

Many steps are followed in the phytochemical analysis of plants or plant products:

- Collection and identification of the plant, followed by separation and drying of the plant material.
- Extraction, preparation and chromatographic analysis by TLC and ^1H NMR.
- Bioassay screening of crude or pure crude extracts.
- Chromatographic separation, with several successive steps to be followed to separate plant compounds.
- Identification of the isolated compounds, then structural evaluation by phytochemical methods (Hamburger and Hostettmann, 1991).
- Testing for bioactivity and screening tests for compound toxicology using various animal and human cell lines.

Plants are commonly used for the management of T2-DM in folk medicine in many countries, and in India in particular, the anti-hyperglycaemic property of many plants such as *Cassia kleinii* leaves was revealed (Babu *et al.*, 2003).

Many studies have shown that the free radicals are involved in the patho-physiology of several diseases such as T2-DM, cancer and cardiovascular diseases (Weisburger, 2002; Ramkumar *et al.*, 2007). Antioxidant compounds found in plants were able to deactivate these free radicals, therefore showing an interesting action in the prevention of these chronic diseases (Urquiaga and Leighton, 2000; Niki *et al.*, 2005). In addition, the roles of these free radicals are essentially determined by their structures (Bravo, 1998). For example, phytochemicals, such as phenolic compounds, have antioxidative, and antidiabetic actions, in addition to other actions (Arts and Hollman, 2005; Scalbert *et al.*, 2005).

1.12.2 Methods of extraction and isolation

Homogenisation (powdering or comminution) is used when plant cells or tissues require to be disrupted so that they release their chemical contents. This can be done using pestle and mortar under liquid nitrogen, or they can be dried first at normal temperature and then the dry tissues are crushed using a pestle and mortar.

After homogenisation, the plant tissues are extracted with a solvent. The solvent is chosen to improve the extraction of the intended phytochemical as both phytochemicals and solvents differ in their polarity. Three different polarity indexes are commonly used: a polar solvent, methanol; a medium-polar solvent, ethyl acetate, chloroform, acetone and dichloromethane, and; non-polar solvents, hexane, toluene and petroleum.

Two common methods of extraction are maceration and hydro-distillation using steam and Soxhlet extraction. In chemistry, maceration is defined as the preparation of an extract by solvent extraction where the plant material is soaked in the solvent extraction. Maceration of *A. cominia* is carried out with the aim of reducing levels of impurity of the plant material. With maceration, the dried plant tissues are immersed solvent in a closed container and left at normal temperatures. Then the solvent is decanted and filtered to remove debris. Otherwise, in the hydro distillation method or Soxhlet extraction, the liquid or vapour mixture of two or more substances is separated into its component fractions of required purity by the application and the removal of heat. Using a distillation method, the plants are exposed to high temperature and moisture; then the resulting vapour mixture is cooled in order to separate compounds carried in the oil and water phases.

1.12.3 Methods of separation

Advances in screening and separation skills are currently employed to analyse bioactivity with greater effectiveness and exactness. Recently a method of direct screening of natural product extracts using mass spectrometry that does not require any sample preparation or fractionation work was reported. Hundreds of crude extracts can be screened for their biological activities. Direct bioaffinity screening

mass spectrometry method followed by the use of ligand mass information for mass-directed purification makes the screening of crude extracts and identification of active compounds very efficient (Vu *et al.*, 2008). Bioaffinity mass spectrometry is a novel technology for analysis of binding proteins and their ligands.

The separation and purification of compounds in a plant extract maybe performed using one or more combined chromatographic techniques:

- Paper chromatography (PC)
- Thin layer chromatography (TLC)
- High performance liquid chromatography (HPLC)
- Column chromatography (CC)
- Gas liquid chromatography (GLC)
- Electrophoresis

All these chromatographic techniques aim to separate compounds based on their size, shape or charge and their ability to interact with a surface or stationary phase (Heftmann, 1992). They have been used to separate different macro and micro-molecules. The separation is based on the interactions between the analyte and two phases (mobile phase: MP, and stationary phase: SP) (Miller, 2004). Separation of the sample is based on the polarity of components and their partitioning between the adsorbent and the mobile phases (Salituro and Dufresne, 1998).

The choice of technique depends generally on the solubility properties and the volatilities of the compounds to be separated (Table 1.3).

The SP is either liquid or solid while the MP is mainly liquid. The relative retardation of the analytes in the SP is determined by their physical and chemical properties in that once in the MP. Selectivity is therefore achieved by varying either the MP or SP or both. The significant progress of the chromatography is mainly due first, to the ability of LC to analyse practically all pharmaceutical samples adequately and second, to the rapid development in column technology (Belanger *et al.*, 1997).

Chromatographic technique	Compounds
TLC	Lipid soluble components, such as lipids, steroids, carotenoids, simple components and chlorophylls.
GLC	Volatile compounds, derivatised fatty acids, mono and sesquiterpenes, hydrocarbons, and sulphur compounds.
HPLC and LC	Less volatile compounds

Table 1.3 Methods of separation and their specific compounds.

Chromatographic analysis involves the introduction, separation, and detection of analytes in mixtures. The separation of sample components in a mixture is based on the different physicochemical and chemical interactions between the sample components and the SP and MP. The differences in these interactions for various analytes result in their separation on the chromatographic column (Braithwaite *et al.*, 1990).

Separation in HPLC is achieved by the chemical interactions of the SP and the sample with the MP, which determines the degree of migration and separation of the components contained in the sample. For example, samples which have stronger interactions with the SP than with the MP elute from the column less quickly and thus have a longer retention time, while those samples which have stronger interactions with the MP than with the SP elute from the column faster and thus have a shorter retention time. The mechanism of separation depends on the MP composition and the type of SP. The mechanism of retention involved depends on whether the type of SP is liquid-solid adsorption, liquid-liquid partition, size exclusion, ion exchange, and affinity.

In adsorption chromatography, the interaction between the analyte and the SP operates on the basis of polarity. Compounds that possess functional groups capable of strong hydrogen bonding will adhere more tightly to the SP than less polar compounds. Thus, less polar compounds elute from the column faster than

compounds that are highly polar. SP is column packing of silica gel or alumina and the MP solvents are chosen according to their strength of adsorption (ϵ_0) with respect to alumina or silica, as the measure of polarity.

In size exclusion chromatography, compounds are separated on the basis of their molecular size. The SP consists of porous beads. The larger compounds are excluded from the interior of the bead and are eluted first. The smaller compounds enter the beads and elute according to their ability to exit from the same sized pores into which they were internalised. The column can be either silica or non-silica based.

Ion-exchange operates on the basis of the selective exchange of ions in the sample with counterions in the SP. IE is performed with columns containing charge-bearing functional groups attached to a polymer matrix. The functional ions with counterions are permanently bonded to the SP. The sample is retained by replacing the counterions of the stationary phase with its own ions.

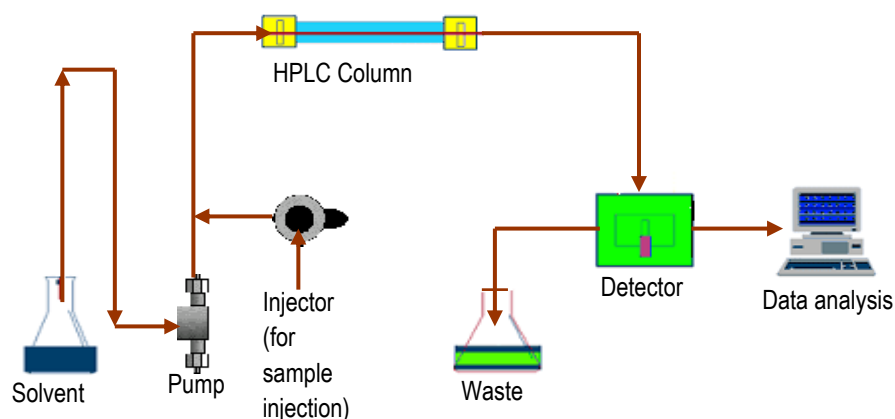


Figure 1.13 Schematic representation of an HPLC.

Finally, reversed-phased HPLC is the most commonly used form of HPLC. It is performed with a column same size as the other techniques, but the silica is modified to make it non-polar by attaching long hydrocarbon chains to its. A polar solvent is usually used. Where a strong attraction between the polar solvent and polar molecules in the mixture being passed through the column. There won't be as much attraction between the hydrocarbon chains attached to the silica (SP) and the polar molecules in the solution (MP). Non-polar compounds in the mixture will tend to

form attractions with the hydrocarbon groups because of van der Waals dispersion forces.

Affinity operates by using immobilised biochemicals that have a specific affinity with the compound of interest. Separation occurs as the MP and sample pass over the SP. The sample compound or compounds of interest are retained as the rest of the impurities and MP pass through. The compounds are then eluted by changing the MP conditions approximately.

There are many types of detector that can be used with LC, depending on the type of compounds present. The most common ones include Refractive Index (RI), Ultra-Violet (UV), Fluorescent, Radiochemical, Electrochemical, Near-Infra Red (Near-IR), Mass spectrometry (MS), Nuclear Magnetic Resonance (NMR), and Light Scattering (LS).

The value of the MS is that it requires only microgram amounts of material that can provide an accurate molecular weight; it may yield a complex fragmentation pattern which is often characteristic of that particular compound and may identify it (Harborne, 2006). In general, MS consists of degradation trace amounts of an organic compound and records the fragmentation pattern according to the mass.

1.12.4 Methods of identification

To identify a plant constituent after isolation and purification, it is important to know the class or combined different classes of the specific compound. The class of the compound can be revealed by its response to colour tests (e.g. Dragendorff's for alkaloids), its solubility, its R_F and its UV spectral characteristics. A known plant compound can generally be identified by using authentic plant examples. Otherwise, when the compound is new, it is preferable to confirm it through chemical degradation (Harborne, 2006).

The UV values and visible spectra in identifying unknown compound using mass spectrometry (which should have a chromophore or conjugated double bonds), are related with the complexity of the spectrum and to the position of the highest

wavelength. For example, if the compound shows a single peak between 250 and 260 nm, it may be one of a considerable number of substances, however if there are three different peaks in between 400 and 500 nm, it could be α -carotenoid.

Mass spectrometry is also employed to determine the molecular weight of compounds, to identify an atom existing in a molecule, and to elucidate the chemical structures of these chemical molecules (Heinrich *et al.*, 2004). It can be used to determine elemental composition of a compound. Its action comprises ionisation of chemical compounds for the generation of charged molecules or fragments of molecules and the measurement of the mass-to-charge ratios of these. Fragmentation patterns which can be seen in mass spectra demonstrate the ionized compound by electron impact ionization.

Liquid chromatography–mass spectrometry (LC-MS) is a sensitive and selective technique employed for a number of applications, particularly for the general detection and potential identification of compounds, even in a complex mixture. Preparative LC-MS system can be employed for the rapid and mass-directed purification of natural-product extracts (Lee and Kerns, 1999).

1.12.5 Nuclear magnetic resonance spectroscopy (NMR)

NMR is a non-destructive technique considered to be a robust and reliable method for the elucidation of compound structures. It is employed to describe the type and number of atoms existing in a compound, and their effect on each other (chemical environments). Radiation in the radio-frequency is used in NMR to excite nuclei. The most commonly detected atoms are hydrogen (^1H) and Carbon (^{13}C), as well as other atoms (^{15}N) according to their quantity and level of purity. Information about measured parameters such as chemical shifts (expressed as delta δ scale or parts per million ppm) are also included in ^1H and ^{13}C spectral data, showing the resonance position of the nuclei in the spectrum, the integral which is peak area of an approximate number of atoms in the signal, Coupling constant J (expressed in hertz Hz), which defines the values of multiplets (m) which in turn give information about the number of other nuclei coupled to the atom. Currently, one-dimensional NMR

methods (^1H and ^{13}C) are still used, but two-dimensional NMR techniques are also used, as these are known to obtain a better identification of molecule structures, including COSY (Correlation Spectroscopy), used to obtain the splitting patterns for a specific proton and to interpret it to discover the number of protons located on the adjacent carbons, with the aim of clarifying ^1H - ^1H connectivity. The hydrogen is plotted on two axes resulting in a cross peaks placed around the diagonal of the square graph. NOESY (Nuclear Overhauser Effect Spectroscopy) is similar to COSY, with diagonal peaks and cross peaks related to resonances from nuclei that are spatially close rather than are through-bond coupled to each other. HMBC and HSQC (Heteronuclear Multiple/Selective Single Quantum Coherence/Correlation) detect heteronuclear correlations over longer ranges of around 2–4 bonds (Williams and Flemming, 1995; Heinrich *et al.*, 2004).

1.12.6 Analysis of results

Two different types of analysis of results are normally carried out: qualitative and quantitative.

- *Qualitative analysis*: much plant analysis is dedicated to the isolation and identification of secondary constituents in a particular compounds or a number of compounds in the belief that some of the species may be novel or unusual structures. Another intention of the phytochemical analysis is the characterisation of an active compound responsible for some toxic or beneficial effect shown by a crude plant extract when tested against cell lines.
- *Quantitative analysis*: this is a method of determining the quantities of substances in a sample (e.g. amount of active substance in plant extract).

1.13 Aims and Objectives

The essential aim of this study was to assess the anti-diabetic activities of compounds extracted from the Cuban *Allophylus cominia* (*A. cominia*) and identify their mechanism of action (Fig 1.14). The specific objectives are to:

- Establish a reliable *in vitro* method for screening possible anti-diabetic activities, covering effects on insulin action and effects on other hypoglycaemic signalling pathways.
- Establish biochemical assays such as PTP1B, DPPIV, α -glucosidase and α -amylase using samples of extracts or compounds from *A. cominia* that might have positive results and then follow up with concentration-effect curves and study the kinetics of their mechanisms of action.
- Use HepG2, L6 myoblasts and differentiated 3T3-L1 cells to perform a fluorescent assay to monitor the stimulation of glucose uptake by using 2-(N-(7-nitrobenz-2-oxa-1,3-diazol-4-yl) (2-NBDG), which is a fluorescent D-glucose analogue.
- Study the effect of the extracts from *A. cominia* on adipogenesis following different stages of the differentiation process of 3T3-L1 cells.
- Show the effect of extracts from *A. cominia* on lipid metabolism using differentiated 3T3-L1 adipocytes.
- Demonstrate the effect of active compounds on GLUT4 transporters.
- Using phytochemical techniques, isolate active compounds from the plant extracts, then identify those compounds using different chromatographic methods such as column chromatography, preparative TLC and HPLC.
- Assay plant extracts using screening tests in order to establish their effect on DPPIV activity and the action of the insulin-like hormone, PTP1B, as well as their activity on the glucose uptake assay using 2-NBDG glucose analogue fluorescent and 2-deoxy-D-glucose.

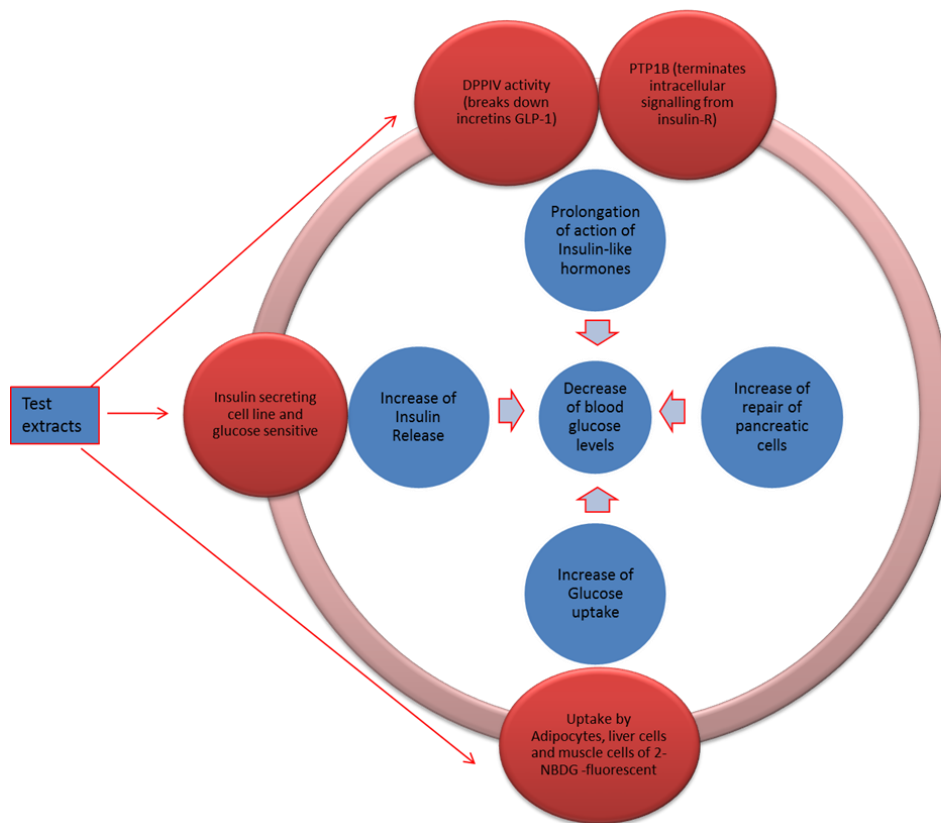


Figure 1.14 Various possible extract tests for T2-DM.

Chapter 2

2 Phytochemical separation and identification of compounds from *Allophylus cominia*

2.1 Introduction

This chapter outlines the characterisation of metabolites isolated from the leaves of *A. cominia*. Phytochemical techniques (UV, IR, NMR, MS and HPLC) and comparison of the spectrum with literature data were used to confirm the structures of the isolated compounds. These techniques are described in Chapter 1, section 1.8. The spectra of the isolated compounds are included in the appendices at the end of the thesis.

Several studies have reported the hypo-glycaemic activity of *A. cominia* aqueous extracts in normoglycaemic and type 1 diabetic animal models (Melchor *et al.*, 1999; Valls *et al.*, 2000; Veliz, 2001). This plant showed anti-diabetic actions after a decrease in the urine glucose levels immediately after its use was discovered. Its branches, leaves and roots have been used, and extracts of the leaves of *A. cominia* have shown an effect on the peripheral uptake of glucose, specifically in muscular tissue. The active metabolites in this plant extract appear to act by an insulin-mimetic type mechanism, facilitating the peripheral uptake of glucose by muscle cells (Veliz *et al.*, 2003; Marrero, 2007).

The preliminary phytochemical studies of the aqueous extract of leaves from *A. cominia* revealed the presence of tannins, free amines, phenols, triterpenes and steroids. In addition, carbohydrates such as arabinose, xylose, galactose, glucose and fatty acids (lauric, myristic, palmitic, stearic and arachidonic) have been identified (Veliz *et al.*, 2005). Phytochemical separation of the plant constituent was carried out using flash chromatography by Dr. Eva Marrero and Dr. Janet Sanchez. However, they did not identify the active compounds. Hence, the aim of this study was to use a number of phytochemical techniques to separate and identify the active compounds (Marrero, 2007).

2.2 Materials and Methods

2.2.1 Solvents, reagents and chemicals

The following solvents were used: acetonitrile, n-pentane, n-hexane, ethyl acetate, and methanol. All were purchased from Fisher Scientific UK or VWR UK, and were either of HPLC or analytical grade. Chloroform, DMSO-d₆, acetone-d₆ (Deuterated 99.9%) and Shigemi NMR tubes were purchased from Sigma-Aldrich, UK Ltd. Acetonitrile and HPLC water were purchased from Fisher Scientific, UK

The following reagents were used: *p*-anisaldehyde, vanillin, and sulphuric acid, all purchased from Fisher Scientific UK.

Other materials used included: TLC grade silica gel coated aluminium sheet (Merck, Germany Pre-coated Silica gel PF₂₅₄), TLC grade silica gel (Merck, Germany), column grade silica gel (Silica gel 60, mesh size 20-200 µm. Merck, Germany), and HPLC vials (purchased from Thermo Scientific, UK).

The equipment used included freeze dryer Epsilon 2-4 LSC, Christ®, SCIQUIP.

2.2.2 Plant material

The plant material used [leaves of *Allophylus cominia* (L.) Sw. (Sapindaceae), *A. cominia*] was collected from San José de Las Lajas, Mayabeque, Cuba in February 2008 by Dr Eva Marrero. Plants were authenticated by Prof. Fernando Franco Flores, in the Laboratory of Botany at the Agriculture University of Havana, Cuba. A voucher specimen of the plant was kept for reference (HFA-1769) in the Herbarium of the institute (CENSA). Fresh leaves of *A. cominia* were dried in an oven at 37°C for 96 h. The dry leaves were milled to fine particles.

Two different extraction methods were carried out: maceration with n-hexane, ethyl acetate and then methanol. Then the residue of the plant material (from the maceration) was used for hot extraction by Soxhlet using the same solvents.

2.2.3 Maceration

The plant material (582.0 g) was extracted using three litres of n-hexane, ethyl acetate and methanol. Plant material was left in each solvent for three days.

After each extraction, the solvent was filtrated through Whatman™ filter paper and filtrates were evaporated at 40°C under vacuum using a rotary evaporator (Büchi Rotavapour) until all solvents were removed. Then the extracts were transferred into small vials using small amounts of the same solvent used for extraction and left under a fume hood at room temperature to obtain solvent-free extracts. TLC and NMR spectroscopies of the three different crude extracts were carried out.

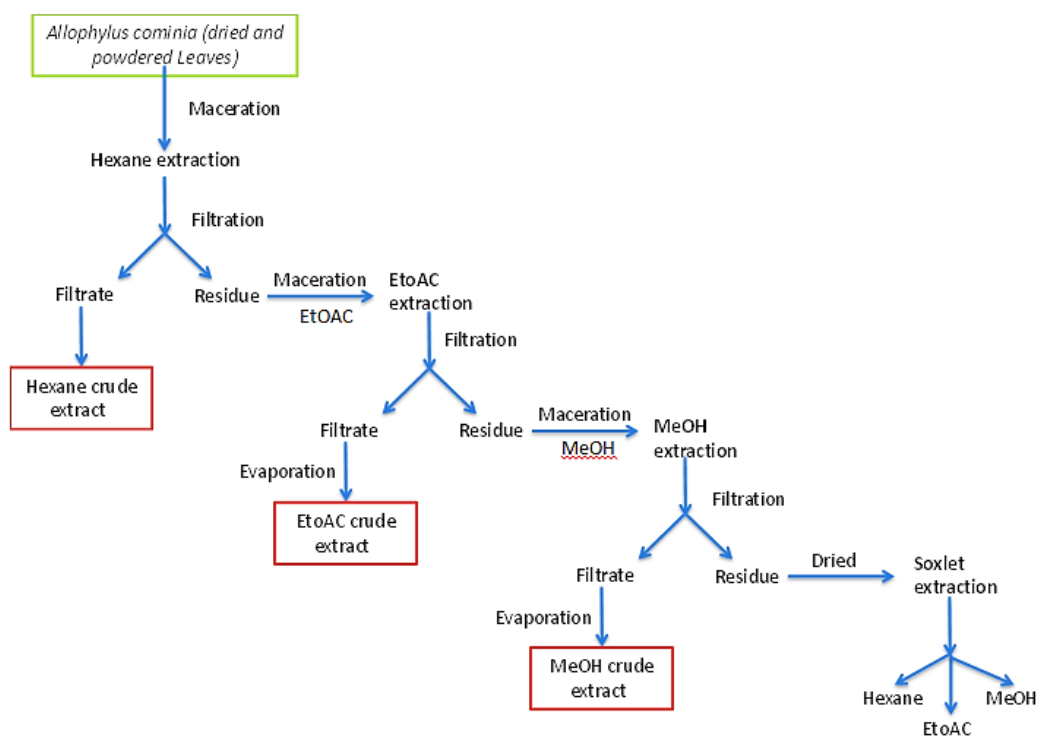


Figure 2.1 Extraction scheme for the leaves of *Allophylus cominia*

2.2.4 Chromatographic techniques

A. Thin layer chromatography (TLC)

This method was used for a rapid, initial screening of the crude extracts. The crude extracts were dissolved in a specific solvent, depending on the polarity of the extracts. Chloroform was used for most of the non-polar samples. Then, with a capillary tube, the samples were spotted directly above 1 cm of the end of a TLC plate. TLC plates were immersed in suitable solvent systems in a TLC tank (a piece of filter paper was added to the TLC tank to saturate the environment with the solvent before immersing the TLC plate). The plate was left to develop for 2-4 min. The solvent system was a 50/50 (v/v) of n-hexane and ethyl acetate. Finally the TLC plate was taken out of the tank and detected under UV or by reagent.

- Detection by UV light: the developed TLC plates were observed under UV light using a short wavelength $\lambda = 254$ nm and another long wavelength $\lambda = 366$ nm. Short UV is useful to detect aromatic compounds, while compounds with conjugated double bonds are visible under long UV light.
- Detection by anisaldehyde-sulphuric acid spray reagent (prepared by adding 0.5 ml of *p*-anisaldehyde to 10 ml of glacial acetic acid and 85 ml of methanol. Then 5 ml of sulphuric acid was added to the mixture).

The dried TLC plates were sprayed with this reagent then heated with a hot air gun for one minute.

In this study, after comparing the samples by TLC, the crude extracts from the maceration of *A. cominia* with hexane and ethyl acetate were observed to have the same components. NMR was carried out to confirm this, and then hexane and ethyl acetate extracts were combined for further separation by silica gel column.

B. Vacuum liquid chromatography (VLC)

This was used for the rapid fractionation of the crude *A. cominia* extracts. The column was prepared in a sintered glass funnel by packing it with a TLC grade silica gel, under vacuum. TLC silica gel particle size was less than 45µm. The sample to be fractionated (powder) was uniformly loaded onto the top of the VLC column. Gradient elution was used and the column was allowed to run dry after each fraction's elution.

In this study, only the methanolic extract from maceration was fractionated. The crude extract was completely dissolved in a minimal solvent (methanol). Soluble extract was absorbed onto silica gel for column chromatography and left under the hood to dry. It was ground into fine powder ready to be used for VLC separation.

At each addition, the silica gel was compressed to a hard layer using a glass stopper and a filter paper was placed at the top of the silica gel layer. 80% hexane and 20% ethyl acetate was used to wet the silica gel and to ensure the uniformity of the packed silica gel.

An elution technique was used (Table 2.1). The column was eluted first using 100% hexane. And then the polarity of the solvent was increased gradually with 5 to 10% ethyl acetate. When 100% ethyl acetate has been eluted, the polarity was increased again by 5-10% methanol until 50% of the methanol was eluted. The column was allowed to dry in between elution to ensure that all the solvent containing extracts was collected. The collection was carried out in round-bottomed flasks and the eluates were dried using the rotary evaporator. Methanol crude extract was separated into sub-fractions A to O. Then chromatographic features were determined by TLC by using the appropriate solvent system. Elutes with similar components were combined (Fig 2.2). NMR was carried out for the determination of the different components and only fractions D, and combined fractions KLMN were subjected to further purification and structure elucidation.

Fraction Name	Hexane %	Ethyl acetate %	Methanol %	Cycles
AC-MeOH-A	80%	20%	–	2
AC-MeOH-B	70%	30%	–	2
AC-MeOH-C	60%	40%	–	2
AC-MeOH-D	50%	50%	–	3
AC-MeOH-E	40%	60%	–	3
AC-MeOH-F	30%	70%	–	3
AC-MeOH-G	20%	80%	–	2
AC-MeOH-H	10%	90%	–	2
AC-MeOH-I	–	100%	–	2
AC-MeOH-J	–	90%	10%	2
AC-MeOH-K	–	70%	30%	3
AC-MeOH-L	–	60%	40%	3
AC-MeOH-M	–	50%	50%	3
AC-MeOH-N	–	40%	60%	3

Table 2.1 A step gradient elution technique used for separation of the methanol crude extract of the maceration extraction.

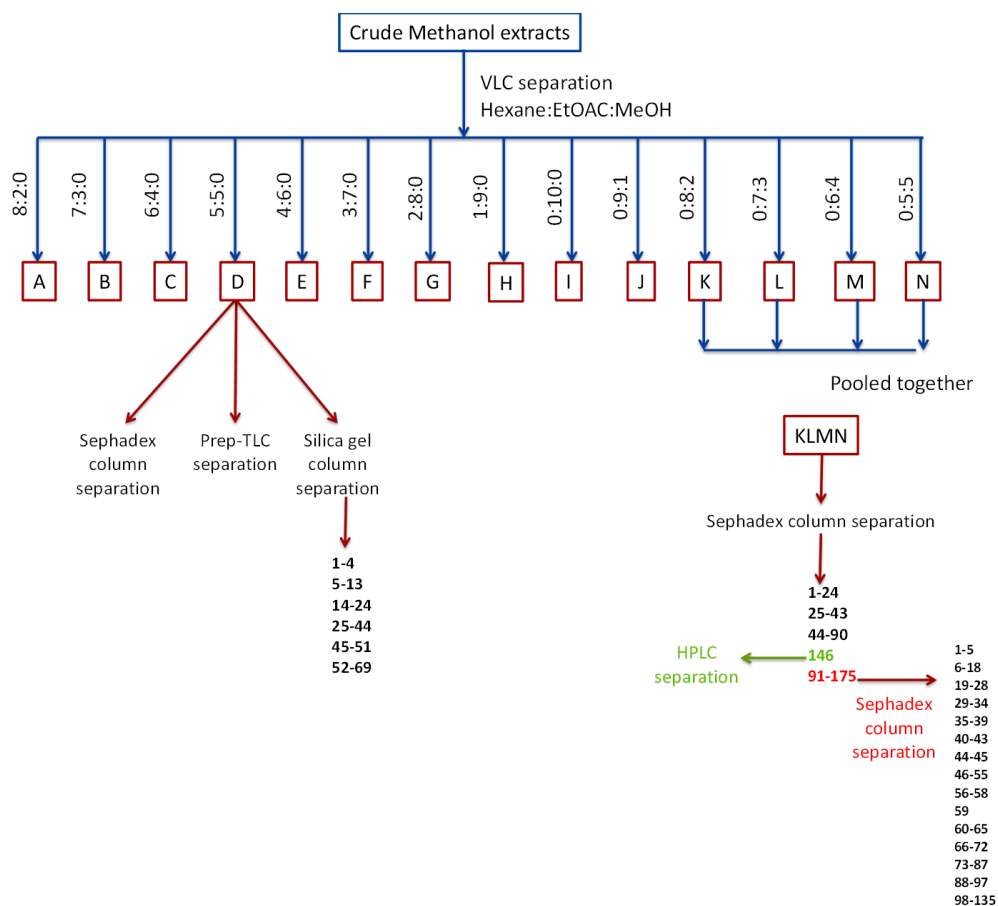


Figure 2.2 Fractionation scheme for the crude methanol extract of *Allophylus cominia* obtained from maceration.

E. Sephadex column chromatography

The dried fraction KLMN (from VLC) was dissolved in methanol.

Column preparation: two thirds of the column was filled with Sephadex LH-20 (from Merck, Germany) dissolved in methanol. The KLMN fraction was then added slowly to the top of the Sephadex using a pipette. Once the crude extract was absorbed by the Sephadex, MeOH was added, and fractions were collected in vials (5 ml in each) and dried under a fume hood at room temperature.

TLC was carried out using 60:40 (v/v) EtOAc:methanol as solvent for the collected fractions. Then after anisaldehyde-sulphuric acid spraying, samples having similar bands were pooled as shown in Fig 2.2. And then NMR was carried out for all the fractions. Only samples collected in vials 91 to 175 showed a mixture of flavonoids. The other fractions were only pigments, fatty acids and tannins.

Further chromatographic separation and structure elucidation for the components of sample AC-MC-KLMN-91-175 was carried out.

F. Silica gel column chromatography

To determine and identify compounds from *A. cominia*, hexane and ethyl acetate extracts which were comparable after TLC were combined (HEC). Then column chromatography separation of HEC extracts from *A. cominia* was carried out. HEC crude extracts were subjected to TLC and compared under UV to review any similarities. Combined together (Fig 2.3), the extracts were dissolved in ethyl acetate with some silica gel to allow the adsorption of the extracts, and then dried under the hood at room temperature.

Column preparation: two thirds of the column was filled with silica gel mixed with n-hexane. The crude HEC extract was added on top of the column. 10:90 (v/v) of ethyl acetate:n-hexane was used at the start of the elution. Depending on the polarity requirements; this solvent elution was changed by increasing the polarity until reaching a solvent system of 10:90 (v/v) ethyl acetate:methanol.

Fractions 1 to 53 were collected and dried in small vials (25ml in each). TLC and NMR were carried out for the fractions, and similar fractions were combined as shown in Fig 2.3. Further chromatographic separation and structure elucidation for the components were carried out.

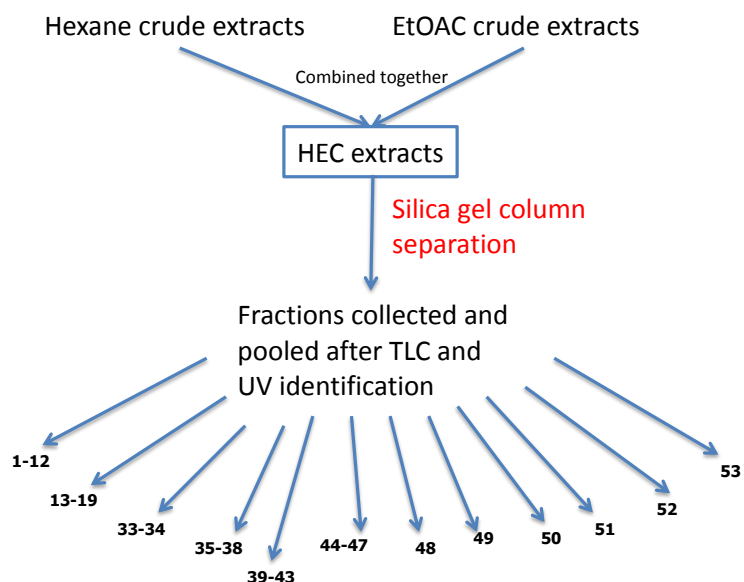


Figure 2.3 Fractionation scheme for the crude hexane and ethyl acetate extracts of *Allophylus cominia* from maceration.

G. Preparative thin layer chromatography (prep-TLC)

This separation method was used for final purification of different compounds. The same procedure as the normal TLC plate was followed but on larger scale. A large developing tank and 20x20 cm TLC plates were used. A solvent system which would adequately separate our compounds and develop the plate was selected.

For coating the plates (glass square plates 20x20 cm), the silica gel was prepared (silica gel 60 PF₂₅₄ for preparative layer chromatography) as 20 g of silica mixed with 40 ml of cooled distilled water, and then mixed well. After stabilising the clean and clear plates on the TLC plate maker, the silica gel was spread over the dried plates keeping the same thickness (0.5 mm). The plates were left to dry in the oven (at 70°C) over 12 to 24 hours.

The dried VLC fraction D, MeOH-D, was dissolved in chloroform (10 mg/ml), then streaked 2.5 cm from the bottom of the prep-TLC plates. The plate was placed in 20:80 (v/v) EtOAc: hexane until developed. The plate was then removed from the tank and left to dry. Different bands were scraped into a clean filter paper. Each band was soaked with different solvents: hexane, EtOAc and MeOH successively then filtered through Whatman™ filter paper. Left under the hood, the solvents were dried

off and the separated fractions were analysed by TLC and then characterized by ^1H NMR.

2.2.5 Structural elucidation

For the structural elucidation of compounds in different *A. cominia* fractions, ultraviolet-visible absorption, nuclear magnetic resonance (NMR) spectroscopy, mass spectrometry (MS) and LC-MS were carried out.

In this study, the majority of these techniques were used to elucidate the structure of the compounds isolated from *A. cominia*.

2.2.6 Nuclear magnetic resonance spectroscopy (NMR)

The first structural characterisation of the isolated compounds was carried out by using ^1H NMR spectroscopy. The spectrophotometer used was JEOL (JNM LA400) 400MHz. The samples were dissolved in chloroform CDCl_3 or DMSO- d_6 and transferred into Shigemi NMR tubes.

2.2.7 Mass spectrometry (MS)

MS is an analytical technique frequently used to determine the molecular weight of a charged species. High (and low) resolution electron impact mass spectra were recorded on a JEOL 505HA spectrometer using direct probe at elevated temperature (110-160°C) at 70 eV. Negative ion mode ESI experiments was performed on a ThermoFinnigan LCQ-Decaiontrap or Orbitrap HRESI mass spectrometer (mass analyser set up at 100,000 ppm, externally calibrated at 3 ppm). According to the polarity, samples were dissolved in water (HPLC grade) at a concentration of 1 mg/mL. Sample solution (20 μl) was injected along with acetonitrile: water in a gradient elution. The method followed was shown in Table 2.2. The flow rate was 1 ml/min. Solvents used for mobile phase were acetonitrile and HPLC water. MS data acquisition was carried out by Dr. Tong Zhang.

Time (minute)	A: HPLC water	B: Acetonitrile
0-29	5%	95%
30-31	80%	20%
31-45	5%	95%

Table 2.2 The gradient method followed in the mass spectrometry.

2.2.8 Liquid chromatography-Mass spectrometry (LC-MS)

Samples were dissolved in HPLC-grade water at a concentration of 1 mg/ml in HPLC vials. Then the vials were loaded into the Orbitrap. A modified amino column (IBL-SIL 5 NH₂, 240 x 4.60 mm purchased from Phenomenex®) was used. The amino column produces hydrophobic interaction chromatography. 20 µl was injected into the spectrophotometer. The method followed was the same as the one for MS (Table 2.2). The flow rate was 1 ml/min. Solvents used for mobile phase were Acetonitrile and HPLC water. UV detection was set at 245 nm.

2.2.9 High performance liquid chromatography (HPLC)

The same conditions, amino column, flow rate, injection volume and solvents were used as for LC-MS. Concentrations from 0.05 to 1 mg/ml of the plant extract AC-MC-KLMN-91-175 were used. 30:70 (v/v) water:acetonitrile was used. The HPLC was carried out using an HP Hewlett Packard Series 1100 HPLC.

2.2.10 Separation of pheophytins by silica gel column chromatography

Fractions were collected in small vials (5 ml in each) and dried. TLC using 70:30 (v/v) hexane:ethyl acetate as solvent was carried out for all the collected fractions. After spraying with anisaldehyde-sulphuric acid, fractions having similar bands were pooled as in Fig 2.2. NMR was carried out for all the fractions. Fraction 14-24 was pheophytin A and fraction 25-44 was pheophytin B.

2.2.11 Isolation of the flavonoids from fatty acids by Sephadex

Fractions from AC-MC-KLMN-91-175 were collected in vials and dried. TLC was carried out using 60:40 ethyl acetate:methanol as solvent for all the collected fractions. After spraying with anisaldehyde-sulphuric acid, fractions with similar bands were combined, as shown in Fig 2.2. NMR was then carried out with all the fractions. Only fractions 66 to 72 had a mixture of flavonoids free of fatty compounds. The other fractions consisted only of pigments, fatty acids and tannins.

2.2.12 Separation of flavonoids by HPLC

Further separation by HPLC was necessary. AC-MC-KLMN-(91-175)-66-72 fraction of *A. cominia* was dissolved in water at 1 mg/ml in an HPLC vial. Analytical reversed-phase HPLC was carried out with an Agilent 1200 series HPLC system. Samples were injected as 100 µl onto an amino column (IBL-SIL 5 NH₂) using an injector fitted with a 100 µl injection loop. Materials eluting from the column were detected using a programmable detector, set at 280 and 340 nm, equipped with an analogue interface module. 100 µl of the sample was injected into the HPLC and 80:20 (v/v) acetonitrile:water was run isocratically at 1ml/min as a flow rate. Detected peaks were estimated and retention times were recorded. The separation and collection of the compounds was carried out following the retention times. Collection of the fractions was carried out from the waste tube. The retention time of quercitrin was between 7-8 minutes and for the mearnsitrin, it was between 8-9 minutes. These two compounds were the major compounds detected.

Fifty injections were carried out to obtain sufficient quantity for the bio-assays. The collection of the samples was in vials, and MS was carried out to confirm the identity of the compounds in the collected fractions. These samples (1 and 2) were then freeze-dried using Epsilon 2-4 LSC.

2.3 Results

2.3.1 Characterisation of the compounds in *A. cominia*

HEC solid and KLMN (methanol fraction) were identified as a mixture of flavonoids, more than 5 compounds were found (Appendix 1), in addition to fatty acids and tannins. The flavonoids were separated from the fatty acids by Sephadex but remained as a mixture in terms of the similarity in the structures and the molecular weights of the major compounds (quercitrin and mearnsitrin). The two major flavonoids were separated by HPLC using an amino column.

MeOH-D was identified as a mixture of pheophytins A and B with other pigments. Pheophytins were separated and purified using prep-TLC and over silica gel.

2.3.2 Characterisation of HEC solid as a mixture of flavonoids

¹H NMR spectrum of HEC fractions confirmed that only fractions 44-47 showed the presence of a mixture of flavonoids mearnsitrin and quercitrin as major compounds and other minor compounds, which were confirmed by further mass spectrometry. To confirm the structures of the compounds ¹³C NMR spectroscopy, HMBC and HMQC for the mixture were carried out (Appendices 6,7 and 8).

Fraction KLMN was separated by Sephadex and ¹H NMR was carried out for fractions 91 to 175. The same compounds were found in them as in the HEC containing a mixture of flavonoids. Fractions 91 to 175 were combined and the solid collected after evaporation of the solvent was 2.17 g. Further chromatographic analysis, MS, LC-MS and NMR, were used to characterise the compounds. HEC and KLMN fractions were identified by NMR as a mixture of flavonoids. The first compound with molecular formula C₂₂H₂₁O₁₂ was obtained from the [M+H]⁺ peak at

m/z 477 in the LC-MS. The other major compound with molecular formula $C_{21}H_{20}O_{11}$ was also obtained from the $[M+H]^+$ peak at m/z 447 in the LC-MS. Supported by data from 1H NMR (Appendix 5.A) and ^{13}C NMR (Appendix 6), compounds and their chemical structures were identified. TLC analysis of the flavonoids showed a red spot under UV at 254 nm before spraying with anisaldehyde-sulphuric acid reagent and heating (Fig 2.4).

The 1H and ^{13}C NMR (Table 2.3) revealed two sets of signals, with features indicating the presence of two or more flavonoids, where only two were major and easily identified. For the quercitrin, a 1,3,4-Trisubstituted benzene ring with proton signals appearing at around 7.29, 7.25 and 7.24 ppm. For the mearnsitrin a singlet (integrated for two protons) representing a 1,3,4,5-Tetrasubstituted benzene ring at 6.86, 6.85 and 6.81 ppm, implying similar substituents at position 3' and 4'.

Both compounds showed meta coupled protons at around 6.37 and 6.20 ppm from A ring disubstituted B ring of a flavone.

The absence of a proton singlet usually observed for the H-3 of flavones implies that this position is substituted and therefore it could be α -glycoside and this is confirmed by the presence of an anomeric sugar proton for the compounds at 5.15 and 5.25 ppm. The sugar from the proton spectrum was identified to be a rhamnose by the methyl doublet appearing at 0.81 ppm for both compounds as integrated for 6-protons (2 x CH_3 groups).

The 1H NMR signals were attributed by comparison to spectral data presented by Jung *et al.* (1999) for the quercitrin and Mahmoud *et al.* (2001) for mearnsitrin structure indicating that the two flavonoids had a rhamnose moiety attached. The 1H NMR signals (400 MHz, in DMSO- d_6) of the quercitrin (also known as quercetin-3-rhamnoside) attributed to the aglycone δ ppm; 12.6 (1H, brs.C5-OH), 7.24 (2H, d, H-6' and H-2'), 6.86 (1H, d, H-5'), 6.36 (1H, d, H-8) and showed the characteristic pattern of 5-7-dihydroxy-flavone, in addition to 6.20 (1H, d, H-6), 3.16-3.97 (m), 0.81 (3H, d, H-6'') . The 1H NMR spectrum also showed signals at δ 5.20 (1H), 3.97 (1H), 3.49 (1H, d), 3.16 (1H, d) and 3.21 (1H), which related the presence of one rhamnose moiety attached to the compound. ^{13}C NMR (100 MHz, DMSO- d_6) δ ppm; 178.2 (C-4), 157.0 (C-9), 161.9 (C-7), 161.9 (C-5), 157.7 (C-2), 148.9 (C-4'), 145.8 (C-3'), 134.7 (C-3), 121.1 (C-1'), 116.1 (C-2'), 116.0 (C-5'), 121.6 (C-6'),

104.5 (C-10), 99.3 (C-6), 94.1 (C-8), 102.6 (C-1''), 70.88, 70.6, 70.2, 70.2, 70.0 (rhamnoside) and 18.0 (C-6'').

The identification of the mearnsitrin was determined from the chemical shifts and the signals by comparison to Mahmoud *et al.* (2001). Mearnsitrin was also known as mearnsetin 3-O-(4''-O-acetyl)- α -L-¹C₄-rhamnopyranoside. The ¹H NMR (400 MHz, in DMSO-d₆) of the mearnsitrin δ ppm; 6.81 (2H, d, H-6' and H-2'), 6.38 (1H, d, H-8), 6.19 (1H, s, H-6), and 0.81 (3H, d, H-6''). The ¹H NMR spectrum also showed signals which related the presence of one rhamnose moiety attached to the compound. In addition, OCH₃, methoxy group, was identified by the singlet at δ 3.73 ppm. ¹³C NMR (100 MHz, DMSO-d₆) δ ppm; 178.2 (C-4), 156.9 (C-9), 165.1 (C-7), 161.9 (C-5), 157.9 (C-2), 138.3 (C-4'), 151.0 (C-3'), 134.9 (C-3), 124.4 (C-1'), 108.16 (C-2'), 151.0 (C-5'), 108.6 (C-6'), 104.6 (C-10), 99.2 (C-6), 94.1 (C-8), 70.88, 70.6, 70.2, 70.2, 70.0 (rhamnoside) and 18.0 (C-6'').

Position	Appendix 5		Jung <i>et al.</i> , 1999		Appendix 5		Mahmoud <i>et al.</i> , 2001	
	Quercitrin		Quercitrin		Mearnsitrin		Mearnsitrin	
	δ_H	δ_C	δ_H	δ_C	δ_H	δ_C	δ_H	δ_C
1	–	–	–	–	–	–	–	–
2	–	157.7	–	156.4	–	157.9	–	157.28
3	–	134.7	–	134.1	–	134.9	–	134.80
4	–	178.2	–	177.7	–	178.2	–	177.80
5	–	161.9	–	157.2	–	161.9	–	161.30
6	6.20	99.3	6.22 (d)	115.5	6.19	99.2	6.21 (s)	98.75
7	–	161.9	–	161.3	–	165.1	–	164.35
8	6.36	94.1	6.41 (d)	115.0	6.38	94.1	6.38 (d)	93.60
9	–	157.0	–	164.4	–	156.9	–	156.50
10	–	104.5	–	115.6	–	104.6	–	104.18
1'	–	121.1	–	121.1	–	124.9	–	124.80
2'	7.29	116.1	7.29 (d)	120.7	6.81	108.6	6.82 (s)	108.10
3'	–	145.8	–	145.2	–	151.0	–	150.60
4'	–	148.9	–	148.5	–	138.3	–	137.70
5'	6.86	116.0	6.88 (d)	115.7	–	151.0	–	150.60
6'	7.24	121.6	7.29 (d)	115.7	6.81	108.6	6.82 (s)	108.10
1''	5.15	102.6	–	101.0	5.25	102.4	5.12	102.17
2''	3.97	70.88	–	71.2	3.97	70.88	3.97 (dd)	70.03
3''	3.49	71.04	–	70.6	3.49	71.04	3.51	70.31
4''	3.16	71.68	–	70.4	3.16	71.68	3.15	71.13
5''	3.22	70.53	–	70.0	3.22	70.53	3.32	70.53
6''	0.81	18.0	0.82	17.5	0.81	18.0	0.88	17.45
4'-OCH ₃	–	–	–	–	3.73	60.3	–	59.75
5-OH	12.6	–	12.65 (s)	–	12.7	–	12.7	–

Table 2.3 ¹H and ¹³C NMR for quercitrin and mearnsitrin (in DMSO-d₆) including rhamnose moiety by comparison to quercitrin. Jung *et al.*, 1999 and Mahmoud *et al.*, 2001.

This complete assignment using ¹H NMR and ¹³C NMR spectra confirmed the configuration, confirmation and the complete structure of the quercitrin and mearnsitrin. More confirmation of the structures of the quercitrin and meansitrin using the correlation between H-C (HMBC spectrum, Appendix 7) is shown in Table 2.4 below. The hydroxy's did not show any correlation however an expansion of the HMBC spectrum was studied. The chemical structures of quercitrin and mearnsitrin are presented in Fig 2.8. Appendices 5.B to 5.E explain the assignment of the most important peaks to the hydrogens of each compound (mearnsitrin as first major and quercitrin as second) by referring to their chemical shifts. Appendices 5.B, 5.C, 5.D,

and 5.E represent the expansions of the ^1H NMR of the aromatic, sugar, aliphatic and hydroxyl regions respectively.

HMBC correlation (H-C) Quercitrin (2)	HMBC correlation (H-C) Mearnsitrin (1)
H-6/C-5, C-8, C-10	H-6/C-5, C-8, C-10
H-8/C-6, C-10	H-8/C-6, C-9, C-7, C-10
H-2'/C-1', C-2, C-4	H-2'/C-2', C-6', C-3', C-4', C-5', C-2
H-6'/C-2, C-5', C-4'	H-6'/C-2', C-6', C-3', C-4', C-5', C-2
H-5'/C-1', C-3'	–
H-1''/C-3, C-3'', C-5''	H-1''/C-3, C-3'', C-5''
H-6''/C-4'', C-5''	H-6''/C-4'', C-5''
–	5-OH/C-5
–	4'-OCH ₃ /C-4'

Table 2.4. Selected HMBC correlations of quercitrin (2) and mearnsitrin (1).

The composition of this mixture was confirmed by studying the peaks of MS of the AC HEC solid (at a concentration of 1 mg/ml), as shown in Fig 2.4, which allows identification of the molecular weight of the major compounds. Peak at 478 (within 1.54 ppm of the theoretical value) corresponded to the molecular formula of $\text{C}_{22}\text{H}_{22}\text{O}_{12}$ for mearnsitrin, and peak at 448 (within 1.66 ppm) corresponded to the molecular formula of $\text{C}_{21}\text{H}_{20}\text{O}_{11}$ for quercitrin.

The other minor compounds in HEC solid extracts were determined by further LC-MS studies, as shown in Fig 2.5, following the same method used for MS but using an amino column for the separation. Three minor compounds appearing in the LC-MS spectrum, showing a peak at 463.09 (within 2.10 ppm), which corresponded to the molecular formula of $\text{C}_{22}\text{H}_{20}\text{O}_{11}$ for naringenin and two peaks at 461.1692 corresponding to the same molecular formula of $\text{C}_{22}\text{H}_{21}\text{O}_{11}$ for two isomers of flavonol (azalein) and isoflavonol (tectoridin). Further chromatographic studies could be carried out to confirm the chemical structures of these minor compounds.

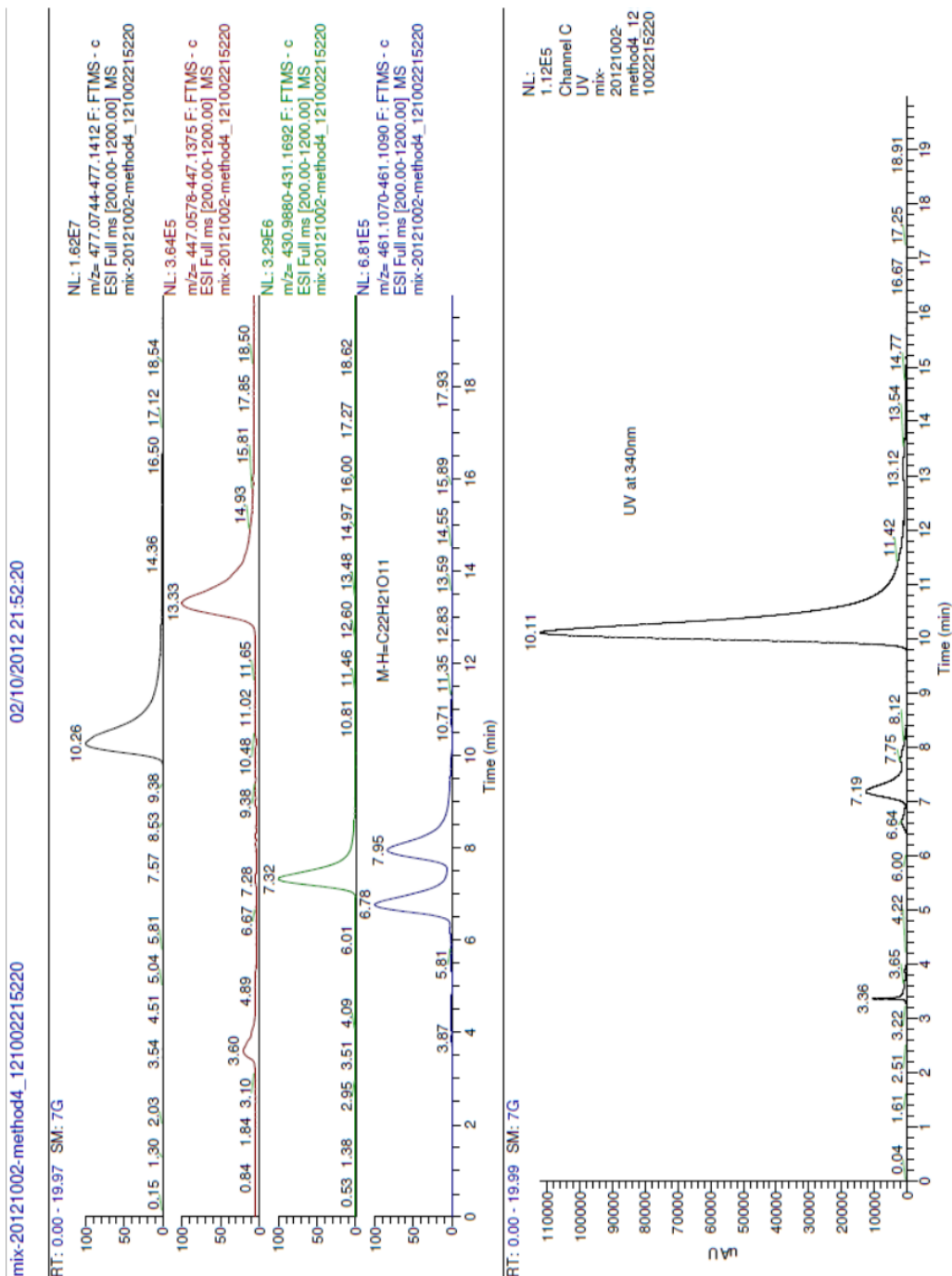


Figure 2.4 Separation of compounds by LC-MS from HEC solid of *A. cominia*. HEC extract from *A. cominia* was dissolved in methanol at 1 mg/ml. Then submitted for LC-MS using Orbitrap. Using 20 μ l injection of the sample, the flow rate was 1 ml/min. Solvents used for mobile phase were acetonitrile and HPLC water. Method followed was gradient. UV detection was set at 340 nm.

C:\Xcalibur\... \20120229\Dima-ACEC 29/02/2012 11:16:25

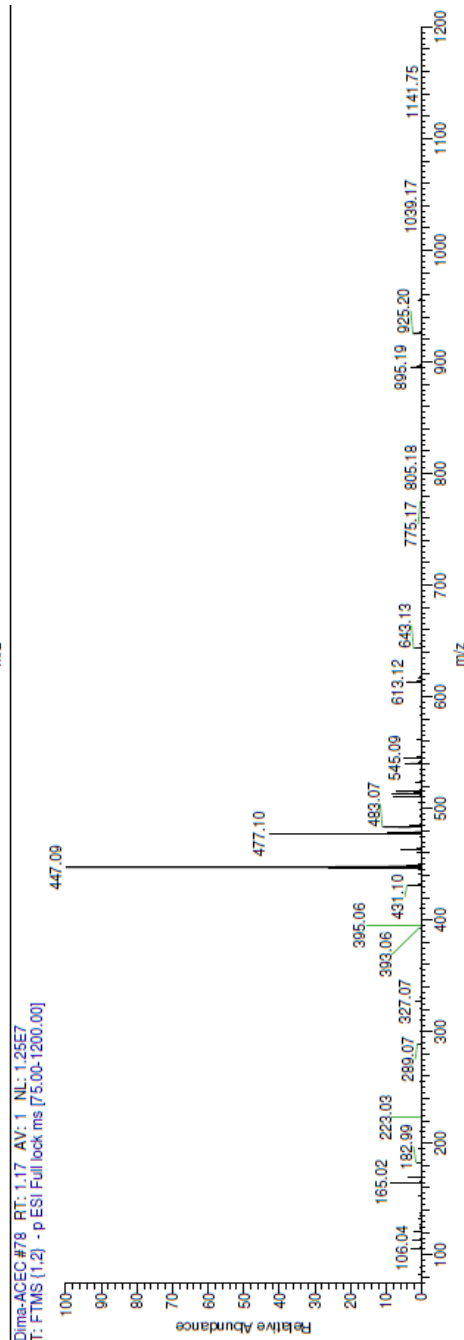
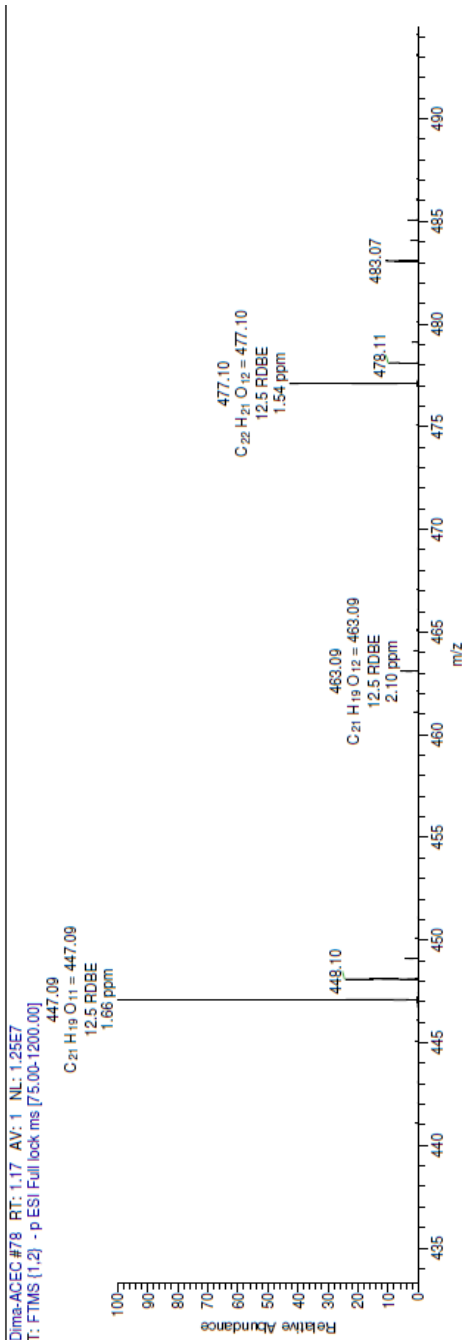


Figure 2.5 Identification of compounds by LC-MS for HEC solid of *A. cominia*. HEC extract from *A. cominia* was dissolved in methanol at 1 mg/ml. Then submitted for LC-MS using Orbitrap. Using 20 μ l injection of the sample, the flow rate was 1 ml/min. Solvents used for mobile phase were acetonitrile and HPLC water. Method followed was gradient. UV detection was set at 245 nm.

For further separation of the flavonoids, prep-TLC was necessary. LC-MS was carried out to study the retention times of the fractions with the aim for a separation by HPLC using the same amino column.

As shown in Fig 2.6, the retention time of the meansitrin was around 10.10 minutes, for quercitrin 7.23 minutes, and for the other flavonol isomers, 6.70 minutes and 7.78 minutes.

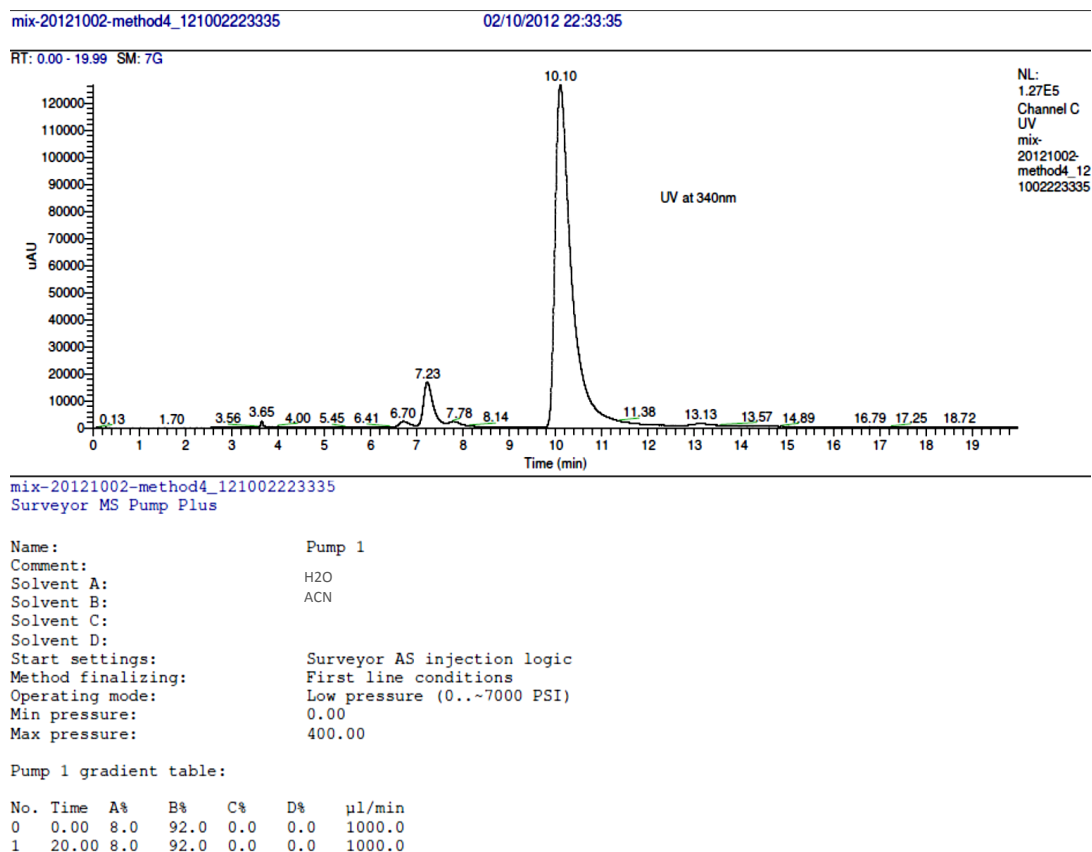


Figure 2.6 LC-MS spectrum of HEC solid of *A. cominia* showing the retention times of different compounds and the method followed for the separation. Solvents used were water and acetonitrile. Flow rate was 1 ml/min. The solvent system used was 08:92 (v/v) A:B. A was water and B was acetonitrile.

For further confirmation of the method and optimisation of the concentration of the extracts, more analytical HPLC studies were carried out, as shown in Fig 2.9, and comparable results were obtained by the same retention time as the LC-MS (Fig 2.6).

There was 2.22 minutes between the peak of quercitrin and the peak of mearnsitrin. There was also time between the peaks of the other two flavonols and the peak of quercitrin, which confirmed that the separation of these compounds using prep-HPLC could be applicable.

Separation by HPLC was carried out, samples were collected at around 7-9 minutes and 10-13 minutes, and MS was carried out to confirm that these samples were quercitrin and mearnsitrin. Further separation using a specific amino column for the HPLC could be carried out.

2.3.2.1 Purification of the flavonoids

The mixture of flavonoids (as shown in Appendix 1) contained fatty compounds which affected the 3T3-L1 cells. The cells were differentiated into the fatty cells even before the differentiation process had initiated, as shown in Fig 2.7. Seven days after cell seeding in a clear 96-well plate, the crude sample containing flavonoids and fatty acids at a concentration of 100 µg/ml was added to the 3T3-L1 pre-adipocytes cells. Twenty-four hours after incubation with the crude sample in DMEM containing 10% FBS, some of the cells were transformed into rounded and fatty cells containing fat droplets. Eight days after differentiation, there was 100% differentiation of the cells compared to the differentiation without the addition of the crude extract of *A. cominia* containing the flavonoids and the fatty compounds. Therefore, the effect of the fraction of *A. cominia* on enhancing the 3T3-L1 differentiation is clearly from the fatty compounds in comparison to the effect of the pure flavonoids from *A. cominia* on the 3T3-L1 differentiation shown in Fig 2.7. For accurate results, the fats had to be separated from the mixture of flavonoids by Sephadex column chromatography.

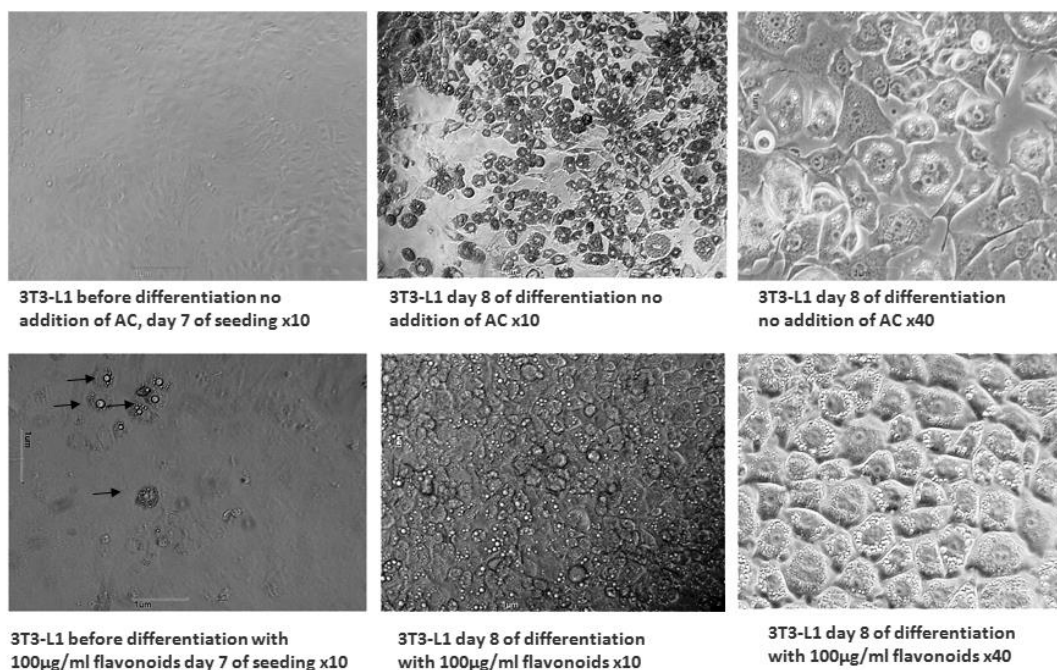
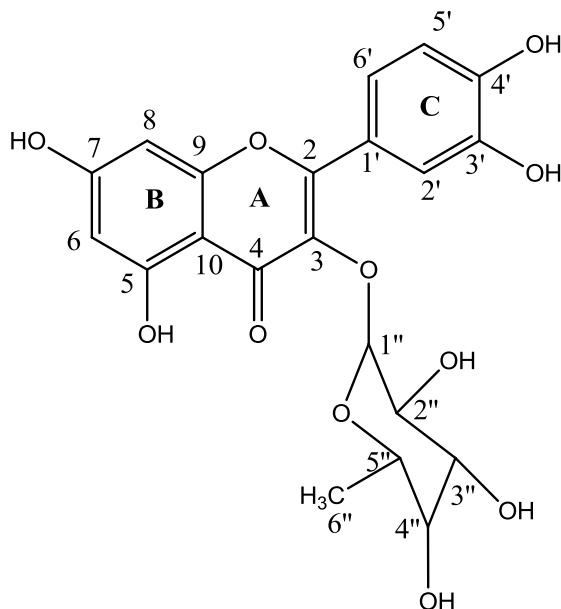


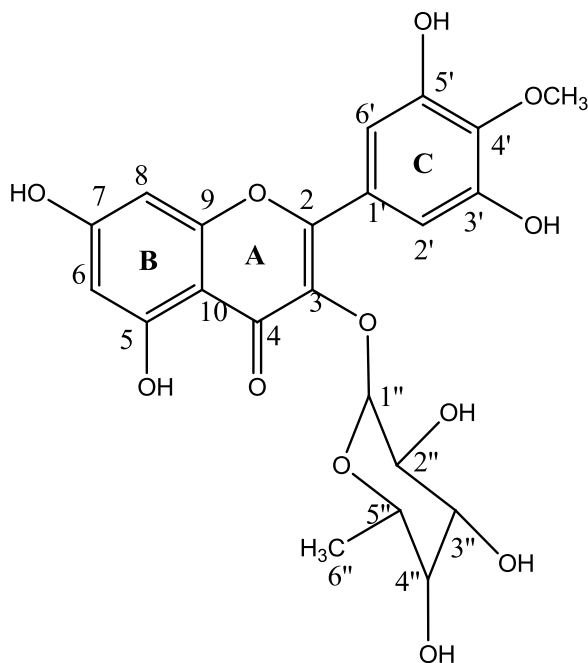
Figure 2.7 Photomicrographs illustrating the effect of crude extracts of AC-MC-KLMN-91-175 (mixture of flavonoids and fats) on the 3T3-L1 differentiation (before and after differentiation process). Arrow (→) shows the 3T3-L1 differentiated cells in the well (96-well plate) before the differentiation process in the presence of flavonoid mixture.

AC-MC-KLMN-91-175 (mixture of flavonoids and fatty acids) was added to 3T3-L1 fibroblasts at 100 µg/ml differentiated some of the cells without the differentiation process being started. As also shown in the Fig 2.7, AC-MC-KLMN-91-175 enhanced the differentiation of 3T3-L1 into adipocytes in comparison to the control, where the cells were differentiated using the same conditions in the absence of AC extracts. The enhancement of the differentiation could be the result of the presence of fat in AC-MC-KLMN-91-175. Therefore, separation of the compounds was carried out.

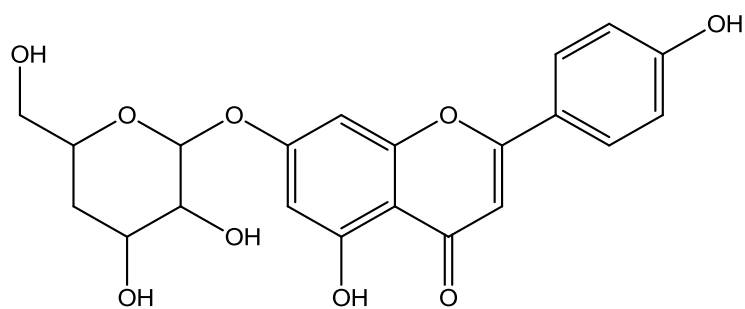
By comparison with prior literature, analysing the NMR spectrum of AC crude extract and by following the mass spectrometry showing the molecular weight and formula of each compound, the structures of mearnsitrin, quercitrin, naringenin and two isomers are shown in Fig 2.8.



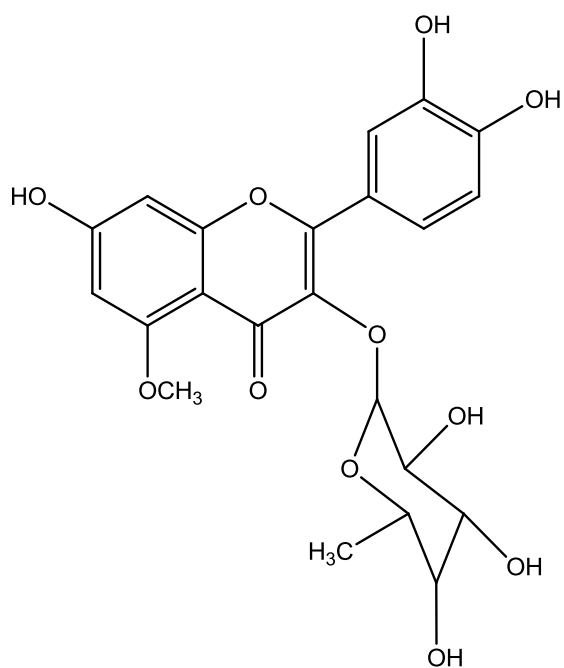
Chemical structure of quercitrin (rhamnoside), Major



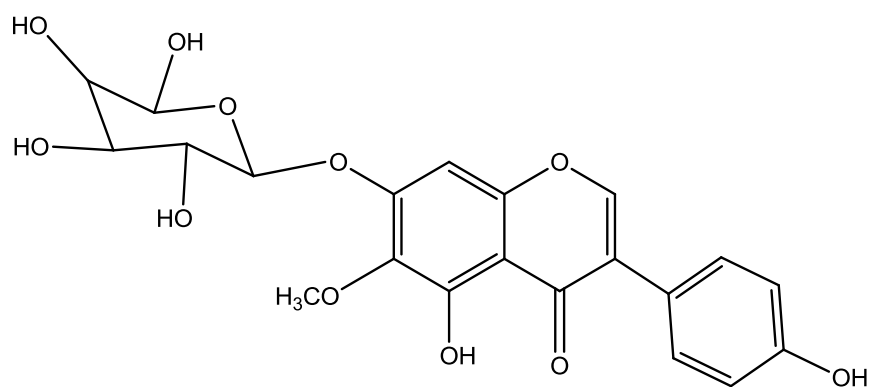
Chemical structure of mearnsitrin (rhamnoside), Major



Chemical structure of naringenin, Minor



Chemical structure of azalein, Minor



Chemical structure of tectoridin, Minor

Figure 2.8 Chemical structures of the different compounds in *A. cominia* extracts from HEC and MeOH-D extracts.

2.3.2.2 Separation of quercetin and mearnsitrin

In Fig 2.9, two fractions were collected at specific retention times and compounds were identified as mearnsitrin collected between 8.5 and 9.5 minutes and quercetin collected between 9.5 and 11 minutes. MS was carried out for both samples and characterisation of the molecular weight of the major compound in fraction 1 suggested quercetin 447 C₂₁H₁₉O₁₁ (Fig 2.10), while the major compound in fraction 2 suggested mearnsitrin 477 C₂₂H₂₁O₁₂ (Fig 2.11). Confirmation of the separation of the two major compounds of flavonoids was carried out by ¹H NMR, with only mearnsitrin collected in fraction 2 (appendix 13). No compounds were shown in fraction 1 (appendix 14) because of the low quantity of the compound collected by HPLC. Even after increasing the number of scans from 16 to 128 (appendix 15), the low concentration of sample 1 did not enable a good ¹H NMR for characterisation.

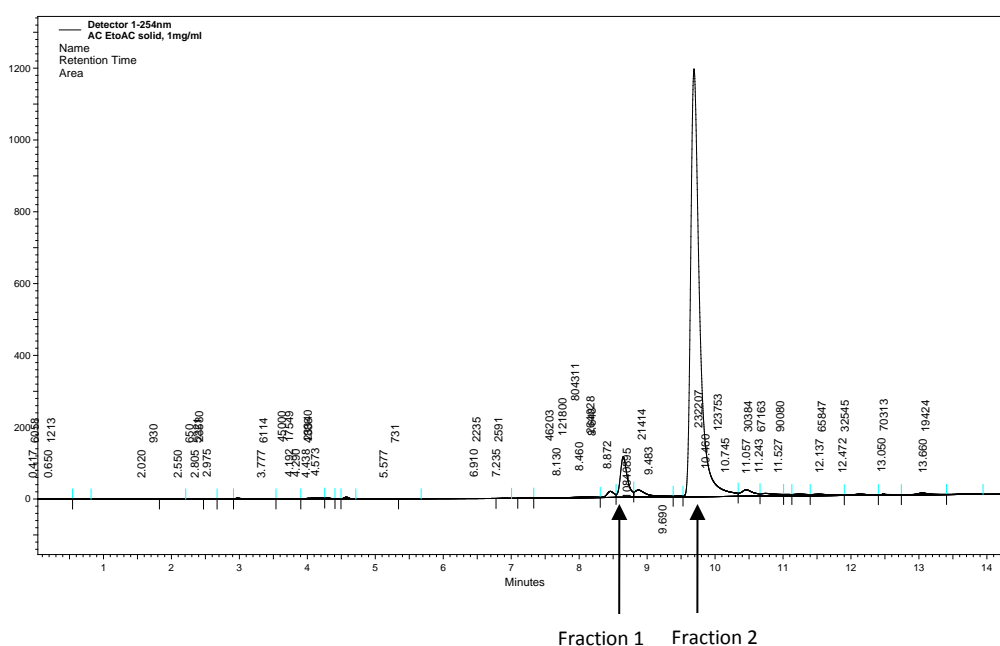


Figure 2.9 HPLC chromatogram showing different peaks for the flavonoids. Their retention times were used for the separation of the compounds. Analytical reversed-phase HPLC was carried out with Agilent 1200 series HPLC system. Samples were injected as 100 μ l onto an amino column. UV detection was set at 280 and 340 nm. 100 μ l of the sample was injected into the HPLC and 80:20 (v/v) acetonitrile:water was run isocratically at 1ml/min as a flow rate.

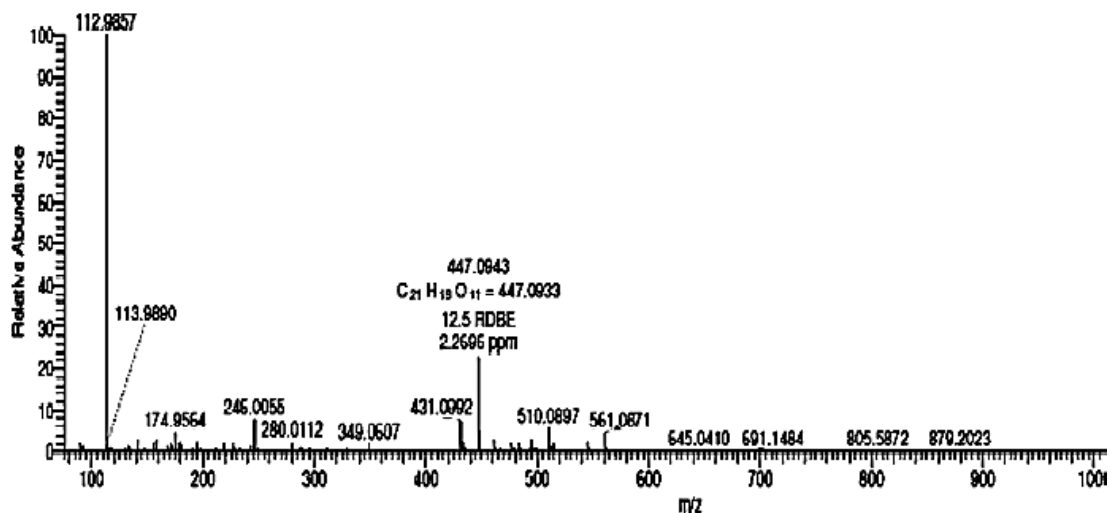


Figure 2.10 MS for fraction 1 collected at 8.5-9.5 minutes. The major compound was with MW 447.

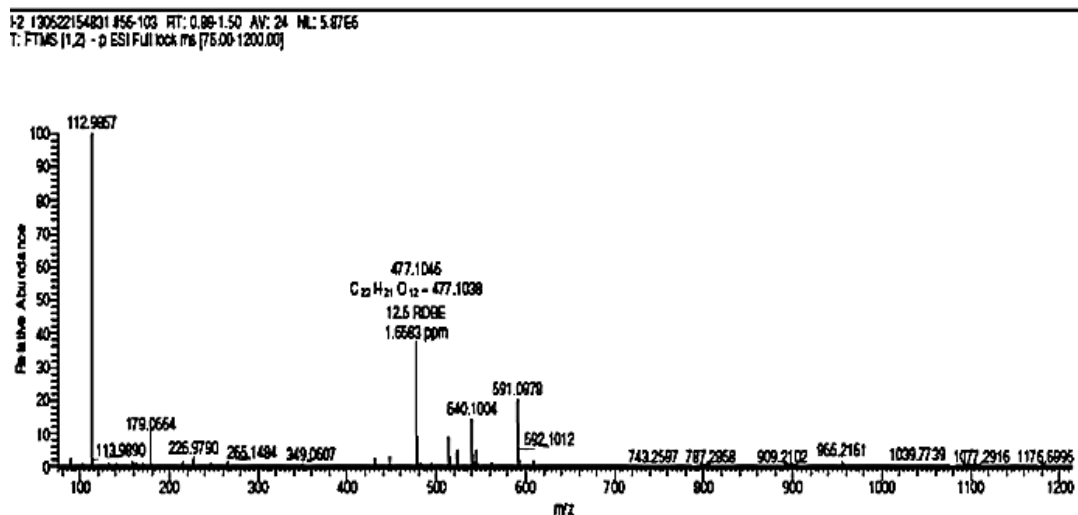


Figure 2.11 MS of fraction 2 collected at 9.5-11 minutes. The major compound was with MW 477. Fractions 1 and 2 from *A. cominia* were dried out using Epsilon freeze dryer, and dissolved in water at 1 mg/ml. Then submitted for LC-MS using Orbitrap. 20 μ l injection of the sample, the flow rate was 1 ml/min. Solvents used for mobile phase were acetonitrile and HPLC water (80:20 v/v). Method followed was isocratic. UV detection was set at 245 nm.

2.3.3 Characterisation of MeOH fraction D as a mixture of pheophytins

The NMR spectra (Appendices 9, 10, 11 and 12) showed the existence of pheophytins in addition to fatty compounds. Comparison of the spectral data with literature (Oba *et al.*, 1997; Ina *et al.*, 2007) identified the compounds as pheophytin A and B (chemical structures in Fig 2.12).

¹H NMR spectrum (Appendix 2) revealed three proton singlets in the region of δ_H 8.5 to 10 ppm, a singlet around 6.2 ppm and a multiplet around 8 accounting for a -CH=CH₂ group. Singlets were also observed between 3 and 4 ppm for the methoxy groups and singlets detected between 1.55 and 1.9 ppm for the methyl.

In addition, the ¹³C-NMR spectrum of MeOH-D indicated the number of carbons in both molecules (Appendix 10). HMBC and HSQC were used for the identification of the compounds and spectrum assignments (Appendices 11 and 12).

Further chromatographic separation was necessary for a full separation of the pheophytins and for the removal of fatty compounds which affected the biological activities of pheophytins. Appendices 3 and 4 represent the assignments of some hydrogen positions of pheophytin A and B respectively.

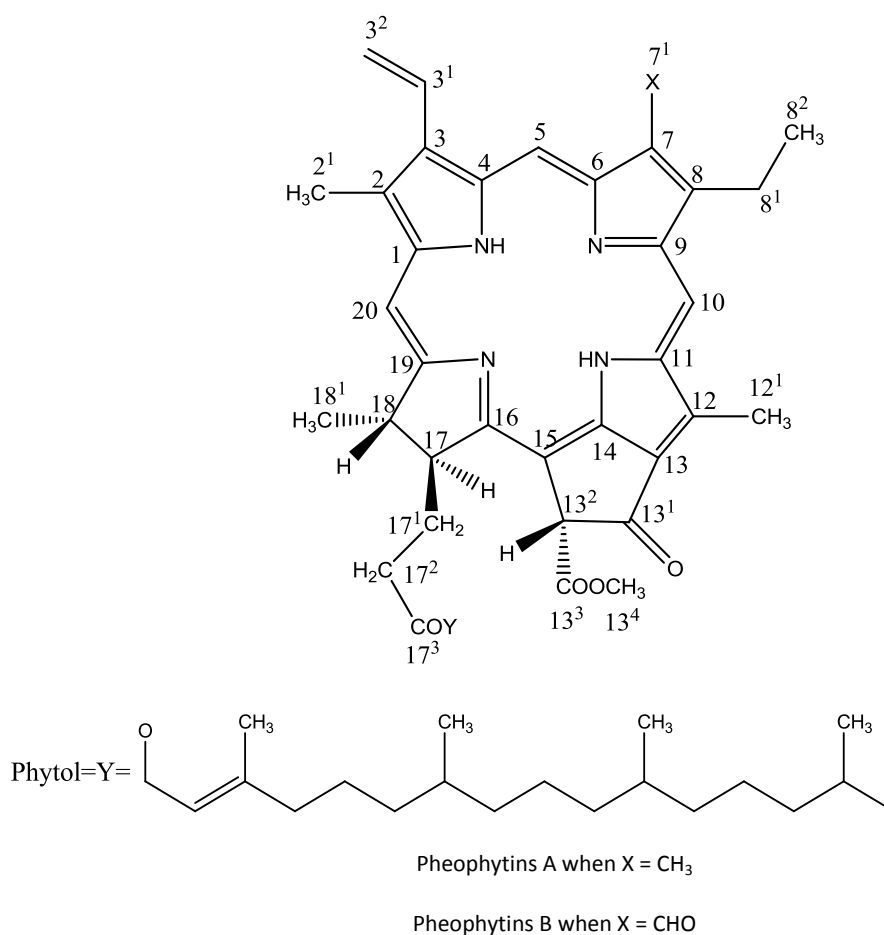


Figure 2.12 Chemical structures of pheophytins A and B.

2.3.3.1 Purification of pheophytins

TLC for fraction MeOH-D was carried out in 70:30 (v/v) hexane:EtOAc and separation of the bands was clear. They showed a quenching spot under short UV light and a red fluorescence under long UV. The spot turned green to yellowish-green after anisaldehyde-sulphuric acid spraying and heating, as shown in Fig 2.13.

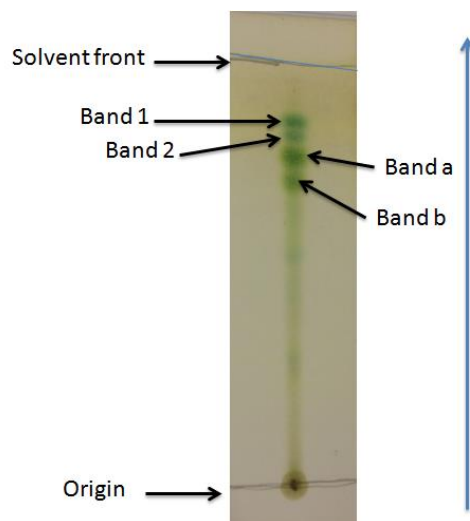


Figure 2.13 TLC plate for MeOH-D dissolved in chloroform in 70:30 hexane:EtOAc.

2.3.3.2 Prep-TLC

Prep-TLC was carried out following the same protocol and same solvent system for the separation of pheophytin A and B (the first and second bands in Fig 2.14).

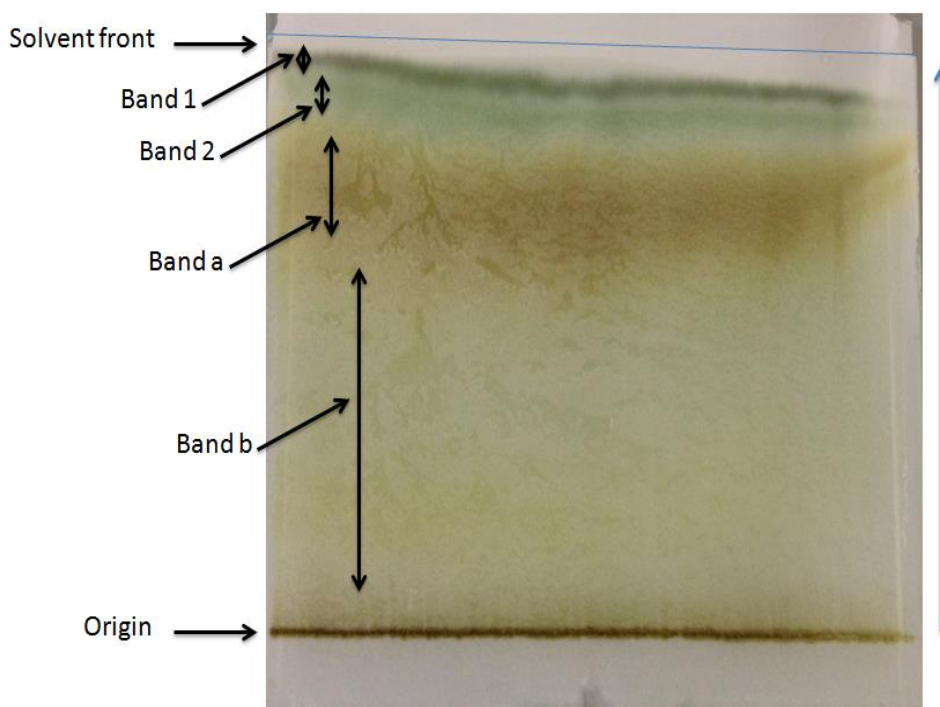


Figure 2.14 Prep-TLC for MeOH-D sample of *A. cominia* in TLC solvent 70:30 hexane:EtOAc.

After scraping each band, each band was eluted in three different solvents: hexane, EtOAc and MeOH. TLC was carried out as shown below using the same solvent system used in the separation (Fig 2.15).

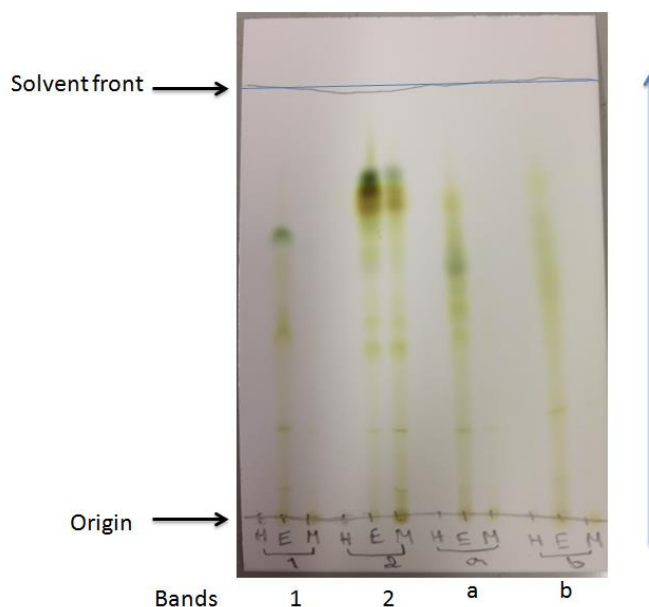


Figure 2.15 TLC plate for fractions separated by prep-TLC from the crude MeOH-D extracts of *A. cominia*. Four samples been separated 1, 2, a, and b. Each sample was soaked in three different solvents successively. H for hexane, E for EtOAc, and M for MeOH. Dissolved in chloroform, TLC solvent was 70:30 Hexane:EtOAc.

Only the EtOAc, fraction 1 showed the presence of a pure compound (one band). In addition, ^1H NMR was carried out for all the samples 1, 2, a, and b EtOAc and only fraction 1, EtOAc, as expected, was pure pheophytin A (Appendix 2). Pheophytin B was not obtained, therefore silica gel chromatography separation was carried out with the aim of purifying more of the pheophytin A and B.

With the aim of obtaining sufficient compounds for bioassays tests, prep-TLC separation was repeated ten times, under the same conditions. Therefore, starting from 40 mg of MeOH-D crude extracts, only 1.2 mg of pheophytin A was collected.

2.3.3.3 Silica gel column chromatography

Using the same solvent system as in the separation of the MeOH-D crude extract by prep-TLC (70:30 Hexane:EtOAc), the separation was carried out using column chromatography. Collection of fractions was carried out as 5 ml per vial then evaporated under hood; TLC was carried out and bands were visualised under UV and anisaldehyde spraying, and then similar fractions were combined and submitted for ^1H NMR. As shown in Fig 2.16, all the samples showed different single bands, then ^1H NMR showed that samples 5-13 were pheophytin A and samples 14-24 were pheophytin B (Appendices 3 and 4)

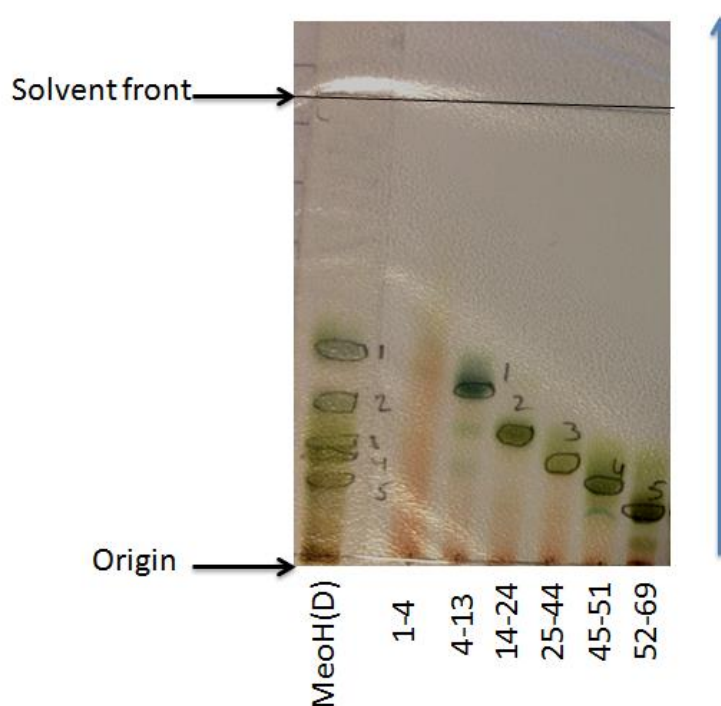


Figure 2.16 TLC plate for fractions separated by silica gel column chromatography from the crude MeOH-D extract of *A. cominia*. Six samples were separated (1-4, 5-13, 14-24, 25-44, 45-51, and 52-69). Dissolved in chloroform, TLC solvent was 70:30 Hexane:EtOAc.

The separated pheophytin A (fractions 5 to 13) was identified by ^1H NMR. ^1H NMR spectrum showed the presence of a pyrrole ring, by comparison to Ina *et al.*, 2007 at around 1.7 ppm, 5.9-7.9 ppm peaks from the vinyl group, then the methyl group at 9.5 ppm (Appendix 3). These chemical shifts were similar to those of pheophytin A as represented by Cahyana *et al.*, 1991 and Hargus *et al.*, 2007, where chemical shifts of all the related peaks were presented in Table 2.5. Fractions between 14 and 24 were identified as pheophytin B. The NMR results were in agreement with previous reports (Oba *et al.*, 1997; Fank and Xu, 2008).

^1H NMR spectra showed pheophytin A (Appendix 4) and B (Appendix 5) to have similar features. Pheophytin A was observed with three deshielded protons at 9.73 ppm (1H, s, H-10), 9.39 ppm (1H, s, H-5) and 8.88 (1H, s, H-20) and another three signals between 6 to 8 ppm for H-3¹, H-3² and H-13². In addition, an oxymethylene and some methyl signals at 0.81 ppm (6H, d), 0.87 (6H, d) and 1.61 (3H, s) were observed, suggesting the presence of the phytol group. By comparison to the chemical shifts of the ^1H NMR presented by Tomaz *et al.*, 2008, the structure of pheophytin A was elucidated. In addition, the HMBC spectrum (Appendix 11) showed all typical correlations between H and C (Table 2.6) that confirm the presence and the structure of pheophytin A and B.

Data from ^1H NMR spectra of fractions 25-44 (pheophytin B, as compared to Oba *et al.*, 1997) was similar to the data obtained for pheophytin A, the only difference being the four deshielded protons at 11.25 (1H, s), 10.50 (1H, s), 10.05 (1H, s) and 8.90 (1H, s) instead of three in the pheophytin A (Table 2.5), as well as two methyls between $\delta 3$ and $\delta 4$ ppm instead of three protons.

^{13}C NMR spectrum (in both pheophytins) was used to reveal the number of carbons, which was 55 (Appendix 10).

Position	δ_{H} (ppm) Pheo A	Tomaz <i>et al.</i> , 2008	δ_{H} (ppm) Pheo B	Oba <i>et al.</i> , 1997
1	-	-	-	-
2	-	-	-	-
2 ¹	3.35 (3H, s)	3.39 (3H, s)	3.34 (3H, s)	3.37 (s)
3	-	-	-	-
3 ¹	8.25 (1H, dd)	7.95 (1H, dd, <i>J</i> =17.85, 11.48 Hz)	8.1 (dd)	7.95 (dd, <i>J</i> =12, 18Hz)
3 ²	6.20 (1H, d) /6.28 (1H, d)	6.27 (1H, d, <i>J</i> = 17.95Hz/6.18 (d, <i>J</i> = 11Hz)	6.20 (1H, d) /6.30 (1H, d)	6.21 (dd, <i>J</i> =1, 12 Hz) trans
4	-	-	-	-
5	9.39 (1H, s)	9.35 (1H, s)	10.50 (1H, s)	9.43 (s)
6	-	-	-	-
7	-	-	-	-
7 ¹	3.16 (3H, s)	3.19 (3H, s)	11.25 (1H, s)	11 (s)
8	-	-	-	-
8 ¹	3.71 (2H, m)	3.63 (2H, m)	3.34 (2H, m)	3.85 (q, <i>J</i> = 8Hz)
8 ²	1.74 (m)	1.66 (m)	0.84 (3H, t, <i>J</i> =7.03 Hz)	-
9	-	-	-	-
10	9.73 (1H, s)	9.51 (1H, s)	10.05 (1H, s)	10.2 (1H, s)
11	-	-	-	-
12	-	-	-	-
12 ¹	3.61 (3H, s)	3.69 (3H, s)	3.75 (3H, s)	3.63 (3H, s)
13	-	-	-	-
13 ¹	-	-	-	-
13 ²	6.37 (1H, s)	6.30 (1H, s)	6.45 (1H, s)	6.25 (1H, s)
13 ³	-	-	-	-
13 ⁴	3.81 (3H, s)	3.91 (3H, s)	3.34 (3H, s)	3.93 (3H, s)
14	-	-	-	-
15	-	-	-	-
16	-	-	-	-
17	4.06 (m)	4.15 (m)	4.18 (dt)	4.20 (dt, <i>J</i> =3,9 Hz)
17 ¹	2.36 (1H, m) /2.66 (1H, m)	-	2.37 (1H, m) /2.69 (1H, m)	2.15 (m)
17 ²	2.23 (1H, m) /2.54 (1H, m)	-	2.41 (1H, m) /2.54 (1H, m)	2.45 (m)
17 ³	-	-	-	-
18	4.30 (1H)	4.34 (m)	4.18 (1H)	4.25 (m)
18 ¹	1.98 (3H, d)	1.84 (d)	1.98 (3H, d)	1.85 (3H, d)
19	-	-	-	-
20	8.88 (1H, s)	8.60 (s)	8.90 (1H, s)	8.53 (1H, s)

Table 2.5 ¹H NMR spectral assignments for pheophytin A and B. Tomaz *et al.*, 2008 and Oba *et al.*, 1997.

Position	HMBC correlation (H-C) Pheo A	HMBC correlation (H-C) Pheo B
1	-	-
2	-	-
2 ¹	H-2 ¹ /C-2, C-1, C-3, C-2 ¹	H-2 ¹ /C-2, C-1, C-3, C-2 ¹
3	-	-
3 ¹	H-3 ¹ /C-3, C-2, C-4	H-3 ¹ /C-3 ² , C-2, C-4
3 ²	H-3 ² /C-3, C-3 ¹	H-3 ² /C-3, C-3 ¹
4	-	-
5	H-5/C-7, C-3, C-4	H-5/C-7, C-3, C-4
6	-	-
7	-	-
7 ¹	H-7 ¹ /C-6, C-8, C-7	H-7 ¹ /C-6, C-7, C-7 ¹
8	-	-
8 ¹	H-8 ¹ /C-8 ² , C-9, C-7, C-8	H-8 ¹ /C-8 ¹ , C-8 ² , C-9, C-7, C-8
8 ²	H-8 ² /C-8 ¹ , C-8	H-8 ² /C-8 ¹ , C-8
9	-	-
10	H-10/C-12, C-11, C-8	H-10/C-12, C-11, C-8
11	-	-
12	-	-
12 ¹	H-12 ¹ /C-11, C-13, C-12	H-12 ¹ /C-11, C-13, C-12
13	-	-
13 ¹	-	-
13 ²	H-13 ² /C-15, C-14, C-13 ¹ , C-13 ³	H-13 ² /C-16, C-15, C-14, C-13 ¹ , C-13 ³
13 ³	-	-
13 ⁴	H-13 ⁴ /C-13 ³	H-13 ⁴ /C-13 ³
14	-	-
15	-	-
16	-	-
17	H-17/C-17 ¹ , C-17 ² , C-16	H-17/C-18 ¹ , C-17 ¹ , C-17 ² , C-16
17 ¹	-	C-17 ³
17 ²	-	C-17 ¹ , C-17, C-17 ³
17 ³	--	-
18	H-18/C-18 ¹ , C-17 ²	H-18/C-18 ¹ , C-17 ¹ , C-19, C-16,
18 ¹	H-18 ¹ /C-17, C-18, C-19	H-18 ¹ /C-17, C-18, C-19
19	-	-
20	H-20/C-2, C-18, C-1	H-20/C-2, C-18, C-1

Table 2.6 Selected HMBC correlations of pheophytin A and B. Appendices 11 and 12.

2.4 Conclusion and discussion

Allophylus cominia was identified as an antidiabetic plant, which was used for the treatment and management of T2-DM by Cuban patients (Mechlor *et al.*, 1999; Oliva *et al.*, 2013). Furthermore, *in vivo* experiments were carried out confirming that extracts from *A. cominia* were enhancing glucose uptake, especially fractions 6 and 10 collected after flash chromatography (Sanchez *et al.*, 2014). However, studies carried out for the separation and identification of compounds from *A. cominia* were not leading to the identification of the active constituents in *A. cominia* (Veliz *et al.*, 2003). The phytochemical investigation of *A. cominia* provided many compounds, mainly including some simple phenolics or derivatives and some pheophytins. This is the first report of the isolation and identification of these compounds in *A. cominia*.

In our research, a mixture of flavonoids and pheophytins were identified as major compounds. By comparison to studies carried out by Jung *et al.*, 1999, Cahyana *et al.*, 1991, Mahmoud *et al.*, 2001 and Lopes *et al.*, 2004; Hargus *et al.*, 2007, Ina *et al.*, 2007; these compounds were identified as quercitrin, mearnsitrin in addition to other minor compounds (naringenin, azalein and tectoriden) which could have an effect in the biological assays. The separation of the flavonoids was carried out by HPLC using an amino column. Only mearnsitrin and quercitrin were identified. A conventional HPLC separation was a robust method of separation. However, separation should be carried out using a preparative HPLC for a robust, fast and less costly separation. In addition, pheophytin A and pheophytin B were identified in *A.cominia*. All These compounds are added to the preliminary chemical identification by Rodriquez *et al.*, 2005 and Veliz *et al.*, 2005 (fatty acids such as lauric acid, myristic acid, palmitic acid, stearic acid, and arachidic acid in addition to carbohydrates such as arabinose, galactose, and glucose).

Among the extracts fractionated from *A.comina*, all were investigated for anti-enzymes activity (DPPIV, PTP1B, α -glucosidase and α -amylase). Fractions that showed more than 70% inhibition of PTP1B enzyme activity were followed by investigating their effect on the glucose uptake using various cell lines. Only the mixture of flavonoids and pheophytin A were used in the glucose uptake assay.

Chapter 3

3 *In vitro* determination of the effect of *A. cominia* on the glucose uptake in HepG2, L6 and 3T3-L1 cells

3.1 Introduction

Several drugs are used for the treatment of T2-DM. However, these agents have unexpected treatment-limiting side effects (more information are presented in chapter 1 section 1.2.1.1). Therefore, there is a need for new anti-diabetic substances (Laville and Andreelli, 2000; De Souza *et al.*, 2001) that have fewer side effects on patients with diabetes and do not induce obesity. Several studies carried out using plant extracts have shown significant effects on the glucose uptake (Alonso-Castro *et al.*, 2006; Alonso-Castro *et al.*, 2008; Nomura *et al.*, 2008; Rahul *et al.*, 2009; Alonso-Castro *et al.*, 2011; Hassanein *et al.*, 2011) and have the potential to be used in the treatment of diabetes.

In this project, HepG2 cells were used as a model system for the study of the glucose uptake (Hu and Wang, 2011; Wang *et al.*, 2011). L6 cell line was also one of the most useful models for testing glucose uptake (Wang *et al.*, 1999; Jia *et al.*, 2010).

Fully differentiated adipocytes are insulin-responsive and take up glucose more effectively than pre-adipocytes, with a high number of glucose transporter-4 (GLUT4) enhanced by the insulin from the intracellular compartment to the cytoplasmic membrane, resulting in an increase in the glucose uptake with lower insulin concentrations. The 3T3-L1 cell line is one of the most useful established models for the study of insulin responsiveness and for testing the activity and mechanism of action of anti-diabetic drugs and plants extracts (Xu *et al.*, 2006, Wang *et al.*, 2011). 3T3-L1 cells were also a good model for testing the effect of the extracts from *A. cominia* on the glucose uptake as well as their effect on the 3T3-L1 differentiation and fat accumulation.

2-NBDG a novel fluorescence glucose analog probe that was initially developed to measure the glucose uptake rates in cells, has proven to be of great utility to also measuring glucose uptake rates in a wide range of non-mammalian and mammalian cells in recent years. 2-NBDG has shown to be transported intracellularly by the same glucose transporters (GLUT4) as glucose. 2 Deoxy-D-glucose was also used

which is known to compete with 2-NBDG in mammalian cells (Hassanein *et al.*, 2011). However, 2-NBDG are known to be phosphorylated by the same kinases (hexokinases) as glucose. Therefore, 2-NBDG can be trapped within the cells for an extended period of time, which might be essential to monitor the glucose uptake, although the phosphorylation of 2-NBDG leads to rapid degradation into non-fluorescent products. For such reason 2-DG was a better glucose analog for testing the effect of the extracts from *A. cominia* on the glucose uptake by mass spectrometry (Jo *et al.*, 2013). 2-DG uptake experiment can be considered as an orthogonal assay of the 2-NBDG uptake. Mass spectrometry analysis of the glucose uptake was carried out in this project for further confirmation of the effect of the extracts on the glucose uptake as well as the quantification of the uptake. The aim of this chapter is to study the effect of the extracts from *A. cominia* on the glucose uptake using HepG2, L6 and 3T3-L1 cell lines as well as the effect of these extracts on insulin activity.

3.2 Material and Methods

3.2.1 Preparation of *Allophylus cominia* extracts

Samples (crude and pure compounds) were dissolved in DMSO (pheophytins and tannins) or distilled water (flavonoids) at a concentration of 10 mg/ml and kept at -20°C as stock solutions. Further dilution of the plant stock samples was carried out using either assay buffer or cell growth medium as appropriate.

3.2.2 HepG2 liver cells

HepG2 (*human liver hepatocellular carcinoma cell lines*) are adherent, epithelial-like cells in morphology, growing as monolayers and in small aggregates (islands).

The HepG2 (SIDR cells bank) were removed from the liquid nitrogen (-210°C), and were thawed rapidly (37°C) and then transferred into warm growth medium in 25 cm² clear and sterile flask (purchased from Thermofisher, Nunc). The cells were seeded in 5 ml of DMEM (Dulbecco's Modified Eagle's Medium from Gibco,

Invitrogen, UK) supplemented with 10% FBS (foetal bovine serum), 100 U/mL of penicillin, and 100 µg/mL of streptomycin (Hu and Wang, 2011). The flask was incubated at 37°C in 95% humidified air and 5% CO₂ for 10 to 15 days, depending on the growth rate of the cells. The growth medium was replaced every two days.

A. HepG2 seeding

The growth medium was removed from the 25 cm² flask and the cells washed twice with 5 ml (10 ml for the 175 cm² flask) of Hank's saline solution (from Sigma Aldrich, UK). Cells were detached from the bottom of the flask following the addition of 5 ml of Hank's and trypsin mixture (trypsin EDTA X10 was purchased from Gibco, Invitrogen, UK) The flask was incubated for 5 to 6 min at 37°C in a 95% air and 5% CO₂, after which DMEM was added to the cells to deactivate the trypsin. The cells were then divided into two tubes and centrifuged at 1000 RPM for 2 minutes (IEC/Medispin, 6PL centrifuge, Life Sciences International). The supernatant was removed and 10 ml of DMEM with 10% FBS were added to the cell pellet. Cells were counted using a haemocytometer viewed under an inverted microscope (Olympus IM, Japan). The cells were seeded in 175 cm² clear and sterile flasks (Nunclon Delta, Thermo Scientific Nunc) at a density of 2x10⁶ cells per 175 cm² flask when seeding for 3 days growth, and 1.5x10⁶ cells per 175 cm² flask when seeding for 4 days growth.

In general, the cells were seeded and grown in 175 cm² flasks in 25 ml of DMEM with a 10% FBS, incubated at 37°C in air containing 5% CO₂ (Zhang *et al.*, 2010) for 2 to 5 days, depending on the cells' growth.

B. HepG2 culture

The HepG2 cells were cultured both in black and clear bottom 96-well plates purchased from Fisher Scientific, UK; and in 96-well clear plates purchased from TPP, Switzerland, at three different seeding densities: 0.5×10^4 , 1×10^4 , and 2×10^4 cells/well. For the cytotoxicity assays, all the cells were seeded at 1×10^4 cells/well. The culture medium (DMEM) was supplemented with 10% FBS, 100 U/mL of penicillin, and 100 $\mu\text{g/mL}$ of streptomycin (Hu and Wang, 2011). Plates were incubated at 37°C in an atmosphere containing 5% CO_2 for 24 or 48 hours.

C. HepG2 storage

Cells were re-suspended at 2.5×10^6 cells/ml in 1ml of DMEM supplemented with 10% FBS and 5% of DMSO. The cells were placed in cryovials (CryotubeTM vials purchased from Nunc), kept for a few days in a -80°C freezer (Sanyo, CFC free) and then transferred into liquid nitrogen when longer storage was required.

3.2.3 3T3-L1 cell culture and adipocyte differentiation

A. Cell growth

3T3-L1 cells from Swiss mouse embryo tissue were purchased from ATCC (American Type Culture Collection), cultured in DMEM (high glucose) with 10% FBS (foetal bovine serum), supplemented with 1% glutamine and 1% penicillin/streptomycin and then grown at 37°C in an atmosphere containing 5% CO_2 . 3T3-L1 cells with passage number 4 (from liquid nitrogen) defrosted quickly at 37°C in water bath. Then the cells were transferred into a 75 cm^2 flask in 15 ml of DMEM supplemented with 10% FBS, and incubated for 24 hours at 37°C in an atmosphere containing 5% CO_2 . The medium was changed after 48 hours when the cells reach no more than 70% confluence after which the cells were passaged in DMEM with 10% FBS into 75 cm^2 flask with 15 ml of media. The cells were divided every two to three days using the same protocol that was used for the HepG2 cells

where 6 ml of TrypLE Express was added to the flask, incubated for two minutes to allow the cells to become detached from the surface of the flask. After which 4 ml of growth medium was added to the flask to terminate the action of the TrypLE Express. The cell suspension was centrifuged for 2 minutes at 1000 RPM, and then the supernatant was discarded and the pellet of cells was re-suspended in 5 ml of DMEM 10% FBS to be seeded at a specific concentration in flasks or plates. The cells were triturated with a Pasteur pipette and were counted using a haemocytometer with the aid of an inverted microscope. The cells were seeded at a density of between 0.4 and 0.8×10^5 cells/ml in 75 cm^2 flask with 15 ml of DMEM supplemented with 10% FBS.

B. Cell storage

DMEM medium was aspirated from the flask and 5 ml of TrypLE Express [0.05% (v/v) in EDTA] was added to each flask. Flasks were then incubated at 37°C for 3-5 min until the cells were just beginning to come off the flask. The trypLE Express solution was gently spread over the surface of the flask until all of the cells were detached. 5 ml of DMEM 10% FBS was added to each flask. The cell suspension was then transferred to a 15 ml universal tube. The trypLE/cell mix was then centrifuged at $1000 \times g$ for 2 min and the supernatant was discarded. The cell pellet was then re-suspended in 1 ml of freeze medium; DMEM with 40% FBS containing 10% dimethyl sulphoxide (DMSO). The re-suspended cell pellet was transferred into 1.8 ml polypropylene cryogenic tubes (1 ml/tube). The cryogenic tubes were then placed into a polycarbonate container and stored overnight at -80°C . The following day, the vials were transferred to liquid nitrogen when longer storage was required.

C. 3T3-L1 cell differentiation

After splitting and seeding 3T3-L1 cells (passage 2-12) in Corning 75 cm^2 flasks, the flasks were incubated at 37°C in 5% CO_2 until they reached no more than 70% confluence. Then they were seeded in DMEM 10% NBS (new-born serum) in black

clear bottom 96-well plate; the cells were left until 100% confluence (200 µl of medium was added to each well). The cells were differentiated using the following procedure: at day 1, the growth medium was replaced with the differentiation media which was prepared with DMEM supplemented with 10% FBS, 1 µg/ml of insulin (Sigma I2643 - 50 mg), 0.25 µM dexamethasone (Sigma D1756 - 100 mg) and 0.5 mM IBMX (Sigma I5879 - 250 mg). IBMX was freshly made on each occasion while the insulin and dexamethasone were prepared from stock solutions. The solutions were filter sterilisation via a 0.22 mm syringe filter. At day 3, the medium was replaced by DMEM 10% FBS with 1 µg/ml insulin. On day 5, the medium was replaced with DMEM supplemented with 10% FBS, after which the media was replaced by a fresh cell growth medium (DMEM 10% FBS) every 48 hours. The cells were fully differentiated and used between days 8 and 12 of the induction of differentiation protocol.

3.2.4 Oil Red-O staining of 3T3-L1 adipocytes

Fixing solution

10% of formalin (from 37% of formalin stock) in PBS was prepared and stored at room temperature. It can be used for up to 6 months.

Oil Red-O stock

500 mg of Oil Red-O was dissolved in 100 ml of isopropanol (2-propanol) in a dark bottle and left overnight without stirring at room temperature for at least 24 hours. Oil Red-O working solution was prepared fresh on the day of the assay. 60% of Oil Red-O stock in distilled water (40%) was kept at room temperature for at least half an hour, and then was filtrated through Whatman paper to remove particulate matter.

Staining protocol

The media from the differentiated 3T3-L1 cells were removed from the 6-well plates and the cells were washed twice with 1 ml of PBS. 1 ml of the fixing solution (to cover the bottom of wells) was added to each well, and then the plate was incubated at 37°C in an atmosphere containing 5% CO₂ for 1.5 h, after which the fixing solution was removed and the cells were washed three times with distilled water. 1ml

of Oil Red-O dye was added to each well and left at room temperature for one hour. The dye was removed, the cells were washed three times with distilled water and pictures of the stained cells were taken under the microscope.

Optical density measurement

1 ml of isopropanol was added to each well of the 6-well plate and the plate was left at room temperature for 10 minutes to allow the cells to release the dye. Then they were transferred into 200 μ l per well of a 96-well clear plate, and the optical density was measured at 540 nm using a Spectramax plate reader.

3.2.5 L6 muscle cells

A. Cell growth

L6 cells from rat skeletal muscle cells purchased from ECACC (European Collections of Cell Cultures, donated from the SIDR library) cultured in DMEM containing 10% FBS supplemented with 1% sodium pyruvate, 1% glutamine and 1% penicillin/streptomycin and then incubated at 37°C in an atmosphere containing 5% CO₂. L6 cells with passage number 2 (from liquid nitrogen) were defrosted quickly in a water bath at 37°C. Then the cells were transferred to a 25 cm² flask in 5 ml of DMEM with 10% FBS, and incubated for 24 hours at 37°C in an atmosphere containing 5% CO₂. The medium was changed no more than 72 hours to a fresh DMEM with 10% FBS, and when they reached no more than 80%, the cells were passaged in DMEM with 10% FBS into 75 cm² flask with 15 ml of medium. Then the cells were split using the same protocol used for splitting HepG2 cells (trypsinisation), described in section 3.2.2.1.1. The cells were seeded at 1×10^4 cells/ml in 15 ml of DMEM 10% FBS.

B. Cell storage

Following trypsinisation, the cell pellet was re-suspended in 5 ml of the freezing medium containing 90% FBS and 10% sterile DMSO. Cells were counted using a haemocytometer, and only 0.5 - 1×10^6 cells/ml was frozen down in 1.8 ml

polypropylene cryogenic tubes for two days before being transferred into liquid nitrogen when longer storage was required.

C. L6 cell differentiation

L6 cells were seeded at 8×10^3 cells/well, in a 96-well plate, in DMEM containing 10% FBS and incubated for 48 hours at 37°C in air at 5% CO₂. Once the cells were 100% confluent, the medium was replaced with DMEM containing 1% FBS for five days.

3.2.6 Cytotoxicity assays

A. cominia extracts used in bioassays were first tested for their effect on the viability of the different cells. The extracts containing the active components of *A. cominia* were tested on HepG2, L6, 3T3-L1 pre-adipocyte and adipocyte cell lines, using two different assays, Alamar blue and MTT. The assays incorporated a fluorometric growth indicator, based on the detection of metabolic activity.

3.2.6.1 Alamar blue assay

HepG2, L6, 3T3-L1 fibroblasts and adipocytes cell lines were seeded in 96-well clear plate and incubated for 24 hours at 37°C in an atmosphere containing 5% CO₂. Gradient concentrations of each sample (stock was 10 mg/ml) diluted in DMEM with 10% FBS were added to the plate (the final volume added to each well was 100 µl). The plate was incubated for 24 hours at 37°C in an atmosphere containing 5% CO₂, following which the Alamar blue test was performed in order to test the cell viability. Alamar blue (Resasurin) is a redox indicator for testing cell growth or viability; in metabolically active cells it can be reduced to resorufin by NADH (dehydrogenase activity). Resorufin exhibits fluorescence (563/587 nm) and can be detected fluorometrically. Alamar blue taken by the living cell penetrates into the mitochondria, where it changes colour from blue to pink (Fig 3.1) (AlamarBlue®ox + 2H + 2e⁻ gives AlamarBlue®RED) (Goegan *et al.*, 1995). 10 µl of Alamar blue in addition to 90 µl of DMEM with 10% FBS were added to each well. After 6 hours at 37°C in an atmosphere containing 5% CO₂, the fluorescence intensity was measured with a Wallac Victor² 1420 Multilabel counter using Alamar Blue with absorbance reading between 560 nm and 590 nm (AB 560/590).

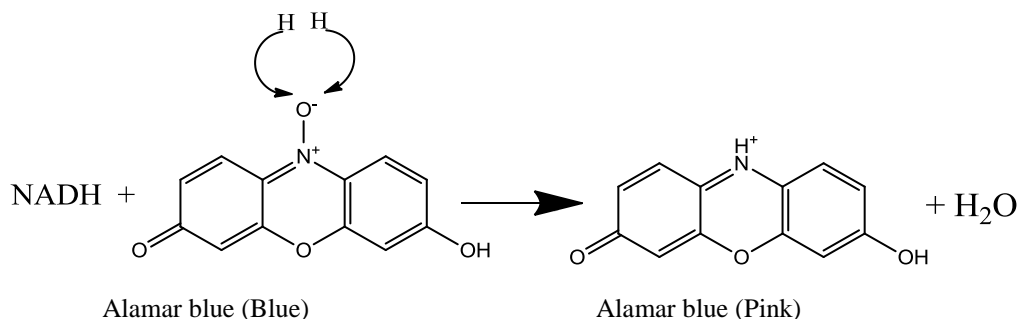


Figure 3.1 Alamar blue reaction that occurs in the mitochondria of the living cells leading to the change in the colour of the Alamar blue from blue to pink.

3.2.6.2 MTT assay

MTT (3-(4,5-Dimethylthiazol-2-yl)-2,5-diphenyltetrazolium bromide) is a yellow tetrazole, a colorimetric dye used for cell viability tests. MTT is reduced to purple formazan in the presence of NADH and NADPH (Fig 3.2).

At day 1, different cell lines were plated in a 96-well plate at 1×10^4 cells/well, then incubated for 24 hours at 37°C in air at 5% CO₂, to allow the cells to attach to the bottom of the wells. After 24 hours, *A. cominia* extracts were added to the plate at different concentrations (1 µg/ml to 100 µg/ml), then incubated for another 24 hours at 37°C in an atmosphere containing 5% CO₂. On day 3, the working solution of MTT was prepared at 5 mg/ml in phosphate buffer saline (PBS) and filtrated through a 0.22 µm syringe filter.

After preparation the MTT working solution, the growth media was removed from the wells and 20 µl (20%) of MTT was added to each well and the volume was made up to 100 µl with DMEM, with 10% FBS. The plate was then incubated for 4 hours at 37°C in an atmosphere containing 5% CO₂. The growth media was then removed and the cells were lysed by the addition of 150 µl of DMSO to each well. The plate was left for 5 minutes at room temperature, and then shaken to allow the cells to detach from the plate. The absorbance was measured on a Spectramax instrument using 560 nm and 690 nm. Finally, the values obtained at 670 nm reading were subtracted from the values obtained at 560 nm reading and the results were presented as percentages of the mean counts of the untreated cells (control).

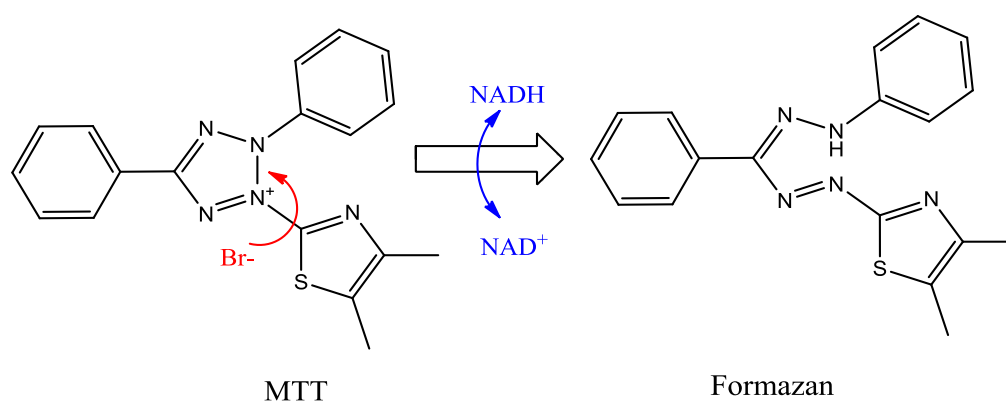


Figure 3.2 MTT reaction mechanism that occurs in the mitochondria of the living cells leading to a change in the colour of the MTT from yellow to purple (Formazan).

3.2.7 2-NBDG uptake assay

2-N-7-(nitrobenz-2-oxa-1,3-diazol-4-yl)amino-2-deoxy-D-glucose (2-NBDG, Fig 3.3) is a fluorescent glucose analogue; it allows for direct and very sensitive measurements of glucose uptake by the cells.

To promote the uptake of the 2-NBDG by different cell lines, an enhanced buffer replacement medium was prepared (Krebs Ringer Bicarbonate HEPES) in the absence of glucose.

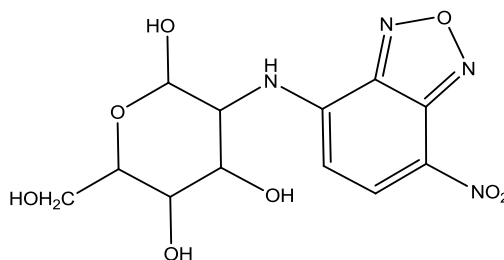


Figure 3.3 Chemical structure of the 2-N-7-(nitrobenz-2-oxa-1,3-diazol-4-yl)amino-2-deoxy-D-glucose (2-NBDG).

Buffer preparation

The Krebs Ringer Bicarbonate HEPES (10X stock) were prepared using 4 stock solutions:

Stock A: 7 g of Sodium chloride (NaCl 1.2 M), 0.544 g of potassium di-hydrogen phosphate (KH_2PO_4 40 mM) and 2.46 g of magnesium sulfate (MgSO_4 10 mM) in a 100 ml of distilled water.

Stock B: 0.11 g of Calcium Chloride (CaCl_2 7.5 mM) in 100 ml of distilled water.

Stock C: 0.84 g of Sodium Carbonate (NaHCO_3 100 mM) in 100 ml distilled water.

Stock D: 7.14 g of HEPES (300 mM) in 100 ml distilled water.

1X buffer was made fresh just prior to the start of the glucose uptake assay by adding 10 ml of each stock (in the order A, B, C and D); then the pH was adjusted to 7.4 and made up to 100 ml with distilled water.

Material

2-NBDG ($\text{C}_{12}\text{H}_{14}\text{N}_4\text{O}_8$), from Sigma stored at -20°C , stock 5 mg dissolved in 1462 μl of distilled water.

Insulin (100 mM stock 1) was purchased from Sigma and stored at -20°C, while insulin stock 2 (1 mM) was prepared by 10 µl of insulin stock 1 in 990 µl ABCD buffer. Then the insulin working solution (final concentration per well was 100 nM) was prepared by 30 µl from stock 2 added to 2.5 ml of ABCD buffer.

Method

HepG2, 3T3-L1 fibroblasts, 3T3-L1 adipocytes and L6 myoblasts were seeded in DMEM supplemented with 10% FBS at 1×10^4 cells/well for HepG2, L6 and 3T3-L1 fibroblasts in black 96 well clear bottom plate and incubated for 24 hours. Therefore, seeded at 8×10^3 cells/well, 3T3-L1 fibroblasts were differentiated into adipocytes following the protocol explained in 4.2.2.2.3; then the plate was used for 2-NBDG glucose uptake assay. *A. cominia* (flavonoids and pheophytins extracts) was added to the wells at 100 µg/ml and incubated at 37°C in 5% CO₂ for 24 hours.

The medium was replaced by 50 µl of the enhanced buffer prepared “Krebs Ringer Bicarbonate Hepes” in order to starve the cells.

The plate was incubated for 5 hours at 37°C in an atmosphere containing 5% CO₂. The cells were treated with and without 100 nM of insulin (25 µl per well) in the presence or absence of 100 µg/ml of *A. cominia* extracts, and incubated for 45 minutes at 37°C in 5% CO₂. Wortmannin (10 µM), which is a steroid metabolite of the fungi *Penicillium funiculosum* and an irreversible inhibitor of phosphoinositide 3-kinases, a key point in the insulin signalling pathway (Liu *et al.*, 2007). The half-life time of the wortmannin in cell culture is 10 minutes. This was followed by the addition of 2-NBDG (1 µM to 100 µM) to all wells (25 µl/well) and the plate was incubated at 37°C in an atmosphere containing 5% CO₂ for one hour. After incubation, the plate was washed twice with 100 µl of chilled PBS (pre-cold) in each well (Leira *et al.*, 2002; Zou *et al.*, 2005). Finally, 200 µl of pre-cold PBS (phosphatase buffer solution) was added to each well. The fluorescence intensity of 2-NBDG was measured on a Wallac Victor² 1420 Multi-label counter using the following wavelengths: 485 nm/535 nm, 1 s.

The experiment was repeated by adding insulin (1 nM to 100 nM) to all wells (25 µl) and 100 µM of 2-NBDG in the presence or absence of 100 µg/ml of *A. cominia* extracts.

3.2.8 2-Deoxy-D-glucose uptake assay

2-Deoxy-D-glucose $C_6H_{12}O_5$ is a glucose analogue (MW 164.16 g/mol) in which the hydroxyl group was replaced with hydrogen (Fig 3.4). It can also bind to the glucose transporters (GLUT4) located in the cell membranes. 2-Deoxy-D-glucose has been a fluorescent target in many projects (Sheth *et al.*, 2009). It allows a direct quantification of the glucose uptake by many cells, such as cancer cells, adipocytes and liver cells.

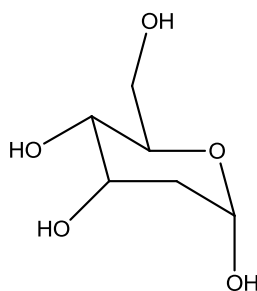


Figure 3.4 Chemical structure for 2-deoxy-D-glucose.

3.2.8.1 2-Deoxy-D-glucose uptake by 3T3-L1 adipocytes

3T3-L1 cells were seeded and differentiated in 24-well plates in the presence of 1 μ M of troglitazone. Twelve days from the differentiation initiation, *A. cominia* extracts at 100 μ g/ml were added to the cells, and then the plate was incubated at 37°C for 24 hours. The glucose uptake assay was performed using the same method as 2-NBDG (section 3.2.5) but using 2-deoxy-D-glucose at 200 μ M. 2-DG uptake was also measured by the differentiated 3T3-L1 pre-treated cells in the absence or presence of *A. cominia* extracts, TNF- α or troglitazone to study the effect of these treatments on the 2-DG glucose uptake.

2-DG glucose uptake by 3T3-L1 adipocytes was measured after metabolite extraction and mass spectrometry analysis (explained in sections 3.2.6.2 and 2.2.8).

3.2.8.2 Metabolite extraction

The cell concentration in each well of the 24-well plates was counted before the differentiation with a haemocytometer. Five days after differentiation 2-Deoxy-D-glucose assay was carried out, and the cells were washed twice with PBS. 3T3-L1 adipocytes were detached from the bottom of the wells using TrypLE Express and a cell scraper. Cells were collected in Eppendorf tubes and cooled rapidly in a dry-ice and ethanol bath and stored in ice. Cells were collected by centrifugation (10 min at 1800 x g at 4°C) and the supernatant or spent medium was transferred to a separate Eppendorf tube and stored on ice. The cell pellet was mixed by gentle pipetting with ice-cold PBS (wash number 1). 1 ml of the cell suspension, containing the same number of differentiated 3T3-L1 cells was centrifuged for 10 min at 1800 x g at 4°C. The supernatant was discarded and the cell pellet was mixed with 1 ml ice-cold PBS (wash number 2) and the cells were collected in a fresh Eppendorf tube by centrifugation as described above.

Cell extracts were prepared by mixing the cell pellet with 200 µl of ice-cold extraction buffer 1 [chloroform/methanol/water - 1/3/1 (v/v)] and shaking at 12°C for 1 hour in a thermo-mixer (Incubator shaker Incu-shake Maxi from Sciquip ZHWY-200D). The extract was cleared by centrifugation for 10 minutes at 13000 x g at 4°C and the supernatant stored at -80°C.

3.2.8.3 Mass spectrometry

Extracts of the 3T3-L1 adipocytes were submitted for mass spectrometry using an Orbitrap mass spectrometry detector. The column used was a BEH-amide sugar-95-70 from Waters (C18 21x30mm, 1.7 µm). The mobile phase A was 90:10 (v/v) water:acetonitrile and B was 10:90 (v/v) water:acetonitrile in the presence of 0.3% ammonium hydroxide in both mobile phases (A and B). The wavelength used was 150 nm. The flow rate was 0.5 ml/min and the injection volume was 20 µl. The gradient method used is presented in Table 3.1.

	Time (min)	% A	% B
1	0	5	95
2	0	5	95
3	0.1	5	95
4	35	30	70
5	36	93	8
6	41	92	8
7	42	5	95
8	52	5	95

Table 3.1 Mass spectrometry gradient method used for the quantification of 2-deoxy-D-glucose in the 3T3-L1 adipocytes metabolite extracts. A was 90:10 (v/v) water:acetonitrile and B was 10:90 (v/v) water:acetonitrile plus 0.3% ammonium hydroxide. Flow rate was 0.5 ml/min.

3.2.9 Statistical Analysis

Results are expressed as mean +/- SEM. Statistically significant differences were determined using PRISM version 4 software by a one-way ANOVA analysis of variance and Dunnett post-test where appropriate, with $p < 0.05$ as significant.

Chemical structures were drawn using Chem Bio Draw ultra-version 12.0.2 software.

3.3 Results

3.3.1 Cell culture

3.3.1.1 3T3-L1 adipocytes morphology

3T3-L1 fibroblasts that are used for the differentiation of adipocytes were grown as explained in section 3.2.3 until reaching 100% confluence (Fig 3.5.A to E). Three days over confluence, the cells were differentiated into round fat cells full of droplets of triglycerides as explained in chapter 4 section 4.2.1 (Fig 3.5.F to I). Pictures of 3T3-L1 fibroblasts and adipocytes were taken over the days of the cell growth and differentiation (Fig 3.5).

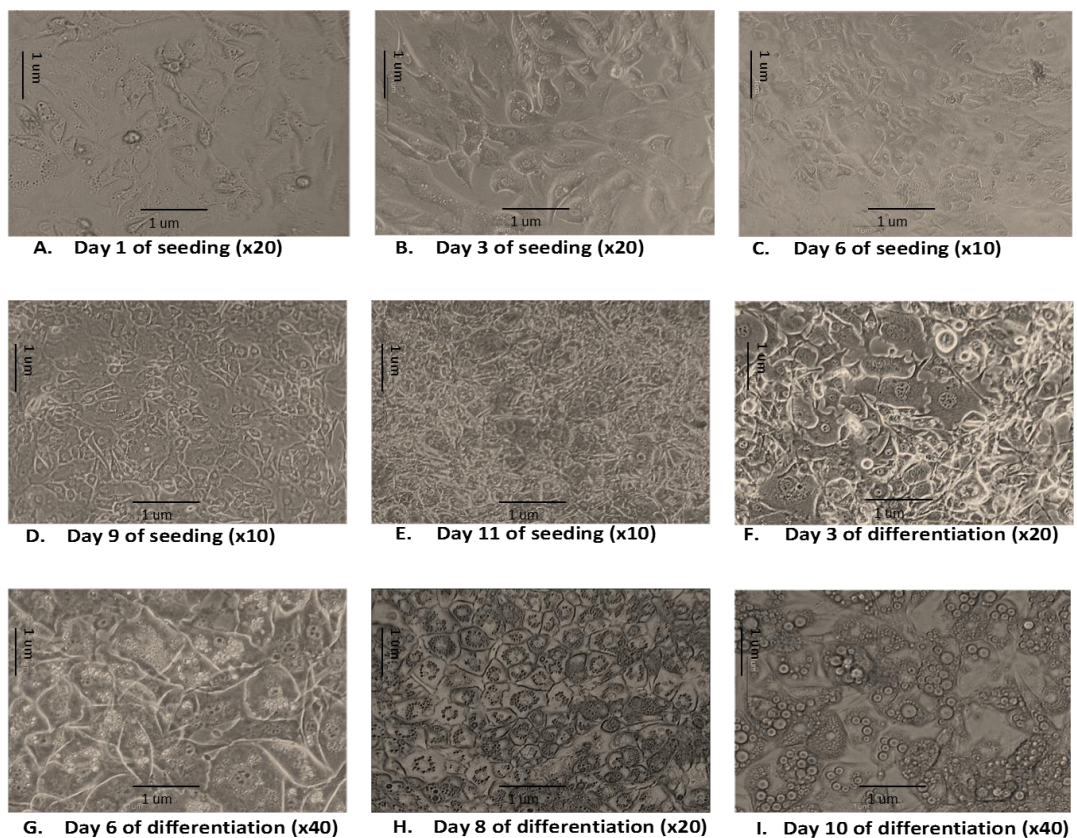


Figure 3.5 Series of images depicting the 3T3-L1 fibroblast differentiation. Cell growth was followed over a period of eleven days (A to E), and adipocyte differentiation over a period of ten days (F to I). Cells were treated with differentiation media and incubated at 37°C in an atmosphere containing 5% CO₂.

3.3.1.2 Oil Red-O staining for 3T3-L1 cells

To identify whether the cells were differentiated or not, quantifying lipid droplets was performed by Oil Red-O (as explained in section 3.2.4) 12 days after the differentiation. Pictures of different wells from the 12-well plates were therefore taken before and after the staining, as shown in Fig 3.6. Fat droplets were stained in red (Fig 3.6.B) and could be easily detected under microscope. The non-differentiated cells were washed away with the distilled water after staining.

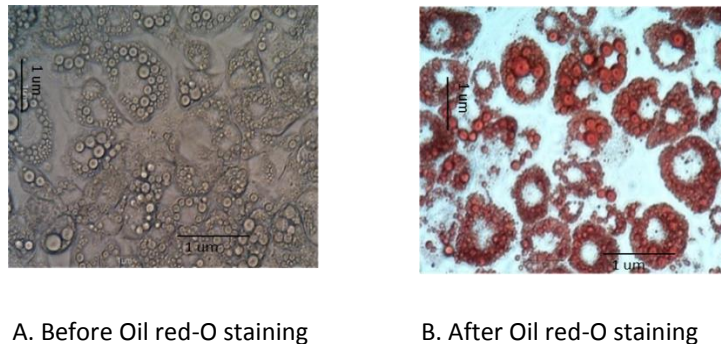


Figure 3.6 Microscopy of mature 3T3-L1 cells adipocytes before and after Oil Red-O staining. (A) 3T3-L1 adipocytes in DMEM supplemented with 10% FBS. (B) 3T3-L1 adipocytes in distilled water after Oil Red-O staining. (x40).

3.3.1.3 L6 cells morphology

L6 (Skeletal cells) were seeded in DMEM supplemented with 10% FBS in a 75 cm² flask at 1x10⁶ cells/ml and left over 5 days until reaching 60-70% confluence. The cells confluence followed and was depicted over the 5 days, as shown in Fig 3.7. Reaching 100% confluence, the media replaced with DMEM supplemented with 1% FBS allow L6 cells to use in culture to form multinucleated myotubes and striated fibers (Fig 3.8).

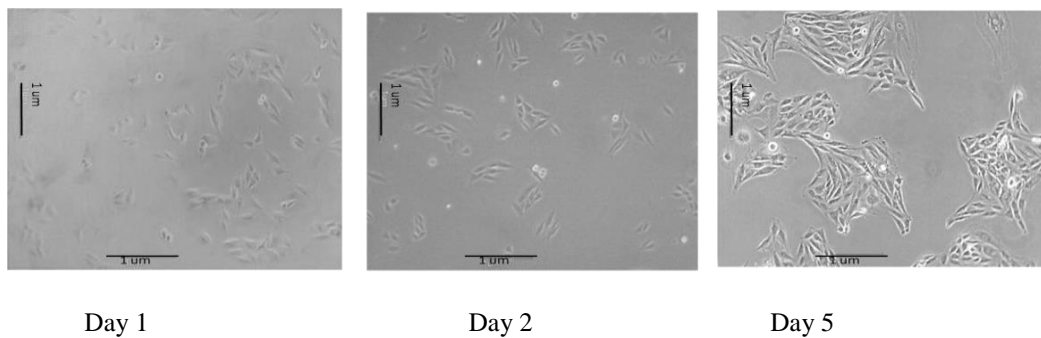


Figure 3.7 Images depicting the growth of L6 cells over a period of five days following seeding in 75 cm² flask at 1x10⁶ cells/ml in DMEM supplemented with 10% FBS at 37°C in an atmosphere containing 95% air and 5% CO₂ (x10).

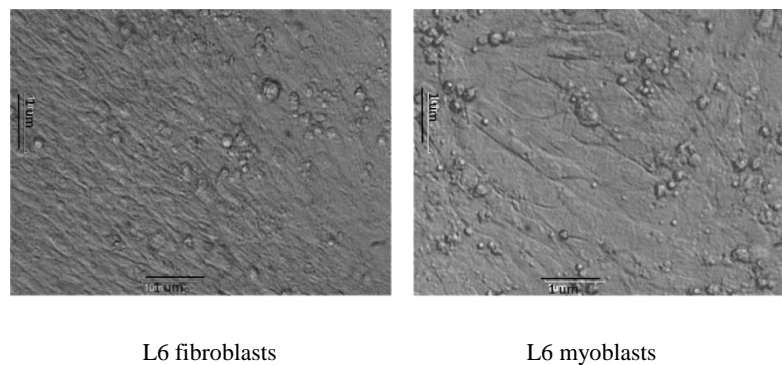


Figure 3.8 Images depicting the differentiation of L6 cells over a period of five days following differentiation in a 96-well black clear bottom plate (x40).

3.3.2 Effects of extracts from *A. cominia* on cell viability

Extracts from *A. cominia* were tested on HepG2, L6, 3T3-L1 fibroblasts and differentiated adipocytes to determine effects on the viability of cells grown in culture. As explained previously, among the several alternative assays available, measuring the levels of cell metabolism is the most sensitive, reliable, and convenient method for monitoring cell viability. Alamar blue and MTT assays were used to test for cell viability. For each assay, cell viability was calculated by comparing to the mean cell viability for each extract concentration or the vehicle (DMSO) as a percentage of the mean viability of the untreated cells (control). The control cells had a viability of 100% (see below). The differences between control and extract concentration of the treated cells were analysed for statistical significance by a one-way ANOVA Dunnett post-test. A *P* value of < 0.05 was considered significant.

3.3.2.1 Effects of extracts from *A. cominia* on HepG2 cell viability

The crude methanolic extract from *A. cominia* was tested on HepG2 cell viability. After 24 h of the addition of the extracts on HepG2 cells, no difference in cell viability between the control and the pre-treated HepG2 cells with the crude methanolic extract was shown by the Alamar blue test. There was no effect of the vehicle (1% DMSO) on the HepG2 viability. The results showed that the crude methanolic extracts from *A. cominia* (below 100 µg/ml) were not toxic on HepG2 cells (Fig 3.9).

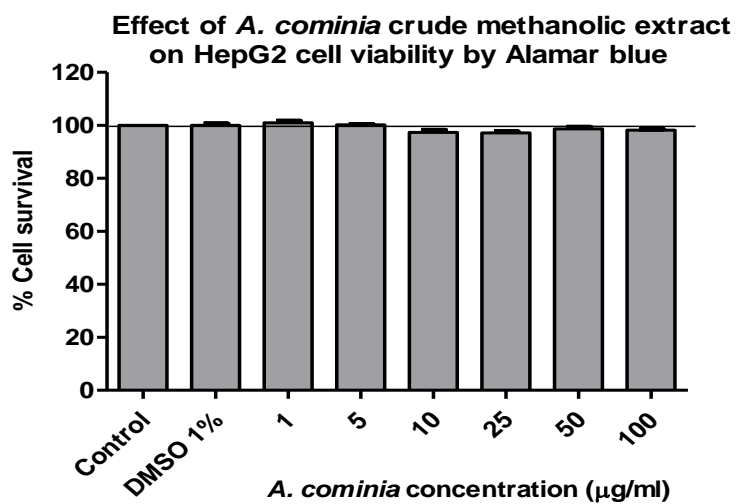


Figure 3.9 A lack of cytotoxic effect of the crude methanolic extract from *A. cominia* on HepG2 cell viability by Alamar blue test. Values are presented as percentage of control (\pm SEM) of three independent experiments. The data were analysed by Dunnett post-test, and no significant difference was shown by comparison to the control/DMSO 1%.

3.3.2.2 Effects of extracts from *A. cominia* on 3T3-L1 fibroblasts and adipocytes cell viability

A. Effect of crude AC extract on fibroblast viability

The effect of the methanolic crude extract of *A. cominia* on 3T3-L1 fibroblast viability was tested using Alamar blue to determine cell viability (Fig 3.10). There was no difference in cell viability between the control and treated 3T3-L1 cells with DMSO 1% or with *A. cominia* crude methanolic extract at 2.5 µg/ml. However, from 5 µg/ml, the AC methanolic crude extract produced a small (less than 10%) but significant reduction in the number of 3T3-L1 fibroblast viability compared to the control, with *P* value less than 0.05.

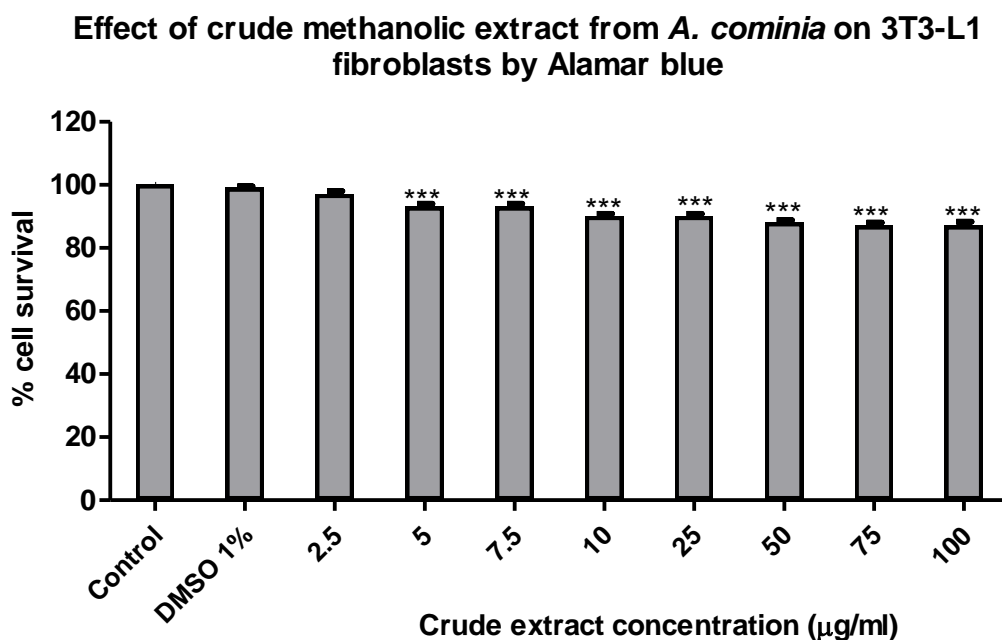


Figure 3.10 Cytotoxic effect of the methanolic crude extract from *A. cominia* on 3T3-L1 fibroblast viability by Alamar blue test. After 24 h of 3T3-L1 fibroblasts cell seeding in a 96-well clear plate. *A. cominia* crude methanolic extract was added to the wells (at different concentrations 1-100 µg/ml) and incubated at 37°C in an atmosphere containing 5% CO₂ for another 24 h. Then Alamar blue was added to the wells (10%) and incubated in the same conditions as before for 6 hours. Values are presented as percentage of control (± SEM). n=5. The data were analysed by Dunnett post-test, ****P*<0.05 versus control.

B. Effect of the crude methanolic extract from *A. cominia* on 3T3-L1 fibroblasts using Alamar blue and MTT assays

To confirm whether the cell viability results were affected by the Alamar blue test, MTT assay was done and results were compared. In both assays, vehicle controls did not change and the crude methanolic extract of *A. cominia* ($\geq 75 \mu\text{g/ml}$) produced a small but significant ($P < 0.05$) reduction in the number of viable 3T3-L1 fibroblast cells compared to the control (Fig 3.11).

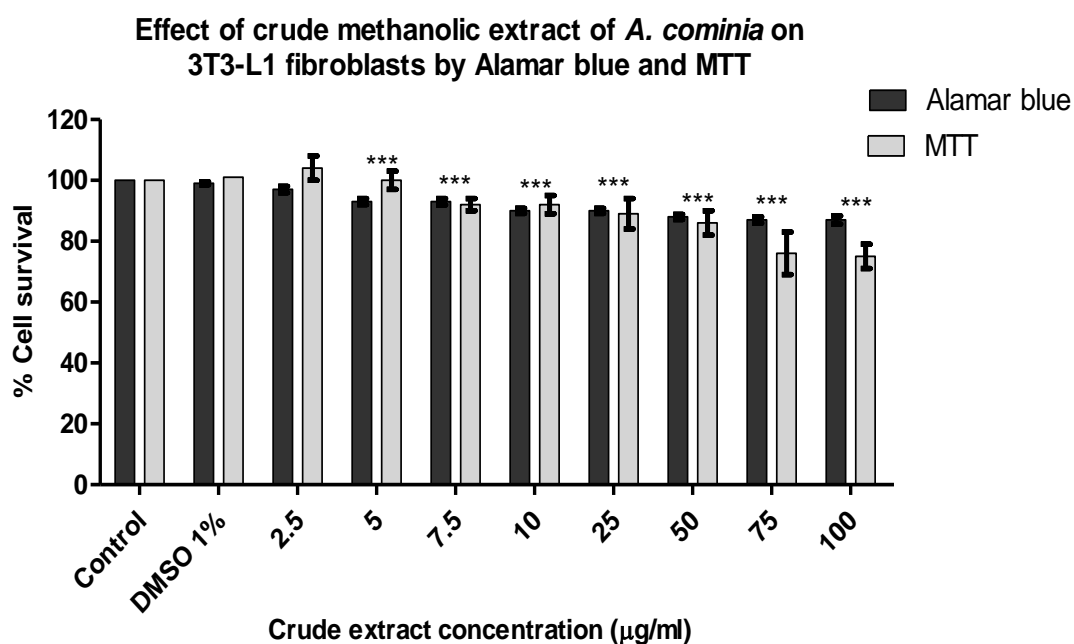


Figure 3.11 The methanolic crude extract from *A. cominia* cytotoxicity effect on 3T3-L1 fibroblast viability using Alamar blue test and MTT assays. Values are presented as percentage of control (\pm SEM). Both assays (Alamar blue and MTT) for testing the *A. cominia* crude extracts on 3T3-L1 fibroblasts were performed in a 96-well plate using the same conditions to compare their effects on the cell viability. The data were analysed by Dunnett post-test, *** $P < 0.05$ versus control of each assay.

C. Effect of extracts from *A. cominia* on 3T3-L1 fibroblasts viability

After the separation of the crude methanolic extract from *A. cominia*, the extracts were tested on the viability of non-differentiated 3T3-L1 fibroblasts using an MTT assay. Extracts from *A. cominia* (≤ 100 $\mu\text{g/ml}$), flavonoids (Fig 3.12.A), pheophytins (Fig 3.12.B) and tannins (Fig 3.12.C) were tested on the viability of 3T3-L1 fibroblasts. There was a significant decrease in the viability of 3T3-L1 fibroblasts at 100 $\mu\text{g/ml}$ of the flavonoids and tannins; therefore this decrease was acceptable (less than 10%).

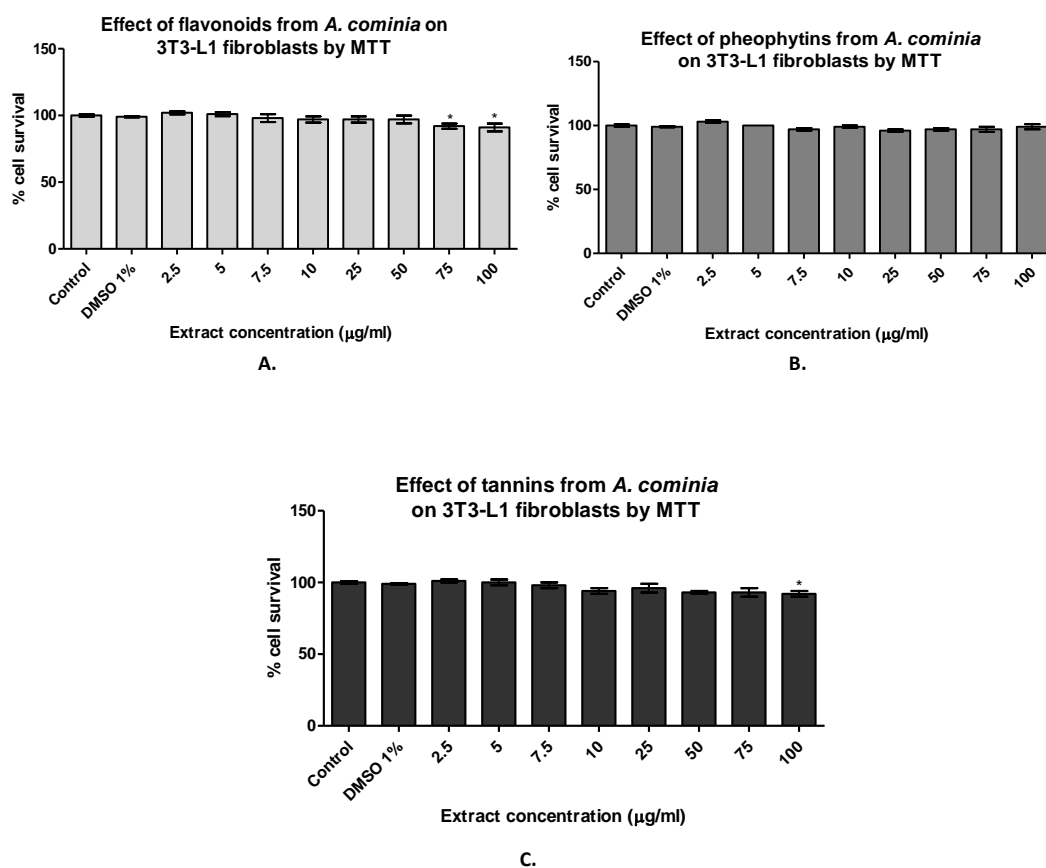


Figure 3.12 A lack of cytotoxic effect of different extracts from *A. cominia* on 3T3-L1 fibroblast viability by MTT test. A. Flavonoids, B. Pheophytins and C. Tannins. After 24 hours of cells seeding in a 96-well clear plate for 3T3-L1 fibroblasts, *A. cominia* extracts were added to the cells (at different concentrations) and incubated at 37°C in an atmosphere containing 5% CO₂ for another 24 h. Then the Alamar blue was added to the wells (10%) and incubated in the same conditions as before for 6 hours. Values are presented as percentages of cell viability (\pm SEM). n= 3. The data were analysed by Dunnett post-test, * $P < 0.05$ versus control.

D. Effect of extracts from *A. cominia* on 3T3-L1 adipocytes viability

The effect of 100 µg/ml of *A. cominia* extracts (flavonoids, pheophytins and tannins) on the viability of 3T3-L1 fibroblasts and adipocytes was tested using an MTT assay. On 3T3-L1 preadipocytes (Fig. 3.13.A), and adipocytes (Fig 3.13.B), there was no difference between control and vehicle controls (DMSO 1% or water 1% as the flavonoid sample was dissolved in water, pheophytins and tannins were dissolved in DMSO). The only significant decrease in cell number was found with flavonoids and tannins on both cell types; however, the decrease was less than 10% (4±3% with flavonoids, 8±2.7% with tannins on pre-adipocytes and 9±6% with flavonoids and 8±4% with tannins on adipocytes) and was not considered to be biologically important or relevant.

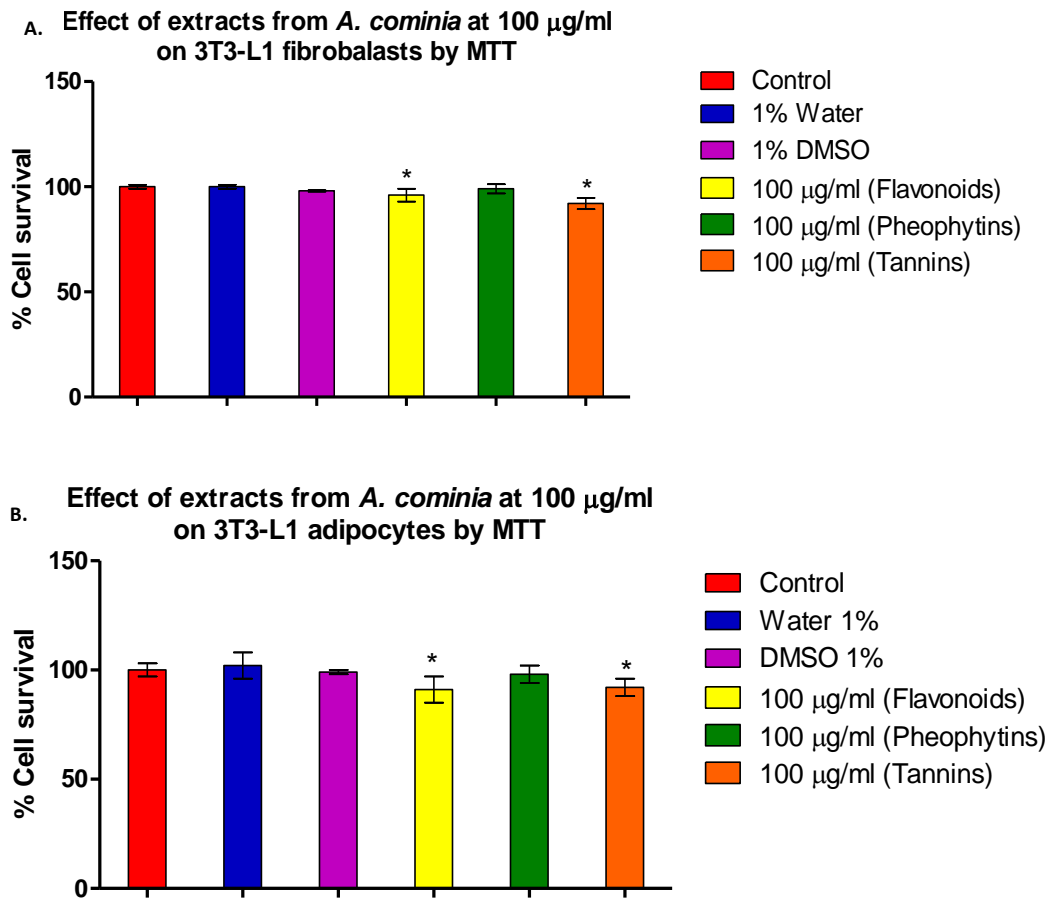
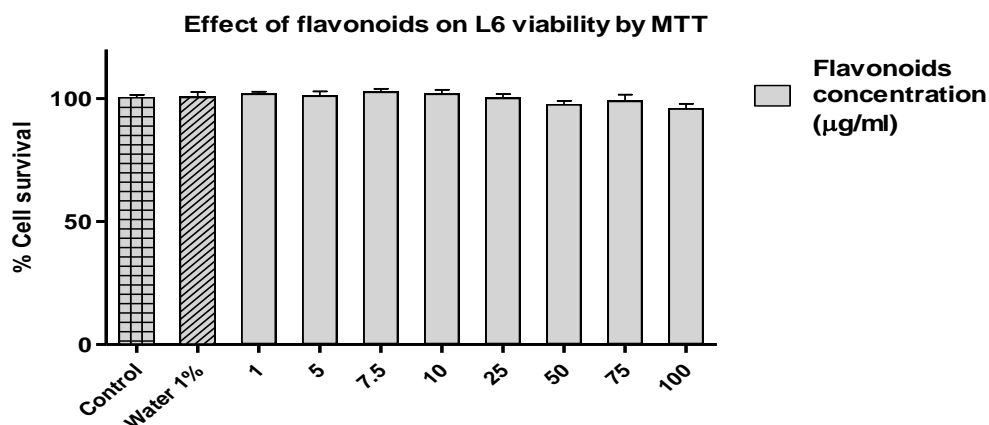


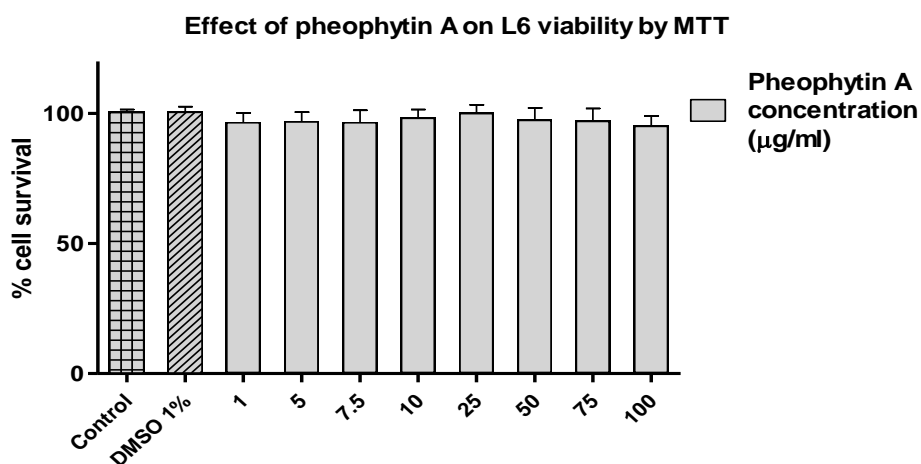
Figure 3.13 Lack of cytotoxic effect of different extracts of *A. cominia* (100 µg/ml) on 3T3-L1 fibroblasts (A) and 3T3-L1 adipocytes (B) viability by Alamar blue test. Values are presented as percentage of control (\pm SEM). $n=3$. The data were analysed by Dunnett post-test, * $P < 0.05$ versus control.

3.3.2.3 Effects of extracts from *A. cominia* on L6 myoblast viability

The effect of a range of concentrations of *A. cominia* extracts (flavonoids and pure pheophytin A) on the viability of L6 cells was tested. As shown below in Fig 3.14, there was no difference between control and vehicle controls. Neither extracts of *A. cominia*, flavonoids (Fig 3.14.A) and pheophytin A (Fig 3.14.B) had an effect on the viability of L6 cells, even at 100 µg/ml which was used later in the glucose uptake assay.



A. Effect of flavonoids containing extract from *A. cominia* on L6 cell viability.



B. Effect of pheophytin A compound from *A. cominia* on L6 cell viability.

Figure 3.14 No cytotoxic effect of a range of concentration of flavonoids (A) and pheophytin A (B) from *A. cominia* on L6 cell viability by MTT assay. Values are presented as percentage of control (\pm SEM). $n=5$. The data were analysed by Dunnett post-test, and no significant difference was shown.

3.3.2.4 Conclusion and discussion

To determine whether or not *A. cominia* extracts affected the cell viability of different cell lines *in vitro*, Alamar blue and MTT assays were used to test the effect of crude methanolic extract of *A. cominia* (AC) on different cell lines used (HepG2, 3T3-L1 fibroblasts, 3T3-L1 adipocytes and L6 cells). Comparing Alamar blue (AB) and MTT assays, the number of cells was greater in the former than in the latter. The reason for this could be that some of the floating or apoptotic cells may show some of the fluorescence in the presence of AB. Apoptotic cells were removed by MTT. The comparison between MTT and Alamar blue results confirmed that both are useful assays for testing cell survival, and that the MTT assay was more sensitive than the Alamar blue assay. Therefore, further cytotoxic assays were performed using MTT dye.

Vehicle controls did not affect the viability of any of the cell lines used, nor did extracts of *A. cominia* at different concentrations affect the viability of HepG2, 3T3-L1 fibroblasts, adipocytes or L6 cells. However, high concentrations of the extracts (particularly flavonoids and tannins >100 µg/ml) caused a small but statistically significant reductions in viable cells. A larger percentage of the cells (more than 90%) were still viable. This level of viability was acceptable for the glucose uptake assay because of the fragile nature of 3T3-L1 cells evidenced during the experiments where the cells were easily detached from the bottom of the cell culture plates.

3T3-L1 fibroblasts are a less frequently used model for studying glucose uptake. Previous studies on the expression of glucose transporters in 3T3-L1 fibroblasts have shown their translocation to the cell surface upon differentiation into adipocytes (Govers *et al.*, 2004).

3.3.3 Effect of extracts from *A. cominia* on 2-NBDG glucose uptake

To establish whether *A. cominia* extracts were able to stimulate the 2-NBDG uptake in cells or enhance the activity of exogenous insulin, we evaluated the effect of the flavonoid mixture and pheophytins on the glucose uptake by HepG2, L6, 3T3-L1 fibroblasts and differentiated 3T3-L1 adipocytes.

3.3.3.1 Effect of extracts from *A. cominia* on 2-NBDG glucose uptake by HepG2 cells

As shown below in Fig 3.15.A, insulin produced a concentration-dependent increase in 2-NBDG glucose uptake in HepG2 cells with EC_{50} 93 ± 21 nM. In the presence of 100 μ g/ml of AC crude extracts, the potency of insulin in increasing 2-NBDG uptake by HepG2 cells increased, with a 6.7-fold reduction in EC_{50} to 13 ± 2 nM.

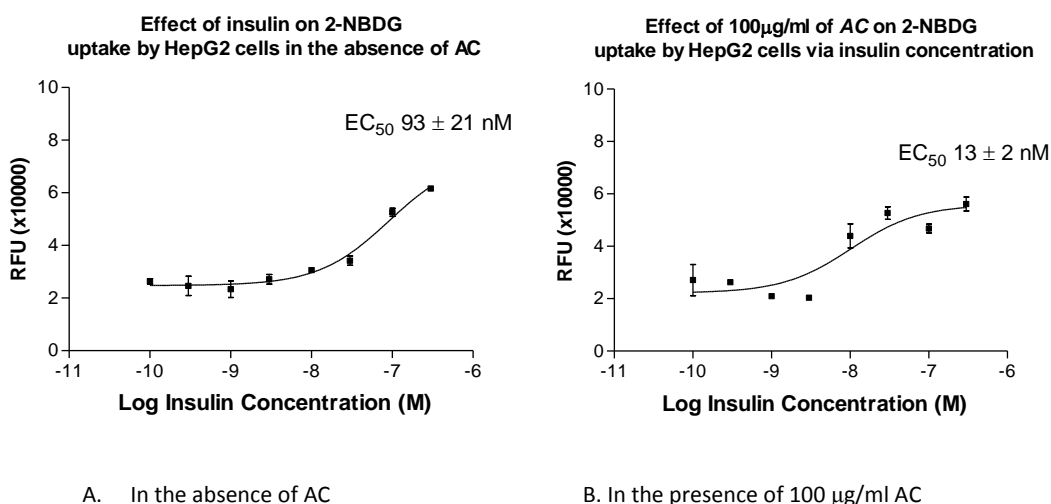


Figure 3.15 Concentration-dependent increase of 2-NBDG uptake by HepG2 produced by insulin. In the absence (A) or presence (B) of 100 μ g/ml of the crude methanolic extract of *A. cominia* (AC). HepG2 cells were incubated in the presence or absence of 100 μ g/ml of the extract for 24 hours, and then assayed for 2-NBDG glucose uptake. The data represent the mean of $RFU \pm SEM$ of three independent experiments. Insulin (0.1-300 nM) in the presence or absence of AC, EC_{50} 93 ± 21 nM and 13 ± 2 nM respectively.

Insulin produced a concentration-dependent increase in 2-NBDG glucose uptake in HepG2 cells (Fig 3.16). A significant enhancement of insulin-stimulated glucose uptake was observed from 50 nM, which increased by almost twice the basal level

where no insulin was added ($P < 0.05$). A marked enhancement of insulin-stimulated glucose uptake was observed in the presence of 100 $\mu\text{g/ml}$ of the crude methanolic extract of *A. cominia*. However, a significant difference was apparent through all the concentrations of insulin, in the presence of the extract in comparison to the basal level in the absence of both insulin and AC extract.

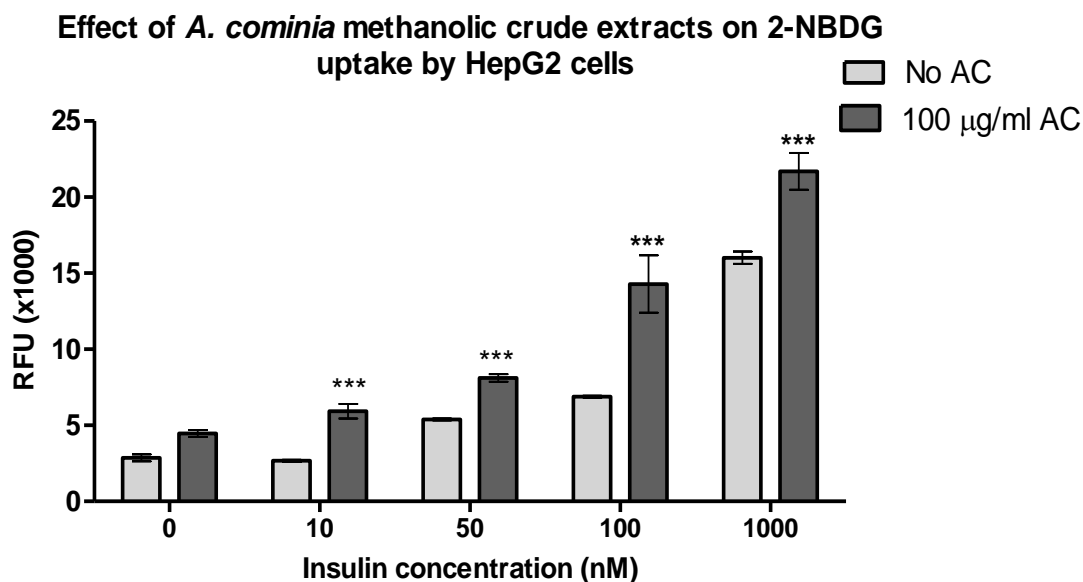


Figure 3.16 The methanolic crude extract of *A. cominia* (AC) produces an insulin concentration- dependent increase of 2-NBDG uptake by HepG2 cells. The data represent the mean of RFU \pm SEM of three independent experiments. The data were analysed by Dunnett post-test, *** $P < 0.05$ versus basal level of the non-AC insulin treated cells.

Uptake of 2-NBDG by HepG2 cells was enhanced by the addition of the crude methanolic extract of *A. cominia* in the presence or absence of 100 nM insulin. In the absence of insulin, the 2-NBDC uptake by HepG2 cells increased nine-fold. In the presence of insulin, the uptake of 2-NBDG was five-fold higher than it was without 100 nM insulin; however. In the presence of both 100 nM insulin and 100 $\mu\text{g/ml}$ of the methanolic extracts from *A. cominia*, the 2-NBDG uptake increased eleven-fold, as shown in Fig 3.17.

Effect of extracts from *A. cominia* on 2-NBDG uptake by HepG2 cells in the presence or absence of insulin

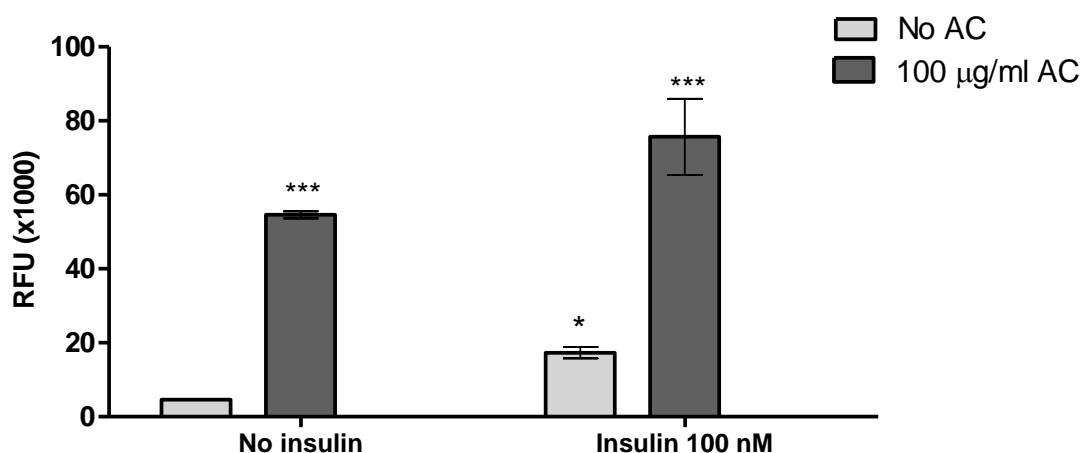


Figure 3.17 The methanolic extract from *A. cominia* increases 2-NBDG uptake by HepG2 liver cells in the presence or absence of 100 nM insulin. The data represent the mean \pm SEM of relative fluorescence unit (RFU) of three independent experiments. The data were analysed by Dunnett post-test, *** P <0.01 and * P <0.05 versus control untreated cells.

3.3.4 Effect of extracts from *A. cominia* on 2-NBDG glucose uptake by 3T3-L1 fibroblasts

Insulin produced a concentration-dependent increase in glucose uptake in 3T3-L1 fibroblasts and fully-differentiated adipocytes. A marked enhancement of insulin-stimulated glucose uptake by 3T3-L1 fibroblasts was seen from 50 nM in the absence of *A. cominia* (Fig 3.18). A significant increase in 2-NBDG glucose uptake was shown in the presence of *A. cominia* methanolic crude extract (starting from 10 nM of insulin) by comparison with the control (in the absence of insulin) was added to the 100 µg/ml of *A. cominia* methanolic extract. In the presence of 100 µg/ml of the crude methanolic extract from *A. cominia* (AC), insulin produced a concentration-dependent increase in glucose uptake. No significant difference was shown in the presence of AC extract. However, AC extract did not enhance insulin activity in comparison to the cells untreated by AC.

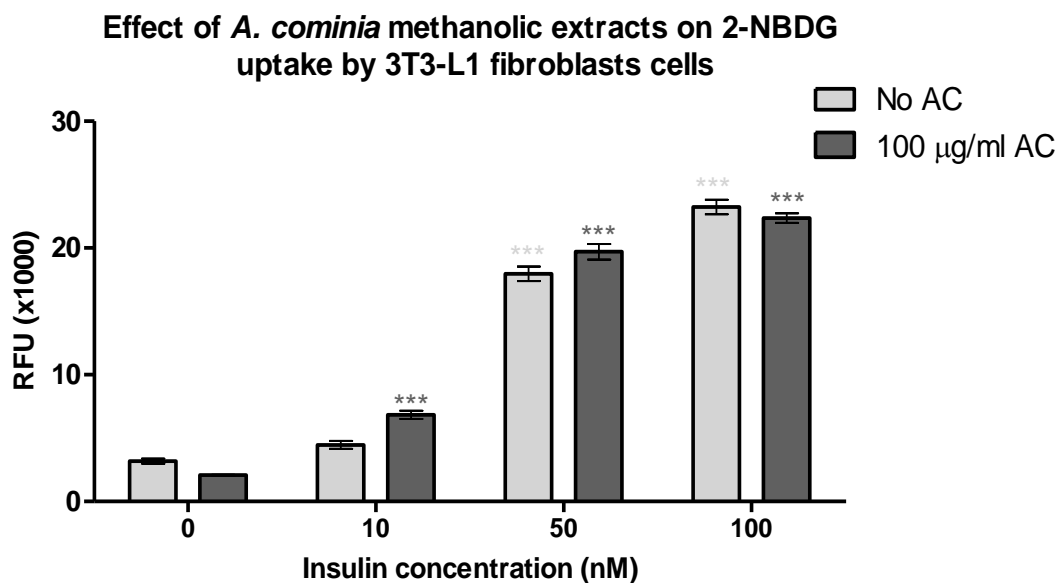


Figure 3.18 No effect of AC on insulin activity on 2-NBDG glucose uptake by non-differentiated 3T3-L1 fibroblasts. Insulin concentration-dependent effect on glucose uptake in the presence or absence of methanolic crude extracts of *A. cominia*. The data represent the mean \pm SEM of relative fluorescence unit (RFU) of three independent experiments. The data were analysed by Dunnett post-test, *** $P < 0.05$ versus basal level of the non-insulin treated cells in the absence of AC and *** $P < 0.05$ versus basal level of the non-insulin treated cells in the presence of AC.

An increase in 2-NBDG uptake by 3T3-L1 fibroblasts was shown (Fig 3.18) in the presence and absence of the methanolic crude extract from *A. cominia* with increases in insulin concentrations; however, the effect of the extract was small (Fig 3.19). The EC_{50} of insulin without AC was >1000 nM and in the presence of the extract, the EC_{50} was 38 ± 4 nM. Thus, AC enhances insulin activity,

Effect of 100 $\mu\text{g/ml}$ of *A. cominia* methanolic extract (AC) on 2-NBDG uptake by 3T3-L1 fibroblasts via insulin concentration

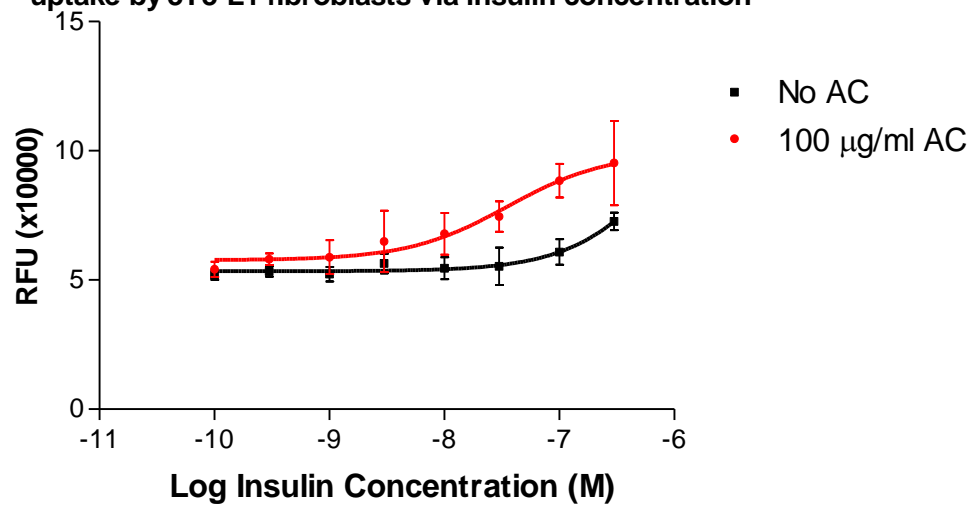


Figure 3.19 The crude extracts from *A. cominia* produce a concentration-dependent uptake of 2-NBDG in non-differentiated fibroblasts via insulin concentration. The data represent the mean \pm SEM of relative fluorescence unit (RFU) of $n=4$. EC_{50} without AC was >1000 nM, and EC_{50} in the presence of AC was 38 ± 4 nM. Insulin concentration range was 0.1 to 300 nM.

3.3.5 Effect of insulin, 2-NBDG and cell density on the glucose uptake by 3T3-L1 adipocyte cells

To confirm the optimum 2-NBDG concentration, insulin concentration and 3T3-L1 density, glucose uptake was carried out using various concentrations of 2-NBDG, insulin and two 3T3-L1 cell densities. Differentiated 3T3-L1 adipocytes showed an increase in the uptake with the increasing concentrations of 2-NBDG in the presence or absence of 100 nM of insulin (Fig 3.21). Insulin produced an increase in glucose uptake in the absence of *A. cominia* (Fig 3.20). The highest uptake in the presence or absence of insulin was with 100 μ M of 2-NBDG (Fig 3.21). The effect of insulin in producing a concentration-dependent increase in 2-NBDG uptake in fully differentiated 3T3-L1 adipocytes was then observed, as shown in Fig 3.20.

Different concentrations of 3T3-L1 fibroblasts were seeded and fully differentiated into adipocytes and then assayed for 2-NBDG uptake in the presence of 100 nM insulin and in the presence of different concentrations of 2-NBDG. The highest cell density (8000 cells/well) showed an increase in the uptake of more than twofold compared to 4000 cells/well (Fig 3.22).

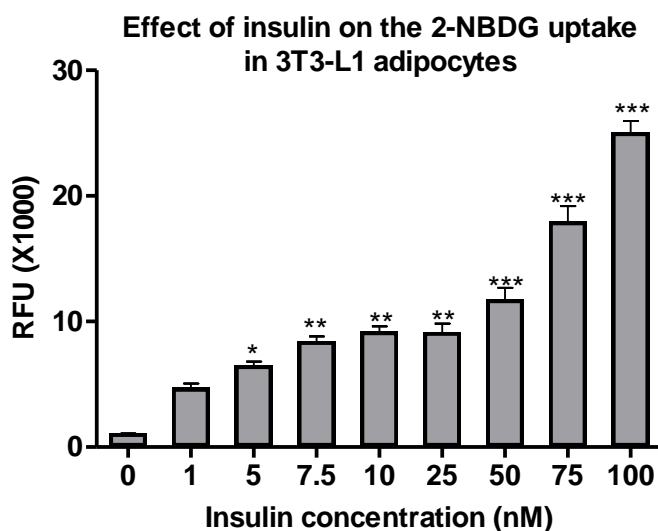


Figure 3.20 Insulin produces a concentration-dependent increase of 2-NBDG glucose uptake in fully differentiated adipocytes in the absence of crude extracts of *A. cominia*. The data represent the mean \pm SEM of relative fluorescence unit (RFU) $n=3$. The data were analysed by Dunnett post-test, *** $P<0.05$ versus basal level of the non-insulin treated cells.

Effect of insulin on the 2-NBDG uptake by 3T3-L1 adipocytes via 2-NBDG concentration

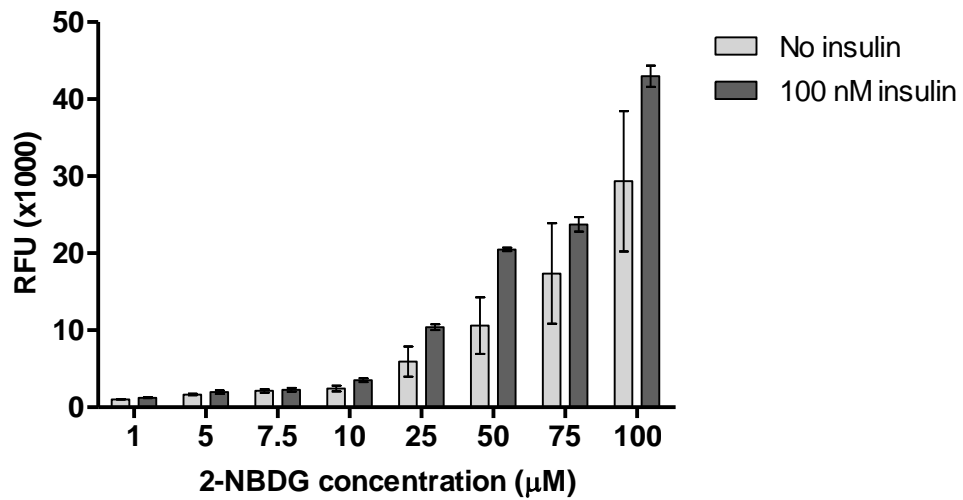


Figure 3.21 2-NBDG produces a concentration-dependent uptake by fully-differentiated 3T3-L1 cells in the absence of *A. cominia*. The data represent the mean \pm SEM of relative fluorescence unit (RFU) n=3.

Effect of fibroblasts cell density on glucose uptake by 3T3-L1 adipocytes in the presence of 100nM insulin via 2-NBDG concentration

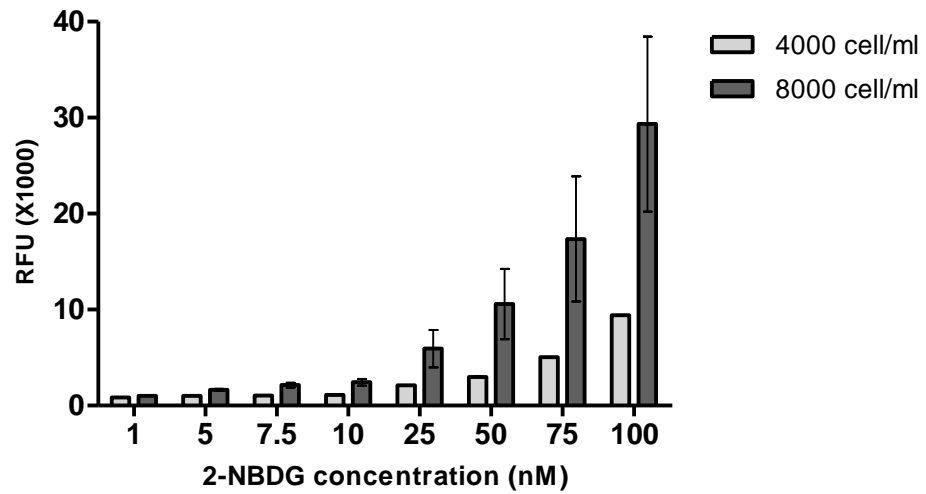


Figure 3.22 Increased fibroblast seeding density increases 2-NBDG glucose uptake in fully-differentiated adipocytes. The data represent the mean \pm SEM of relative fluorescence unit (RFU) n=4.

3.3.6 Effect of extracts from *A. cominia* on 2-NBDG glucose uptake by 3T3-L1 adipocytes

Insulin (100 nM) produced an increase of glucose uptake in fully differentiated 3T3-L1 adipocytes by comparison to the basal level where no insulin was added (Fig 3.23). The crude extract of *A. cominia* did not show any enhancement of 2-NBDG uptake by 3T3-L1 adipocytes in the presence or absence of 100 nM insulin (Fig 3.24).

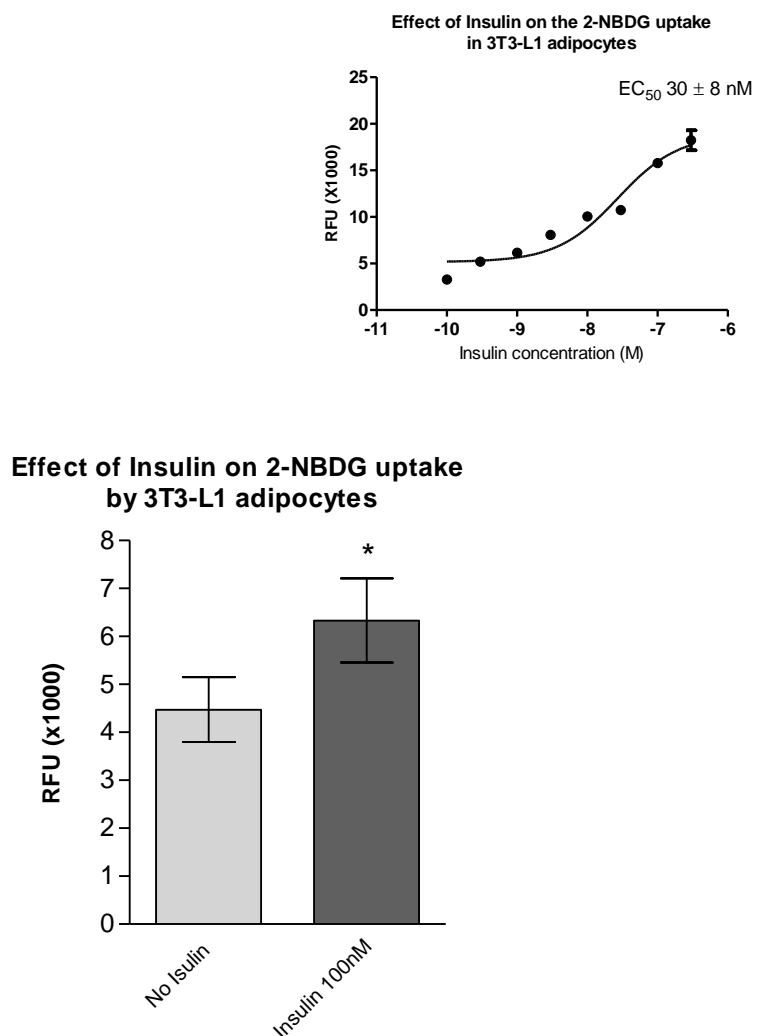


Figure 3.23 Effect of *A. cominia* on 2-NBDG uptake by fully-differentiated adipocytes in the presence or absence of 100 nM insulin. Insert shows the insulin concentration-dependent curve (0.1-300 nM) with EC₅₀ 30 ± 8 nM.

Effect of insulin and methanolic crude extract from *A. cominia* (AC) on 2-NBDG uptake by 3T3-L1 adipocytes

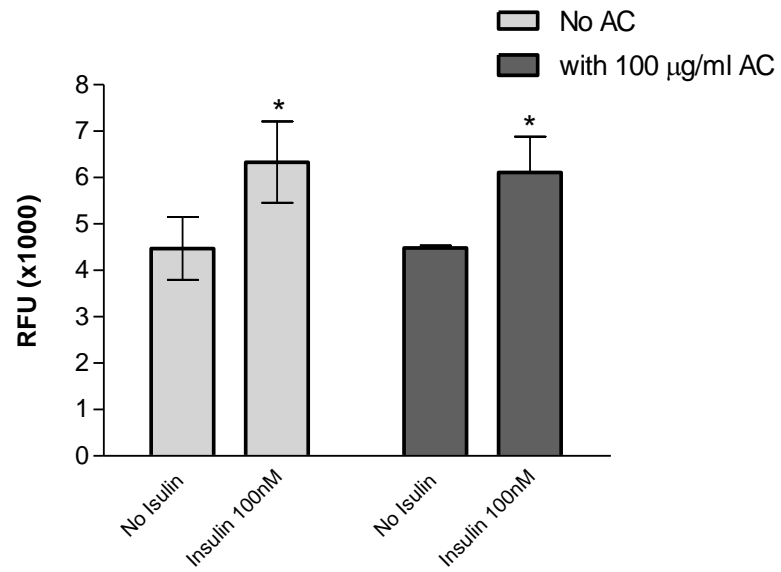


Figure 3.24 Effect of *A. cominia* crude extract on 2-NBDG uptake by differentiated 3T3-L1 fibroblasts in the presence or absence of 100 nM insulin. The data represent the mean \pm SEM of relative fluorescence unit (RFU) $n=3$. The data was analysed by Dunnett post-test, $*P<0.05$ versus basal level of the non-insulin treated cells in the presence or absence of AC.

3.3.7 Effect of extracts from *A. cominia* on 2-NBDG glucose uptake by L6 cells

As shown in Fig 3.25, there was a small increase in 2-NBDG glucose uptake by L6 cells with increasing concentrations of insulin in the absence of AC ($EC_{50} 28.6 \pm 0.7$ nM). L6 cells were treated for 24 hours with 10 and 100 $\mu\text{g/ml}$ of flavonoids or pheophytin A. As shown in Figs 3.26 and 3.27, insulin produced a concentration-dependent increase of glucose uptake. In the presence of 100 $\mu\text{g/ml}$ flavonoids and pheophytins, the uptake increased and EC_{50} decreased to 0.08 ± 0.02 nM and 5 ± 0.9 nM, respectively.

Flavonoid and pheophytin samples produced an increase of glucose uptake in differentiated L6 cells in the presence of 100 nM insulin. The data in the presence of flavonoids and pheophytin A extracts were not sigmoid; therefore, EC_{50} would not be accurate (Figs 3.28 and 3.29).

Insulin (100 nM) increased the uptake of 2-NBDG by L6 cells two-fold compared to the control (non-treated cells). A significant increase in glucose uptake and enhancement of insulin activity were observed in the presence of 100 $\mu\text{g/ml}$ of flavonoids containing extracts ($P < 0.05$). Four fold increase in the glucose uptake and two fold increase of insulin activity were observed in the presence of flavonoids sample. A significant increase in 2-NBDG uptake was also marked in the presence of 100 $\mu\text{g/ml}$ of pheophytin A. An eight-fold increase in the glucose uptake and a four-fold enhancement of insulin activity were observed in the presence of pheophytin A. Insulin activity was not enhanced in the presence or absence of either extract at 10 $\mu\text{g/ml}$ (Fig 3.30).

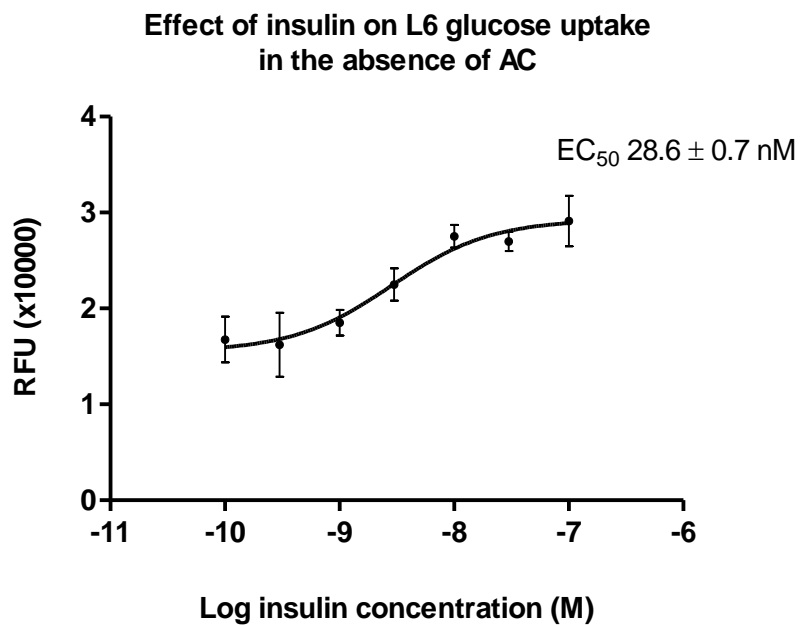


Figure 3.25 Insulin produces an increase in 2-NBDG uptake by L6 cells in the absence of *A. cominia*. Data represent the mean \pm SEM relative fluorescence unit (RFU). n=3.

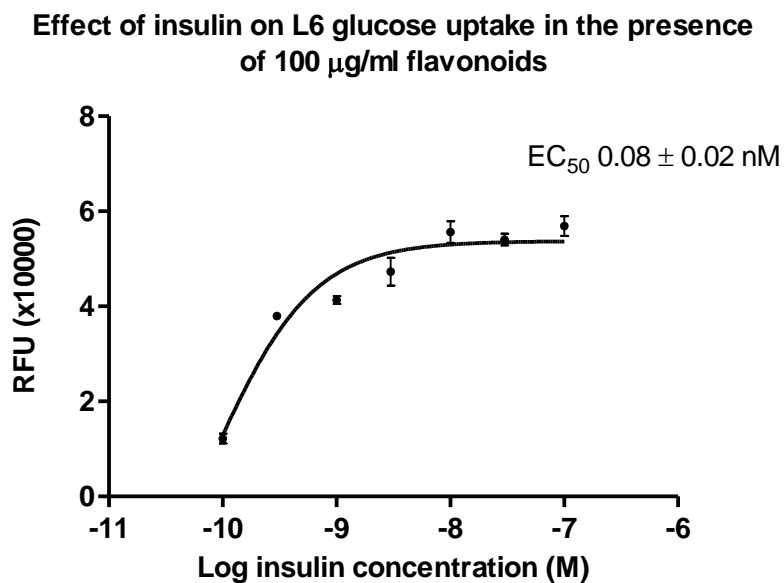


Figure 3.26 Insulin produces a concentration-dependent uptake of 2-NBDG by L6 cells in the presence of 100 $\mu\text{g/ml}$ of flavonoids from *A. cominia*. The data represent the mean \pm SEM of relative fluorescence unit (RFU) n=3.

Effect of insulin on L6 glucose uptake in the presence of 100 $\mu\text{g/ml}$ pheo A

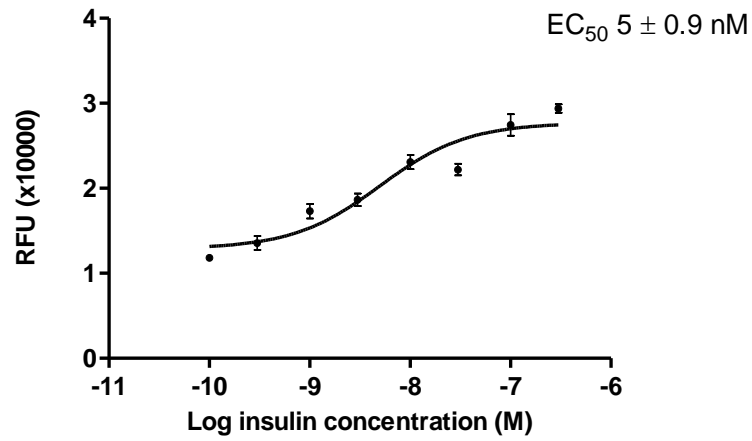


Figure 3.27 Insulin produces a concentration-dependent uptake of 2-NBDG by L6 cells in the presence of 100 $\mu\text{g/ml}$ of pheophytin A from *A. cominia*. The data represent the mean \pm SEM relative fluorescence unit (RFU) $n=3$.

Effect of flavonoids on L6 glucose uptake in the presence of 100 nM insulin

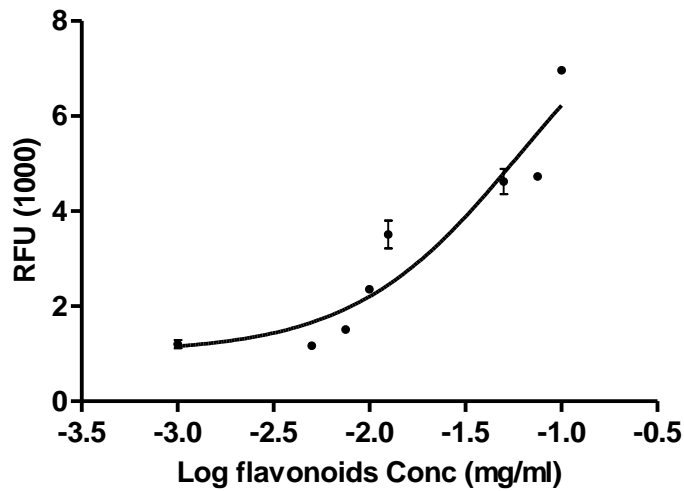


Figure 3.28 Flavonoid extract from *A. cominia* produces a concentration-dependent uptake of 2-NBDG by L6 cells in the presence of 100 nM insulin. The data represent the mean \pm SEM of relative fluorescence unit (RFU) $n=3$.

Effect of pheophytins on L6 glucose uptake in the presence of 100 nM Insulin

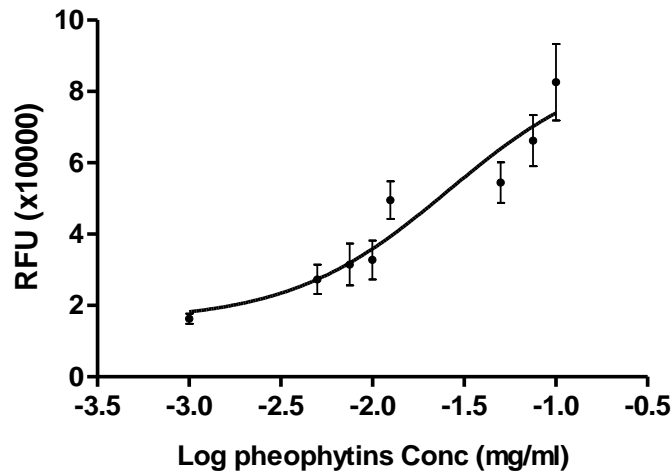


Figure 3.29 Pheophytin A extract from *A. cominia* produces a concentration-dependent uptake of 2-NBDG by L6 cells in the presence of 100 nM insulin. The data represent the mean \pm SEM of relative fluorescence unit (RFU) n=3.

Effect of insulin and AC extract on 2-NBDG uptake by L6 cells

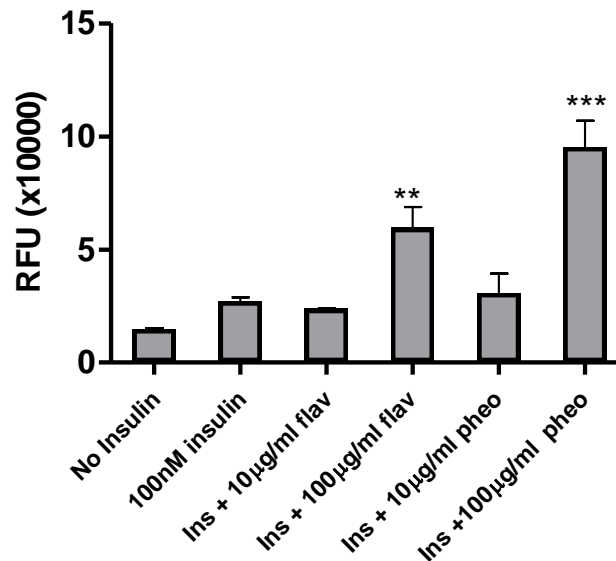


Figure 3.30 Flavonoids and pheophytin A from *A. cominia* enhance insulin activity in 2-NBDG uptake by L6 cells. Extracts (flav for flavonoids and phoe for pheophytins) were used at 10 or 100 μ g/ml. L6 cells were seeded and differentiated in 96-well plates and incubated for 24 hours with the *A. cominia* extracts (10 or 100 μ g/ml) at 37°C in an atmosphere containing 5% CO₂ and then assayed for 2-NBDG glucose uptake. The data represent the mean \pm SEM of relative fluorescence unit (RFU) n=3. The data were analysed by Dunnett post-test. ** $P < 0.05$ and *** $P < 0.01$ versus basal level of the non-insulin treated cells.

3.4 Conclusion and discussion

Insulin produced a concentration-dependent stimulation of 2-NBDG uptake (compared to the control untreated cells) by HepG2, 3T3-L1 fibroblasts, adipocytes and L6 cells, which confirms that these cell lines were responsive to insulin. HepG2 cells were reaching 70% confluence in three days. However, for unknown reasons, these cells were growing on top of each other in a way affecting the results of the glucose uptake, and therefore the usage of L6 cells as another cell line for the study of the glucose uptake was necessary. An important functional aspect of these cells, particularly differentiated 3T3-L1 adipocytes, is insulin sensitivity. Insulin EC₅₀ of 93 ± 21 nM in HepG2 cells decreased to 13 ± 2 nM in the presence of the methanolic crude extract of AC. In 3T3-L1 fibroblasts, insulin had an EC₅₀ of >1000 nM that decreased to 38 ± 4 nM in the presence of AC extract. However, in adipocytes, insulin produced a significant concentration-dependent increase and an EC₅₀ of 30 ± 8 nM was a further confirmation of the insulin responsiveness of the adipocytes to the insulin. The results are consistent with the general observation that newly developed adipocytes show increased insulin responsiveness and take up more glucose than fibroblasts (Xu *et al.*, 2006). In L6 cells, insulin also produced a concentration-dependent increase with an EC₅₀ of 28.6 ± 0.7 nM; EC₅₀ decreased to 0.08 ± 0.02 nM and 5 ± 0.9 nM in the presence of 100 µg/ml of flav and pheo, respectively. This serves to confirm the importance of AC extracts in lowering the insulin concentration needed in diabetic models by enhancing insulin activity.

An incubation time of 1 h was chosen to avoid insulin degradation. For the glucose uptake assay, an incubation time of 24 h was chosen for the extracts because of the experience with the *in vivo* studies carries out by Veliz *et al.* (2003) on *A. cominia*. Cell density of 8x10³ cells/ml, 100 nM insulin and 100 µM of 2-NBDG were chosen for higher glucose uptake.

Methanolic crude extract of *A. cominia*, flavonoids and pheophytins produced significant ($P < 0.05$) increases in 2-NBDG glucose uptake compared to the control of untreated cells (HepG2, 3T3-L1 adipocytes and L6).

Differentiation of 3T3-L1 cells done *in vitro* was having difficulties while the differentiation process. In 96 black well plates, 25 cm² flasks and 12 well plates the differentiation of the cells was not similar. Therefore, the experiments carried out on 3T3-L1 differentiated adipocytes in a 96-well plate and the well-to-well variation affected the activity of AC extracts on 2-NBDG glucose uptake. However, the differentiation was better in 25 cm² flasks; then 2-deoxy-D-glucose uptake followed and measured by MS analysis, which is assumed to be more accurate.

Many researchers have shown that the stimulation of glucose uptake by HepG2, L6 and 3T3-L1 fibroblasts is a well-recognised mechanism of action of anti-diabetic drugs and plants which have insulin-like activities (Wang *et al.*, 2011; Wang *et al.*, 1999; Xu *et al.*, 2006; Alonso-Castro *et al.*, 2008; Hu and Wang, 2011). However, the activity of *A. cominia* extracts on 2-NBDG glucose uptake reported in this project did not provide any information on the mechanism pathways involved in producing this activity, thus requiring further work, including enzymes tests.

3.5 Effect of extracts from *A. cominia* on 2-deoxy-D-glucose uptake by 3T3-L1 by MS

3.5.1 Effect of wortmannin on insulin activity

3T3-L1 cells were differentiated using troglitazone as to enhance differentiation. The glucose uptake assay was then performed using insulin and wortmannin. After blocking the uptake of 2-deoxy-D-glucose using pre-cold PBS, cells were harvested and the metabolites were extracted. Samples were submitted for MS (method explained in chapter 3, section 3.2.6.3) for further confirmation of the insulin activity. MS results were obtained from the Metabolomics Facility at Strathclyde University. The parameters measured to detect the 2-deoxy-D-glucose uptake in 3T3-L1 adipocytes were peak time (retention time, RT) and the area under the peak curve of it (MA) for quantifying the glucose uptake in each treatment. Firstly, the parameters were measured for the standard (2-deoxy-D-glucose), and then were compared with the results of the samples to confirm the glucose uptake in 3T3-L1 adipocytes. 2-Deoxy-D-glucose produced a concentration-dependent increase of the area under the curve (Fig 3.31). R^2 was 0.98. The unknown 2-DG concentration uptake by 3T3-L1 cells after each reading was calculated using the equation presented in Fig 3.31 ($y = 0.1042 x - 0.0937$; where x is the 2-DG concentration).

By comparing with the control cells (in the absence of insulin), the glucose uptake increased significantly by three-fold in the presence of 100 nM insulin (Fig 3.32). Wortmannin (inhibitor) decreased the glucose uptake by two-fold in comparison to insulin-treated cells. 34.4 $\mu\text{g/ml}$ of 2-DG was uptake by 3T3-L1 adipocytes in the presence of insulin (tested in 25 cm^2 flask). 2-DG concentrations uptake by 3T3-L1 adipocytes in the presence of insulin, inhibitor and both insulin and inhibitor were 8.6 $\mu\text{g/ml}$, 14 $\mu\text{g/ml}$ and 18.5 $\mu\text{g/ml}$ respectively (Table 3.2).

Standard curve of 2-deoxy-D-glucose by MS

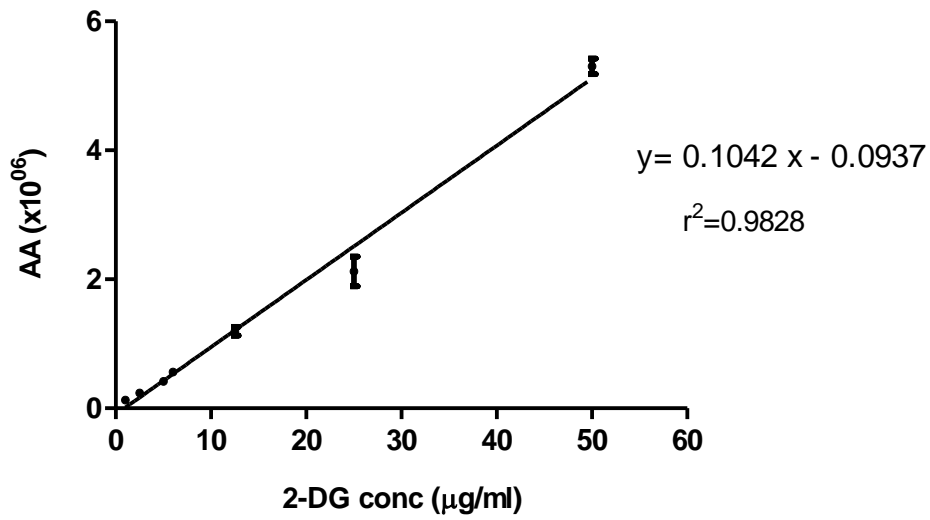


Figure 3.31 2-Deoxy-D-glucose standard curve. Data are presented as mean \pm SEM of AA ($\times 10^6$) via 2-deoxy-D-glucose concentration ($\mu\text{g/ml}$) of three independent experiments. AA represents the area under the curve obtained by MS.

Effect of insulin and wortmannin on 2-DG glucose uptake by 3T3-L1 adipocytes

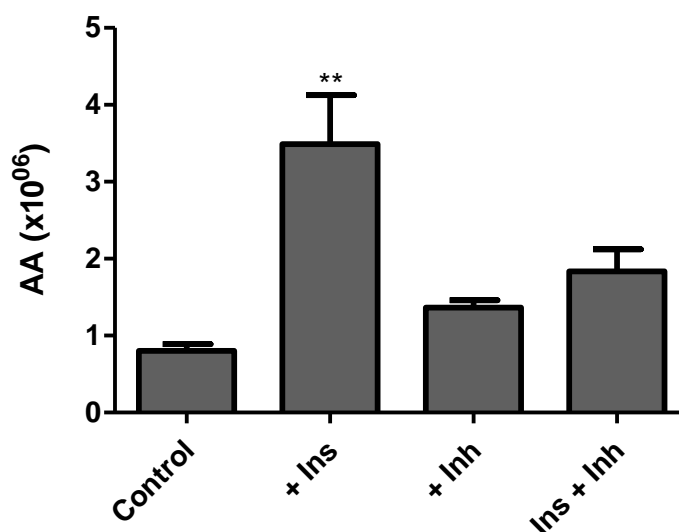


Figure 3.32 100 nM insulin increases 2-deoxy-D-glucose (2-DG) uptake by differentiated 3T3-L1 (metabolites), whereas Inh is the inhibitor which is wortmannin (10 nM) inhibits insulin activity. AA represents the area under the curve. Results are presented as AA± SEM of three independent experiments. Data was analysed by Dunnet post-test, ** $P < 0.05$ versus control.

Treatment	Mean AA	2-DG (µg/ml)
No addition	0.8	8.6
+ Inh	1.4	14.0
+ Ins	3.5	34.4
Ins + Inh	1.8	18.5

Table 3.2 Concentration of 2-deoxy-D-glucose uptake uptake by 3T3-L1 cells of different pre-treated cells in the presence or absence of insulin 100 nM (Ins) and 10 nM of wortmannin (Inh). 2-DG concentration expressed in µg/ml were calculated with relevance to the AA (area under the curve by MS).

3.5.2 Effect of pheophytins on 2-DG uptake analysed by MS

The data presented in Fig 3.33 were used to quantify glucose uptake by 3T3-L1 adipocytes in the presence or absence of 100 µg/ml of pheophytin A extracted from *A. cominia*. In comparison with the control (non-treated cells), 2-DG uptake increased two-fold in the presence of 100 nM insulin. 100 µg/ml pheophytin increased 2-DG uptake by two folds in the absence of insulin. However, 2-DG uptake by 3T3-L1 adipocytes increased in the presence of both 100 nM insulin and 100 µg/ml pheophytin by comparison with the control, although the increase was not statistically significant (Fig 3.33).

2-DG uptake by the untreated 3T3-L1 adipocytes was 10.3 µg/ml. Treated with 100 nM insulin, the uptake was 18.5 µg/ml and in the presence of 100 µg/ml of pheophytin, the uptake was 16.6 µg/ml in the absence of insulin. In the presence of 100 nM insulin, pheophytin (100 µg/ml) increased the uptake 18.6 µg/ml of 2-DG (Table 3.3).

Effect of insulin and pheophytin A on 2-DG glucose uptake by 3T3-L1 adipocytes

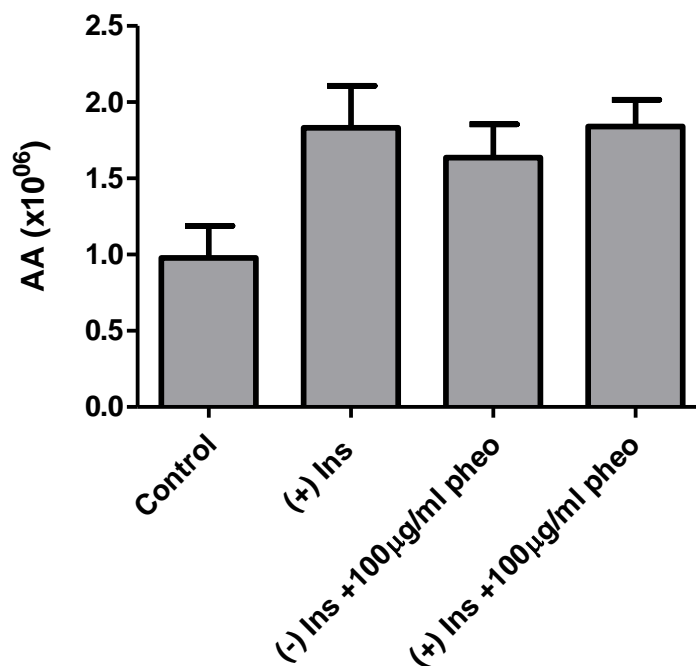


Figure 3.33 Pheophytin A increases 2-deoxy-D-glucose uptake by differentiated 3T3-L1 adipocytes. Values are presented as AA \pm SEM. AA represents the area under the curve of three independent experiments. Data were analysed by Dunnet post-test, no significant difference was shown.

Treatment	Mean AA	2-DG ($\mu\text{g/ml}$)
(-) Ins - pheo	1.0	10.3
(+) Ins	1.8	18.5
(-) Ins +100µg/ml pheo	1.6	16.6
(+) Ins +100µg/ml pheo	1.8	18.6

Table 3.3 Concentration of 2-deoxy-D-glucose uptake by 3T3-L1 cells of different pre-treated cells in the presence or absence of insulin 100 nM (Ins) and 100 $\mu\text{g/ml}$ of pheophytin A (pheo). 2-DG concentrations expressed in $\mu\text{g/ml}$ were calculated in relevance to the AA (area under the curve by MS).

3.5.3 Effect of flavonoids on 2-DG uptake analysed by MS

The data, presented in Fig 3.34 were used to quantify glucose uptake by 3T3-L1 adipocytes in the presence or absence of 100 µg/ml of flavonoids containing extract from *A. cominia*. In comparison to the control (non-treated cells), 2-DG uptake was not affected by the presence of 100 nM insulin as well as in the presence of 100 µg/ml flavonoids (in the absence of 100 nM insulin). However, in the presence of both insulin and 100 µg/ml flavonoids, the uptake increased two-fold (Fig 3.34).

2-DG uptake by the untreated 3T3-L1 adipocytes was 9.3 µg/ml. Treated with 100 nM insulin, the uptake was 6.7 µg/ml and in the presence 100 µg/ml of flavonoids, the uptake was also 8 µg/ml. Flavonoids at 100 µg/ml increased the uptake to 15.6 µg/ml of 2-DG in the presence of 100 nM insulin (Table 3.4).

Effect of insulin and flavonoids on 2-DG glucose uptake by 3T3-L1 adipocytes

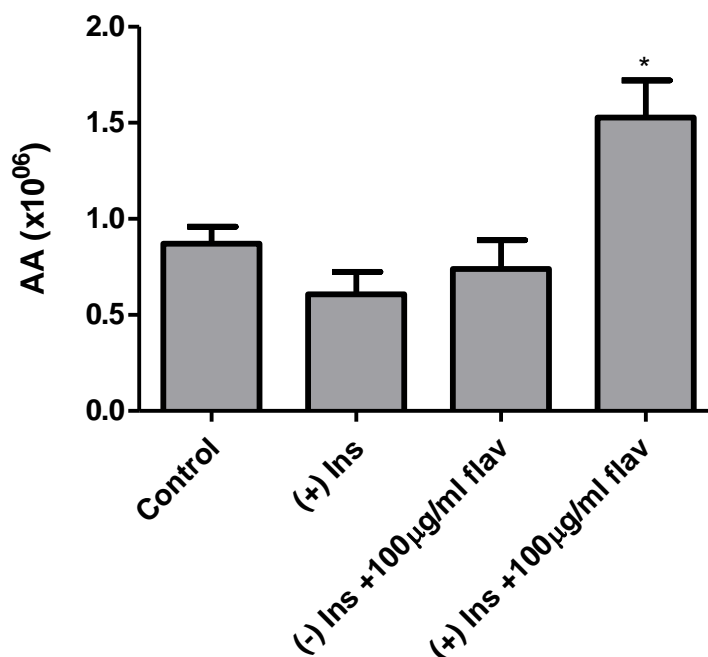


Figure 3.34 Flavonoid extract from *A. cominia* enhances insulin activity in 2-deoxy-D-glucose uptake by differentiated 3T3-L1 (metabolites). AA represents the area under the curve of three experiments. Data were analysed by Dunnet post-test, * $P < 0.05$ versus control.

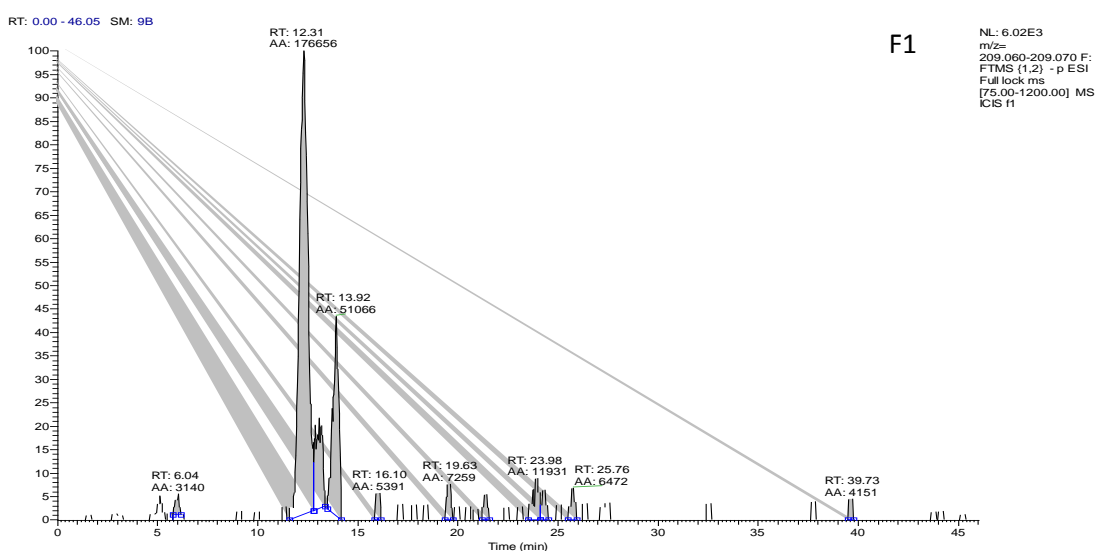
Treatment	Mean AA	2-DG ($\mu\text{g/ml}$)
(-) Ins	0.9	9.3
(+) Ins	0.6	6.7
(-) Ins +100µg/ml flav	0.7	8.0
(+) Ins +100µg/ml flav	1.5	15.6

Table 3.4 Concentration of 2-deoxy-D-glucose uptake by 3T3-L1 cells of different pre-treated cells in the presence or absence of insulin 100 nM (Ins) and 100 µg/ml of flavonoids (flav). 2-DG concentrations expressed in µg/ml were calculated with relevance to the AA (area under the curve by MS).

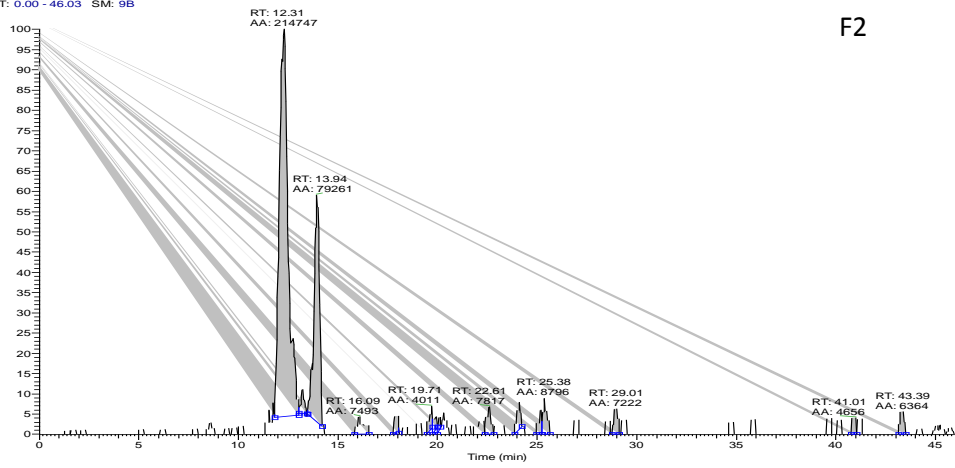
3.5.4 Effect of differentiation on 2-deoxy-D-glucose uptake analysed by MS

The cells were differentiated in the absence or presence of troglitazone, TNF- α , flavonoids or pheophytins in 25 cm² flasks, then 2-deoxy-D-glucose uptake was quantified by MS. The data presented in Fig 3.35 were followed to measure the glucose uptake by the cells. As shown below, peak F1 is control, while peaks F2, F3, F4 and F5 are for cells treated with troglitazone, TNF- α , flavonoids, and pheophytin A respectively. A significant increase (2.5 fold) in 2-DG glucose uptake was shown by 3T3-L1 pre-treated cells by flav and pheo, as well a low but statistically significant decrease of the 2DG uptake in the TNF- α (2.5 fold decrease) pre-treated cells by comparison with the control/untreated cells (F1) (Fig 3.36).

2-DG concentration uptake by the untreated control 3T3-L1 adipocytes was very low, 2.7 μ g/ml as well as in the pre-treated cells with troglitazone, 3.3 μ g/ml. In the pretreated cells with 100 μ g/ml of flavonoids and pheophytin A, the uptake was higher (2-DG uptake was 6.1 and 5.2 μ g/ml respectively). In cells pre-treated with TNF- α 2-DG uptake was significantly decreased by comparison to the control untreated cells (2-DG uptake was 1.8 μ g/ml) (table 3.5).



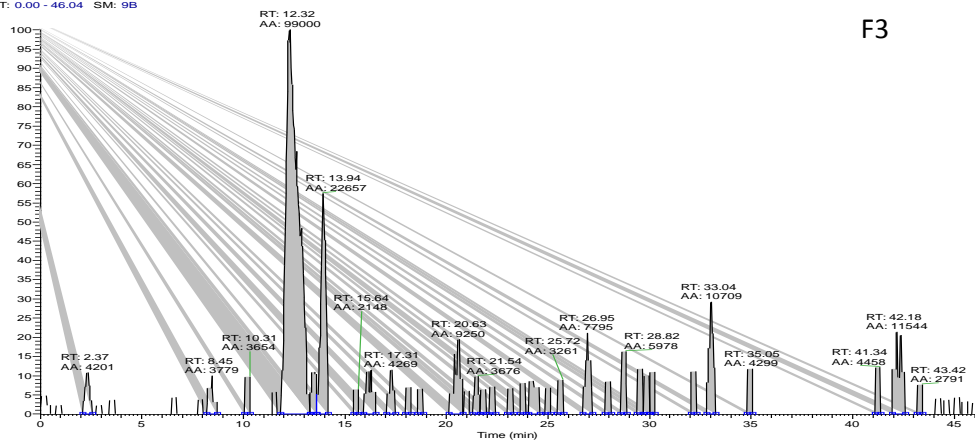
RT: 0.00 - 46.03 SM: 9B



F2

NL: 7.28E3
m/z= 209.060-209.070 F:
FTMS (1.2) - p ESI
Full lock ms
[75.00-1200.00] MS
ICIS F2

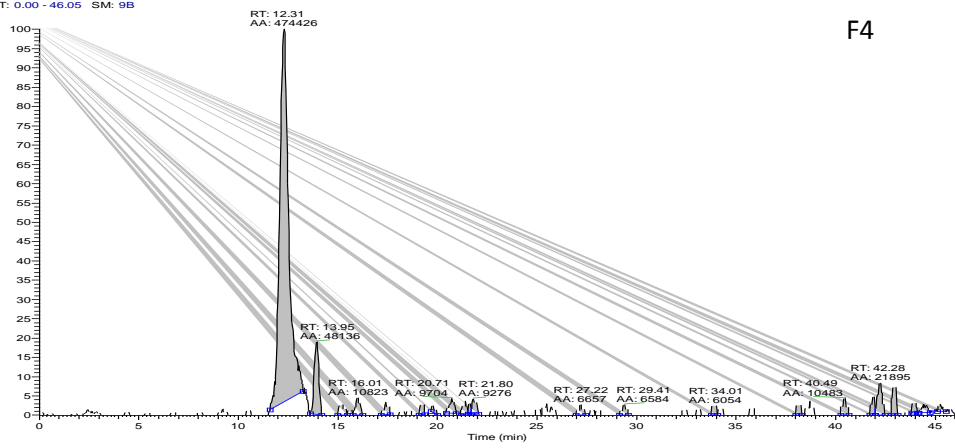
RT: 0.00 - 46.04 SM: 9B



F3

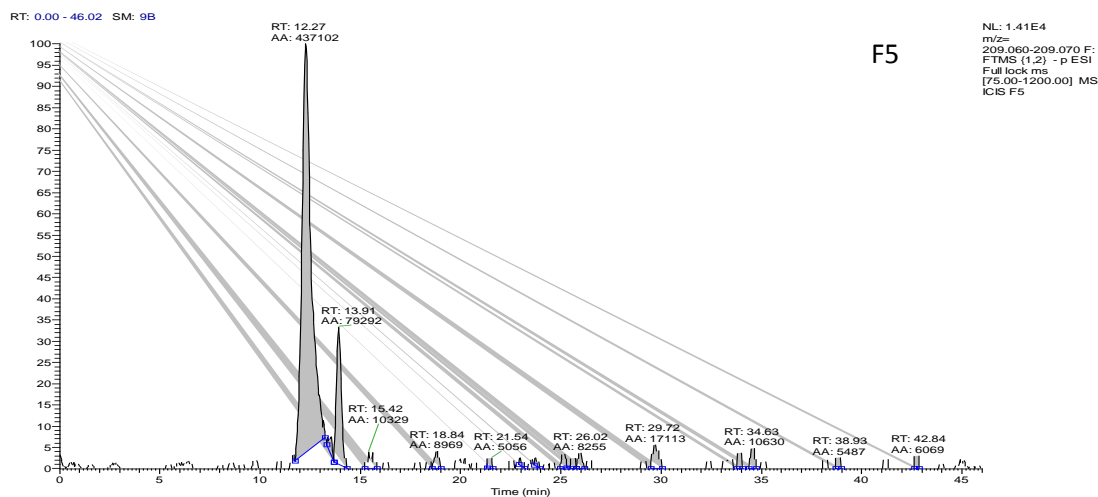
NL: 2.34E3
m/z= 209.060-209.070 F:
FTMS (1.2) - p ESI
Full lock ms
[75.00-1200.00] MS
ICIS F3

RT: 0.00 - 46.05 SM: 9B



F4

NL: 1.56E4
m/z= 209.060-209.070 F:
FTMS (1.2) - p ESI
Full lock ms
[75.00-1200.00] MS
ICIS F4



Peak	F1	F2	F3	F4	F5
Treatment	No addition	Troglitazone	TNF- α	Flav	Pheo
concentration		1 μ M	10ng/ml	100 μ g/ml	100 μ g/ml

Figure 3.35 MS spectrum representing the 2-deoxy-D-glucose uptake by differentiated 3T3-L1 in 25cm² flasks following different treatments (metabolite extracts) in the presence of 100 nM insulin. RT is retention time, MA is area under the curve, m/z represents the molecular weight of 2-deoxy-D-glucose. RT for 2-deoxy-D-glucose around 12.3 minutes. The 2-deoxyglucose is mainly present as its formate adduct with a mass of 209.0670. The table insert explains the treatments followed during the differentiation process of the 3T3-L1 cells starting from day 1. F1: control, F2, F3, F4 and F5 are cells treated with troglitazone, TNF- α , flavonoids and pheophytin A respectively.

Effect of different pre-adipocytes treatments on 2-DG glucose uptake by MS

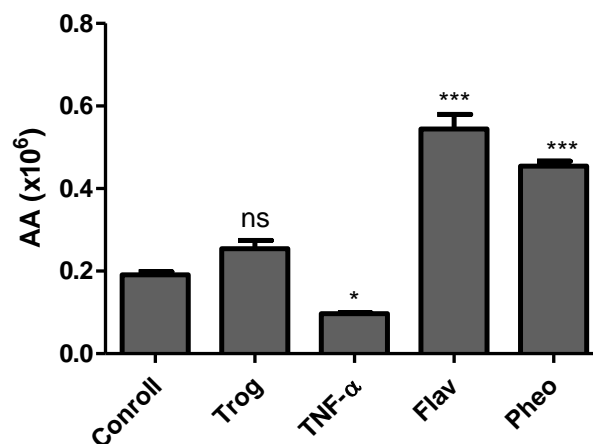


Figure 3.36 2-Deoxy-D-glucose uptake by differentiated 3T3-L1 (metabolite extracts) in the presence of 100 nM insulin and the effect of different treatments on the glucose uptake assay after differentiation. AA is area under the curve. Results are presented as mean AA \pm SEM

of three independent experiments. Data were analysed by Dunnett post-test,* $P<0.05$, and *** $P<0.01$ versus control.

Treatment	Mean AA	2-DG ($\mu\text{g/ml}$)
Control	0.19	2.7
Trog	0.25	3.3
TNF-α	0.097	1.8
Flav	0.54	6.1
Pheo	0.45	5.2

Table 3.5 Concentration of 2-deoxy-D-glucose uptake by 3T3-L1 cells of different pre-treated cells with TNF- α , flavonoids and pheophytins. 2-DG concentrations (expressed in $\mu\text{g/ml}$) were calculated with relevance to the AA (area under the curve by MS).

3.6 Conclusion and discussion

Insulin increased the glucose uptake by three-fold. Wortmannin blocked insulin activity. The presence of 100 $\mu\text{g/ml}$ pheophytin increased glucose uptake but did not enhance insulin activity. However, flavonoids containing extract alone did not increase the glucose uptake, although it did enhance insulin activity by two-fold. No effect of flavonoids and pheophytins extracts was found on the glucose uptake when they were added to the cells during the differentiation process. The stimulation of glucose uptake by 3T3-L1 adipocytes is a well-recognised mechanism of action of anti-diabetic drugs. Active compounds such as the pheophytins extract from *A. cominia* have insulin-like activities (Xu *et al.*, 2006; Alonso-Castro *et al.*, 2008; Wang *et al.*, 2011). All these MS results were confirming the results obtained by 2-NBDG uptake by 3T3-L1 cells in the presence of the extracts, as well the discussion in section 3.3.3.6. MS results also emphasize the importance of the metabolomic study for testing and quantifying the glucose uptake by cell lines by comparing to the 2-NBDG glucose uptake. 2-Deoxy-D-glucose uptake can be considered an orthogonal experiment providing and confirming the 2-NBDG uptake experiment.

3.7 Summary of *in vitro* studies involving the *A. cominia* extracts in the glucose uptake

In summary, the *in vitro* assays using HepG2 cells, L6, 3T3-L1 fibroblasts and 3T3-L1 adipocytes confirmed the anti-diabetic effect of the Cuban *Allophylus cominia*. The crude methanolic extract from *A. cominia* and different fractions from the eluted extracts containing a mixture of flavonoids and pheophytins was safe and did not affect cell viability of different cell lines, although higher concentrations of the extracts were reduced less than 10% of 3T3-L1 cell viability. According to the non-toxic characteristic of the extracts of *A. cominia*, a glucose uptake assay was carried out using 2-NBDG and 2-Deoxy-Glucose glucose as fluorescent probes. In HepG2 cells, the crude methanolic extract produced an increase in 2-NBDG uptake. In 3T3-L1 fibroblasts, no significant enhancement of insulin activity was shown, although the data of 2-NBDG glucose uptake assay were not conclusive of a significant effect of AC. Furthermore, a 2-DG uptake assay was performed using MS. Results were confirming that the extracts had produced significant increase in the uptake (pheophytin) and significant enhancement of the insulin activity (flavonoids). In L6 myoblasts, both flavonoids and pheophytins extracts produced an increase in 2-NBDG uptake. Therefore, all these results confirmed the importance of *A. cominia* as a natural anti-diabetic product which has been used by diabetic patients in Cuba.

Chapter 4

4 *In vitro* determination of lipid accumulation in 3T3-L1 adipocytes

4.1 Introduction

Adipocytes are the primary functional units of the adipose tissue. The terminal differentiation of the fibroblast precursor cells to adipocytes is an essential component of glucose and lipid metabolism. Adipocytes are responsible for the storage and balance of energy and fat (Gregoire *et al.*, 1998). In the last 20 years, the cellular and molecular mechanisms of adipocyte differentiation have been widely studied using pre-adipocyte culture systems. The process of adipocyte differentiation has been implicated in many studies in human diseases, particularly in the search for a treatment for T2-DM and obesity (Calabro *et al.*, 2005). Recently, pre-adipocyte differentiation has been primarily studied using *in vitro* tissue culture models of adipogenesis.

Insulin promotes glucose uptake by many tissues that express the glucose transporter GLUT4, e.g. skeletal muscle cells and fat cells. It also increases the transporter's activities by the number of transporters in the cell membrane.

Many studies have shown that TNF- α inhibits adipogenesis and 3T3-L1 differentiation by down regulation of microRNAs (Cawthorn *et al.*, 2008). TNF- α has also been reported in some studies to contribute to apoptosis in many cell lines. Apoptosis is a mechanism by which cells respond to a full damage by activating a program of cell death (Krown *et al.*, 1996).

In type 2 diabetic patients, troglitazone acts as insulin-sensitising agent. It improves insulin sensitivity by combining to PPARs. Troglitazone prevents the inhibitory effects of inflammatory cytokines such as TNF- α on insulin-induced adipocyte differentiation in 3T3-L1 cells (Bouaboula *et al.*, 2005). Troglitazone were used by many studies for enhancing adipocytes differentiation *in vitro*.

In our project, we have tested the extracts from *A. cominia* on 3T3-L1 adipogenesis, their effect on the lipid accumulated in the cells, then investigate their ability to induce or not apoptosis in 3T3-L1 adipocytes. TNF- α was used as adipogenesis inhibitor and troglitazone as adipogenesis enhancer. Many researchers suggested that

the decrease in lipid accumulation in 3T3-L1 cells may be associated to the expression of GLUT4 transporters translocation in the cell membrane (Moon *et al.*, 1990; Khil *et al.*, 1999). The aim of this chapter is to study the effect of the extracts from *A. cominia* on 3T3-L1 differentiation, on lipid droplets that already are accumulated in 3T3-L1 adipocytes and on the number of GLUT4 transporters.

4.2 Methods

4.2.1 Adipogenesis

Differentiation of 3T3-L1 was also carried out in the presence of extracts of *A. cominia* (flavonoids and pheophytin A) at day 1 and day 3 of the differentiation protocol. TNF- α at 10 ng/ml (tumour necrosis factor, purchased from Sigma T7539) was used as control to inhibit the differentiation of the cells. Troglitazone at 1 μ M (purchased from Sigma T2573-5MG) was used to enhance the differentiation of 3T3-L1.

3T3-L1 cells were seeded in 25 cm² flasks (at 8x10³ cells/ml); 3 days after the cells were confluent troglitazone and TNF- α was added to the differentiation medium at both: day 1 and day 3 as well as the extracts of *A. cominia* (flavonoids and pheophytins both at 100 μ g/ml). At day 5, the differentiation medium was replaced with fresh DMEM with 10% FBS. Twelve days after the differentiation induction, the lipid droplets were measured with oil Red-O (as explained in section 3.2.2.3).

4.2.2 Lipid accumulation

Five days after differentiation, *A. cominia* extracts (flavonoids and pheophytins) were tested on 3T3-L1 adipocytes, with the aim of exploring the effects of these extracts on the lipid metabolism. 3T3-L1 cells were differentiated in 12 and 24 well plates as explained in section 3.2.2.2.3 in the presence of troglitazone (1 μ M). The effect of the extract of *A. cominia* on lipolysis was followed over 3 days post differentiation using 100 μ g/ml of the extract in DMEM containing 10% FBS. For

some wells, the media were replaced with DMEM free FBS in order to starve the cells. Then Oil Red-O staining followed.

4.2.3 Caspase-3 assay

Caspase-3 is a protein from the family of caspases that mediate cell death and is considered a critical apoptotic enzyme of (Porter and Janicke, 1999) leading to chromatin condensation, DNA fragmentation and blebbing of cell membranes (destruction of cell cytoskeleton).

The caspase-3 colorimetric assay is based on the hydrolysis of the peptide substrate (acetyl-Asp-Glu-Val-Asp p-nitroanilide) by the caspase-3 enzyme liberated during apoptosis into a p-nitroaniline moiety with high absorbance (405 nm, and ϵ^{mM} 10.5) which can be easily detected on a plate reader.

To determine whether or not the inhibition of 3T3-L1 differentiation, by TNF- α , flavonoids and pheophytins, was the result of apoptosis, a caspase-3 assay was performed using a caspase-3 colorimetric assay kit purchased from Sigma Aldrich, UK.

3T3-L1 cells were differentiated in 25 cm² flasks (F) using different cell treatments where control was the untreated, undifferentiated cells. F1 is the untreated, differentiated cells in the flask. F2 is the differentiated cells in the presence of troglitazone (1 μ M). F3 is the flask containing differentiated cells in the presence of TNF- α . F4 is the flask containing differentiated cells in the presence of flavonoids, and F5 is the flask containing differentiated cells in the presence of pheophytins. Twelve days after differentiation initiation, the cell medium was removed and cells were washed twice with PBS. Two ml of triple Express was added to each flask and harvested cells were transferred into Eppendorf tubes then centrifuged at 600 x g for 5 minutes at 4°C using a microfuge Sigma 1-15K (Laborzentrifugen, Germany). Supernatant was discarded and cell pellets were washed twice with 1ml of PBS, where the supernatant was discarded with each wash. Cell pellets were re-suspended in 1ml of lysis buffer 5X (Lysis buffer L2912, including 250 mM of HEPES, pH 7.4, 25 mM CHAPS and 25 mM DTT). Eppendorfs were incubated on ice for 20 minutes,

and then centrifuged at 18000 x g for 15 minutes at 4°C. The supernatants containing cell metabolites were transferred into new Eppendorfs and analysed immediately or stored at -80°C if further storage was required.

Assay buffer preparation: 1X assay buffer was prepared by a 10-fold dilution of 10x stock (20 mM HEPES, PH 7.4, 2 mM EDTA, 0.1% CHAPS, 5 mM DTT) with 17 megohm water.

Substrate preparation: Caspase-3 substrate, acetyl-Asp-Glu-Val-Asp p-nitroanilide stock solution was 20 mM (1 mg of substrate dissolved in 78.5 µl of DMSO) and stored at -20°C. Working solution was needed, and 2 mM was prepared by diluting 10-fold the stock substrate with the assay buffer (1X).

Caspase-3 enzyme preparation: Caspase-3 enzyme was only added to the positive control wells. 100 µg/ml of stock solution was prepared (5 µg of the enzyme was dissolved in 50 µl of 17 megohm water and stored at -20°C). The working solution was 5 µg/ml, where a 20-fold dilution of the stock solution was made with assay buffer (1X).

Standard preparation: P-nitroaniline standard was used for developing a calibration curve for assays in 96-well clear plate. A stock solution was made by dissolving 1mg of p-nitroaniline in 0.72 ml of DMSO and stored at -20°C. The working solution was prepared by diluting 100-fold the stock solution in assay buffer (1X).

Staurosporine was used as a positive control to induce apoptosis in the cells, used at 1 µg/ml (stock solution 10 µg/ml) added to the cells and incubated for 24 hours at 37°C in an atmosphere containing 5% CO₂ in air before lysing the cells.

Caspase-3 inhibitor: Acetyl-Asp-Glu-Val-Asp-al (Sigma A0835, 0.5 mg) was diluted from 20 mM stock solution (0.5 mg dissolved in 500 µl of DMSO) to 2 mM with 1X Assay Buffer.

Assay experiment: An appropriate volume of assay buffer was added to each well of a 96-well plate (the final volume in the well was 100 µl). 5 µl of cells lysate, caspase-3 inhibitor and caspase-3 positive control were added to their appropriate wells as well as the p-nitroaniline which was added at different concentrations to the appropriate wells. The reaction was then started by the addition of 10 µl of caspase-3 substrate to all wells except those for the p-nitroaniline calibration curve, after

mixing the plate gently. The plate was then covered with aluminium foil and incubated at 37°C for 90 minutes (further incubation was done if the signals were too low). Absorbance was measured using Spectramax at 405 nm and the results were analysed by comparison to the calibration curve of p-nitroaniline.

The caspase-3 activity was calculated in μmol of p-nitroaniline released per minute per 1 ml of cell lysate or positive control, using the formula below:

$$\text{Activity } (\mu\text{mol of p – nitroaniline}) = \frac{\text{OD} * \text{d}}{\epsilon^{\text{mM}} * t * v}$$

Where ϵ^{mM} was 10.5, v is the volume of sample in ml (5 μl used), d is the dilution factor (20-folds as 100 μl total volume was used) and t is the reaction time in minutes (90 minutes followed).

Then the calculation of the concentration of p-nitroaniline produced per well in μmol was made following Table 4.1 below as guideline:

μM p-NA	μmol p-NA per 100 μl
10	0.001
20	0.002
50	0.005
100	0.01
200	0.02

Table 4.1 Guideline table presenting the amount of p-nitroaniline (p-NA) in μmol produced per 100 μl per well and their relative concentration in μM of p-NA.

4.2.4 Protein assay

Protein assay (Quick Start Bradford protein assay kit purchased from BioRad Laboratories, USA) was used for a simple and accurate procedure to determine the concentration of protein in solution.

3T3-L1 cells were pre-treated and differentiated in 25 cm^2 flasks and cells were harvested in lysis buffer as explained in section 4.2.3. BSA and Gamma-Globulin

were used as standards for studying the linear range of the assay, which was 125-1000 µg/ml with BSA and 125-1500 µg/ml with Gamma-Globulin. Standards or unknown samples from the pre-treated 3T3-L1 cells with troglitazone, TNF- α , flav and pheo were added to a 96-well clear plate (5 µl/well). Fibroblast cells were used as control. Blank was made using water and dye reagent. 1X dye reagent was then added to each well (250 µl/well). The dye reagent was removed from the 4°C storage and warmed up at room temperature before each use. Samples and standards were incubated with the dye reagent at room temperature for 10 min (not more than an hour) and then the absorbance was read with a Spectramax micro-plate reader using 595 nm.

4.2.5 Western blot

3T3-L1 cells were seeded and differentiated as described in before, in a 25 cm² flask, treatment with TNF- α (10 ng/ml), flavonoids and pheophytins from *A. cominia* at 100 µg/ml was done from the beginning of the differentiation process. Three days post differentiation; cells were washed twice with PBS. Cells were harvested and transferred into Eppendorf tubes in PBS. The PBS was removed by centrifugation at 600 x g for 5 minutes at 4°C using microfuge Sigma 1-15K. Supernatant was discarded and cell pellet was washed twice with 1 ml of PBS, the supernatant was discarded after each wash. Cell pellets were re-suspended in 1ml 1X lysis buffer (10X lysis buffer stock were diluted 10-fold with 9 ml of 18 megohm water). Cells were incubated on ice for 20 minutes then centrifuged at 18000 x g for 15 minutes at 4°C. The supernatants containing cell proteins were transferred into new Eppendorfs and analysed immediately or stored at -80°C if further storage was required. SDS PAGE was carried out by preparing 12% of resolving gel (RB, about 4.65 ml/gel) and 4% of Stacking gel (SB, about 1 ml/gel), where RB was prepared by 5 ml (2X) RB, 4 ml acrylamide, 1 ml distilled water, 200 µl of APS and then 8 µl TEMED. SB (4%) was prepared by 4 ml (2X) SB, 1.2 ml acrylamide, 2.8 ml distilled water, 200 µl of APS and finally the addition of 10 µl TEMED. Then the gel was poured on top of the set resolving gel, and a comb was inserted to allow it to set (isopropanol was added before then removed to polymerise the gel). The comb was removed and the

lanes were washed three times with running buffer. The gel cassettes were transferred to the electrophoresis tanks and filled with running buffer. The samples were then loaded at 30 µl per lane and a marker with low molecular weight was used as a control (15 µl), using a Hamilton syringe. The gel was running for half an hour at 80 mV then increased to 150 mV for one hour. The transfer of the proteins was done by disassembling the gel plates; the gel was placed in transfer cassettes, and then the transfer was run in transfer buffer (25 mM Tris base, 0.2 M glycine, 20% methanol and pH 8.9) at 120 mA at constant AMPS and left overnight. The blockage was made with 5% SCHIM (proteins) for an hour at room temperature and then incubated with Abcam antibody (1:1000, Glucose Transporter GLUT4). The cyclophilin B antibodies were purchased from Abcam PLC (Cambridge, U.K.). The polyclonal GLUT4 antibody was raised in rabbit with the immunogen located in the C-terminus of GLUT4. The polyclonal cyclophilin B antibody was raised against a C-terminal peptide of human cyclophilin B), and then a secondary antibody IRdye (1:12500) was added. The plate was washed three times with PBST (phosphate buffer saline Tween 0.02% volume) for 10 minutes after the addition of the first and the second antibodies. Finally, the plate was scanned under a LI-COR Odyssey infrared scanner and the results were analysed by Licor Studio Image Lite software.

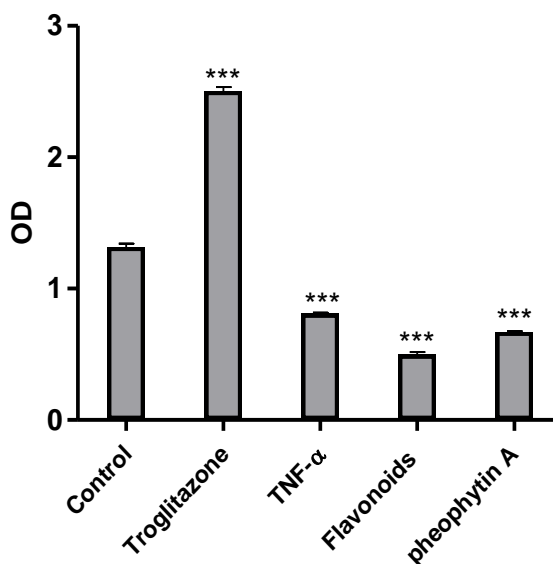
4.3 Results

4.3.1 Effect of extracts from *A. cominia* on 3T3-L1 adipogenesis on the first day of differentiation

To establish whether the extracts from *A. cominia* affected adipogenesis, 3T3-L1 fibroblasts were grown to over 100% confluence, and then treated with or without both of the extracts of *A. cominia* in the presence of insulin from day 1 of the differentiation process. In control wells, the medium was replaced at the first, third and fifth days. In some wells, troglitazone was added to enhance the differentiation, and TNF- α was used as inhibitor of 3T3-L1 differentiation. Twelve days after initiating the differentiation, lipid droplets accumulated in the cells were measured as optical density after staining the cells with Oil red-O (Fig 4.2). Compared to the control cells, where the differentiation process was followed without any treatment, there was an increase of the optical density by one fold in the presence of

troglitazone (Fig 4.1), and a significant decrease of the optical density was shown with TNF- α . Both flavonoids and pheophytins decreased lipid accumulation by 50% compared with the control ($P<0.05$) (Fig 4.1).

Effect of *A. cominia* extracts on 3T3-L1 on first day of differentiation



Day 1	IBMX Dexamethasone Insulin	IBMX Dexamethasone Insulin Troglitazone 1 μ M	IBMX Dexamethasone Insulin TNF- α 10 ng/ml	IBMX Dexamethasone Insulin Flavonoids 100 μ g/ml	IBMX Dexamethasone Insulin Pheophytin A 100 μ g/ml
Day 3	Insulin	Insulin Troglitazone 1 μ M	Insulin TNF- α 10 ng/ml	Insulin Flavonoids 100 μ g/ml	Insulin Pheophytin A 100 μ g/ml
Day 5	DMEM 10% FBS	DMEM 10% FBS	DMEM 10% FBS	DMEM 10% FBS	DMEM 10% FBS

Figure 4.1 Inhibitory effects of *A. cominia* extracts on 3T3-L1 differentiation starting from day 1 of the differentiation. Values are mean \pm SEM of three independent experiment. The data were analysed by Dunnett post-test, *** $P<0.05$ versus control. Oil Red O staining was done. Table insert is showing different additions over three days of the differentiation protocol for each treatment.

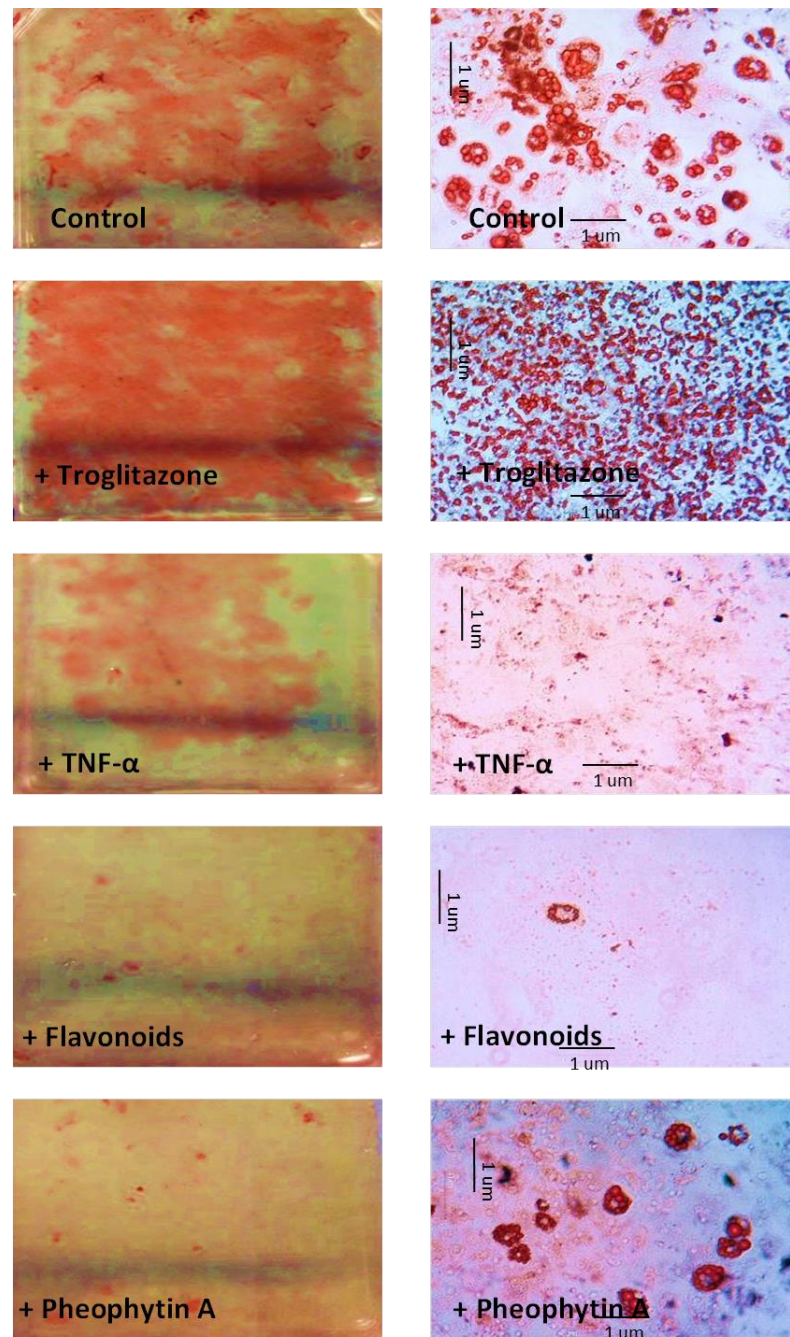
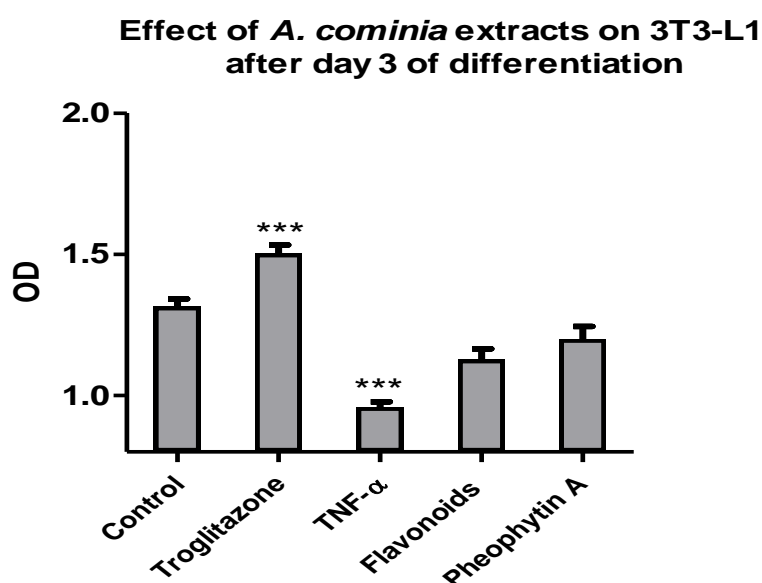


Figure 4.2 Morphological examination of adipocyte differentiation influenced by extracts of *A. cominia* and drugs treatments. Control: fully differentiated 3T3-L1 adipocytes untreated. + Troglitazone: fully differentiated 3T3-L1 adipocytes treated with troglitazone (1 μ M). + TNF- α : fully differentiated 3T3-L1 adipocytes treated with TNF- α (10 ng/ml). + Flavonoids: fully differentiated 3T3-L1 adipocytes treated with flavonoids containing extract from *A. cominia* (100 μ g/ml). + Pheophytin A: fully differentiated 3T3-L1 adipocytes treated with pheophytin A from *A. cominia* (100 μ g/ml).

4.3.2 Effect of extracts from *A. cominia* on 3T3-L1 adipogenesis on the third day of differentiation

The addition of extracts of *A. cominia* (both flavonoids and pheophytin A at 100 µg/ml) on the third day of the differentiation process did not significantly affect the differentiation of 3T3-L1 adipocytes by comparison to the control cells (Fig 4.3). A significant increase in the lipid droplets was shown after addition of troglitazone on the third day of the differentiation process (Fig 4.3) but not as potent as that of the addition at the beginning of the differentiation.



Day 1	IBMX Dexamethasone Insulin	IBMX Dexamethasone Insulin	IBMX Dexamethasone Insulin	IBMX Dexamethasone Insulin	IBMX Dexamethasone Insulin
Day 3	Insulin	Insulin Troglitazone 1 µM	Insulin TNF-α 10 ng/ml	Insulin Flavonoids 100 µg/ml	Insulin Pheophytin A 100 µg/ml
Day 5	DMEM 10% FBS	DMEM 10% FBS	DMEM 10% FBS	DMEM 10% FBS	DMEM 10% FBS

Figure 4.3 Inhibitory effects of *A. cominia* extracts on 3T3-L1 differentiation starting from day 3 of the differentiation. Values are mean OD ± SEM of three independent experiment. The data was analysed by Dunnett *post-test*, *** $P < 0.05$ versus control. Table insert is showing different additions over three days of the differentiation protocol for each treatment.

4.3.3 Apoptotic effect of extracts from *A. cominia* in 3T3-L1 adipocytes

To confirm whether the flavonoids and pheophytins from *A. cominia* inhibited 3T3-L1 adipogenesis by causing apoptosis and cell death, caspase-3 assay was done. Expected apoptosis was due to the appearance of the cells when viewed under an inverted microscope (Fig 4.4), cells treated with TNF- α appeared to be apoptotic (cell shrinkage) by comparison to the vehicle controls. Therefore, the cells treated with both extracts from *A. cominia* were different by comparison with the vehicle controls. Cells treated with flavonoids and pheophytin A at 100 $\mu\text{g/ml}$ were unlike the cells pre-treated with TNF- α during the differentiation. Significant increase of the optical density OD (11 fold versus control cells) was observed with cells pre-treated with staurosporine. In cells pre-treated with TNF- α , 100 $\mu\text{g/ml}$ of flavonoids and pheophytin A; a lack of increase of the OD was shown by comparison to the control cells. Significant decrease in the OD was observed in the presence of the inhibitor by comparing to the cells pre-treated with staurosporine. OD was very low therefore; no hydrolysis of the substrate resulting from the absence of caspase-3 enzyme was observed (Fig 4.6). By comparison to the p-nitroaniline concentration curve (Fig 4.5), the concentration of p-nitroaniline produced in the caspase-3 positive control in the presence of the substrate was 50 μM . In the cells pre-treated with staurosporine, p-nitroaniline produced by the cell lysate in the presence of substrate was 12.5 μM . Caspase-3 activity of staurosporine in μmol of p-nitroaniline released per min per ml of cell lysate was calculated using the formula presented in section 4.2.3 and the activities are presented in Table 4.2.

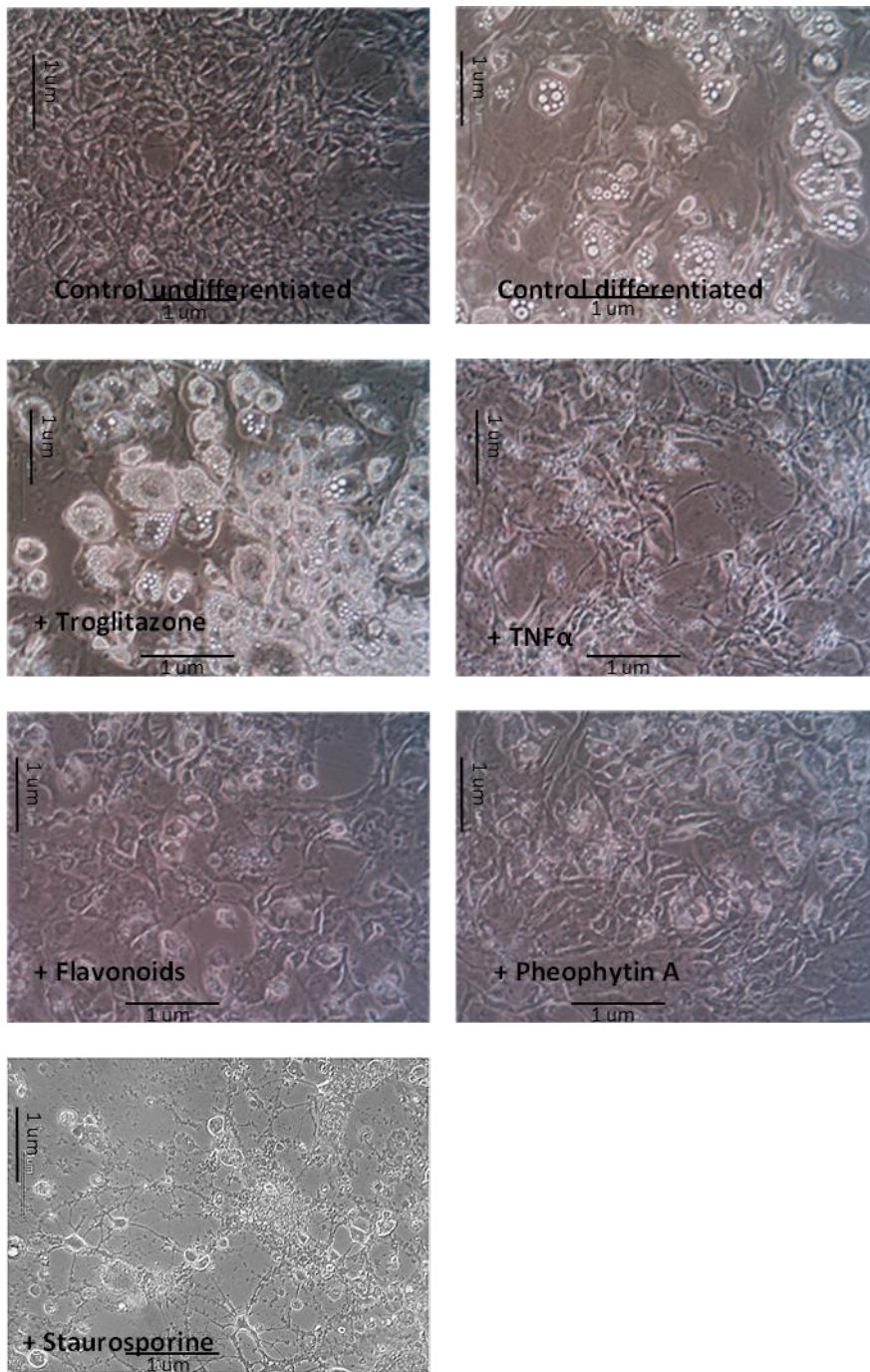


Figure 4.4 Series of pictures of 3T3-L1 cells depicting the effect of TNF- α , flavonoids, pheophytin A and staurosporine effect on the morphology of 3T3-L1 at day 8 of differentiation by comparison to the undifferentiated cells. (x20). Vehicle controls represented fibroblasts and fully differentiated adipocytes in the presence of troglitazone. TNF- α (10 ng/ml), flavonoids (100 μ g/ml) and pheo (100 μ g/ml) were added to the cells during the differentiation process. Staurosporine (1 μ g/ml) was added to the cells for 24 hours.

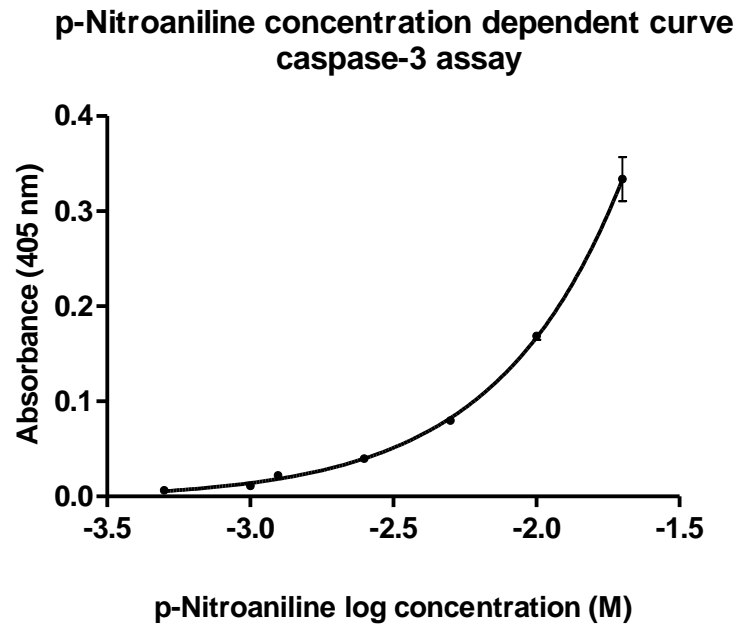


Figure 4.5 p-Nitroaniline concentration dependent curve. Absorbance was measured at 405 nm. Results are presented as mean \pm SEM of absorbance reading of three independent experiments.

Effect of TNF- α , flavonoids and pheophytins on 3T3-L1 differentiation caspase-3 assay

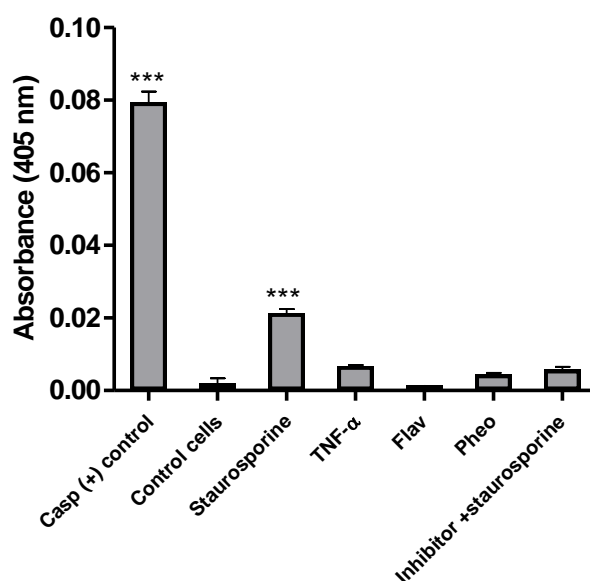


Figure 4.6 TNF- α , flavonoids and pheophytins extracts from *A. cominia* do not induce apoptosis in 3T3-L1 adipocytes. Caspase-3 assay was done. Control represented the differentiated cells in the presence of troglitazone. TNF- α (10 ng/ml), flavonoids (100 μ g/ml) and pheophytin (100 μ g/ml) were added to the cells during the differentiation process. Staurosporine (1 μ g/ml) was added to the cells for 24 hours. Inhibitor used was Acetyl-Asp-Glu-Val-Asp-al (2 mM). Absorbance was measured at 405 nm. The data was analysed by Dunnett post-test, *** P <0.05 versus control cells. Results are presented as mean \pm SEM of absorbance reading of three independent experiments.

	OD	p-NA activity	μ M of p-NA
Caspase positive control	0.079333	0.00503	50
Control cells	0.002	0.000126	< 1
Staurosporine	0.021333	0.001306	13
TNF- α	0.006667	0.00042	4
Flav	0.001333	0.000085	< 1
Pheo	0.004333	0.00028	< 1
Inhibitor +staurosporine	0.005667	0.00036	<1

Table 4.2 Caspase-3 activity of different cell lysate of pre-treated cells with staurosporine, TNF- α , flavavonoids (flav) and pheophytin A (pheo). Activity expressed in μ mol of p-nitroaniline released per min per ml of cell lysate.

4.3.4 Effect of addition of extracts from *A. cominia* on the accumulation of lipid in 3T3-L1 cells

To determine whether extracts of AC are affecting the accumulation of lipid droplets in the cells following differentiation, cells were differentiated in 12-well plate as described before in the presence of troglitazone (1 μ M). Lipid droplets accumulated in the cells were measured as optical density after staining the cells with oil red-O. As shown in Figs 4.7 and 4.8, there was no effect of starving the cells over three days on the lipid droplets in the cells. The addition of flavonoids has no effect after 24 h; therefore, a decrease in the lipid droplets was clear after 48 h and 72 h. Pheophytins significantly decreased the lipid droplets in 3T3-L1 adipocytes starting from 24 h after addition of the extract to the adipocytes, and this decrease was greater after 48 h and 72 h.

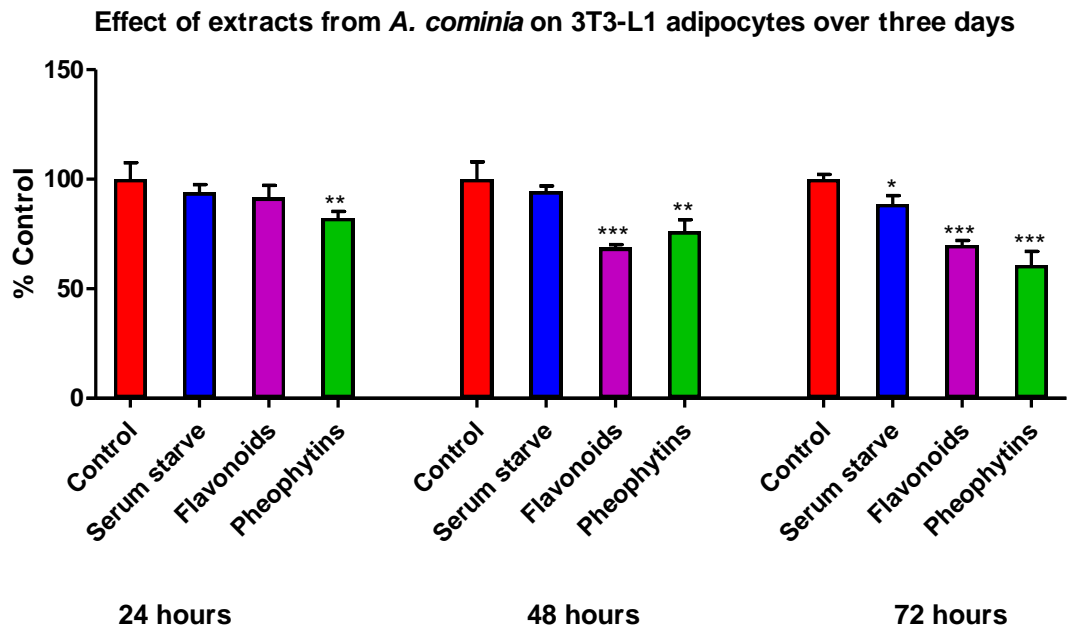


Figure 4.7 Inhibitory effects of *A. cominia* extracts on lipid accumulation in adipocytes for 72 hours. Values are presented as mean % control \pm SEM of three independent experiment. The data was analysed by Dunnett post-test, *** $P < 0.01$ and * $P < 0.05$ versus control. Oil Red O staining for quantifying lipid droplets was done.

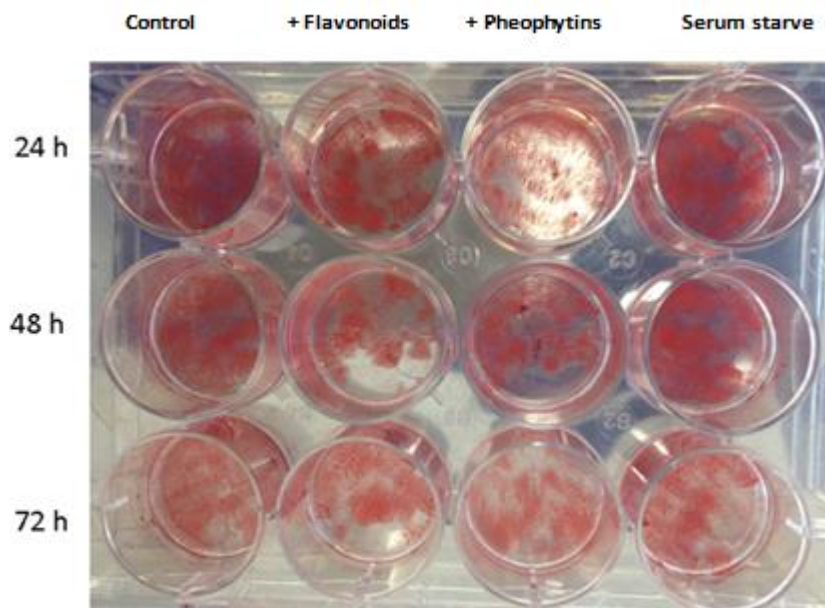


Figure 4.8 12-Well plate representing the inhibitory effects of *A. cominia* extracts on lipid accumulation in adipocytes for 72 hours.

4.3.5 Effect of withdrawal of extracts from *A. cominia* on the accumulation of lipid in 3T3-L1 cells

To confirm whether or not the effect of *A. cominia* was decreasing the lipid droplets already existing in the differentiated 3T3-L1 cells, the experiment was repeated and the extracts of AC were left on the cells over five days. Then the extracts of AC (flav and pheo) were withdrawn and the OD of lipid droplets in the cells (stained with Oil Red-O) was measured after 1, 2, 5 and 6 days. There was a significant decrease of the lipid droplets inside the cells starting from 24 h of the addition of 100 µg/ml of the flavonoids and pheophytins extracts from *A. cominia* (Fig 4.9) The change of the OD was significantly decreasing over days even after 5 days by comparison to the control untreated cells. After 6 days of withdrawal of the extracts, the medium was replaced with normal growth medium supplemented with 10% FBS. By comparison to the control, no fat re-accumulation was observed in the pre-treated cells with extracts of *A. cominia*. The cells pre-treated with the flavonoids containing extract showed fewer fat droplets inside the 3T3-L1 adipocytes after 5 days of the treatment (Fig 4.10.B) compared with the control cells (Fig 4.10.A).

Effect of addition and withdrawal of flavonoids and pheophytin A on 3T3-L1 lipid droplets accumulated in the cells over days

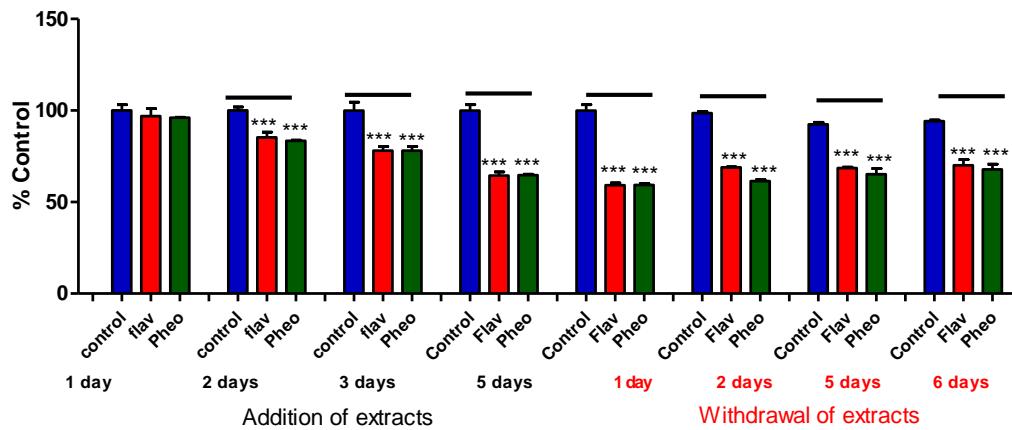
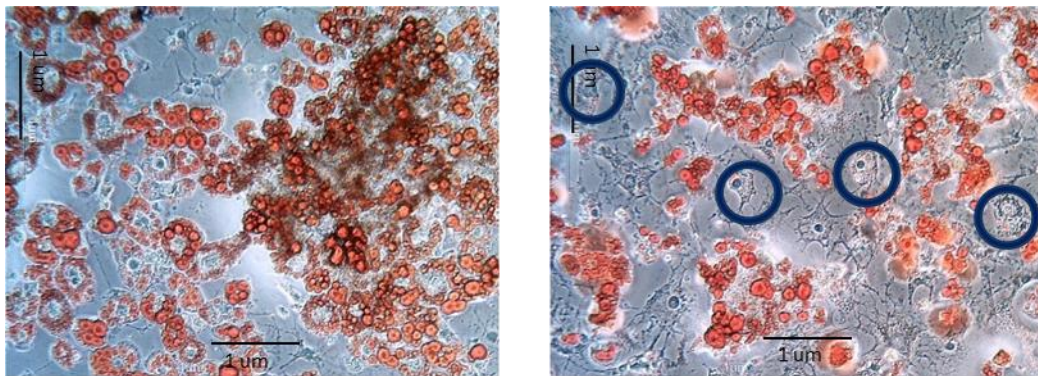


Figure 4.9 The inhibitory effect of *A. cominia* extracts on lipid accumulation in adipocytes over 5 days and the withdrawal effect of the extracts on the adipocytes over 6 days. Cells were differentiated in a 24-well plate and *A. cominia* extracts were added over days at 100 µg/ml. After 5 days of the incubation of the cells with the extracts and on the withdrawing days, extracts were replaced by fresh DMEM supplemented with 10% FBS. Lipid droplets were quantified by Oil Red-O staining. The results represent the mean percentage control of four experimental results ± SEM. The data was analysed by Dunnett post-test, *** $P < 0.05$ versus control at each day.



A.

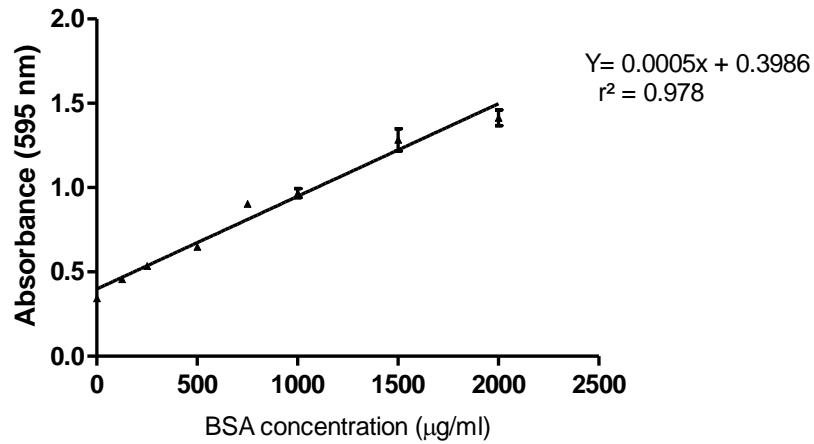
B.

Figure 4.10 Morphological examination of 3T3-L1 adipocytes influenced by the extracts of *A. cominia*. Red droplets are the fat accumulated in the cells. A. Control differentiated 3T3-L1 in the absence of extracts from *A. cominia*. B. Differentiated 3T3-L1 in the presence of flavonoids extract from *A. cominia*. The blue circles surround differentiated cells with fewer fat droplets in them.

4.3.6 Effect of the extracts from *A. cominia* on protein concentrations in 3T3-L1 adipocytes

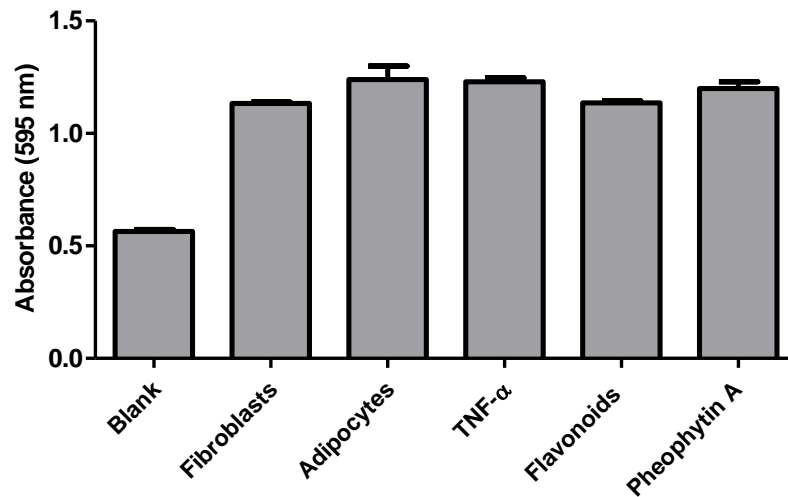
To determine whether the total protein concentration in pre-treated 3T3-L1 cells with troglitazone, TNF- α , flavonoids and pheophytin A was the same, a protein determination assay (Bradford assay kit) was performed. As shown in Fig 4.11.A, BSA was used as standard. BSA produced a concentration-dependent increase in the absorbance at 595 nm. The unknown sample concentrations were calculated using the equation presented in Fig 4.11.A and results are presented in Table 4.3. Lysis buffer was used as blank and did not show high protein concentration. No significant difference between adipocytes, fibroblast and the pre-treated cells with TNF- α , flavonoids and pheophytin A was shown. Furthermore, compared to the protein concentration in the fibroblasts cell lysate that was used as control, all the other metabolites from the pre-treated cells with troglitazone, TNF- α , flavonoids and pheophytin A containing similarity in the total protein concentrations in these cell lysates (Fig 4.11.B). Protein concentration was about 1300 - 1600 $\mu\text{g/ml}$ as calculated from BSA standard curve. All these results confirmed that these cell lysates contain similar protein concentrations and were able to be used for further western blot for the identification and quantification of the GLUT4 transporters in these pre-treated 3T3-L1 cells.

BSA calibration standard in protein quantitation assay



A. Standard curves of BSA standard in the protein determination assay

Total protein determination in 3T3-L1 pre-treated cells



B. Protein determination of samples from pre-treated 3T3-L1 cells

Figure 4.11 Protein determination of the pre-treated 3T3-L1 cells with TNF- α , flavonoids and pheophytin A. A. Standard curves of BSA standard in the protein determination assay. B. Protein determination of samples from pre-treated 3T3-L1 cells. Adipocytes and fibroblasts were used as control. Results were presented as mean absorbance \pm SEM. The data were analysed by Dunnett *post-test*, no significant difference was shown by comparison to the fibroblasts. Standard and cell lysate were added to the plate with 1X dye reagent and incubated at room temperature for 10 min. Then the absorbance were measured using micro-plate reader at $\lambda = 595$ nm.

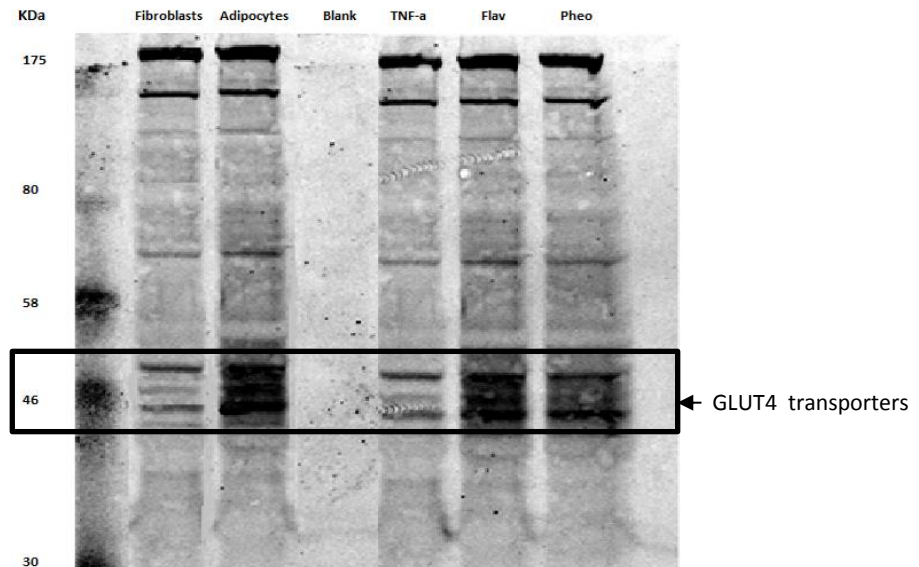
	Protein conc (µg/ml)	
	Absorbance	BSA
Adipocytes	1.24 ± 0.002	1681
Fibroblasts	1.07 ± 0.048	1336
TNF-α	1.23 ± 0.023	1661
Flav	1.14 ± 0.010	1474
Pheo	1.17 ± 0.028	1534

Table 4.3 Protein concentration in pre-treated 3T3-L1 cells. Protein concentration was calculated using BSA standard curve.

4.3.7 Effect of the extracts from *A. cominia* on insulin-mediated GLUT4 transporters

To investigate the effects of flavonoids and pheophytin extracts from *A. cominia* on insulin-mediated glucose transporter 4 (GLUT4) in 3T3-L1 adipocytes, western blot of the pre-treated differentiated cells with TNF- α , flav and pheo was carried out. 3T3-L1 fibroblasts and adipocytes were used as a vehicle controls. As shown in Fig 4.12, the GLUT4 transporters from differentiated 3T3-L1 cells appeared around 46 kDa (Fig 4.12.A), represented by prominent bands, whereas, cells treated with TNF- α showed lighter bands. The effect of TNF- α , flav and pheo was confirmed in Fig 4.12.B, while a significant decrease of GLUT4 transporters only appeared in the TNF- α pre-treated 3T3-L1 cell line. Flavonoids and pheophytin A did not affect the GLUT4 transporters in the 3T3-L1 intracellular-membrane.

A.



B.

Effect of extracts from *A. cominia* on GLUT4 transporters

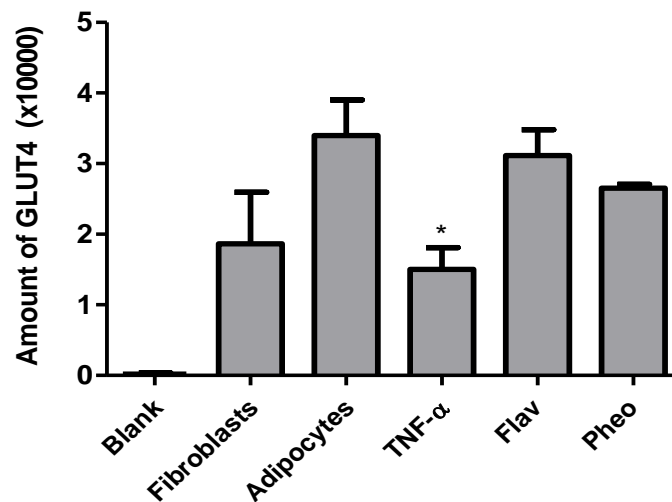


Figure 4.12 Western blot showing the effect of TNF- α , flav and pheo extracts of *A. cominia* on GLUT4 protein in plasma membranes in 3T3-L1 adipocytes. A. Representative Western blot analysis of GLUT4 proteins in 3T3-L1 cells. B. Bar graph representative of GLUT4 transporters in fibroblasts and adipocytes and the effect of the treatments of TNF- α , Flav and pheo. Relative amount of GLUT4 protein was determined by Western blot in total extracts of 3T3-L1 adipocytes. Equal amounts of protein were loaded into each lane. The several bands noticeable for and GLUT4 probably represent differential glycosylation of the transporters. Total bands were quantitated by densitometry, and results are represented as mean amount of GLUT4 \pm SEM of three independent experiments. The data were analysed by Dunnett post-test, * $P < 0.05$ versus adipocytes.

4.3.8 Conclusion and discussion

Flavonoid and pheophytin extracts from *A. cominia* decreased lipid accumulation in 3T3-L1 once added from the first day of the initiation of the differentiation process. No effect was shown once added after three days of the differentiation initiation. This confirms that these extracts, as well as TNF- α , are only active at the beginning of differentiation. This can be related to the expression of PPAR γ , which plays an important role as an essential regulator in adipocytes differentiation (Saito *et al.*, 2007). Extracts from *A. cominia* decreased lipid droplets accumulated in the cells over days. However, no lipid re-accumulation was shown after removal of the extracts over days. This can be related to the lipolytic effect of these extracts. Lipolysis in adipocytes is known to be triggered by an increase of intracellular cAMP level. cAMP activates protein kinase A and downstream lipases (Saito *et al.*, 2007).

Cells pre-treated with TNF- α showed a decrease in GLUT4 transporters in comparison to that of the adipocytes, as in the control undifferentiated fibroblasts, confirming that the decrease in GLUT4 transporters is due to TNF- α (Stephens *et al.*, 1997). Flavonoids seemed to work differently than TNF- α . It has been reported (Moon *et al.*, 1990; Lee *et al.*, 1994; Khil *et al.*, 1999) that the hypo-glycaemic action of compounds may be due to the stimulation of glucose transport and metabolism in insulin target organs, such as 3T3-L1 adipocytes. The translocation of GLUT4 transporters is mediated by the fusion of the plasma membrane and vesicles containing GLUT4 proteins, in which the intracellular calcium causes conformational changes in the membrane compartment to facilitate the translocation process (Muller *et al.*, 2014). Flavonoids' mechanism of action is possibly involved in the blockage of GLUT4 receptors rather than decreasing their translocation, thus preventing the cells from the uptake of nutrients and accumulation of fat droplets, which further implies that glucose uptake by 3T3-L1 adipocytes did not increase in the presence of flavonoids in the absence of insulin. Previous results in adipocytes showed that flavonoids inhibited the uptake of methylglucose, a substrate that enters the cells through GLUT4 transporters in 3T3-L1 adipocytes (Strobel *et al.*, 2005). Flavonoids and their related synthetic compounds such as flavones and isoflavones, are tyrosine kinase inhibitors that cause the inhibition of glucose transport (Vera *et*

al., 2001). As shown in the Western blot, there was an increase in GLUT4 transporters in pheo pre-treated cells but not as much as in the control differentiated cells, which shows that the mechanism of action of pheo in the differentiation process was not similar to that of the TNF- α that is, it blocks the GLUT4 transporters. Lysis buffer was used as blank only in the absence of any cells to ensure that the bands of GLUT4 transporters did not exist. Cells differentiated and treated with staurosporine for 24 hours did not show any GLUT4 transporters, confirming that none of flav or pheo extracts had apoptotic effects. Reduced glucose transporter expression is therefore likely to be a manifestation of impaired differentiation rather than a mechanism to explain reduced differentiation.

4.3.9 Summary of *in vitro* studies involving the *A. cominia* extracts in adipogenesis

AC extracts were tested on adipogenesis at the beginning of the differentiation of 3T3-L1 fibroblasts; both flavonoids and pheophytin A extracts had blocked the differentiation process without having an apoptosis effect on the cells. In addition, we confirmed by Western blot that the flavonoids blocked the lipid accumulation, but by comparison to the control, the extracts did not reduce GLUT4 transporters on the 3T3-L1 cells. After differentiation of 3T3-L1 cells, AC extracts were tested to show their effect on the lipid accumulation and both extracts have produced significant decrease in lipid droplets inside the cells and no lipid accumulation were seen after withdrawal of the extracts from the cell growth medium. The reduction in lipid droplets caused by *A. cominia* extracts, may not be due to reduced differentiation, but a result of impaired fat synthesis or increased lipolysis. Further study should be carried out to determine this and to compare whether or not the mechanism of action of AC extracts in inhibiting the 3T3-L1 differentiation is similar to or different from that of TNF- α .

We conclude that these extracts with their effect on decreasing lipid droplets in the cells could be a new candidate to prevent the fat formation that leads to a decrease in the risks of the obesity when associated with diabetes. Therefore, all these results confirmed the importance of *A. cominia* as a natural anti-obesity product which has been used by diabetic patients in Cuba.

Chapter 5

5 Effect of the extracts from *A. cominia* on the activities of PTP1B, DPPIV, α -glucosidase and α -amylase enzymes

5.1 Introduction

In this chapter, all extracts from *A. cominia* were tested on for their effect on PTP1B, DPPIV, α -glucosidase and α -amylase activity. These enzymes were reported in many studies as new drug targets for the treatment of T2-DM, and possibly, obesity. Many inhibitors have been identified through chemical synthesis and natural products (Chen *et al.*, 2002; Na *et al.*, 2006)

Mechanisms that have a high impact on glucose uptake are numerous, such as activation of glucose transporters GLUT4 in cell plasma membranes, insulin mimetic acting at post-receptor level, activation of AMP Kinase, an increase in nitric oxide, glucose-6P, glycogen stores (Wiernsperger, 2005) and deficiency in PTP1B. Further, many plants extracts may inhibit the action of the enzyme PTP1B that regulates negatively the insulin signalling by dephosphorylating phosphotyrosine residues on the insulin receptor (Chapter 1, Fig 1.11). Plants, such as *Galega officinalis*, can also stimulate the glucose uptake (Mooney *et al.*, 2008). Wiernsperger (2005) found that the inhibition of PTP1B is the main principle underlying the type of approach according to the activation of glucose uptake.

Prolonged DPPIV inhibition has a potential effect on reducing post-prandial glucose levels and HbA1c levels, which confirms that DPPIV inhibitors are novel, efficient and tolerable treatment of T2-DM (Ahrén, 2005).

α -Amylase and α -glucosidase inhibitors such as acarbose act by blocking the activity of these enzymes leading to a reduction in the breakdown of polysaccharides, and thereby decreasing the post-prandial increase in the blood glucose level in addition inducing weight loss (Zhong *et al.*, 2006). The aim of this chapter is to study the inhibitory effect of the extracts from *A. cominia* on PTP1B, DPPIV, α -amylase and α -glucosidase enzymes and study the kinetics of their inhibition in each of these enzyme assays.

5.2 Material and Methods

5.2.1 Z-factor

The Z-factor is a measure of statistical effect size useful during piloting for the quality of assay conditions. It has been proposed for use in high-throughput screening to quantify how well the assay works after at least after three independent experiments. This will produce a statistically significant data set for evaluation (Zhang *et al.*, 1999).

The Z-factor is defined in terms of four parameters: the averages and standard deviations of both the positive and negative controls. Given these values, the Z-factor is defined as:

$$Z - \text{factor} = 1 - \frac{3SD_- + 3SD_+}{Ave_+ - Ave_-}$$

SD₋ is the negative control standard deviation

SD₊ is the positive control standard deviation

Ave₊ is the positive control average

Ave₋ is the negative control average

Once the Z-factor is calculated, Table 5.1 shows the expected potential performance for optimising the assay conditions.

Z-factor	Assay validation
1 > Z > 0.9	Excellent assay
0.9 > Z > 0.7	Good assay
0.7 > Z > 0.5	Benefit assay
Z = 0.5	Minimum recommended assay

Table 5.1 High-throughput screening assay fitness table.

Different assay conditions should be ranked and qualified by the Z-factor's value. Therefore, repetition and modification of assay conditions are needed until suitable conditions are found.

5.2.2 Plant sample preparation

Plant stock concentration was prepared beforehand at 10 mg/ml in DMSO or water (stored at -20°C). In all the enzyme assays, samples of *A. cominia* (crude or pure compounds) were screened at 30 µg/ml in a 96-well round-bottom clear plate (U-shape plate, Greiner bio-one, Germany). 10 µl of the prepared sample was added to the enzyme and substrate in the enzyme assay plate.

5.2.3 DPPIV assay

5.2.3.1 Buffer preparation

7.88 g of Tris-HCl (Trisma hydroxylchloride) was dissolved in 500 ml of distilled water (100 mM). Then 50 mg of bovine serum albumin (BSA) (concentration needed at 0.1 mg/ml) was added. Tris-HCL (T5941) and BSA (A2153) were purchased from Sigma. pH was adjusted to 8 using a Mettler MP220 pH meter.

The buffer for the assay was prepared on a weekly basis and stored at 5°C.

5.2.3.2 Enzyme preparation

Dipeptidyl Peptidase IV enzyme (Sigma D7052) was soluble in Tris-HCl (100mM and PH 8). Stock concentration (0.27 μ M) was stored at -20°C until required. 0.3 nM as final concentration was required. A working solution (0.6 nM) containing 5.6 μ l of the enzyme solution was added to 2.5 ml of the DPPIV buffer.

5.2.3.3 Substrate preparation

Gly-pro-7-amido-4-methylcoumarin hydrobromide (Gly-pro, Sigma G2761, 25 mg) was dissolved in distilled water at 50 mg/ml and stored at -20°C, Km is 22 μ M. 30 μ M final concentration was needed; therefore, 120 μ M stock was prepared.

5.2.3.4 Inhibitor preparation

P32/98 inhibitor (3N-[(2S, 3S)-2-amino-3-methyl-pentanoyl]-1,3-thiazolidine) hemifumarate, and 10 mg (Tocris 2136), stored as powder in the fridge. P32/98 was dissolved in water at a stock concentration of 10 mM. A 1:10 dilution was made for the displacement curve, with a concentration range between 0.0003 and 3 μ M.

5.2.3.5 Assay method

In a 96-half-well black, flat-bottom plate (Costar®), 10 μ l of the standard (P32/98) or samples were added to the plate, then 20 μ l of DPPIV enzyme was added to each well. The plate was incubated for 30 min at 37°C in an atmosphere containing 5%

CO₂. 10 µl of the substrate was added to the wells and then incubated for 30 min. The plate was tested on a Wallac Victor² using ex 355 nm/em 460 nm.

5.2.3.6 Z-factor method

In a 96-half-well black flat-bottom plate, 10 µl of DPPIV substrate was added to the plate. 10 µl of buffer was added to replace the plant sample volume. 20 µl of DPPIV enzyme was added to half of the plate as positive control, and to the other half (negative control) only buffer was added (20 µl). The plate was incubated for 30 min at 37°C in an atmosphere containing 5% CO₂. The umbelliferon was tested using Wallac Victor² using ex 355 nm/em 460 nm.

5.2.3.7 Kinetics of the inhibition of DPPIV enzyme by *A. cominia*

Various concentrations of the *A. cominia* extract (KLMN(91-175)66-72, concentration range 0.01-30 µg/ml) were incubated at 37°C in an atmosphere containing 5% CO₂ with DPPIV enzyme (0.3 nM) for 30 min. Various concentrations of the substrate (Gly-pro, concentration range 0-120 µM) were added and incubated for another 30 min. The mechanism of inhibition of DPPIV by *A. cominia* extract was compared with the commercial inhibitor P32/98. The same procedure was repeated with various concentrations of the DPPIV inhibitor (P32/98, concentration range 0.0003-3 µM). The umbelliferon was tested using a Wallac Victor² using ex 355 nm/em 460 nm.

5.2.4 PTP1B assay

5.2.4.1 Buffer preparation

The buffer was composed of the following: 2.975 g of HEPES (25 mM, Sigma H3375), 1.461 g of sodium chloride (50 mM, Sigma S9625), 0.32 g of dithiothreitol (2 mM, Sigma D5545), 0.365 g of ethylenediaminetetraacetic acid (EDTA 2.5 mM, Sigma E1644) and 5 mg of bovine serum albumin (BSA 0.01 mg/ml). All were dissolved in 500 ml of distilled water and the pH was adjusted to 7.2.

5.2.4.2 Enzyme preparation

100 µl of the enzyme protein tyrosine phosphatase 1B (Sigma P6244- 50 µg, MW 37400) was added to 25 ml of the buffer and aliquoted into 1 ml (100 µl was sufficient for each plate) then stored at -80°C. A working solution of 2 nM was needed. 100 µl of the stock was added to 2.5 ml of PTP1B buffer.

5.2.4.3 Substrate preparation

6,8-difluoro-4-methylumbelliferyl phosphate (DiFMUP) (Invitrogen Ltd, D6567- 5 mg) was stored at -20°C at 5 mg/1.71 ml of DMSO, with a K_m of 6 µM. A 7 µl of the stock (10 mM) was added to 1.75 ml of buffer. 10 µM was needed therefore 40 µM stock was prepared. For each plate, 5 µl of the 10 mM stock was added to 1.25 ml of buffer.

5.2.4.4 Inhibitor preparation

TFMS inhibitor (Bis(4-Trifluoromethylsulfonamidophenyl)-1,4-diisopropylbenzine), (Calbiochem 540211- 10 mg, K_m 6 µM) was soluble in DMSO (10 mg in 1.64 ml). The TFMS displacement curve was done (concentration range 0.0003-3 µM). JA0008 (a sample from Maybridge with K_i is 0.12 µM) was also used as a standard inhibitor for PTP1B as well as a new TFMS inhibitor.

5.2.4.5 Assay method

In a 96-half-well flat-bottom black plate (Costar®), 10 µl of the standard (TFMS) or samples were added. Then 20 µl of PTP1B enzyme was added to each well, and incubated for 30 min at 37°C in an atmosphere containing 5% CO₂. 10 µl of the

substrate was added to the wells then incubated for another 10 min. The plate was tested on a Wallac Victor², (ex 355 nm/em 460 nm).

5.2.4.6 Kinetics of the inhibition of PTP1B enzyme by *A. cominia*

Various concentrations of *A. cominia* extract (both flavonoids and pheophytins, concentration range 0.01-30 µg/ml) were incubated with PTP1B enzyme (2 nM) at 37°C for 30 min. Various concentrations of PTP1B substrate (DiFMUP, concentration range 0-40 µM) was added and incubated at 37°C in an atmosphere containing 5% CO₂ for another 10 min. The mechanism of inhibition of PTP1B by *A. cominia* extract was compared with the commercial inhibitor P32/98. The same procedure was repeated with various concentrations of the PTP1B inhibitor (TFMS, concentration range 0.0003-3 µM). The umbelliferon was tested using a Wallac Victor² using ex 355 nm/em 460 nm.

5.2.5 α -glucosidase assay

5.2.5.1 Buffer preparation

Phosphate buffer at a concentration of 0.1 mM was freshly prepared by mixing 25.5 ml of solution A and 24.5 ml of solution B. The volume was topped up to 100 ml with distilled water. The pH was adjusted to 6.8.

Solution A: sodium phosphate monobasic dehydrate $\text{NaH}_2\text{PO}_4 \cdot 2\text{H}_2\text{O}$ (purchased from Sigma 04269-1k) prepared at a concentration of 0.2 M in distilled water (13.9 g in 500 ml distilled H_2O).

Solution B: sodium phosphate dibasic heptahydrate $\text{Na}_2\text{HPO}_4 \cdot 7\text{H}_2\text{O}$ (purchased from Sigma S9390-500g) prepared at a concentration of 0.2 M in distilled water (26.8 g in 500 ml distilled H_2O).

Stock solutions A and B were kept at room temperature.

5.2.5.2 Enzyme preparation

Yeast α -glucosidase (EC 3.2.1.20) purchased from sigma G0660 was dissolved in distilled water (750 units in 1 ml water). Further stock of 75 units per ml was prepared and stored at -20°C . A working solution of the enzyme of 0.2 units per ml was needed, where 13 μl (of the 75 units per ml) of the enzyme solution was added to 2.5 ml of phosphate buffer.

5.2.5.3 Substrate preparation

4-nitrophenyl- α -D-glucopyranoside purchased from Sigma N1377 (1 g), stored at -20°C was dissolved in phosphate buffer, K_m is 0.83 mM. Final concentration required was 1 mM; therefore, a stock of 4 mM was prepared. 1.8 mg of the substrate was dissolved in phosphate buffer and sonicated before each assay.

5.2.5.4 Inhibitor preparation

Acarbose was purchased from Sigma A8980 (1 g) stored as powder at room temperature. Acarbose was dissolved in distilled water at a concentration of 100 mM, a 1:10 dilution was made for the displacement curve (concentration range from 10 μ M into 30 mM).

5.2.5.5 Assay method

In a 96-half-well clear flat-bottom plate (Costar®), 10 μ l of standard (Acarbose) or samples were added to the wells. 20 μ l of α -glucosidase enzyme was added to each well and incubated for 10 min at 37°C in an atmosphere containing 5% CO₂. 10 μ l of the substrate was added to the wells and then incubated for another 10 min at 37°C in an atmosphere containing 5% CO₂. The optical density was tested on Spectramax plate reader at 450 nm.

5.2.5.6 Kinetics of the inhibition of α -glucosidase by *A. cominia*

Various concentrations of the *A. cominia* extracts (both flavonoids and pheophytins, concentration range 0.01-30 μ g/ml) were incubated with yeast α -glucosidase enzyme. The plate was incubated for 10 min at 37°C in an atmosphere containing 5% CO₂. Various concentrations of the substrate (4-nitrophenyl- α -D-glucopyranoside, concentration range 0-10 mM) were added and the plate was incubated for another 10 min. The mechanism of inhibition of α -glucosidase by *A. cominia* extracts was compared with the commercial inhibitor (acarbose). The same procedure was repeated with various concentrations of the α -glucosidase inhibitor (acarbose, concentration ranges from 10 μ M to 30 μ M). The optical density was tested on Spectramax at 450 nm.

5.2.6 α -amylase assay

5.2.6.1 Buffer preparation

HEPES buffer was prepared and kept at room temperature. HEPES (purchased from Sigma H3375-100 g) was prepared at a concentration of 50 mM, with 5.96 g dissolved in 500 ml of distilled water. pH was adjusted into 7.1.

5.2.6.2 Enzyme preparation

α -amylase (3.2.1.1) from porcine pancreas, purchased from Sigma A6255 (25 mg), was dissolved in distilled water (1402 units per mg) at a concentration of 29 mg/ml. The enzyme was prepared and stored at -20°C . A working solution of the enzyme was needed at 125 units per ml; therefore, a stock of 250 units per ml was prepared. 15.4 μl (625 units) of the enzyme stock solution was added to 2.5 ml of HEPES buffer.

5.2.6.3 Substrate preparation

4-nitrophenyl- α -D-maltohexaside purchased from Sigma 73681 (100 mg), stored at $2-8^{\circ}\text{C}$ was dissolved in water at 50 mg/ml, Km is 1.8 mM. The final concentration was required at 1.5 mM. A stock concentration of 6 mM was prepared; therefore 8.3 mg of the substrate was dissolved in 1.25 ml of HEPES buffer before each assay.

5.2.6.4 Inhibitor preparation

Acarbose purchased from Sigma A8980 (1 g), stored as powder at room temperature, was dissolved in HEPES buffer at 100 mM. A 1:10 dilution was made for the displacement curve at a concentration range from 10 μM to 30 mM.

5.2.6.5 Assay method

In a 96-half-well flat-bottom clear plate (Costar®), 10 μl of standard (acarbose) or samples were added to the plate, then 20 μl of α -amylase enzyme was added to each well. The plate was incubated for 30 min at 37°C in an atmosphere containing 5% CO_2 . 10 μl of the substrate was added to the wells and then incubated for another 30 min at 37°C in an atmosphere containing 5% CO_2 . The optical density was tested using Spectramax plate reader at 450 nm.

5.2.6.6 Results analysis

The following protocols were used in a 40 μ l per well reaction mixture. 10 μ l of buffer (with the equivalent volumes of DMSO or distilled water used in preparing the 10 mg/ml concentration of *A. cominia* extracts) was added to the control wells. The fluorescence or umbelliferon released from the hydrolysis of the substrate by the enzyme when the substrate was alone was considered the control. Hydrolysis of the substrate by the enzymes, in the presence of extracts or inhibitors, was calculated as a percentage of that of the control. The control was assumed to have no inhibitory effect; thus, the substrate underwent 100% hydrolysis. The results were analysed with Prism program version 5. Statistical significance is recognised when P value is less than 0.05. K_i , the dissociation constant of the enzyme-inhibitor complex, was determined from the non-linear regression analysis in Prism 5.

In competition study, alpha which is the ternary complex constant (calculated by Prism) was adapted. Alpha determines the mechanism of inhibition; its value determines the degree to which the binding of inhibitor changes the affinity of the enzyme for substrate. Alpha value is always greater than zero. When Alpha value is one, the inhibitor does not alter the binding of the substrate to the enzyme, and the mixed-model is identical to non-competitive inhibition. When the Alpha is very large, the binding of the inhibitor prevents the binding of the substrate and the mixed-model becomes identical to competitive inhibition. When Alpha is very small (but greater than zero); the binding of the inhibitor enhances the binding of the substrate to the enzyme, and the mixed model becomes almost identical to an uncompetitive model.

5.3 Results

5.3.1 DPPIV enzyme

5.3.1.1 Z-factor of DPPIV assay

DPPIV enzyme assay fitness was screened using DPPIV enzyme at 0.3 nM in the presence of gly-pro-7-amido-4-methylcoumarin hydrobromide as substrate (gly-pro, 30 μ M). The positive control was in the presence of both gly-pro and DPPIV enzyme. The negative control was in the presence of the substrate only. Z-factor was calculated as explained in section 5.2.1.

For the DPPIV assay (Fig 5.1), the value of Z-factor was 0.7. By comparison to the high-throughput screening fitness assay Table 5.1, Z-factor is between 0.7 and 0.9, confirming that the DPPIV assay and its conditions were acceptable and can be followed for further screening tests.

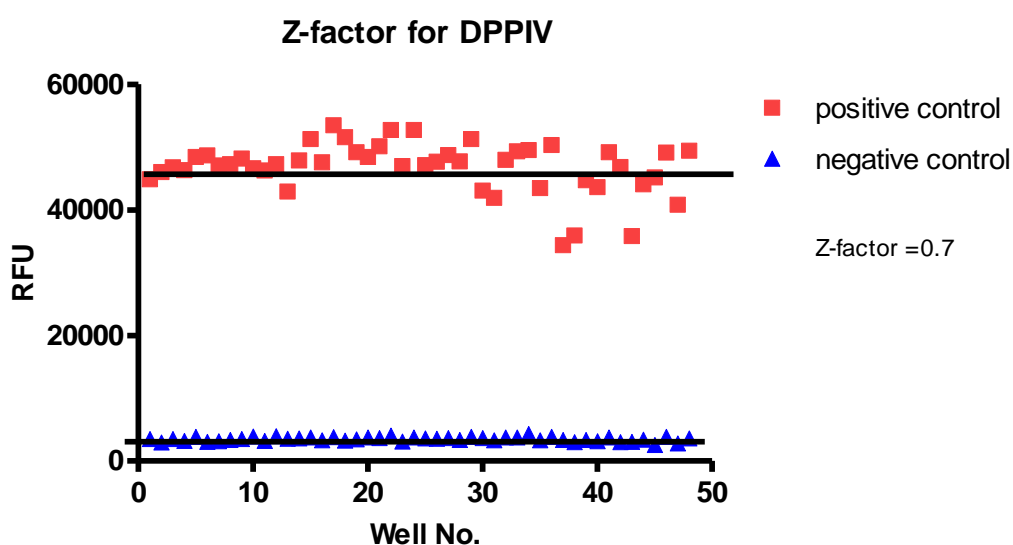


Figure 5.1 High-throughput screening fitness for DPPIV assay using gly-pro-7-amido-4-methylcoumarin hydrobromide as substrate and DPPIV enzyme.

5.3.1.2 Effect of extracts from *A. cominia* on DPPIV enzyme

Extracts of *A. cominia* (crude and eluted samples) were tested on DPPIV enzyme assay at 30 µg/ml. The extracts were compared with the standard DPPIV inhibitor P32/98, which produced a concentration-dependent inhibition (K_i 0.9 ± 0.01 µg/ml; Fig 5.2). Among the samples tested, significant inhibition ($75.3 \pm 2.33\%$) was found only with the flavonoid sample from *A. cominia* (AC-MC-KLMN(91-175)-66-72) (Fig 5.2).

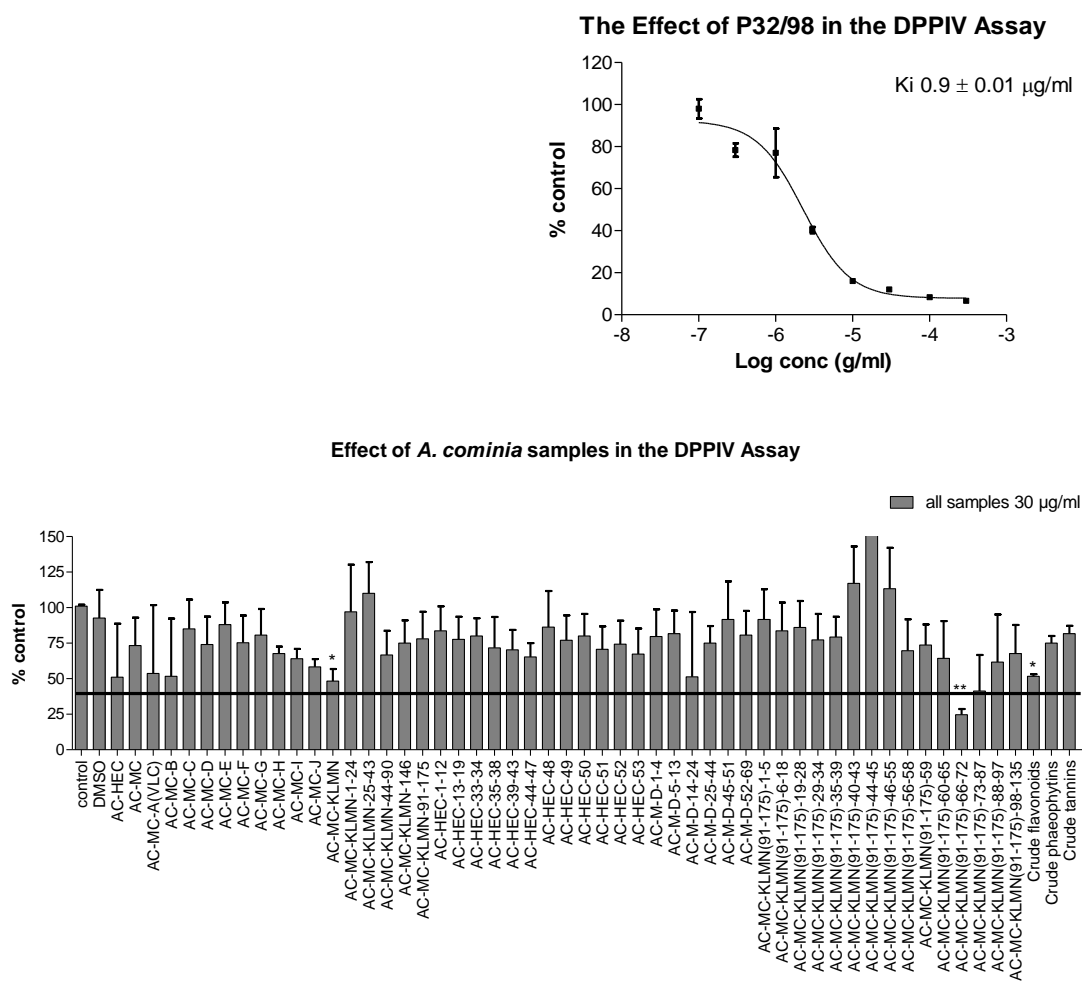


Figure 5.2 Effect of various *A. cominia* extracts on DPPIV enzyme in the presence of Gly-pro substrate. Extracts concentration at 30 µg/ml were incubated with DPPIV enzyme for 30 min at 37°C in an atmosphere containing 5% CO₂. Gly-pro (30 µM) was then added and incubated for 30 min at 37°C. The hydrolysis of Gly-pro by DPPIV enzyme was measured at 355/460 nm. Data represents mean ± SEM of DPPIV enzyme hydrolysis (% control) of three independent experiments. Insert shows the effect of different concentrations of P32/98 standard (0.03-100 µM) on DPPIV enzyme in the presence of Gly-pro. K_i for P32/98 was 0.9 ± 0.01 µg/ml. The data were analysed by Dunnett *post-test*. * $P < 0.05$ versus control.

The effect of fractions from *A. cominia* were repeated at two different concentrations (3 and 30 µg/ml). Significant inhibition was shown at 30 µg/ml in samples AC-MC, AC-MC-KLMN and AC-MC-KLMN(91-175)-66-72 with a decrease in the percentage of control in comparison to that of samples at 3 µg/ml. Sample AC-MC-KLMN(91-175)-66-72, with 30 µg/ml produced a $73 \pm 2.33\%$ inhibition (Fig 5.3) was compared with the inhibition produced by at 3 µg/ml ($17.5 \pm 2.5\%$). Neither pure quercitrin (F1) nor meansitrin (F2) at 30 µg/ml inhibited DPPIV enzyme (Fig 5.4).

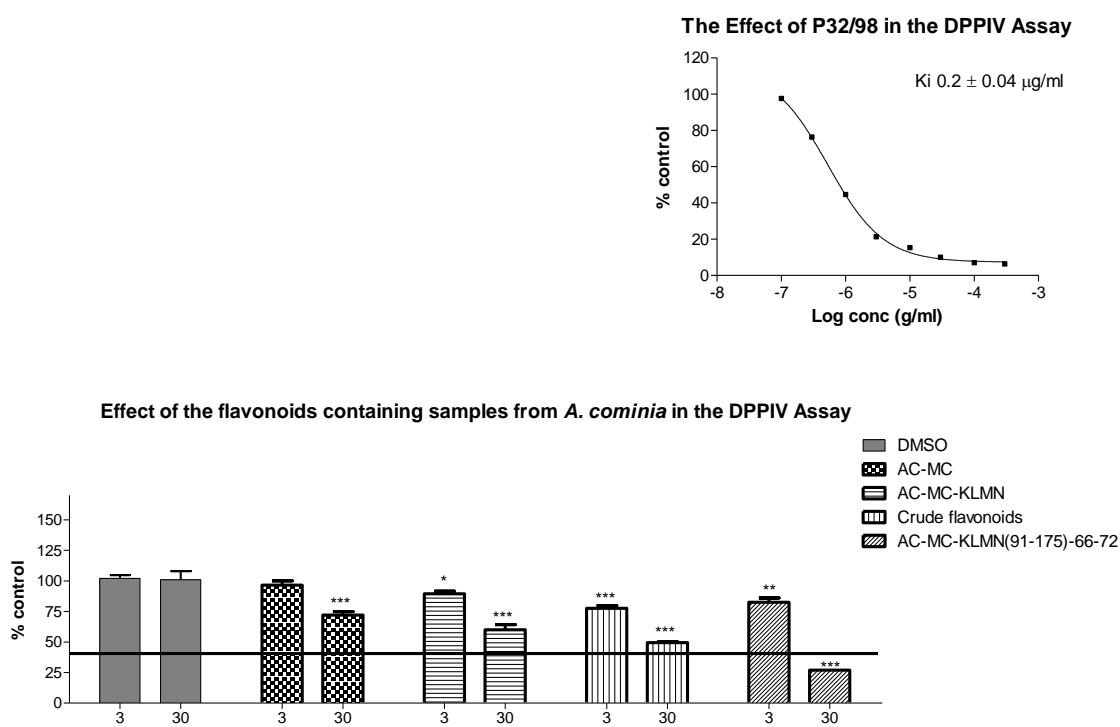


Figure 5.3 Effect of various extracts of AC-MC on DPPIV enzyme at two different concentrations (3 µg/ml and 30 µg/ml) in the presence of Gly-pro substrate. Extract concentrated at 30 µg/ml were incubated with DPPIV enzyme for 30 min at 37°C in an atmosphere containing 5% CO₂. Gly-pro (30 µM) was then added and incubated for 30 min at 37°C. The hydrolysis of Gly-pro by DPPIV enzyme was measured at 355/460 nm. Data represent mean \pm SEM of DPPIV enzyme hydrolysis (% control) of three independent experiments. The insert shows the effect of various concentrations of P32/98 standard (0.03-100 µM) on DPPIV enzyme in the presence of Gly-pro with Ki 0.2 ± 0.04 µg/ml. The data were analysed by Dunnett *post-test*. * $P < 0.05$ versus DMSO (100%).

Effect of flavonoids extracts from AC-KLMN-91-175 on DPPIV

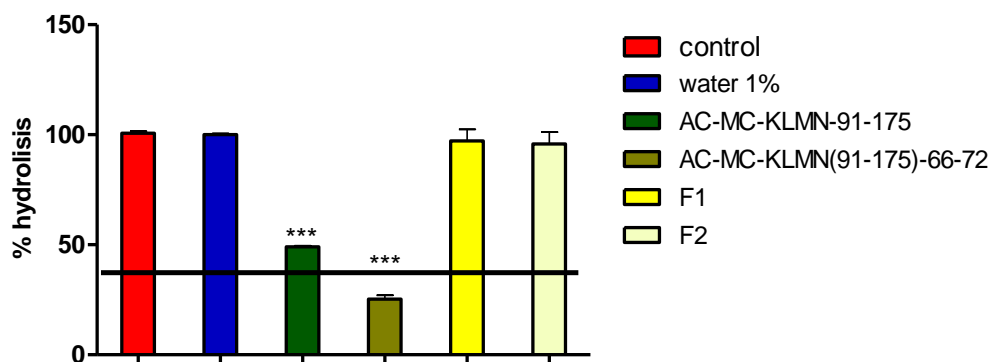


Figure 5.4 Effect of various extracts of AC-KLMN-91-175 on DPPIV enzyme. F1 and F2 are fractions separated from AC-KLMN-91-175 by HPLC. Samples were tested at 30 $\mu\text{g/ml}$ in the presence of Gly-pro substrate. Data were presented as mean \pm SEM of DPPIV enzyme hydrolysis (% control) of three independent experiments. The data were analysed by Dunnett *post-test*. *** $P < 0.05$ versus control (100%).

5.3.1.3 Concentration dependent inhibition of the flavonoids from *A. cominia*

The effect of a range of concentrations of the flavonoid mixture (0.1-30 $\mu\text{g/ml}$) was tested on DPPIV enzyme activity. Flavonoids produced a concentration-dependent inhibition of DPPIV enzyme with a K_i value of $2.6 \pm 0.2 \mu\text{g/ml}$, which was three times the K_i value of P32/98 ($0.9 \pm 0.02 \mu\text{g/ml}$) (Fig 5.5).

The Effect of KLMN(91-175)66-72 in the DPPIV Assay

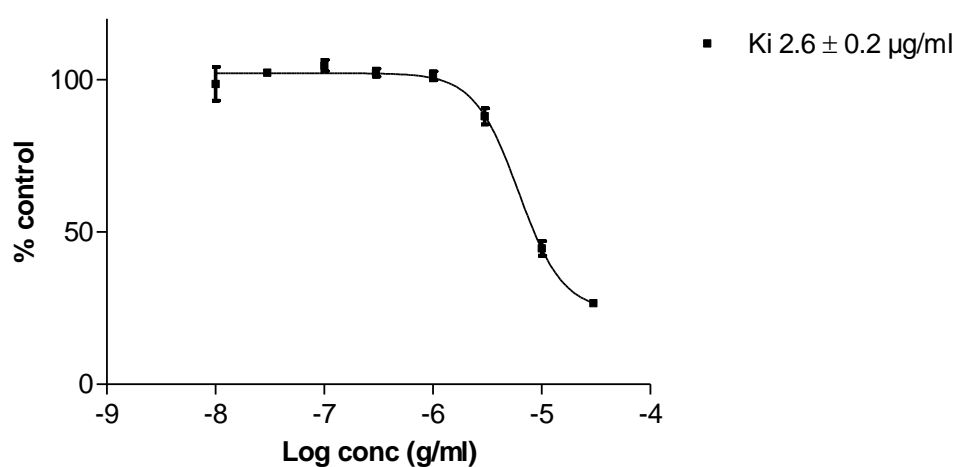
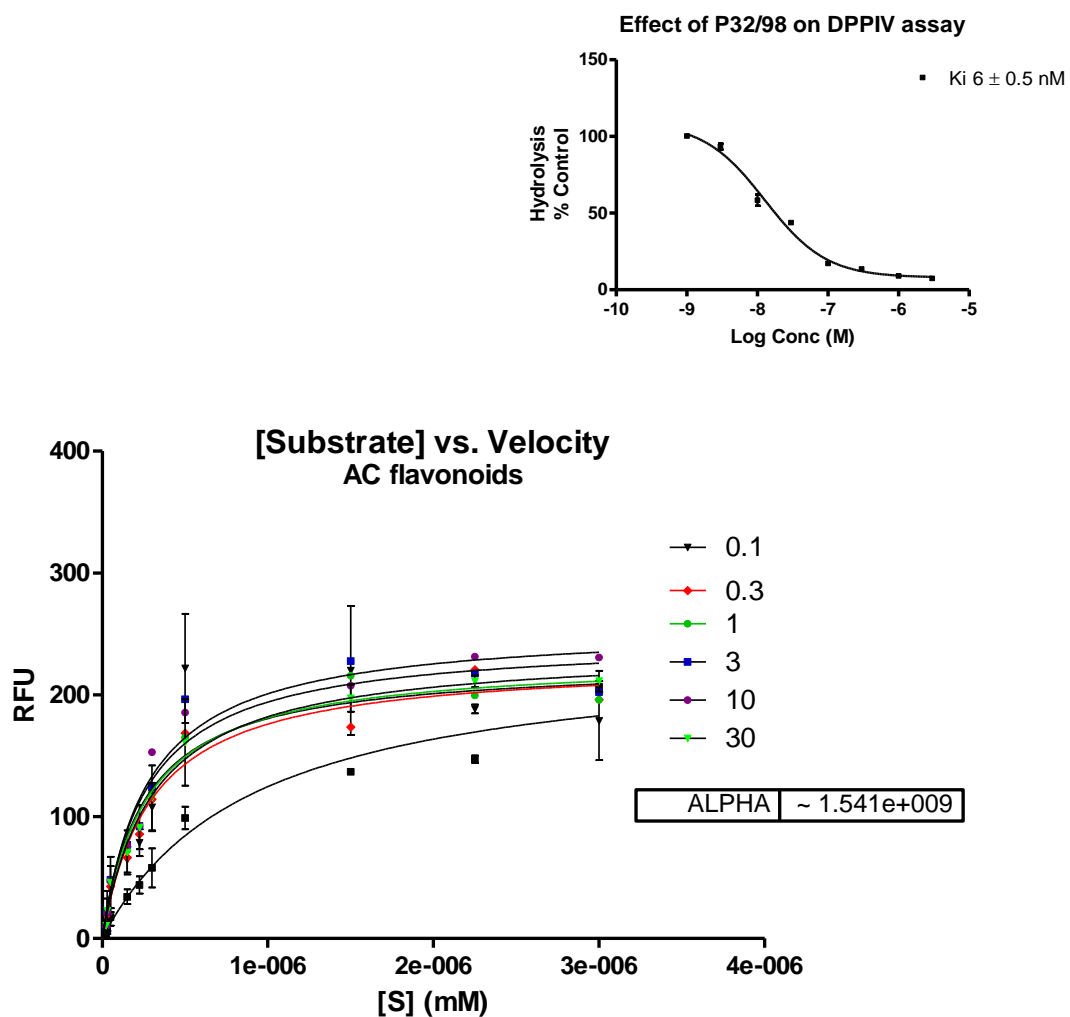


Figure 5.5 Effect of each fraction KLMN(91-175)66-72 (mixture of flavonoids) from *A. cominia* extracts on DPPIV enzyme. Extracts were incubated with DPPIV enzyme for 30 min at 37°C in an atmosphere containing 5% CO_2 . Gly-pro (30 μM) was then added and incubated for 30 min at 37°C. The hydrolysis of Gly-pro by DPPIV enzyme was measured at 355/460 nm. Data represent mean \pm SEM of DPPIV enzyme hydrolysis (% control). n=3.

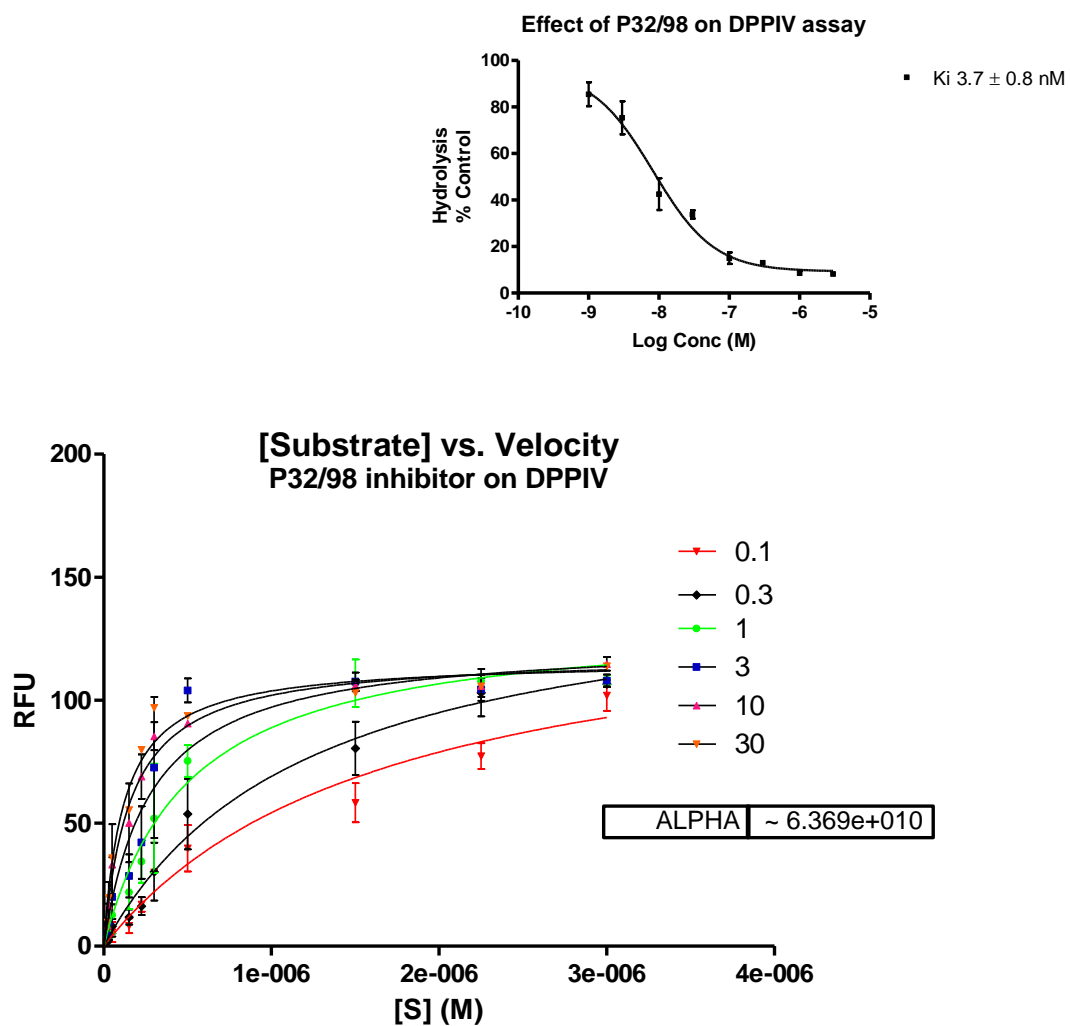
5.3.1.4 Kinetics of the inhibition of DPPIV by the flavonoids from *A. cominia*

Various concentrations of the flavonoid sample were incubated with DPPIV enzyme and increasing concentrations of the substrate. The results were graphed using a Michaelis-Menten plot. V_{max} and K_m were calculated (Fig 5.6). As the flavonoid concentration increased so did the K_m . The V_{max} was unchanged (~230 RFU) with increased concentration of inhibitor (Fig 5.6). The shape of the curve in the Michaelis-Menten plot was hyperbolic. Alpha was around $1.541e+009 > 1$ (very large). All these factors were indicative of a competitive inhibition of the flavonoid sample. The mechanism of action of the P32/98 inhibitor used in the assay also confirmed its competitive inhibition. As the P32/98 concentration increased, the K_m decreased. The V_{max} was unchanged with increased concentration of inhibitor. The shape of the curve in the Michaelis-Menten plot was hyperbolic. Alpha was around $6.369e+010 > 1$ (very large) (Fig 5.7). The mechanism of action of the flavonoid sample extracted from *A. cominia* was comparable to that of the P32/98 inhibitor of DPPIV enzyme activity.



Inhibitor Concentration (μM)	Vmax (RFU)	Km (M)
0.1	226.5	2.55E-07
0.3	228.5	2.99E-07
1	230.2	2.71E-07
3	246.1	2.69E-07
10	256.8	2.79E-07
30	238.1	3.08E-07

Figure 5.6 Michaelis-Menten plot of the inhibitory effect of the flavonoid fraction of *A. cominia* on DPPIV-catalysis hydrolysis of the enzyme. Data are expressed as mean RFU (relative fluorescence unit) for n=3 replicates of each substrate concentration (0.01 to 30 μg/ml). The insert figure shows the effect of P32/98 on DPPIV assay with $K_i 6 \pm 0.5 \text{ nM}$. The table below the figure represents K_m (M) and V_{max} (RFU) with each inhibitor concentration.



Inhibitor Concentration (μM)	Vmax (RFU)	Km (M)
0.1	144.7	1.22E-07
0.3	152.2	1.60E-07
1	133.5	2.80E-07
3	124.3	5.03E-07
10	118.3	1.21E-06
30	116.4	1.67E-06

Figure 5.7 Michaelis-Menten plot of the inhibitory effect of P32/98 inhibitor on DPPiV-catalysis hydrolysis of the enzyme. Data are expressed as mean RFU (relative fluorescence unit) for n=3 replicates of each substrate concentration (0.01 to 30 $\mu\text{g}/\text{ml}$). The insert figure shows the effect of P32/98 on DPPiV assay with a K_i of 3.7 ± 0.8 nM. The table below the figure represents K_m (M) and V_{max} (RFU) with each inhibitor concentration.

5.3.1.5 Conclusion and discussion

The ability of DPPiV inhibitors to improve glucose control in T2-DM, has led to the examination of natural products as DPPiV inhibitors (Mardanyan *et al.*, 2011). Our *in vitro* studies showed that a flavonoid mixture extracted from the Cuban *A. cominia* inhibited the enzymatic activity of DPPiV and the inhibition appeared to be competitive. However, the separated flavonoids did not modify DPPiV activity. Quercitrin and mearnsitrin were active only in synergy. After separation, these compounds lost their activity on the DPPiV enzyme. The flavonoid mixture produced a concentration-dependent inhibition with a K_i three times of that of the P32/98 inhibitor. The inhibition of DPPiV by the flavonoid mixture was competitive, as was P32/98. All the aforementioned findings suggest that *A. cominia* as anti-diabetic treatment contains active DPPiV inhibitors.

5.3.2 PTP1B enzyme

5.3.2.1 Z-factor of PTP1B assay

For PTP1B assay (Fig 5.8), the value of Z-factor was 0.902. By comparison with the high-throughput screening fitness assay (Table 5.1), Z-factor is between 0.9 and 1, which shows that the DPPIV assay and its conditions were excellent and can be highly recommended to follow in further screening tests.

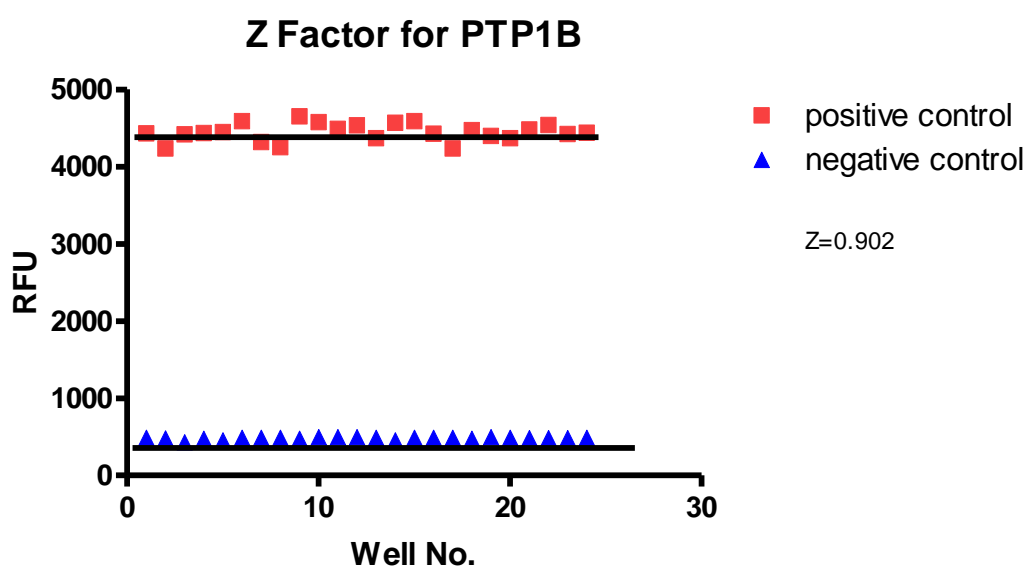


Figure 5.8 High-throughput screening fitness for PTP1B assay using TFMS as substrate and PTP1B enzyme.

5.3.2.2 Effect of extracts of *A. cominia* on the PTP1B enzyme

All plants extracts were tested on the PTP1B enzyme assay at 30 µg/ml and compared with the standard inhibitor, TFMS, which produced a concentration-dependent inhibition with a K_i of 1.1 ± 0.03 µM (Fig 5.9). Plants contain several classes of secondary metabolites and the biological activity of the plant may be the result of all these metabolites working in synergy. Therefore, all the compounds isolated from different crude extracts from *A. cominia*, as well as all the samples eluted by different phytochemical techniques (particularly the active compounds tested in the glucose uptake assay) were also tested in the PTP1B enzyme assay.

5.3.2.3 Effect of compounds isolated from AC-HEC on PTP1B enzyme

DMSO did not produce any effect on PTP1B enzyme compared with the control. All the samples from AC-HEC (hexane and ethyl acetate crude extract and its fractions eluted by silica gel column chromatography) significantly inhibited PTP1B enzyme ($P < 0.05$) (Fig 5.9). A $71.6 \pm 3\%$ inhibition of PTP1B was observed by the crude extract (HEC). More than 70% inhibition was observed only with samples HEC-35-38, 48 and 51-53. These samples were identified to be a mixture of flavonoids, fatty acid and tannins.

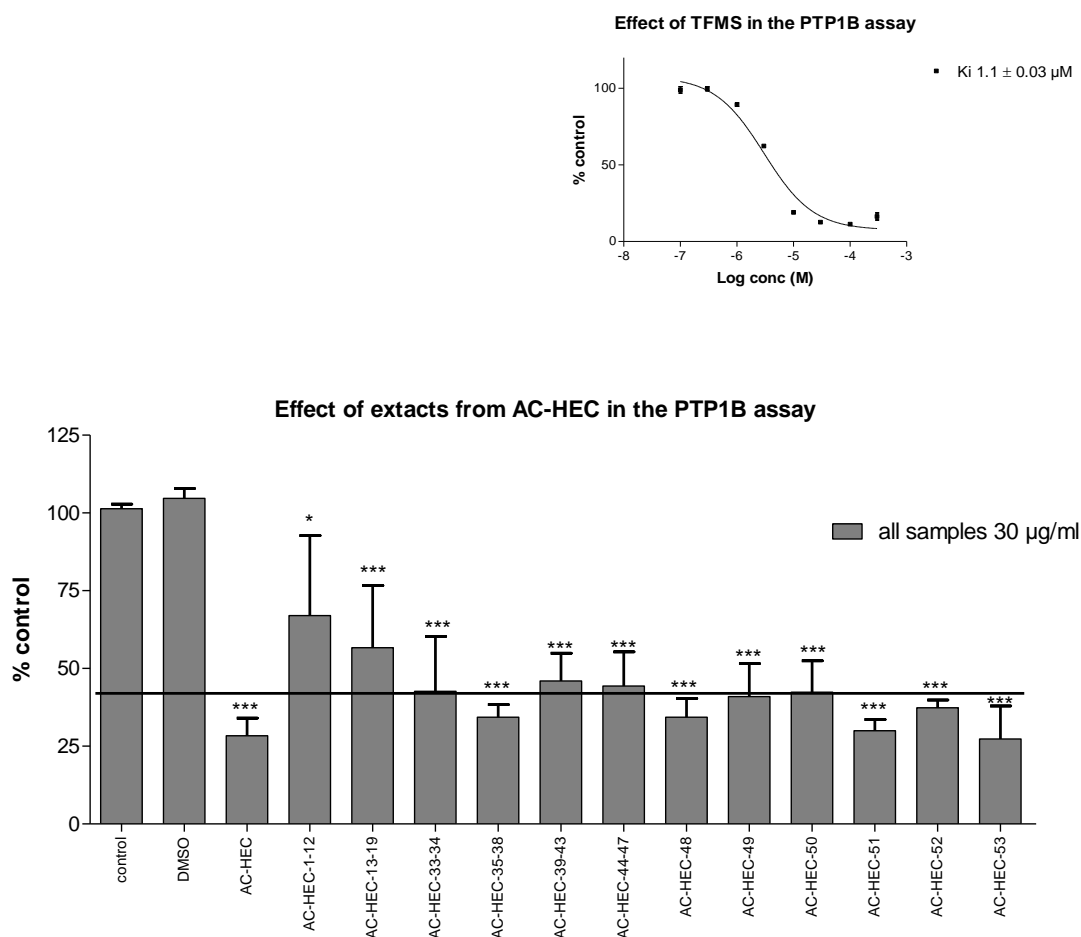


Figure 5.9 Effect of various AC-HEC fractions (separated by silica gel column chromatography) on PTP1B enzyme in the presence of DiFMUP substrate. Extracts concentrated at 30 μg/ml were incubated with PTP1B enzyme for 30 min at 37°C in an atmosphere containing 5% CO₂. DiFMUP (10 μM) was then added and incubated for 10 min at 37°C. The hydrolysis of DiFMUP by PTP1B enzyme was measured at 355/460 nm. Data represent mean ± SEM of PTP1B enzyme hydrolysis (% control) of three independent experiments. Insert shows the effect of various concentrations of TFMS standard (0.03-100 μM) on PTP1B enzyme in the presence of DiFMUP. DMSO was used as control. Ki for TFMS was 1.1 ± 0.03 μM. The data were analysed by Dunnett *post-test*. ****P* value < 0.05 versus control.

5.3.2.3.1 Effect of compounds isolated from AC-MC on PTP1B enzyme

All the samples from AC-MC (methanolic crude extract and its fractions eluted by VLC) significantly inhibited PTP1B enzyme ($P < 0.05$) (Fig 5.10). A $62.6 \pm 0.9\%$ inhibition of PTP1B was observed by the crude extract (MC). More than 70% inhibition was observed only with samples MC-D ($68.3 \pm 4.8\%$), H ($61 \pm 1.5\%$), I ($64.3 \pm 1.3\%$), J ($78.3 \pm 2.6\%$) and KLMN ($79 \pm 4.3\%$). These samples were identified to be a mixture of flavonoids, pheophytins and tannins. A further PTP1B assay was done on the eluted samples from D and KLMN only. Sub-fraction D was found to be a mixture of pheophytins, while KLMN was a mixture of flavonoids. The flavonoid mixture was the most active.

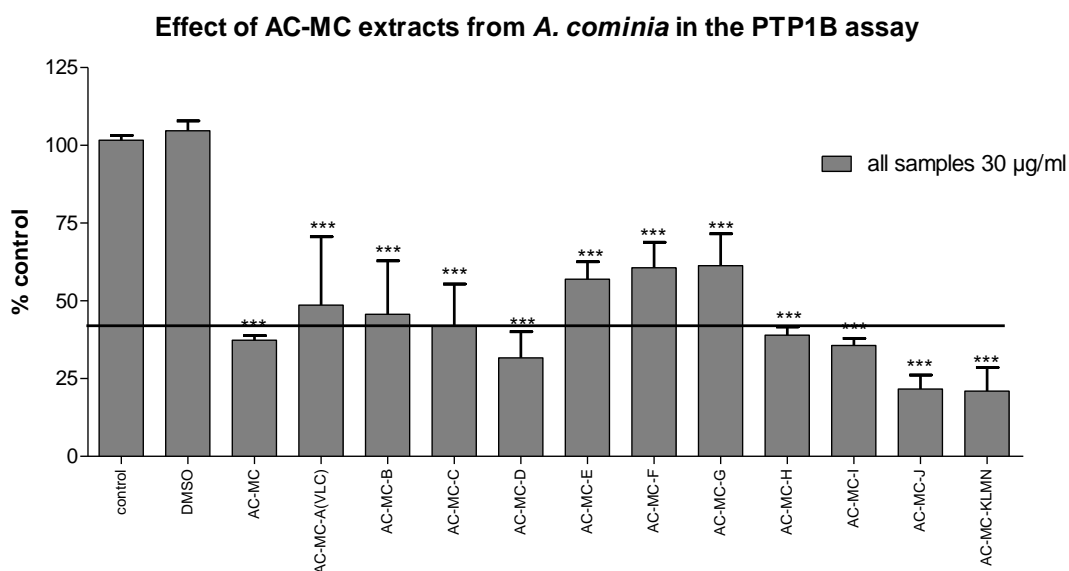


Figure 5.10 Effect of various AC-MC fractions (separated by VLC) on PTP1B enzyme in the presence of DiFMUP substrate. Extracts concentrated at $30 \mu\text{g/ml}$ were incubated with PTP1B enzyme for 30 min at 37°C in an atmosphere containing 5% CO_2 . DiFMUP ($10 \mu\text{M}$) was then added and incubated for 10 min at 37°C . The hydrolysis of DiFMUP by PTP1B enzyme was measured at 355/460 nm. Data represent mean \pm SEM of PTP1B enzyme hydrolysis (% control). $n=3$. The data were analysed by Dunnett *post-test*. *** P value < 0.05 versus control.

7.2.2.3. Effect of compounds isolated from AC-MC-KLMN on PTP1B enzyme

AC-MC-KLMN was identified as a mixture of flavonoids and was then separated by sephadex column chromatography. Samples collected and pooled together (after TLC) were tested in the PTP1B enzyme assay. DMSO had no effect on PTP1B enzyme. The highest inhibition ($77.6 \pm 4.4\%$) of PTP1B was with the mixture sample (KLMN) (Fig 5.11). Separated fractions from KLMN, including 1-24, 44-90 and 91-175, significantly inhibited PTP1B enzyme ($66.3 \pm 3.3\%$, $53.3 \pm 6.2\%$ and $62 \pm 1.7\%$ respectively). More than 60% inhibition was observed only with samples 1-24 and 91-175. Samples 1-24 were identified as tannins. Only samples 91-175 were showing the presence of a mixture of flavonoids separated from the tannins. This sample was then separated by sephadex column chromatography and the activity of the fractions was tested in PTP1B assay (Fig 5.12).

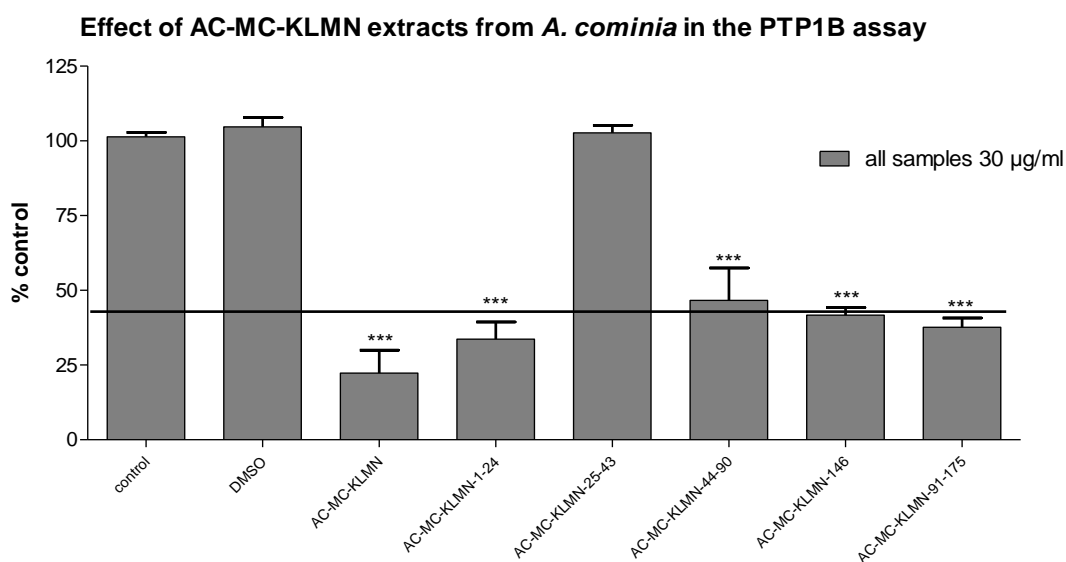


Figure 5.11 Effect of various AC-MC-KLMN fractions (separated by sephadex column chromatography) on PTP1B enzyme in the presence of DiFMUP substrate. Extracts concentrated at $30 \mu\text{g/ml}$ were incubated with PTP1B enzyme for 30 min at 37°C in an atmosphere containing 5% CO_2 . DiFMUP ($10 \mu\text{M}$) was then added and incubated for 10 min at 37°C . The hydrolysis of DiFMUP by PTP1B enzyme was measured at 355/460 nm. Data represent mean \pm SEM of PTP1B enzyme hydrolysis (% control). $n=3$. The data were analysed by Dunnett *post-test*. *** P value <0.05 versus control.

Significant inhibition of PTP1B was observed with samples 1-5, 6-18, 56-58, 59, 60-65, 66-72, and 73-135 (Fig 5.12). The highest inhibition ($100 \pm 5\%$) was with fraction 66-72, which was identified as the mixture of flavonoids separated from the fatty acids. This fraction was further separated by HPLC. Both fractions produced significant inhibition of PTP1B ($25 \pm 6\%$ with F1 and $32 \pm 6\%$ with F2). However, none of the separated compounds produced more than 60% inhibition of the PTP1B enzyme (Fig 5.13). Therefore, individual flavonoid compounds were not accepted as active inhibitors of PTP1B.

Effect of AC-MC-KLMN (91-175) extracts from *A. cominia* in the PTP1B assay

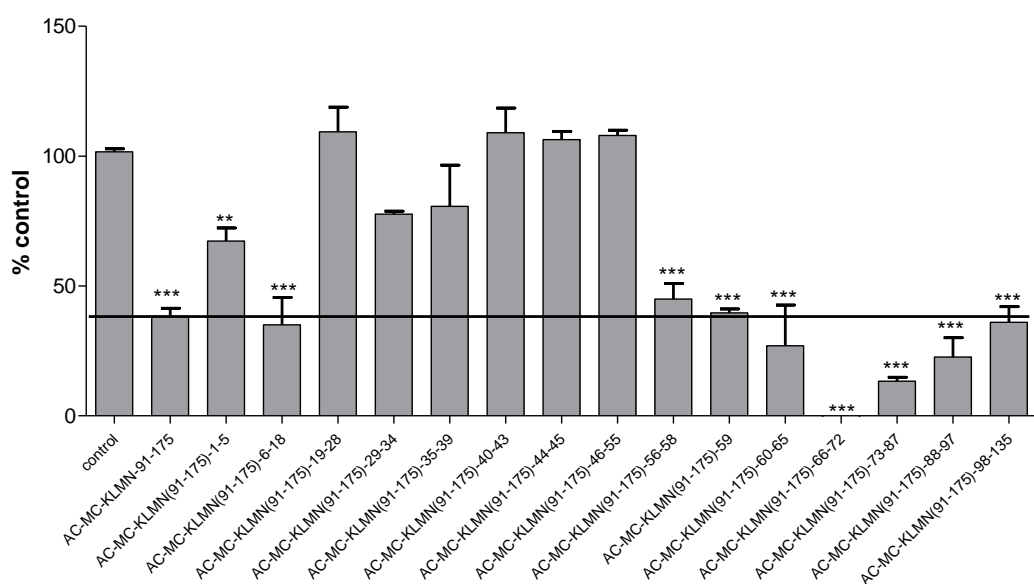


Figure 5.12 Effect of various AC-MC-KLMN-91-175 Fractions (separated by sephadex column chromatography) on PTP1B enzyme in the presence of DiFMUP substrate. Extracts concentrated at $30 \mu\text{g/ml}$ were incubated with PTP1B enzyme for 30 min at 37°C in an atmosphere containing 5% CO_2 . DiFMUP ($10\mu\text{M}$) was then added and incubated for 10 min at 37°C . The hydrolysis of DiFMUP by PTP1B enzyme was measured at 355/460 nm. Data represents mean \pm SEM of PTP1B enzyme hydrolysis (% control). $n=3$. The data were analysed by Dunnett *post-test*. *** P value <0.05 versus control.

Effect of flavonoids extracts from AC-KLMN-(91-175)-66-72 on PTP1B

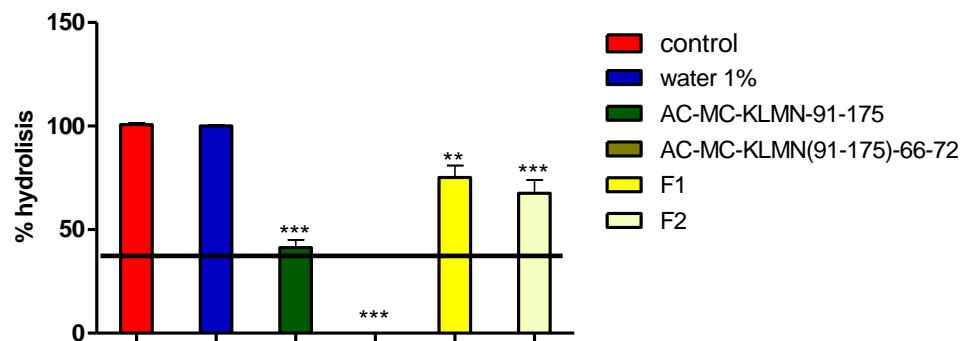


Figure 5.13 Effect of various fractions from AC-KLMN-(91-175)-66-72 (separated by HPLC) on PTP1B enzyme in the presence of DiFMUP substrate. Data represent mean \pm SEM of PTP1B enzyme hydrolysis (% control). $n=3$. The data were analysed by Dunnett *post-test*. *** P value <0.05 versus control.

5.3.2.3.2 Effect of compounds isolated from AC-MC-D on PTP1B enzyme

All the fractions separated from AC-MC-D (by silica gel column chromatography) produced significant inhibition of PTP1B enzyme ($P < 0.05$) at 30 $\mu\text{g/ml}$ (Fig 5.14). Fraction 5-13 was the most active, producing $65 \pm 2\%$ inhibition of the enzyme. Fraction 5-13 was identified as pheophytin A. Fraction 14-24, identified as pheophytin B produced significant inhibition of PTP1B enzyme ($53.3 \pm 1.7\%$). However, fraction 14-24 was not considered to be active (inhibition was less than 60%).

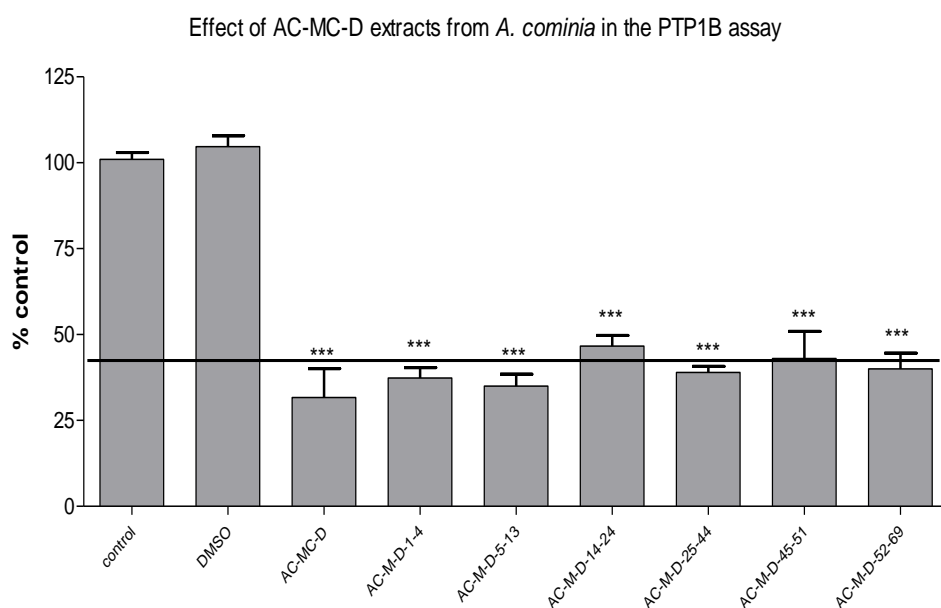


Figure 5.14 Effect of various AC-MC-D fractions (separated by silica gel column chromatography) on PTP1B enzyme in the presence of DiFMUP substrate. Extracts concentrated at 30 $\mu\text{g/ml}$ were incubated with PTP1B enzyme for 30 min at 37°C in an atmosphere containing 5% CO_2 . DiFMUP (10 μM) was then added and incubated for 10 min at 37°C. The hydrolysis of DiFMUP by PTP1B enzyme was measured at 355/460 nm. Data represent mean \pm SEM of PTP1B enzyme hydrolysis (% control). $n=3$. The data were analysed by Dunnett *post-test*. *** P value < 0.05 versus control.

5.3.2.3.3 Concentration dependent inhibition of the flavonoids and pheophytins

TFMS produced a concentration-dependent inhibition of PTP1B enzyme with a K_i value of $1.13 \pm 0.03 \mu\text{M}$. Samples showing more than 60% inhibition of PTP1B enzyme at $30 \mu\text{g/ml}$ are presented in the table in Fig 5.15. Samples AC-HEC, HEC-35-38 and 48 were from the ethyle acetate and hexane extracts. These fractions were identified by NMR to be a mixture of flavonoids. Flavonoids were also identified in the methanolic extracts MC-KLMN, as well as in fraction KLMN-91-175 and fraction KLMN(91-175)-66-72. In addition, pheophytins were identified in MC-D and the separated pheophytin A in MC-D-5-13 and pheophytin B in sample MC-D-24-44. The effect of a range of concentrations of these samples ($0.1\text{-}30 \mu\text{M}$) was tested on the hydrolysis of PTP1B enzyme using DiFMUP as substrate.

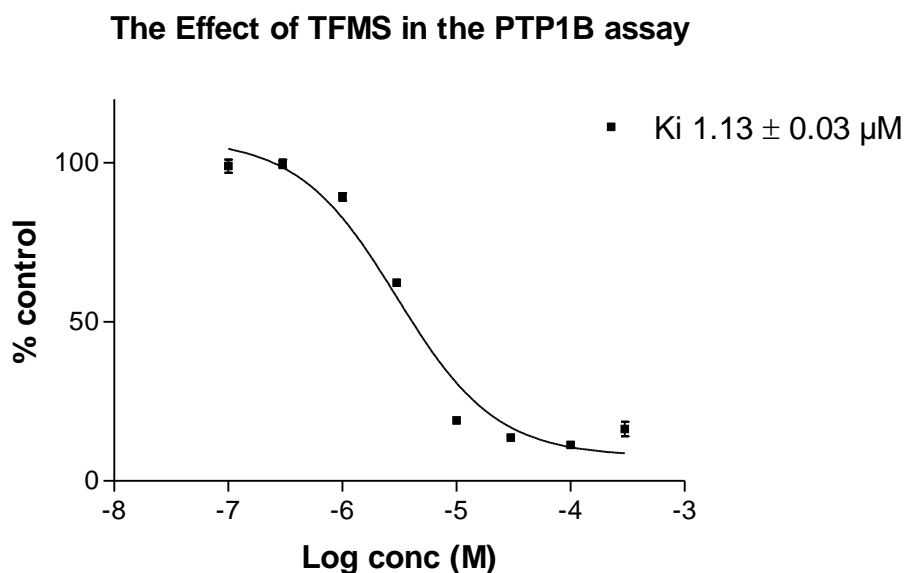


Figure 5.15 Effect of TFMS inhibitor on PTP1B enzyme in the presence of DiFMUP substrate. Inhibitor concentration range was incubated with PTP1B enzyme for 30 min at 37°C in an atmosphere containing 5% CO_2 . DiFMUP ($10 \mu\text{M}$) was then added and incubated for 10 min at 37°C . The hydrolysis of DiFMUP by PTP1B enzyme was measured at 355/460 nm. Data represent mean \pm SEM of PTP1B enzyme hydrolysis (% control). $n=3$. K_i for TFMS was $1.13 \pm 0.03 \mu\text{M}$.

The crude ethylacetate hexane extract produced a concentration-dependent inhibition of PTP1B enzyme with a K_i value of $0.15 \pm 0.01 \mu\text{g/ml}$, which was 7 times less than the K_i value for TFMS ($1.13 \pm 0.03 \mu\text{g/ml}$). Fractions AC-HEC-35-38 and 48 separated from the crude AC-HEC also produced a concentration-dependent inhibition of PTP1B enzyme, with K_i values of $0.13 \pm 0.01 \mu\text{g/ml}$ and $0.12 \pm 0.07 \mu\text{g/ml}$ respectively (Fig 5.16). K_i of the eluted fractions was the same as that of the crude extract. Hence, the inhibition of PTP1B by AC-HEC appeared to be due to the flavonoids present in the extract.

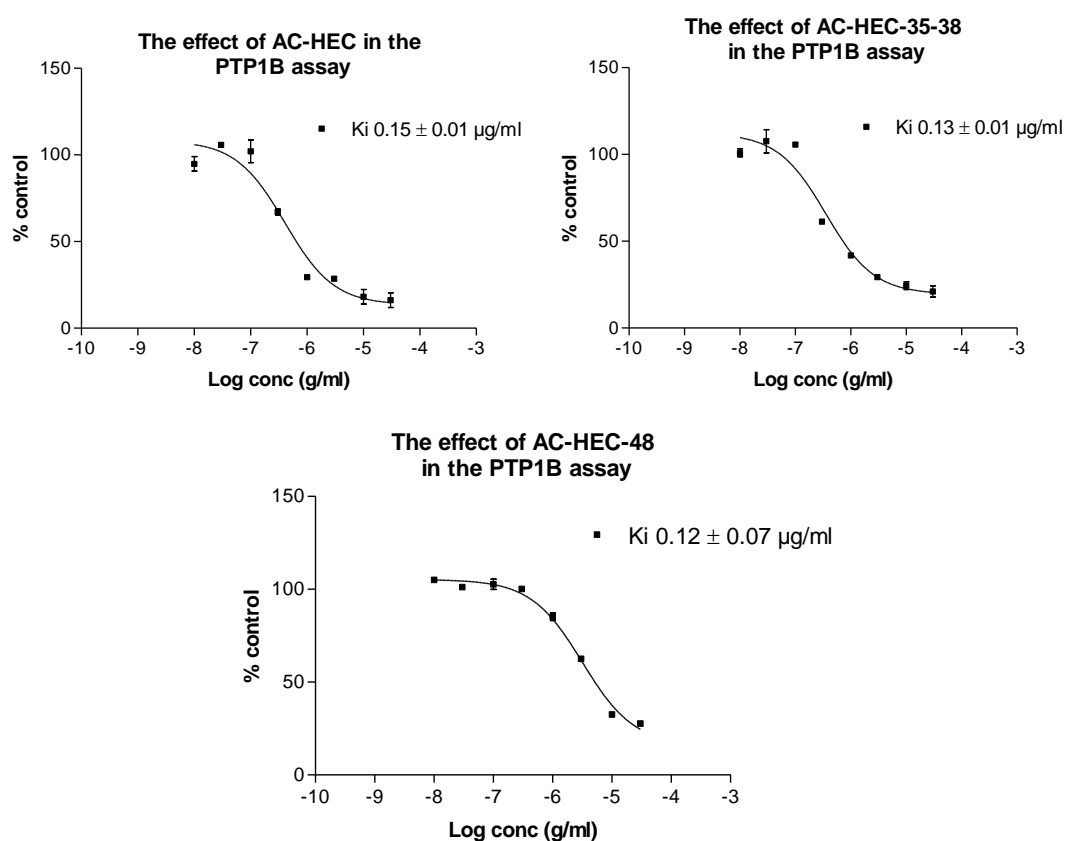


Figure 5.16 Series of graphs showing the effect of various fractions of AC-HEC extracts (AC-HEC, AC-HEC-35-38 and AC-HEC-48) on the PTP1B enzyme. Extracts were incubated with PTP1B enzyme for 30 min at 37°C in an atmosphere containing 5% CO_2 . DiFMUP ($10 \mu\text{M}$) was then added and incubated for 10 min at 37°C . The hydrolysis of DiFMUP by PTP1B enzyme was measured at 355/460 nm. Data represent mean \pm SEM of PTP1B enzyme hydrolysis (% control). $n=3$. K_i for AC-HEC was $0.15 \pm 0.01 \mu\text{g/ml}$, K_i for AC-HEC-35-38 was $0.13 \pm 0.01 \mu\text{g/ml}$ and K_i for AC-HEC-48 was $0.12 \pm 0.07 \mu\text{g/ml}$.

The crude methanolic extract of *A. cominia* produced a concentration-dependent inhibition of PTP1B enzyme with a K_i value of $0.15 \pm 0.02 \mu\text{g/ml}$, which was 7 times less than the K_i value for TFMS ($1.13 \pm 0.03 \mu\text{g/ml}$). Fraction D, a mixture of pheophytins (separated by VLC), produced a concentration-dependent inhibition of PTP1B enzyme with a K_i of $0.5 \pm 0.03 \mu\text{g/ml}$. Fractions AC-MC-D-5-13 and 24-44 separated from AC-MC-D also produced a concentration-dependent inhibition of PTP1B enzyme with K_i values of $0.64 \pm 0.05 \mu\text{g/ml}$ and $0.88 \pm 0.03 \mu\text{g/ml}$ respectively (Fig 5.17). K_i values of the eluted fractions were higher than that of the crude extract. The inhibition of PTP1B enzyme by AC-MC-D was made by the pheophytins in addition to other secondary metabolites in the plant, which may be responsible for the activity of the plant extract.

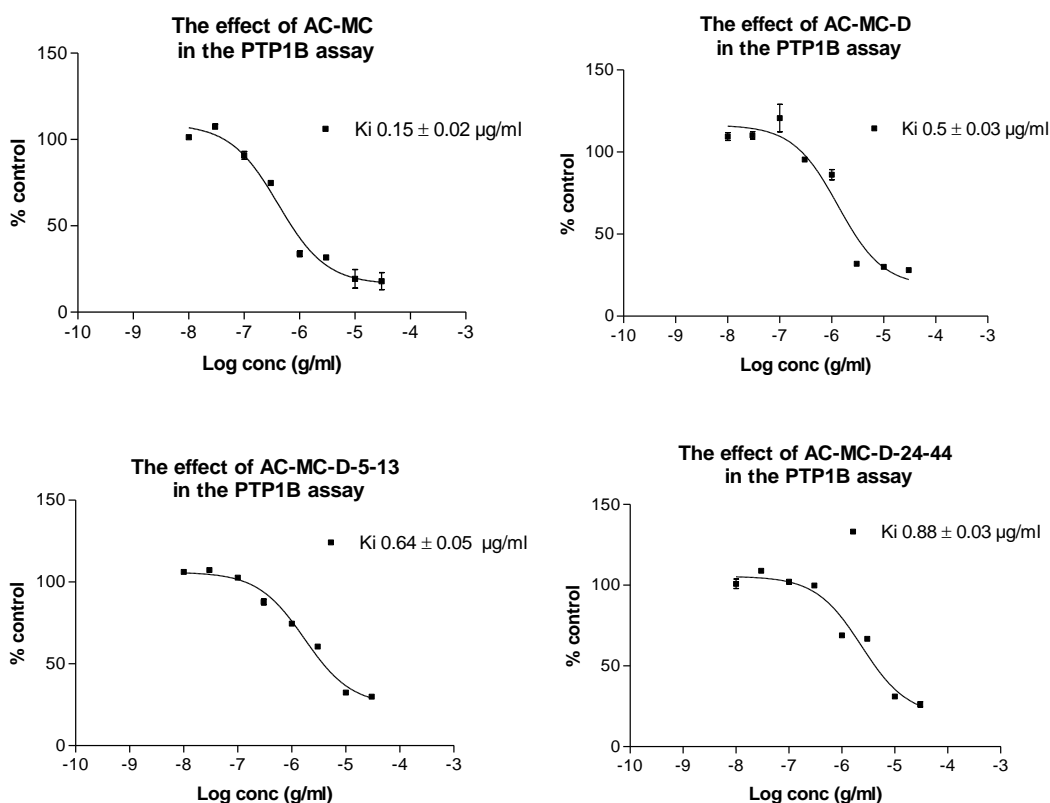


Figure 5.17 Series of graphs showing the effect of various fractions of AC-MC extracts (AC-MC, AC-MC-D, AC-MC-D-5-13 and AC-MC-D-24-44) on the PTP1B enzyme. Extracts were incubated with PTP1B enzyme for 30 min at 37°C in an atmosphere containing 5% CO₂. DiFMUP (10 µM) was then added and incubated for 10 min at 37°C. The hydrolysis of DiFMUP by PTP1B enzyme was measured at 355/460 nm. Data represent mean \pm SEM of PTP1B enzyme hydrolysis (% control). n=3. K_i for AC-MC was $0.15 \pm 0.02 \mu\text{g/ml}$, K_i for AC-MC-D was $0.5 \pm 0.03 \mu\text{g/ml}$, K_i for AC-MC-D-5-13 was $0.64 \pm 0.05 \mu\text{g/ml}$ and K_i for AC-MC-D-24-44 was $0.88 \pm 0.03 \mu\text{g/ml}$.

Fraction KLMN (separated from the crude methanolic extract) produced a concentration-dependent inhibition of PTP1B enzyme with a K_i value of 0.6 ± 0.05 $\mu\text{g/ml}$ which was 2 fold less than the K_i value for TFMS (1.13 ± 0.03 $\mu\text{g/ml}$). Fraction 91-175 (flavonoids and fat) separated from the crude KLMN also produced a concentration dependent inhibition of PTP1B enzyme with a K_i value of 1.08 ± 0.005 $\mu\text{g/ml}$ (Fig 5.18). K_i of the eluted fraction 66-72 (separated from the fat) was higher than that of the crude extract (K_i 3.2 ± 0.09 $\mu\text{g/ml}$). The inhibition of PTP1B enzyme by AC-HEC was made by the flavonoids separated from the crude extract. This inhibition was higher in the presence of fatty acids in the sample.

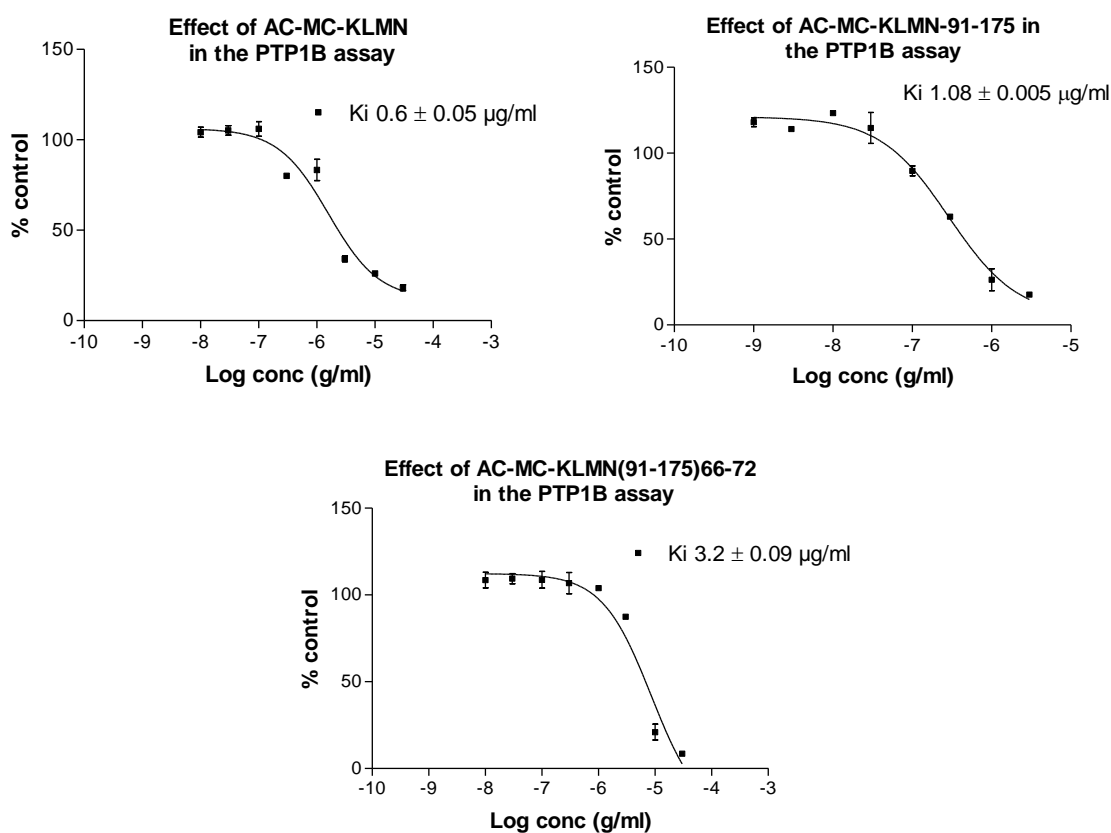
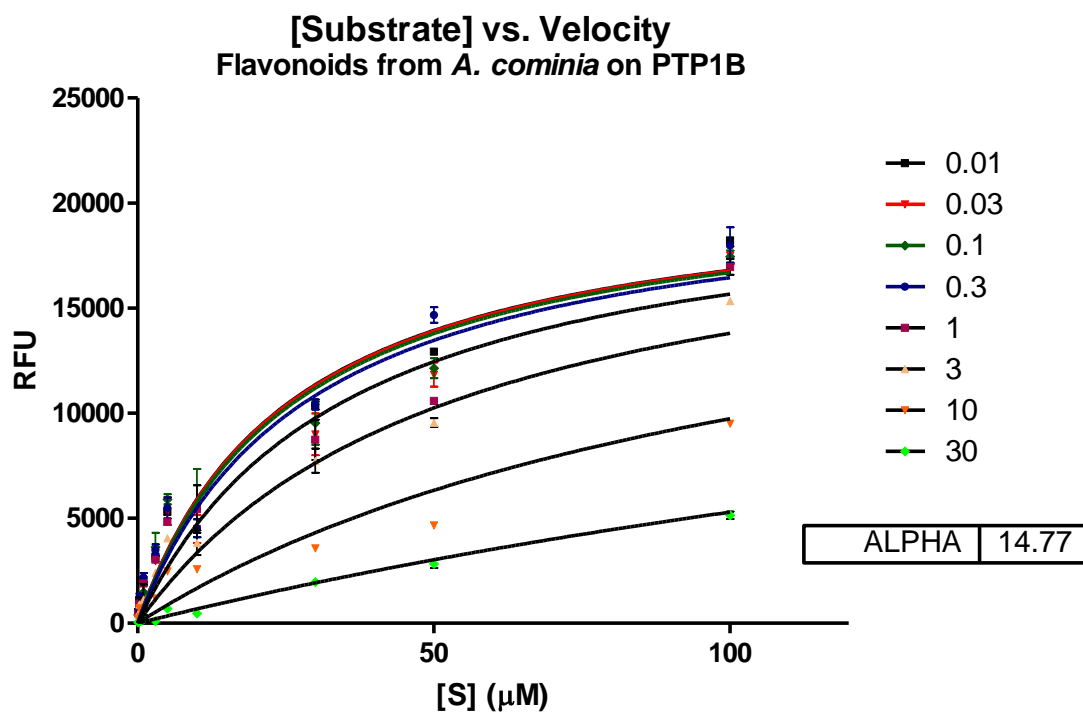


Figure 5.18 Series of graphs showing the effect of various fractions of AC-MC-KLMN extracts (AC-MC-KLMN, AC-MC-KLMN-91-175 and AC-MC-KLMN-(91-175)66-72) on the PTP1B enzyme. Extracts were incubated with PTP1B enzyme for 30 min at 37°C in an atmosphere containing 5%CO₂. DiFMUP (10 μM) was then added and incubated for 10 min at 37°C. The hydrolysis of DiFMUP by PTP1B enzyme was measured at 355/460 nm. Data represent mean \pm SEM of PTP1B enzyme hydrolysis (% control). n=3. K_i for AC-MC-KLMN was 0.6 ± 0.05 $\mu\text{g/ml}$, K_i for AC-MC-KLMN-91-175 was 1.08 ± 0.005 $\mu\text{g/ml}$ and K_i for AC-MC-KLMN-(91-175)66-72 was 3.2 ± 0.09 $\mu\text{g/ml}$.

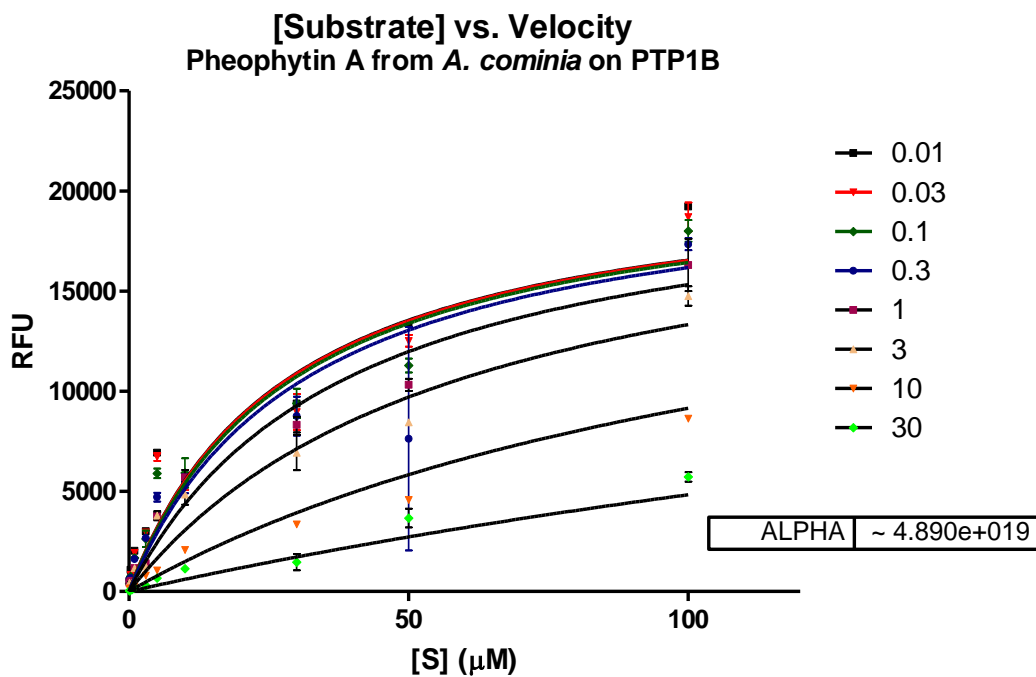
5.3.2.4 Kinetics of the inhibition of PTP1B by the flavonoids and pheophytin A from *A. cominia*

Various concentrations of the flavonoids and pheophytin A samples were incubated with PTP1B enzyme and increasing concentrations of the substrate. The results were graphed using a Michaelis-Menten plot. V_{max} and K_m were calculated (Figs 5.19 and 5.20). As the flavonoids and pheophytin A concentration increased, so did the K_m . The V_{max} was unchanged with increased concentrations of inhibitors. The shape of the curves in the Michaelis-Menten plot was hyperbolic. Alpha was > 1 for both samples. All these factors were indicative of a competitive inhibition of the flavonoid and pheophytin A samples. The mechanism of action of the TFMS inhibitor used in the assay also confirmed its competitive inhibition. As the TFMS concentration increased, so did the K_m . The V_{max} was unchanged with increased concentrations of inhibitor. The shape of the curve in the Michaelis-Menten plot was hyperbolic. Alpha was around $1.941e+015 > 1$ (very large) (Fig 5.21). The mechanisms of action of flavonoid and pheophytin A samples extracted from *A. cominia* were comparable to that of the TFMS inhibitor of PTP1B enzyme activity.



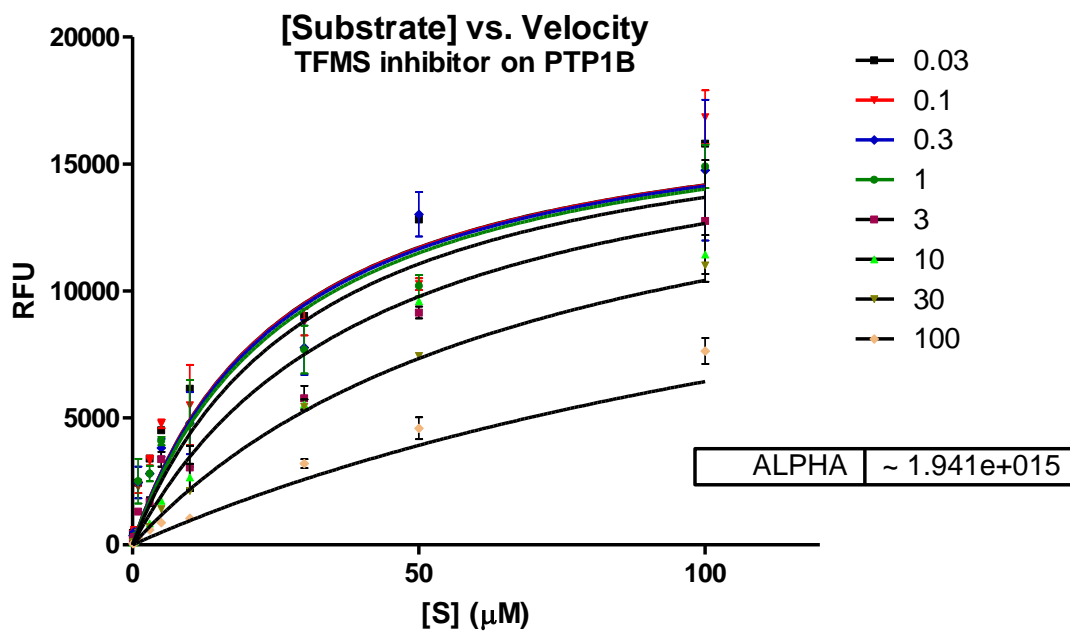
Inhibitor (μM)	Concentration	Vmax (RFU)	Km (μM)
0.01		21482	26.36
0.03		22312	35.98
0.1		19187	21.48
0.3		22474	27.96
1		19725	29.05
3		21214	47.04
10		20901	131.3
30		20313	296.8

Figure 5.19 Michaelis-Menten plot of the inhibitory effect of the flavonoid fractions of *A. cominia* on PTP1B-catalysis hydrolysis of the enzyme. Data are expressed as mean RFU (relative fluorescence unit) for n=3 replicates of each substrate concentration (0.01 to 100 μM). The table below the graph represents Km (μM) and Vmax (RFU) with each inhibitor concentration.



Inhibitor (μM)	Concentration	Vmax (RFU)	Km (μM)
0.01		22729	28.68
0.03		22151	29.93
0.1		20295	26.08
0.3		21838	44.14
1		20940	38.14
3		20189	48.4
10		22671	169.2
30		21659	276

Figure 5.20 Michaelis-Menten plot of the inhibitory effect of the pheophytin A fraction of *A. cominia* on PTP1B-catalysis hydrolysis of the enzyme. Data are expressed as mean RFU (relative fluorescence unit) for n=3 replicates of each substrate concentration (0.01 to 100 μM). The table below the graph represents Km (μM) and Vmax (RFU) with each inhibitor concentration.



Inhibitor (μM)	Concentration	Vmax (RFU)	Km (μM)
0.01		17619	18.59
0.03		18869	26.22
0.1		18520	26.99
0.3		17491	27.77
1		18974	52.8
3		18413	56.94
10		19633	79.19
30		19323	154.4

Figure 5.21 Michaelis-Menten plot of the inhibitory effect of the TFMS on PTP1B-catalysis hydrolysis of the enzyme. Data are expressed as mean RFU (relative fluorescence unit) for n=3 replicates of each substrate concentration (0.01 to 100 μM). The table below the graph represents Km and Vmax with each inhibitor concentration.

5.3.2.5 Conclusion and discussion

Like TFMS, the flavonoid mixture and pheophytins strongly inhibited PTP1B enzyme at 30 $\mu\text{g/ml}$. The flavonoid mixture was highly active (100% inhibition). Pheophytin A (65% inhibition) was more active than pheophytin B (53% inhibition) compared to the control. Therefore, only pheophytin A was used in the glucose uptake assay. After separation by HPLC, quercitrin and mearnsitrin produced much less inhibition, although it was statistically significant (25 and 32 % inhibition respectively). After separation, quercitrin and mearnsitrin did not inhibit PTP1B enzyme, which suggests that these compounds are only active in synergy. Both flavonoid mixture and pheophytins produced a concentration-dependent inhibition of PTP1B enzyme with K_i values of $3.2 \pm 0.09 \mu\text{g/ml}$ for the flavonoids and $0.64 \pm 0.05 \mu\text{g/ml}$ for the pheophytin A. The presence of fatty acids in the sample of flavonoids increased the activity of inhibition. These low K_i values reflect the high potencies of these compounds. Kinetic studies demonstrated that the inhibition of both flavonoids and pheophytin A, as well as the TFMS inhibitor of PTP1B enzyme, were competitive inhibitors. This confirms that these compounds can be reported as PTP1B enzyme inhibitors. Such chemical classes of PTP1B inhibitory compounds from plants including phenols, flavonoids and other compounds have been reported previously (Na., 2006 a, b; Zhang *et al.*, 2010). These reports show that PTP1B enzyme inhibitory compounds from plants belong to a diverse group of chemical compounds. Both flavonoids and pheophytin A also stimulate glucose uptake (as shown in Chapters 3 and 4). It is possible that the inhibition of PTP1B contributed to the enhancement of the glucose uptake as well as to the enhancement of insulin sensitivity in differentiated 3T3-L1, L6 and HepG2 cells. The mixture of flavonoids produced the greatest effect (100% inhibition of PTP1B enzyme). PTP1B enzyme inhibition enhanced insulin activity of *A. cominia* by this mechanism. This is supported by reports on the effect of flavonoids on peripheral insulin sensitivity (Strobel *et al.*, 2005; Nomura *et al.*, 2008; Brahmachari *et al.*, 2011). The hypoglycaemic activity of many plants has been linked to the presence of steroidal glycosides (Kato *et al.*, 1995; Dhanabal *et al.*, 2005; McAnuf *et al.*, 2005).

5.3.3 α -Glucosidase enzyme

5.3.3.1 Z-factor of α -glucosidase assay

α -glucosidase enzyme assay fitness was screened using α -glucosidase enzyme at 0.2 units/ml in the presence of 4-nitrophenyl- α -D-glucopyranoside as substrate (1 mM). The positive control was in the presence of both substrate and α -glucosidase enzyme. The negative control was in the presence of the substrate only.

For α -glucosidase assay (Fig 5.22), the value of Z-factor was 0.79. By comparison to the high-throughput screening fitness assay (Table 5.1), Z-factor is between 0.7 and 0.9, confirming that the DPPIV assay and its conditions were acceptable and can be followed for further screening tests.

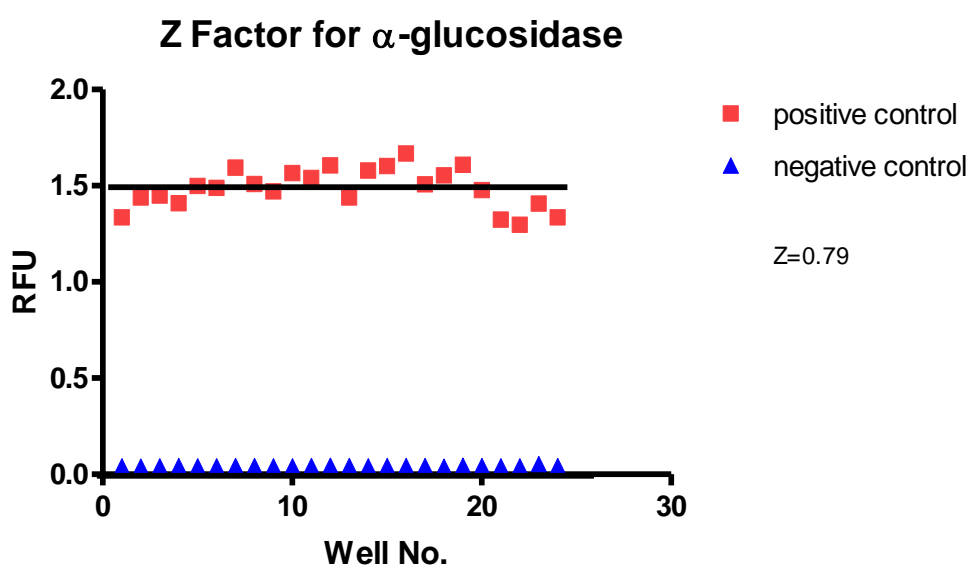


Figure 5.22 High-throughput screening fitness for α -glucosidase assay using 4-nitrophenyl- α -D-glucopyranoside as substrate and α -glucosidase enzyme.

5.3.3.2 Effect of extracts from *A. cominia* on the α -glucosidase enzyme

The control was presented as a displacement curve for the acarbose inhibitor. All *A. cominia* extracts were tested on α -glucosidase assay at 30 μ g/ml. Acarbose produced a concentration-dependent inhibition of α -glucosidase enzyme with a K_i value of 0.22 ± 0.05 mg/ml (Fig 5.23).

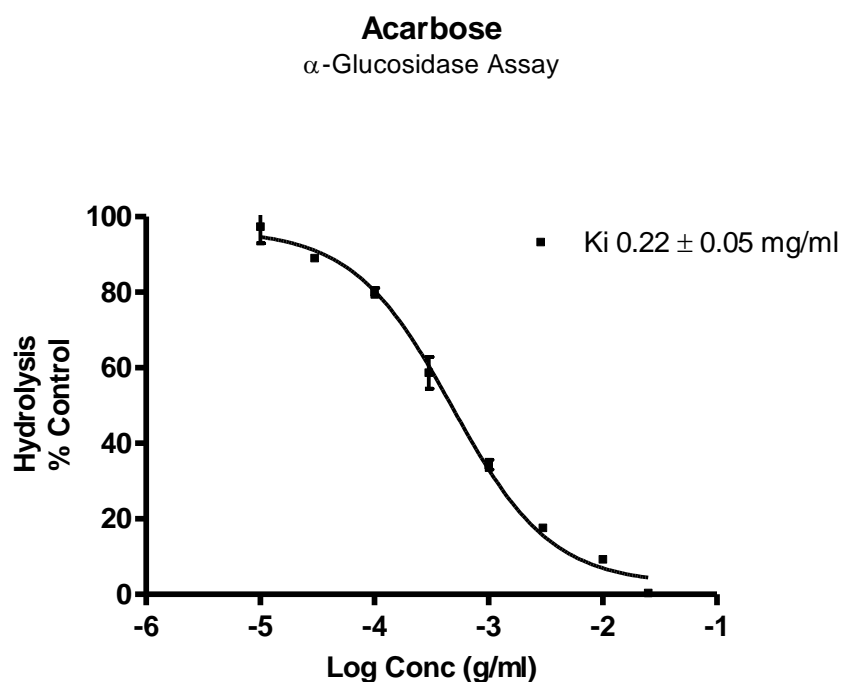


Figure 5.23 Effect of acarbose on the α -glucosidase assay in the presence of 4-nitrophenyl-glucofuranoside (substrate). Acarbose at different concentrations (10 μ g/ml – 30 mg/ml) was incubated with α -glucosidase enzyme for 10 min at 37°C in an atmosphere containing 5% CO₂. 4-nitrophenyl-glucofuranoside (4 mM) was then added and incubated for 10 min at 37°C. The hydrolysis of the substrate by α -glucosidase enzyme was measured at 405 nm. Data represent mean \pm SEM of α -glucosidase enzyme hydrolysis (% control) of three experiments. K_i for acarbose was 0.22 ± 0.05 mg/ml.

5.3.3.2.1 Effect of crude extracts from *A. cominia* on α -glucosidase

Samples which showed 40% or less of the control (more than 60% inhibition) were considered to be potentially active. As shown in Fig 5.24, only methanolic crude extracts of *A. cominia* at 30 μ g/ml showed 94% inhibition (6% of the control). HEC crude extract had no significant effect on α -glucosidase enzyme by comparison to the control. DMSO (1%) did not produce inhibition of the enzyme.

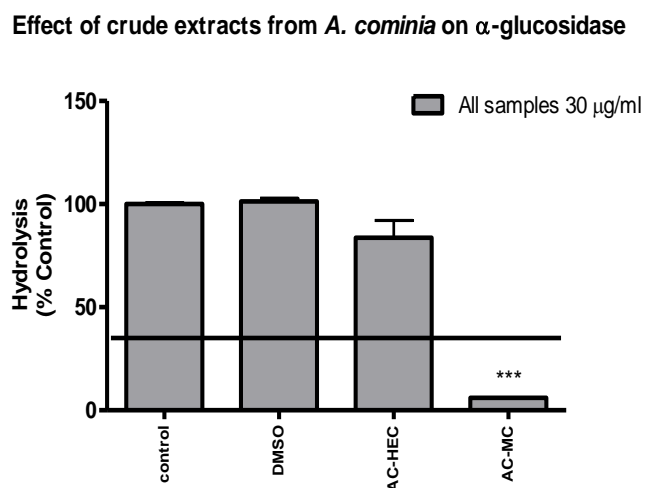


Figure 5.24 Effect of various crude extracts of *A. cominia* from maceration extraction on the α -glucosidase assay in the presence of 4-nitrophenyl-gluco-pyranoside (substrate). Extracts concentrated at 30 μ g/ml were incubated with α -glucosidase enzyme for 10 min at 37°C in an atmosphere containing 5% CO₂. 4-nitrophenyl-gluco-pyranoside (4 mM) was then added and incubated for 10 min at 37°C. The hydrolysis of the substrate by α -glucosidase enzyme was measured at 405 nm. DMSO is a negative control and acarbose is a positive control. Data represent mean \pm SEM of α -glucosidase enzyme hydrolysis (% control) of three experiments. The data were analysed by Dunnett *post-test*, ****P* value < 0.05 versus control.

5.3.3.2.2 Effect of extracts from HEC on α -glucosidase

Of the HEC samples (Fig 5.25) separated by silica gel column chromatography, fraction 52 produced much less inhibition, although it was statistically significant (37% inhibition) by comparison with the control.

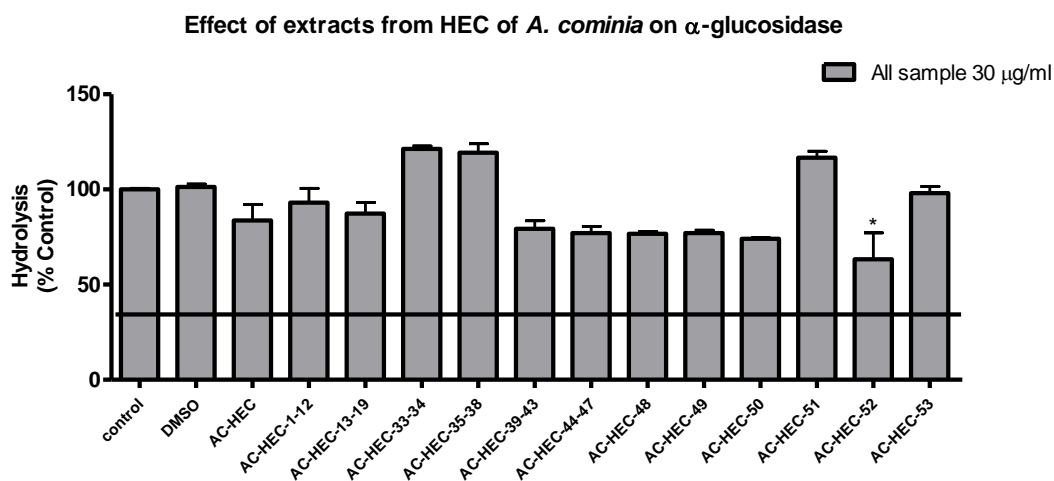


Figure 5.25 Effect of various extracts of *A. cominia* from hexane and ethyl acetate crude extract separated by silica gel column chromatography on the α -glucosidase enzyme. Extracts concentrated at 30 $\mu\text{g/ml}$ were incubated with α -glucosidase enzyme for 10 min at 37°C in an atmosphere containing 5% CO_2 . 4-nitrophenyl-glucopyranoside (4 mM) was then added and incubated for 10 min at 37°C. The hydrolysis of the substrate by α -glucosidase enzyme was measured at 405 nm. DMSO is a negative control and acarbose is a positive control. Data represent mean \pm SEM of α -glucosidase enzyme hydrolysis (% control) of three experiments. The data were analysed by Dunnett *post-test*, **P* value < 0.05 versus control.

5.3.3.2.3 Effect of the methanolic extracts from MC on α -glucosidase

To confirm which fraction of the methanolic extracts is active; α -glucosidase enzyme assay was carried out on all the samples extracted from MC by VLC separation and only samples from fraction F to fraction M showed a significant activity on α -glucosidase enzyme, with p values < 0.05. 79% \pm 2.67, 92%, 87% \pm 0.33, 89% \pm 0.33, 89% \pm 0.33 and 91 \pm 0.33 % of inhibition of α -glucosidase by F, G, H, I, J and KLMN, respectively (Fig 5.26). After chemical identification of all the fractions, fractions D (crude pheophytins) and KLMN (flavonoid mixture) were carried out for further separation and purification, while all separated fractions were tested on α -glucosidase enzyme assay.

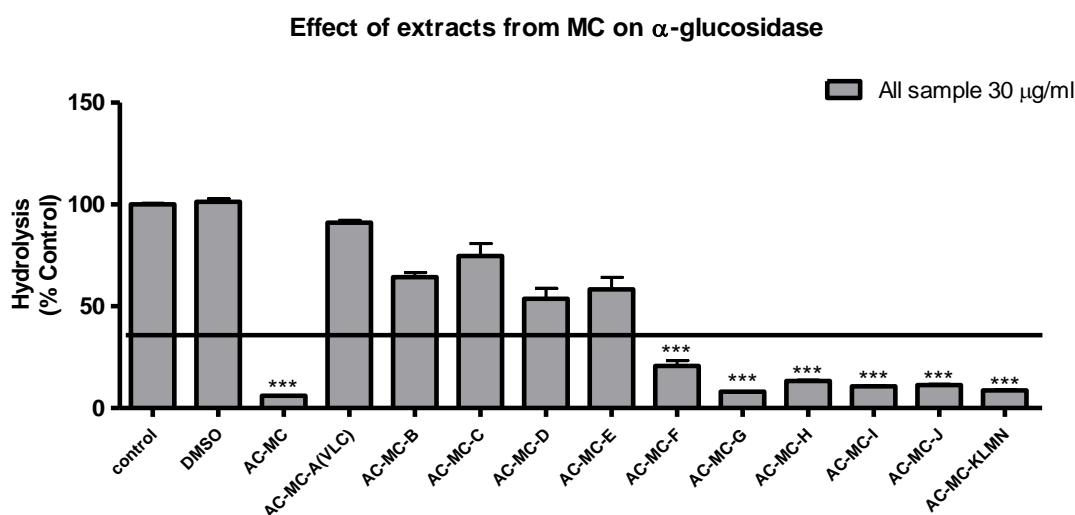


Figure 5.26 Effect of various methanolic extracts of *A. cominia* from vacuum liquid chromatography separation on the α -glucosidase enzyme. Extracts concentrated at 30 μ g/ml were incubated with α -glucosidase enzyme for 10 min at 37°C in an atmosphere containing 5% CO₂. 4-nitrophenyl-gluco-pyranoside (4 mM) was then added and incubated for 10 min at 37°C. The hydrolysis of the substrate by α -glucosidase enzyme was measured at 405 nm. DMSO is a negative control and acarbose is a positive control. Data represent mean \pm SEM of α -glucosidase enzyme hydrolysis (% control) of three experiments. The data were analysed by Dunnett *post-test*, ****P* value < 0.05 versus control.

5.3.3.2.4 Effect of extracts from AC-MC-KLMN on α -glucosidase

As shown in Fig 5.27, all the samples separated by sephadex column chromatography significantly inhibited α -glucosidase enzyme, as did the crude KLMN sample (30 μ g/ml) with P value < 0.05 . The highest inhibition of α -glucosidase (95% inhibition) was with the samples 91-175, identified by chromatographic techniques as a mixture of flavonoids.

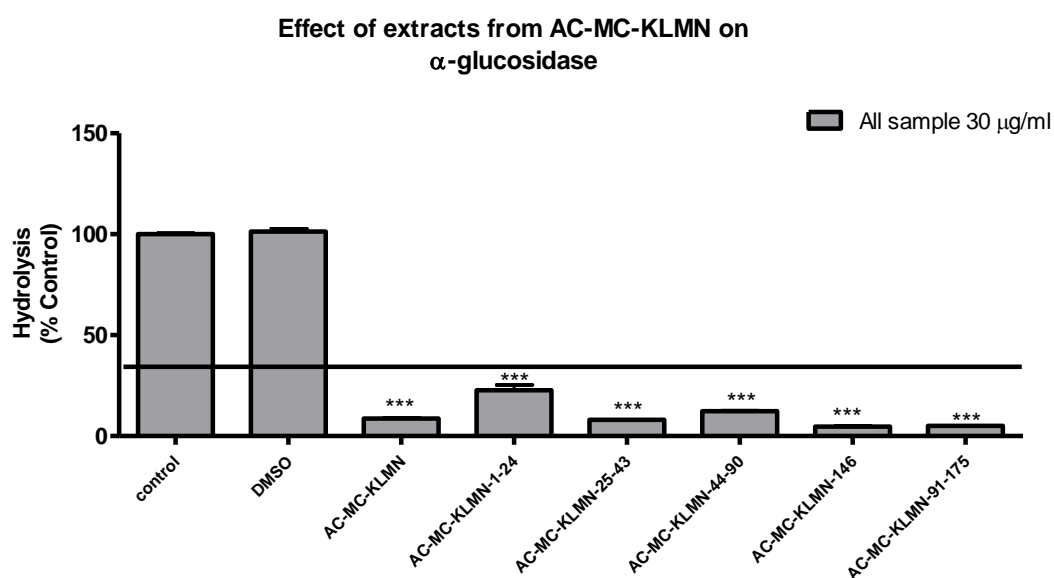


Figure 5.27 Effect of various methanolic extracts of *A. cominia* from KLMN extract fraction separated by sephadex column chromatography on the α -glucosidase enzyme. Extracts concentrated at 30 μ g/ml were incubated with α -glucosidase enzyme for 10 min at 37°C in an atmosphere containing 5% CO₂. 4-nitrophenyl-glucopyranoside (4 mM) was then added and incubated for 10 min at 37°C. The hydrolysis of the substrate by α -glucosidase enzyme was measured at 405 nm. DMSO is a negative control and acarbose is the positive control. Data represent mean \pm SEM of α -glucosidase enzyme hydrolysis (% control) of three experiments. The data were analysed by Dunnett *post-test*, *** P value < 0.05 versus control.

5.3.3.2.5 Effect of extracts from AC-MC-KLMN-91-175 on α -glucosidase

All extracts separated from AC-MC-KLMN-91-175 (except 1-5, 19-28 and 29-34) produced significant inhibition of α -glucosidase enzyme by comparison with the control (Fig 5.28). The highest inhibition of the enzyme was with samples 46 to 59 (95% inhibition). Sample 66-72 (flavonoids mixture) also produced significant inhibition of α -glucosidase enzyme ($79 \pm 1\%$ inhibition). The activity of the extract KLMN-91-175 was affected by all the chemical metabolites in it.

After separation of the flavonoids (quercitrin F1 and mearnsitrin F2) from sample 66-72, neither compound produced inhibition of α -glucosidase (Fig 5.29). This confirms that the effect of the compounds on α -glucosidase occurred when both compounds were in synergy.

Effect of extracts from AC-MC-KLMN-91-175 on α -glucosidase

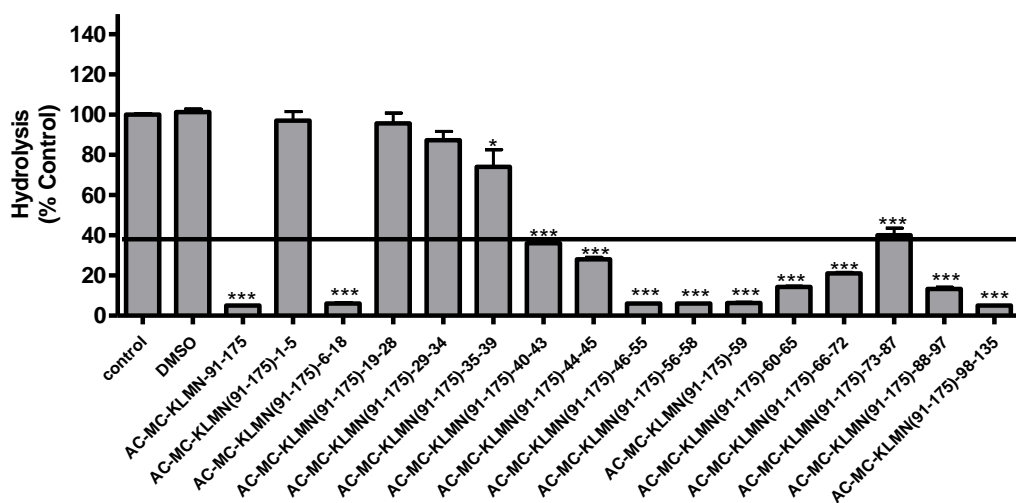


Figure 5.28 Effect of various methanolic extracts of *A. cominia* from fraction KLMN-91-175 separated by sephadex column chromatography on the α -glucosidase enzyme. Data represent mean \pm SEM of α -glucosidase enzyme hydrolysis (% control) of three experiments. The data were analysed by Dunnett *post-test*, ****P* value < 0.05 versus control.

Effect of flavonoids extracts from AC-KLMN-(91-175)-66-72 on α -glucosidase

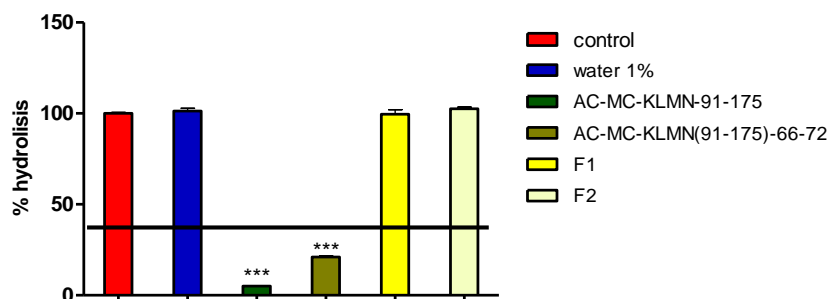


Figure 5.29 Effect of separated flavonoids of *A. cominia* by HPLC (fractions 1 and 2) on α -glucosidase enzyme. Extracts concentrated at 30 μ g/ml were incubated with α -glucosidase enzyme for 10 min at 37°C in an atmosphere containing 5% CO₂. 4-nitrophenyl-glucopyranoside (4 mM) was then added and incubated for 10 min at 37°C. The hydrolysis of the substrate by α -glucosidase enzyme was measured at 405 nm. DMSO is a negative control and acarbose is the positive control. Data represent mean \pm SEM of α -glucosidase enzyme hydrolysis (% control) of three experiments. The data were analysed by Dunnett *post-test*, ****P* value < 0.05 versus control.

5.3.3.2.6 Effect of extracts from AC-MC-D on α -glucosidase

AC-MC-D produced less, but statistically significant inhibition of α -glucosidase (Fig 5.30). None of the extracts of MC-D including the pure pheophytins A and B (respectively fractions 14-24 and 25-44) possessed any inhibitory activity in the α -glucosidase assay.

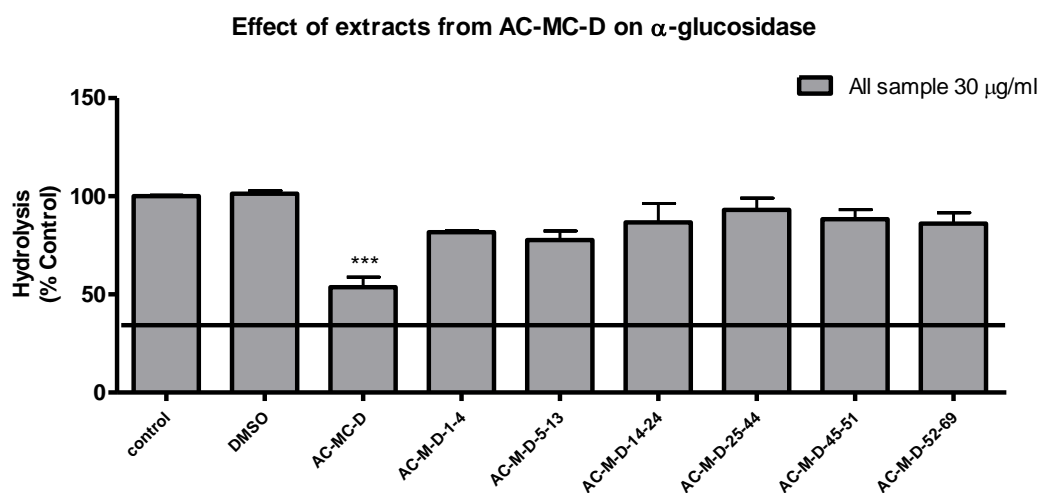


Figure 5.30 Effect of various methanolic extracts of *A. cominia* from fraction D separated by silica gel column chromatography on the α -glucosidase enzyme. Extracts concentration at 30 μ g/ml were incubated with α -glucosidase enzyme for 10 min at 37°C in an atmosphere containing 5% CO₂. 4-nitrophenyl-glucopyranoside (4 mM) was then added and incubated for 10 min at 37°C. The hydrolysis of the substrate by α -glucosidase enzyme was measured at 405 nm. DMSO is a negative control and acarbose is the positive control. Data represent mean \pm SEM of α -glucosidase enzyme hydrolysis (% control) of three independent experiments. The data were analysed by Dunnett *post-test*, ****P* value < 0.05 versus control.

5.3.3.3 Concentration-dependent inhibition of the flavonoids

To study the effect of concentration of the extract on α -glucosidase enzyme, crude methanolic extract, fractions I and KLMN (from VLC), sample AC-MC-KLMN-91-175 and sample AC-MC-KLMN-(91-175)-66-72 were tested. Acarbose produced a concentration-dependent inhibition of α -glucosidase with a K_i value of 0.19 ± 0.0005 mg/ml (Fig 5.31). AC-MC, AC-MC-I and AC-MC-KLMN produced a concentration-dependent inhibition of the enzyme with K_i values of 60 ± 0.02 μ g/ml, 45 ± 0.01 μ g/ml and 32 ± 0.009 μ g/ml respectively (Fig 5.32). However, a concentration-dependent inhibition of α -glucosidase was produced by AC-MC-KLMN-91-175 and AC-MC-KLMN-(91-175)-66-72 with K_i values of 2 ± 0.07 μ g/ml and 1.7 ± 0.5 μ g/ml respectively (Fig 5.33). Purification of the flavonoids decreased the K_i value.

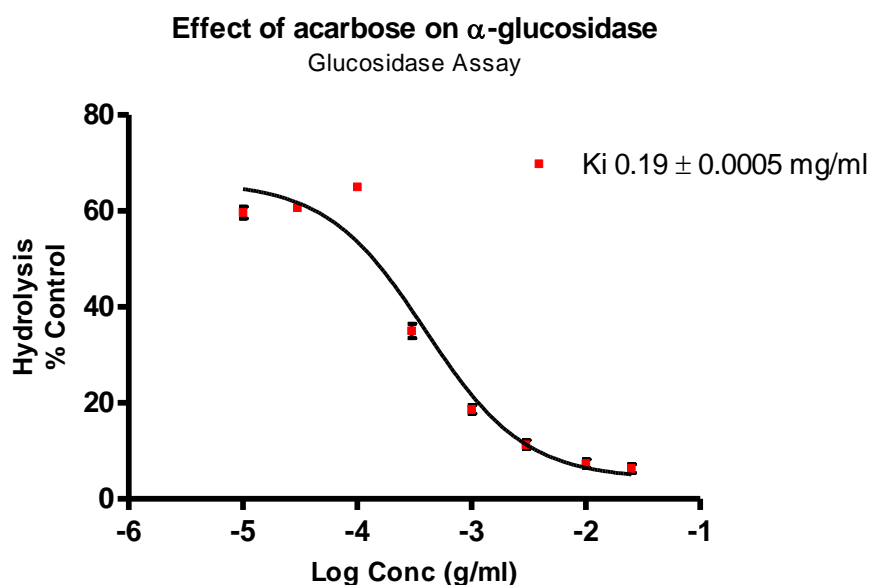


Figure 5.31 Effect of acarbose on the α -glucosidase assay in the presence of 4-nitrophenyl-glucopyranoside (substrate). Acarbose at different concentrations (10 μ g/ml – 30 mg/ml) was incubated with α -glucosidase enzyme for 10 min at 37°C in an atmosphere containing 5% CO₂. 4-nitrophenyl-glucopyranoside (4 mM) was then added and incubated for 10 min at 37°C. The hydrolysis of the substrate by α -glucosidase enzyme was measured at 405 nm. Data represent mean \pm SEM of α -glucosidase enzyme hydrolysis (% control) of three experiments. K_i for acarbose was 0.19 ± 0.0005 mg/ml.

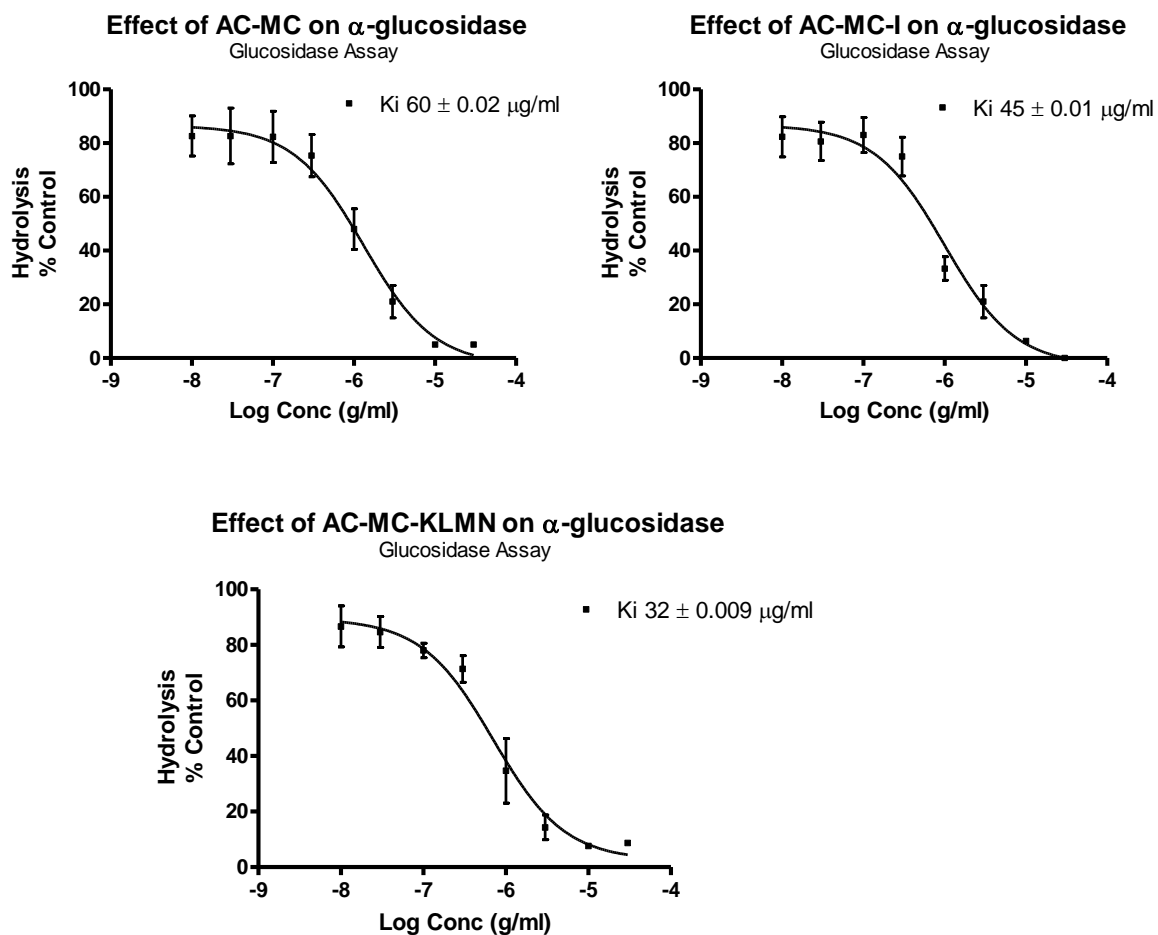


Figure 5.32 The effect of some fractions of AC-MC extracts (AC-MC, AC-MC-I and AC-MC-KLMN) on α -glucosidase enzyme. Extracts were incubated with α -glucosidase enzyme for 10 min at 37°C in an atmosphere containing 5% CO₂. 4-nitrophenyl-glucopyranoside (4 mM) was then added and incubated for 10 min at 37°C. The hydrolysis of the substrate by α -glucosidase enzyme was measured at 405 nm. Data represent mean \pm SEM of α -glucosidase enzyme hydrolysis (% control). n=3. Ki for AC-MC was $60 \pm 0.02 \mu\text{g/ml}$, Ki for AC-MC-I was $45 \pm 0.01 \mu\text{g/ml}$ and Ki for AC-MC-KLMN was $32 \pm 0.009 \mu\text{g/ml}$.

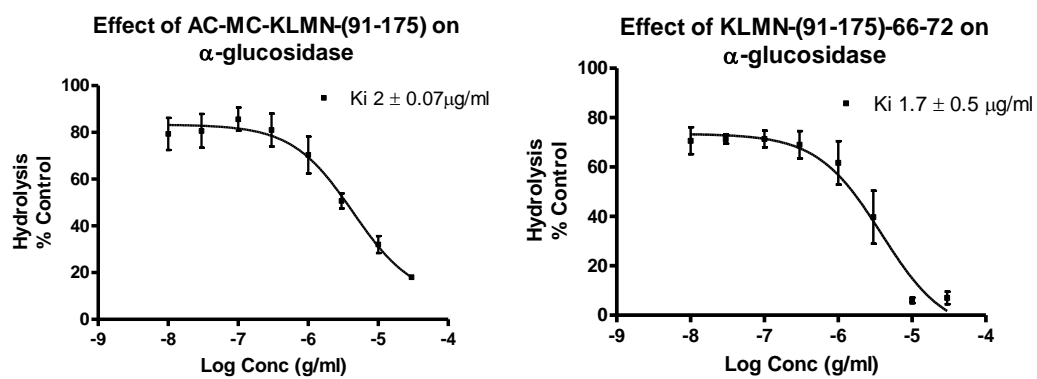
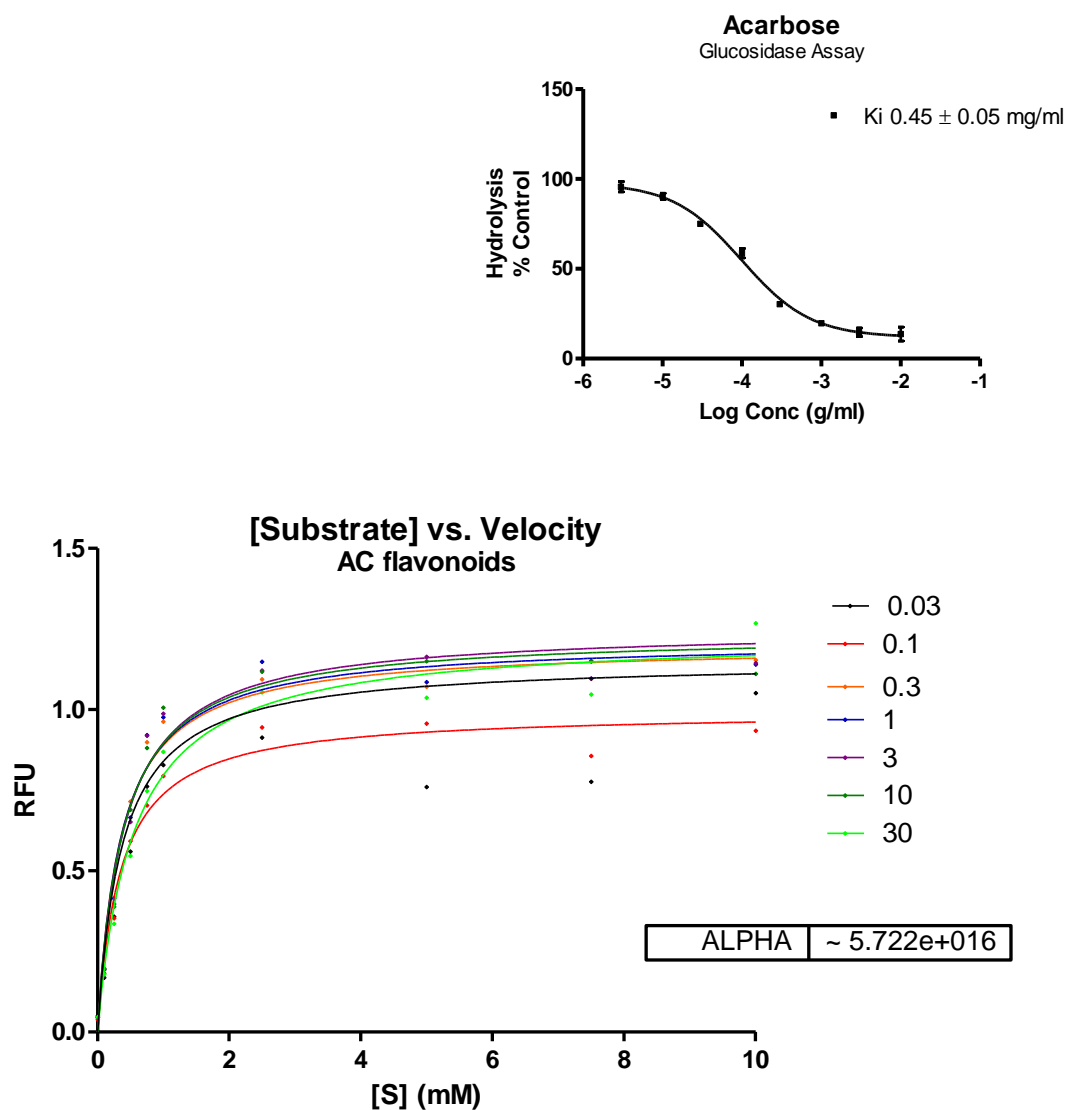


Figure 5.33 The effect of the flavonoids mixture of AC (AC-MC-KLMN-91-175 and AC-MC- KLMN-(91-175)-66-72) on α -glucosidase enzyme. Extracts were incubated with α -glucosidase enzyme for 10 min at 37°C in an atmosphere containing 5% CO₂. 4-nitrophenyl-glucopyranoside (4 mM) was then added and incubated for 10 min at 37°C. The hydrolysis of the substrate by α -glucosidase enzyme was measured at 405 nm. Data represent mean \pm SEM of α -glucosidase enzyme hydrolysis (% control). n=3.

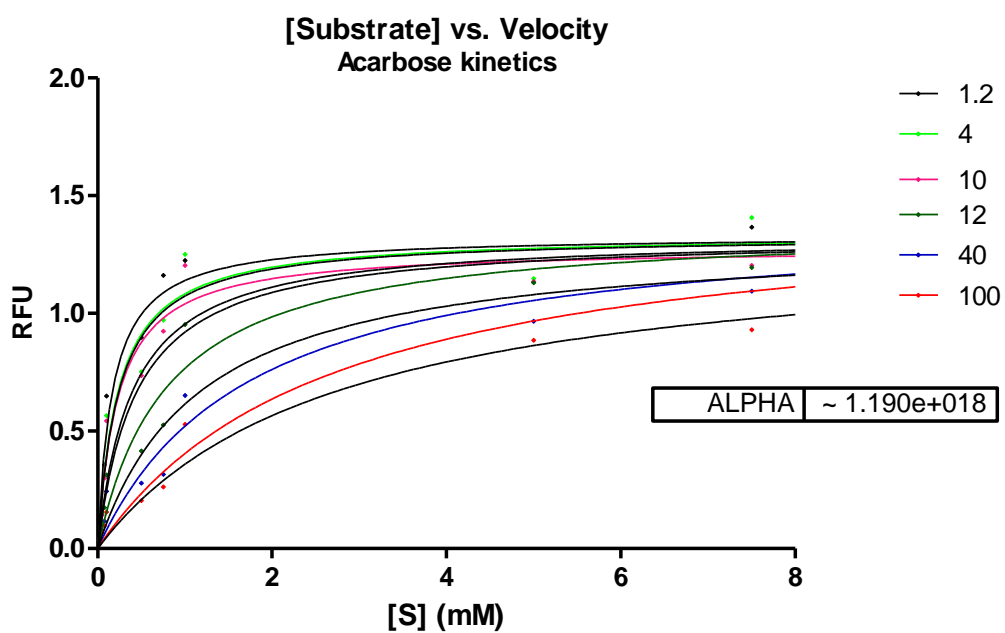
5.3.3.4 Kinetics of the inhibition of α -glucosidase by the flavonoids from *A. cominia*

Acarbose produced a concentration-dependent inhibition of α -glucosidase with a K_i value of 0.45 ± 0.05 mg/ml. Various concentrations of the flavonoids sample were incubated with α -glucosidase enzyme and increasing concentrations of 4-nitrophenyl-glucopyranoside. The results were graphed using a Michaelis-Menten plot. V_{max} and K_m were calculated (Fig 5.34). As the flavonoid concentration increased, the V_{max} remained unchanged. The K_m increased with the increased concentration of inhibitor (Fig 5.34). The shape of the curve in the Michaelis-Menten plot was hyperbolic. Alpha was $5.722e+016$ (very wide). All these factors were indicative of a competitive inhibition of the flavonoids sample. The mechanism of action of the acarbose inhibitor used in the assay was active by competitive inhibition. As the acarbose concentration increased, so did the K_m . V_{max} was unchanged with the increased concentration of inhibitor. The shape of the curve in the Michaelis-Menten plot was hyperbolic. Alpha was around $1.190e+018$ (very large) (Fig 5.35). The mechanism of action of the flavonoids sample extracted from *A. cominia* was similar to that of the acarbose inhibitor of α -glucosidase enzyme activity.



Inhibitor Concentration (mM)	Vmax (RFU)	Km (mM)
0.03	0.9528	0.3112
0.1	0.9948	0.3485
0.3	1.2	0.3496
1	1.215	0.3609
3	1.252	0.3953
10	1.236	0.3806
30	1.231	0.5447

Figure 5.34 Michaelis-Menten plot of the inhibitory effect of flavonoids mixture on α -glucosidase-catalysis hydrolysis of the enzyme. Data are expressed as mean RFU (relative fluorescence unit) for $n=3$ replicates of each substrate concentration (0.05 to 10 mg/ml). The insert graph shows the effect of acarbose on α -glucosidase assay with $K_i 0.45 \pm 0.05$ mg/ml. The table below the graph represents K_m (mM) and V_{max} (RFU) with each inhibitor concentration.



Inhibitor Concentration (mM)	Vmax (RFU)	Km (mM)
1.2	1.327	0.1662
4	1.335	0.2331
10	1.278	0.2298
12	1.377	0.7979
40	1.418	1.727
100	1.485	2.675

Figure 5.35 Michaelis-Menten plot of the inhibitory effect of the acarbose inhibitor on α -glucosidase-catalysis hydrolysis of the enzyme. Data are expressed as mean RFU (relative fluorescence unit) for $n=3$ replicates of each substrate concentration (0.05 to 10 mg/ml). The table below the graph represents K_m (mM) and V_{max} (RFU) with each inhibitor concentration.

5.3.3.5 Conclusion and discussion

Only samples containing flavonoid components inhibited α -glucosidase enzyme. The flavonoid mixture produced a concentration-dependent inhibition of α -glucosidase with a K_i value of 1.7 ± 0.5 $\mu\text{g/ml}$. Kinetic study of the mechanism of action of the flavonoid mixture demonstrated a competitive inhibition of α -glucosidase enzyme. The activity of the flavonoids was comparable to that of the acarbose inhibitor used by patients with T2-DM. Therefore, natural α -glucosidase inhibitors from *A. cominia* could be an attractive source for the management of postprandial hyperglycaemia. However, it is very important to confirm the activity of these extracts *in vivo* as *in vitro* studies do not always correlate with those carried out *in vivo* (Ye *et al.*, 2002).

Many studies have shown potential α -glucosidase inhibitors from extracts of plants such as cranberry, pepper and soy bean (Apostolidis *et al.*, 2006; Georgetti *et al.*, 2006; Pulella *et al.*, 2006). Inhibition of α -glucosidase enzyme, by *A. cominia* extract, involved in the carbohydrates digestion, can decrease blood glucose level and therefore is an important strategy in the management of T2-DM (Ali *et al.*, 2006). And thereby induce weight loss (Zhong *et al.*, 2006; Bhat *et al.*, 2008).

5.3.4 α -Amylase enzyme

5.3.4.1 Z-factor of α -amylase assay

α -amylase enzyme assay fitness was screened using α -amylase enzyme at 125 units/ml in the presence of 4-nitrophenyl- α -D-maltohexaside as substrate (1.5 mM). Positive control was in the presence of both substrate and α -amylase enzyme. The negative control was in the presence of the substrate only.

For α -amylase assay (Fig 5.36), the value of Z-factor was 0.906. By comparison to the high-throughput screening fitness assay (Table 5.1), Z-factor was between 0.9 and 1, confirming that the DPPIV assay and the conditions used were excellent and can be followed for further screening tests.

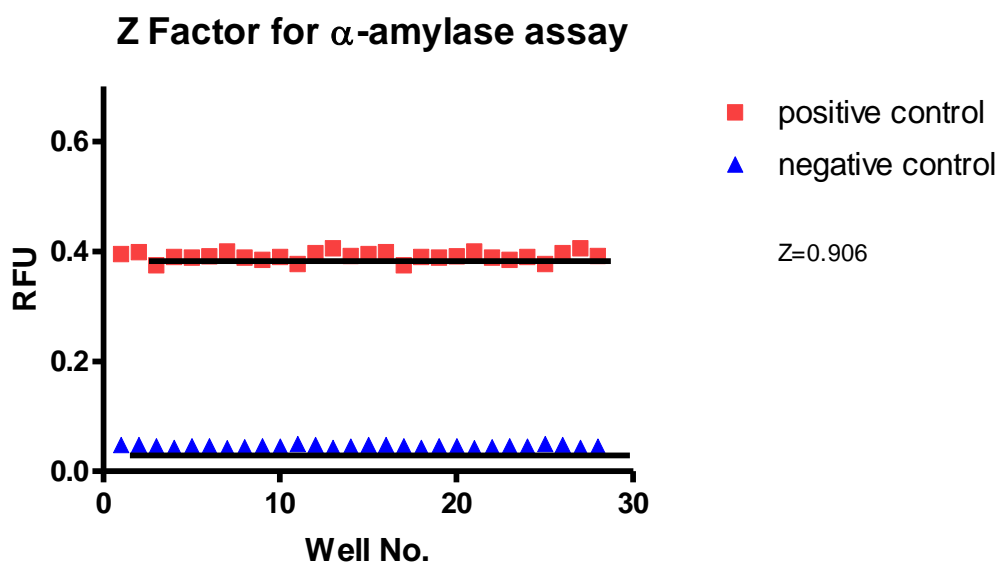


Figure 5.36 High-throughput screening fitness for α -amylase assay using 4-nitrophenyl- α -D-maltohexaside as substrate and α -amylase enzyme.

5.3.4.2 Effect of extracts from *A. cominia* on the α -amylase enzyme

Acarbose produced a concentration-dependent inhibition of α -amylase enzyme with a K_i value of 0.29 ± 0.05 mg/ml. All extracts of *A. cominia* (Fig 5.37) were tested on α -amylase enzyme at $30 \mu\text{g/ml}$. DMSO (1%) did not produce inhibition of α -enzyme in comparison to the control. Only AC-MC-G, K, LMN-91-175 (flavonoids), AC-HEC-53 (tannins), AC-MC-D-25-44 (pheophytin B) and F1 sample (mearnsitrin) produced statistically significant inhibition of α -amylase, although the inhibition was less than 60% (29, 10, 18, 14 and 9 % respectively). However, none of the extracts was considered to be active on α -amylase enzyme.

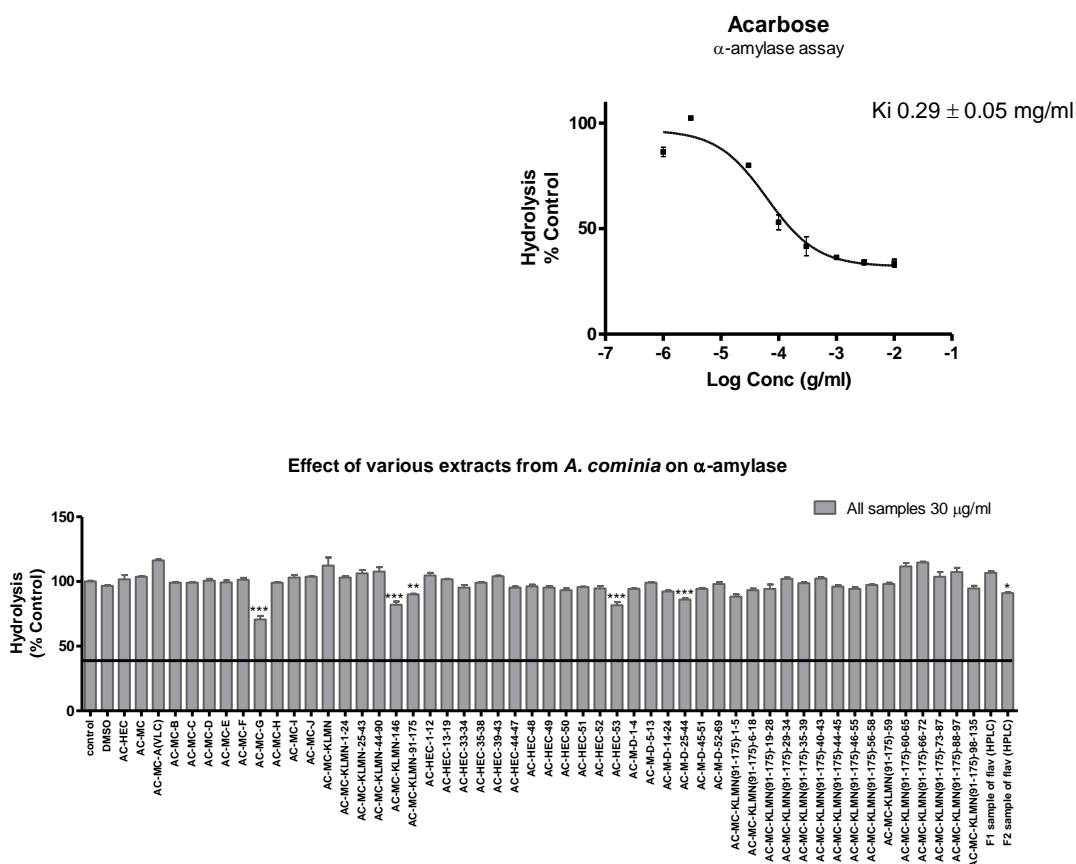


Figure 5.37 Effect of various AC fractions on α -amylase enzyme in the presence of 4-nitrophenyl- α -D-maltohexaside substrate. Extracts concentrated at $30 \mu\text{g/ml}$ were incubated with α -amylase enzyme for 30 min at 37°C in an atmosphere containing 5% CO_2 . 4-nitrophenyl- α -D-maltohexaside (1.5 mM) was then added and incubated for 30 min at 37°C . The hydrolysis of the substrate by enzyme was measured at 450 nm . Data represent mean \pm SEM of enzyme hydrolysis (% control) of three independent experiments. The insert shows the effect of various concentrations of acarbose standard ($10 \mu\text{M}$ – 30 mM) on α -amylase enzyme in the presence of 4-nitrophenyl- α -D-maltohexaside. K_i for acarbose was 0.29 ± 0.05 mg/ml. The data were analysed by Dunnett *post-test*. *** P value < 0.05 versus control.

5.3.4.3 Conclusion and discussion

α -amylase enzyme plays an important role in the digestion of starch and glycogen. Inhibition of α -amylase enzyme was considered an important approach for the management of carbohydrate uptake-related problems (such as diabetes and obesity). *A. cominia* extracts at 30 $\mu\text{g/ml}$ did not inhibit α -amylase enzyme. Higher concentration of these extracts may potentially inhibit the enzyme hydrolysis. Thus, the inhibition of α -amylase enzyme was less with the flavonoid mixture but was statistically significant. Amongst the plant constituents that have been investigated, flavonoids produced the highest inhibitory effect on α -amylase enzyme (Sales *et al.*, 2012; Liu *et al.*, 2013). The potential of inhibition related to a number of hydroxyl groups in the molecule of the compound (Lo *et al.*, 2008; Nickavar *et al.*, 2008; Najafian *et al.*, 2011).

5.3.5 Summary of inhibition studies involving the *A. cominia* extracts

Inhibitory activity of the extracts of *A. cominia* were tested on four enzymes; DPPiV, PTP1B, α -glucosidase and α -amylase.

Only a mixture of flavonoids produced a significant and concentration-dependent inhibition of DPPiV. The inhibition of DPPiV enzyme by the flavonoids was competitive, as shown for the standard inhibitor P32/98.

Among the extracts of *A. cominia*, flavonoids and pheophytin A produced significant inhibition of PTP1B at 30 μ g/ml. Methanolic fractions of the plant were the most active. Competitive inhibition of PTP1B enzyme was observed with the flavonoid mixture and pheophytin A, as well as with the TFMS inhibitor. Furthermore, these fractions significantly stimulated glucose uptake in 3T3-L1 adipocytes, and L6 cells. Only methanolic extracts containing the flavonoid mixture significantly inhibited α -glucosidase. The flavonoid mixture produced a concentration-dependent inhibition of this enzyme and the inhibition was competitive, as was the acarbose inhibitor of α -glucosidase enzyme.

Of all the extracts of *A. cominia*, the least inhibition of the flavonoids on α -amylase enzyme was shown at 30 μ g/ml.

In all the enzyme assays, no significant inhibition of the enzymes was produced by separated flavonoids (identified by LC-MS and NMR after fractionation). This suggests that there is synergism among the components.

Chapter 6

6 General conclusions and suggestions for future work

The present study investigated the anti-diabetic activity of extracts from *Allophylus cominia*, which is used to treat type 2 diabetes mellitus in Cuba. The selection of the plant was based on its importance and some primary results provided by Cuban researchers.

Leaves from *A. cominia* were extracted by maceration using hexane, ethyl acetate and methanol. Successive separation of the fractions from the methanolic extract from *A. cominia* was carried out using various phytochemical methods such as VLC, Sephadex, silica gel and prep-TLC. Fatty acids, tannins, pheophytins (A and B), and a mixture of flavonoids were detected. The identified flavonoids were mearnsitrin (~70%), quercitrin (~30%), quercetin-3-alloside, and naringenin-7-glucoside. Quercitrin and mearnsitrin were separated by HPLC on an amino column.

On HepG2 cells, the crude methanolic extract from *A. cominia* (1 – 100 µg/ml) did not affect the cell count in comparison to the untreated control cells. After separation of the crude extract, three fractions containing flavonoids, pheophytins and tannins were tested for the viability of 3T3-L1 fibroblasts. Extracts from *A. cominia* did not reduce the viability of L6, 3T3-L1 fibroblasts or adipocytes. This provided evidence for a safe and non-toxic natural medicinal plant.

Insulin remains a useful anti-diabetic drug for the treatment of type 2 diabetes. It produces hypoglycaemia through stimulation of glucose uptake into peripheral tissues such as muscles and adipocytes. On 2-NBDG glucose uptake by HepG2 liver cells, insulin produces a concentration-dependent increase of glucose uptake with EC₅₀ value of 93 ± 21 nM. In the presence of the methanolic crude extract from *A. cominia* (100 µg/ml), further confirmation of the insulin responsiveness of HepG2 was shown with a lower value of EC₅₀ 13 ± 2 nM. A significant increase in 2-NBDG uptake was observed with an increase of insulin concentration in the presence of the extract. 100 µg/ml of the extract increased the glucose uptake by five-fold in the absence of insulin and by eleven-fold in the presence of 100 nM insulin in comparison to the basal control uptake. This confirms evidence of the potential anti-

diabetic activity of the methanolic crude extract from *A. cominia* by increasing the glucose uptake and enhancing insulin activity in HepG2 cells.

On 3T3-L1 fibroblasts, insulin produced a low increase in the glucose uptake, starting from 0.3 nM of insulin. However, the crude methanolic extract of *A. cominia* did not enhance insulin activity. 3T3-L1 fibroblasts are not insulin-responsive cell lines, with fewer GLUT4 transporters than the 3T3-L1 adipocytes; furthermore these fibroblasts request higher concentration of insulin. After differentiation of 3T3-L1 into adipocytes, insulin produced a significant concentration-dependent increase of the glucose uptake. 8×10^3 cells/ml of 3T3-L1, 100 nM of insulin and 100 μ M of 2-NBDG were the optimum concentrations used for the better glucose uptake assay. Experiments done *in vitro*, in a black 96-well plate underwent difficulties in differentiation and did hardly show activity of extracts from *A. cominia* on 2-NBDG glucose uptake. 3T3-L1 differentiation was performed in 25 cm² flasks and 12-well plates. And then, 2-deoxy-D-glucose was carried out and the uptake was measured by mass spectrometry. 100 nM insulin produced a 5-fold increase in the glucose uptake, while wortmannin inhibited insulin activity by decreasing glucose uptake by two-fold. Pheophytin A at 100 μ g/ml produced an increase in 2-deoxy-D-glucose uptake without effect on insulin activity. Flavonoids containing extract from *A. cominia* did not produce an increase in 2-deoxy-D-glucose uptake. However, flavonoids enhanced insulin activity by two-fold. This also confirms that both extracts from *A. cominia* (flavonoids and pheophytin) are potential anti-diabetic extracts.

On L6 cells, insulin produced a concentration-dependent increase of 2-NBDG uptake with an EC₅₀ value of 28.6 ± 0.7 nM. This increase was also found in the presence of extracts from *A. cominia*, which lowered EC₅₀ value to 0.08 ± 0.02 nM and 5 ± 0.9 nM in the presence of 100 μ g/ml of flavonoids and pheophytin A extracts respectively. Both flavonoids and pheophytins produced a concentration-dependent increase in the presence of 100 nM insulin. In general, a significant increase of glucose uptake by L6 cells was shown with 100 μ g/ml of both extracts from *A. cominia* in the presence of 100 nM insulin.

During the differentiation process, 3T3-L1 cells were treated with flavonoids and pheophytin extracts. These extracts reduced fat accumulation had no apoptotic effect on 3T3-L1 adipocytes and did not reduce the number of GLUT4 transporters. No significant decrease of lipid droplets was shown when treatment was carried out after 2 days (second stage of differentiation) of the differentiation initiation. A decrease of lipid droplets was shown after 48 h of the treatment of the fully differentiated adipocytes with flavonoids and pheophytins. No fat accumulation was observed after withdrawal of the extracts. We conclude that these extracts with their effect on metabolising the lipid accumulated in the cells could be a new candidate to prevent fat formulation, thus leading to a decrease in the risk of obesity when associated with diabetes.

The activity of *A. cominia* extracts on 2-NBDG glucose uptake reported in this project did not provide any information on the mechanism pathways involved in the production of this activity; thus enzyme tests such as PTP1B, DPPIV, α -glucosidase and α -amylase were carried out. Only flavonoids containing extract from *A. cominia* at 30 $\mu\text{g/ml}$ inhibited the DPPIV enzyme (75% inhibition). Flavonoids produced a concentration-dependent inhibition of the DPPIV enzyme with a K_i value of $2.6 \pm 0.2 \mu\text{g/ml}$. Flavonoids produced a competitive inhibition of DPPIV enzyme in the presence of gly-pro-7-amido-4-methylcoumarin hydrobromide as substrate. DPPIV inhibitors such as the flavonoid extract from *A. cominia* may directly increase incretin levels (GLP-1 and Gastric inhibitory peptide, GIP), which inhibit glucagon release, and in turn improve glucose tolerance and increase insulin secretion in response to glucose levels.

Both flavonoids and pheophytins extracts from *A. cominia* produced a concentration-dependent inhibition of PTP1B, with K_i values of $3.2 \pm 0.09 \mu\text{g/ml}$ and $0.5 \pm 0.03 \mu\text{g/ml}$ for the flavonoids and pheophytins, respectively. Both extracts were competitive inhibitors of PTP1B enzyme in the presence of DiFMUP as substrate. This is evidence of their effect on the insulin secretion and leptin receptors, therefore confirming the increase in the glucose uptake by the 3T3-L1 adipocytes and L6 muscle cells.

The flavonoids containing extract from *A. cominia* was the most active on α -glucosidase enzyme, with 79% of inhibition shown. A concentration-dependent inhibition with a K_i value of $1.7 \pm 0.5 \mu\text{g/ml}$ was produced by the flavonoids. A competitive inhibition of α -glucosidase enzyme was shown with this extract in the presence of 4-nitrophenyl-glucopyranoside as substrate. α -glucosidase inhibitors such as flavonoids containing extract from *A. cominia*, work by preventing the digestion of carbohydrates. Hence, these inhibitors reduce the impact of carbohydrates on blood sugar, which leads to hypoglycaemia.

No effect of the extracts from *A. cominia* on α -amylase which breaks down large, insoluble starch molecules into soluble starches was found.

Separated quercitrin and mearnsitrin did not produce any significant inhibition of DPPIV, PTP1B, α -glucosidase or α -amylase. These results provide the evidence of these compounds only being active in synergy at $30 \mu\text{g/ml}$.

Overall, using three different cell lines, results provided support for the ethnobotanical use of *A. cominia* in treating type 2 diabetes mellitus in Cuba. It also supports the general observation that traditional use of this plant holds great potential for the discovery of new candidates available locally for the management and treatment of type 2 diabetes mellitus.

All these findings suggest further work that could be carried out:

- To determine the effect of these compounds on insulin-induced glycogen accumulation in liver through activating glycogen synthase and inactivating glycogen phosphorylase.
- To determine the effect of the compounds from *Allophylus cominia* (*A. cominia*) on insulin and glucagon secretion in the pancreatic cells. The activity of the flavonoids from *A. cominia* on DPPIV enzyme would be a key achievement of testing this extract on the pancreatic β -cells and the enhancement of insulin release.
- To investigate the effect of extracts from *A. cominia* on blood glucose and its potential side effects in non-insulin-dependent and insulin-dependent diabetics in *in vivo* study.

- Further to confirm the effect of the extracts on the metabolism of lipid droplets. The triglyceride content of adipose tissue depends on both synthesis and lipolysis. Lipolysis could be measured by glycerol release. Fat synthesis could be measured by incorporation of, for example, tritiated glucose, into triglycerides.
- To determine the effect of the extracts from *A. cominia* on kinases and receptors. Kinases such as AMPK (5' adenosine monophosphate-activated protein kinase) could lead to proving the effect of these extracts on lipogenesis and therefore a decrease in lipid accumulation in the adipocytes. Receptors such as PPAR (peroxisome proliferator-activated receptor) play an important role in the pathway involved in lipid metabolism. PPAR agonists are mainly used for lowering triglyceride and blood sugar levels.
- To carry out further work on the effect of Sirtuins in different pathways related to adipogenesis (obesity) and as a new therapeutic approach for the treatment of type 2 diabetes mellitus and its complications. Sirtuins (SIRT) are NAD⁺-dependent deacetylases that regulate metabolism and have beneficial health effects. In adipose tissue, SIRT1 also regulates adiponectin that in turn regulates energy homeostasis. In the liver, SIRT1 plays an important role in lipolysis and gluconeogenesis. In the pancreas, SIRT1 has a direct effect on insulin secretion and on β -cell survival.
- To compare the components of *A. cominia* collected during different seasons for monitoring the active constituents of the plant using the same extraction method for quality assurance of the herbal medicine used in Cuba. Separation and identification of different compounds could be carried out using NMR, HPLC, LC-MS and other techniques.
- The work in this project was only carried out on the leaves from *A. cominia* (the plant was normally used in the herbal medicine). More work could be carried out using other parts of the plant such as stem, roots or even seeds from *A. cominia* with the aim of quantifying the levels of the active compounds in each part of the plant.

Taken overall, it is clear that the current study has opened up a new area of research in the extracts from *A. cominia* may have a limited role in glucose uptake and insulin

activity. Indeed, leaves from *A. cominia* could be a new target for possible therapeutic applications for the treatment of type 2 diabetes mellitus.

7 References

Abdel-Barry, I.A. Abdel-Hassan and M.H.H. Al-Hakiem. (1997). Hypo-glycaemic and anti-hyperglycaemic effects of *Trigonella foenum-graecum* leaf in normal and alloxan induced diabetic rats. *Journal of Ethnopharmacology*; 58: 149-155.

ADA: American Diabetes Association. (2000). Gestational diabetes mellitus. *Diabetes Care* 23 (Suppl. 1): S77-S79.

Agabegi, E. D., and Agabegi, S. S. (2008). *Step-Up to Medicine* (Step-Up Series). Hagerstwon, MD: Lippincott Williams & Wilkins.

Aguilar-Salinas, C.A., Velásquez-Monroy, O., Gomez-Perez, F.J., Gonzalez-Chavez, A., Esqueda, A.L., Molina-Cuevas, V., Rull-Rodrigo, J.A., and Tapia-Conyer, R. (2003). Characteristics of patients with type 2 diabetes in Mexico: results from a large population-based nationwide survey. *Diabetes Care*; 26: 2021-2026.

Ahrén, B. (2005). Inhibition of Dipeptidyl Peptidase-4 (DPP-4): A novel approach to treat type 2 diabetes. *Current Enzyme Inhibition*, 1: 65-73.

Al-Masri, I.M. Mohammad, M.K. and Tahaa, M.O. (2009). Inhibition of dipeptidyl peptidase IV (DPPIV) is one of the mechanisms explaining the hypo-glycaemic effect of berberine. *Journal of Enzyme Inhibition and Medicinal Chemistry*; 24: 1061-1066.

Ali, H., Houghton, P.J., and Soumyanath, A. (2006). Alpha-amylase inhibitory activity of some Malaysian plants used to treat diabetes; with particular reference to *Phyllanthus amarus*. *Journal of Ethnopharmacology* ; 107: 449-455.

Alonso-Castro, A. J., Miranda-Torres, A. C., González-Chávez, M. M., and Salazar-Olivo, L. A. (2008). *Cecropiaobtusifolia* Bertol and its active compound, chlorogenic acid, stimulate 2-NBD glucose uptake in both insulin-sensitive and insulin-resistant 3T3 adipocytes. *Journal of Ethnopharmacology*; 120: 458-464.

Alonso-Castro, A.J., and Salazar-Olivo, L.A. (2008). The anti-diabetic properties of *Guazumaulmifolia*Lam are mediated by the stimulation of glucose uptake in normal and diabetic adipocytes without inducing adipogenesis. *Journal of Ethnopharmacology*; 118: 252-256.

Alonso-Castro, A. J., Zapata-Bustos, R., Romo-Yañez, J., Camarillo-Ledesma, P., Gómez-Sánchez, M., and Salazar-Olivo, L. A. (2010). The antidiabetic plants *Tecomastans* (L.) Juss.exKunth (Bignoniaceae) and *Teucriumcubense* Jacq (Lamiaceae) induce the incorporation of glucose in insulin-sensitive and insulin-resistant murine and human adipocytes. *Journal of Ethnopharmacology*; 127: 1-6.

Alonso-Castro A.J., Zapata-Bustos R., Domínguez F., García-Carrancá A., and Salazar-Olivo L.A. (2011). *Magnolia dealbata* Zucc and its active principles

honokiol and magnolol stimulate glucose uptake in murine and human adipocytes using the insulin-signaling pathway. *Phytomedicine*, 18: 926-933.

Andrade-Cetto, A., and Heinrich, M. (2005). Mexican plants with hypo-glycaemic effect used in the treatment of diabetes. *Journal of Ethnopharmacology*; 93: 248-325.

Andrade-Cetto, A., and Wiedenfeld, H. (2001). Hypoglycemic effect of *Cecropia obtusifolia* on streptozotocin diabetic rats. *Journal of Ethnopharmacology*; 78: 145-149.

Andrade-Cetto, A., Becerra-Jiménez, J., and Cárdenas-Vázquez, R. (2007). Alfa-glucosidase inhibiting activity of some Mexican plants used in the treatment of type 2 diabetes. *Journal of Ethnopharmacology*; 116: 27–32.

Apostolidis, E, Kwon, Y., and Shetty K. (2006). Potential of cranberry- based herbal synergies for diabetes and hypertension management. *Asia Pacific Journal of Clinical Nutrition*; 15: 433-441.

Arredondo, A., Zúñiga, A., and Parada, I. (2005). Health care costs and financial consequences of epidemiological changes in chronic diseases in Latin America: evidence from México. *Public Health*; 119: 711-720.

Arredondo, A., and Zuñiga, A. (2004). Economic consequences of epidemiological changes in diabetes in middle-income countries: the Mexican case. *Diabetes Care*; 27: 104-109.

Arts, I.C. and Hollman, P. C. (2005). Polyphenols and disease risk in epidemiologic studies. *American Journal of Clinical Nutrition*; 81: 317S-325S.

Atkinson, M.A., and Maclaren, N.K. (1994). The pathogenesis of insulin-dependent diabetes mellitus. *The New England Journal of Medicine*; 331: 1428–1436.

Babey, M., Kopp, P. and Robertson, G. L. (2011). Familial forms of diabetes insipidus: clinical and molecular characteristics. *Nature Reviews Endocrinology*; 10.1038: 1759-5029.

Babu V., Gangadevi T., and Subramonian A. (2003). Antidiabetic activity of ethanol extract of *Cassia Kleinii* Leaf in Streptozotocin-induced Diabetic rats and isolation of an active fraction and toxicity evaluation of the extract. *Indian Journal of Pharmacology*; 35: 290-296.

Baggio, L.L., and Drucker, D. J. (2004). Glucagon-like peptide-1 and glucagon-like peptide-2. *Best Practice & Research: Clinical Endocrinology & Metabolism*; 18 (4): 531-554.

Bailey, C. J. and Day, C. (2002). Future therapies. *Current Medical Research and Opinion* 18 (1): s82-88.

- Bailey, C.J., and Turner RC. (1996). Metformin. *The New England Journal of Medicine*; 334(9), 574-9.
- Bakirel, T., Bakirel, U., Keleş, O. Ü., Ülgen, S. G., and Yardibi, H. (2008). *In vivo* assessment of antidiabetic and antioxidant activities of rosemary (*Rosmarinus officinalis*) in alloxan-diabetic rabbits. *Journal of Ethnopharmacology*; 116 (1): 64-73.
- Balkrishnan, R., Rajagopalan, R., Camacho, F.T., Huston, S.A., Murray, F.T., and Anderson, R.T. (2003). Predictors of medication adherence and associated health care costs in an older population with type 2 diabetes mellitus: a longitudinal cohort study. *Clinical Therapeutics*; 25: 2958-2971.
- Bansal P., and Wang, Q. (2008). Insulin as a physiological modulator of glucagon secretion. *American Journal of Physiology - Endocrinology and Metabolism*; 295: E751-E761.
- Barca, A., Politi, M., Sanago, S. H., Morelli, I., and Pizza, C. (2003). Chemical composition and antioxidant activity of phenolic compounds from wild and cultivated *Sclerocarya birrea* (Anacarduaceae) leaves. *Journal of Agricultural and food chemistry* 51: 6689-6695.
- Bhat, M., Ravikumar, A., Zinjarde, S., Bhargava, S., and Joshi, B. (2008). Antidiabetic Indian plants: A good source of potent amylase inhibitors. *Evidenced-based Complementary and Alternative Medicine*; 40: 1-6.
- Bischoff, H. (1994). Pharmacology of alpha-glucosidase inhibition. *European Journal of Clinical Investigation*; 24(3):3.
- Benninger, R. K. P., Head, W., Zhang, M., Satin, L. S., and Piston, D. W. (2011). Gap junctions and other mechanisms of cell–cell communication regulate basal insulin secretion in the pancreatic islet. *The Journal of Physiology*; 589 (22): 5453-5466.
- Bouaboulaa, M., Hilaireta, S., Marchanda, J., Fajas, L., Le Fura, G., and Casellasa, P. (2005). Anandamide induced PPAR γ transcriptional activation and 3T3-L1 preadipocyte differentiation. *European Journal of Pharmacology*; 517(3): 174-181.
- Brahmachari, G. (2011). Bio-flavonoids with promising anti-diabetic potentials: A critical survey. *Opportunity, Challenge and Scope of Natural Products in Medicinal Chemistry*: 187-212.
- Bravo, L. (1998). Polyphenols: chemistry, dietary sources, metabolism and nutritional significance. *Nutrition Review*; 56: 317-33.

- Bray, G. A. and Greenway, F. L. (1999). Current and Potential Drugs for Treatment of Obesity: Table 19: Clinical trials with metformin for the treatment of obese diabetics. *Endocrine Reviews* 20 (6): 805–87.
- Brunton, S., Carmichael, B., Funnell, M., Lorber, D., Rakel, R., and Rubin, R.. (2005). The role of insulin. *Supplement to the Journal of Family Practice* 445-452.
- Butler A. E., Janson J., Bonner-Weir S., Ritzel R., Rizza R.A. and Butler. C. (2003). β -Cell Deficit and Increased β -Cell Apoptosis in Humans With Type 2 Diabetes. *Diabetes*; 52: 102-110.
- Cahyana A. H., Shuto Y. and Kinoshita Y. (1991). Pyropheophytin a as an antioxidative substance from the marine Algs, Arame (*Eisenia bicyclis*). *Bioscience Biotechnology and Biochemistry*; 56 (10): 1533-1535.
- Calabrese A., Caton D., and Meda P. (2004). Differentiating the effects of Cx36 and E-cadherin for proper insulin secretion of MIN6 cells. *Experimental Cell Research*; 294: 379– 391.
- Calabro P., Chang D. W., Willerson J. T. and Yeh E.T.H. (2005). Release of C-Reactive Protein in Response to Inflammatory Cytokines by Human Adipocytes: Linking Obesity to Vascular Inflammation FREE. *Journal of the American College of Cardiology*; 46(6): 1112-1113.
- Cawthorn, W.P., Sethi, J.K. (2008). TNF-[alpha] and adipocyte biology. *FEBS Letters*; 582: 117–131.
- Chan J.C., Malik V., Jia W. (2009). Diabetes in Asia: epidemiology, risk factors, and pathophysiology. *Jama*; 301: 2129-2140.
- Chan, J.M., Rimm, E.B., Colditz, G.A., Stampfer, M.J., Willett, W.C. (1994). Obesity, fat distribution, and weight gain as risk factors for clinical diabetes in men. *Diabetes Care*; 17(9): 961-9.
- Chen, X., Xun, K., Chen, L. and Wang, Y. (2009). TNF- α , a potent lipid metabolism regulator. *Cell Biochemistry and Function*; 27: 407-416.
- Cheadle, W. G. (2006). Risk factors for surgical site infection. *Surgical Infections* (Larchmt); 7(1): S7-S11.
- Cheng, A.Y., and Fantus, I.G. (2005). Oral antihyperglycemic therapy for type 2 diabetes mellitus. *Canadian Medical Association Journal*; 172: 213-226.
- Clayton, P. E., Banerjee, I., Murray, P. G. and Renehan, A. G. (2011). Growth hormone, the insulin-like growth factor axis, insulin and cancer risk. *Nature Reviews Endocrinology*; 7: 11-24.

Collier, C.A., Bruce, C.R., Smith, A.C., Lopaschuk, G., and Dyck, D.J. (2006). Metformin counters the insulin-induced suppression of fatty acid oxidation and stimulation of triacylglycerol storage in rodent skeletal muscle. *American Journal of Physiology: Endocrinology and Metabolism*; 291(1): E182-E189.

Cooke, D.W., Plotnick, L. (2008). Type 1 diabetes mellitus in pediatrics. *Pediatrics Review*; 29 (11): 374-84.

Dallas, J. (2011). Diabetes, Doctors and Dogs: An exhibition on Diabetes and Endocrinology by the College Library for the 43rd St. In *Andrew's Day Festival Symposium, Royal College of Physicians of Edinburgh*.

Daneman, D. (2006). Type 1 diabetes. *The Lancet*; 367(9513): 847-858.

Dean, L., McEntyre, J. (2004). The Genetic Landscape of Diabetes. Bethesda (MD): National Center for Biotechnology Information (US). Chapter 2, Genetic Factors in Type 1 Diabetes.

DeFronzo, R. A., Ratner, R. E., Han, J., Kim, D. D., Fineman, M. S., and Baron, A. D. (2005). Effects of Exenatide (Exendin-4) on Glycemic Control and Weight Over 30 Weeks in Metformin-Treated Patients with Type 2 Diabetes. *Diabetes Care*; 28: 1092-1100.

De Souza, C.J., Eckhardt, M., Gagen, K., Dong, M., Chen, W., Laurent, D., and Burkey, B.F. (2001). Effects of pioglitazone on adipose tissue remodelling within the setting of obesity and insulin resistance. *Diabetes*; 50: 1863-1871.

Dhanabal S. P. Sureshkumar M., Ramanathan M., and Suresh B. (2005). Hypoglycemic Effect of Ethanolic Extract of *Musa sapientum* on Alloxan-Induced Diabetes Mellitus in Rats and Its Relation with Antioxidant Potential. *Journal of Dietary Supplements* 2 (5): 7-19.

Drucker, D. J. (2003). Enhancing incretin action for the treatment of type 2 diabetes. *Diabetes Care*; 26: 2929-2940.

El-Alfy, A.T., Ahmed, A.A.E., and Fatani A.J. (2005). Protective effect of red grape seeds proanthocyanidins against induction of diabetes by alloxan in rats. *Pharmacological Research*; 52: 264-270.

El-Beshbishy, H.A. and Bahashwan, S.A. (2012). α -glucosidase and α -amylase activities: An in vitro study. *Toxicology and Industrial Health*; 28: 42.

Evans, W.C. (2002). Plants with oral hypo-glycaemic activity. In: W. C. Evans (Ed). *Trease and Evans Pharmacognosy*. 15th edition. Edinburgh, London: W.B. Saunders: 46: 419-420.

Fang, L.V., and Xu, X. J. (2008). Studies on the Chemical Constituents of *Rabdosia rubescens*. *Chinese Medicine Material Journal*, 31:1340-1343.

- Georgetti, S.R., Casagrande, R., Vicentini, F.T.M.C., Verri, W.A., and Fonseca, M.J.V. (2006). Evaluation of the antioxidant activity of soybean extract by different in vitro methods and investigation of this activity after its incorporation in topical formulations. *European Journal of Pharmaceutics and Biopharmaceutics*; 64: 99-106.
- Goegan, P., Johnson, G. and Vincent, R. (1995). Effects of Serum Protein and Colloid on the Alamar Blue Assay in Cell Cultures. *Toxicology In Vitro*: 9(3): 257-266.
- Govers, R., Coster, A. C. F., and James, D. E. (2004). Insulin Increases Cell Surface GLUT4 Levels by Dose Dependently Discharging GLUT4 into a Cell Surface Recycling Pathway. *Molecular Cell Biology*; 24 (14): 6456-6466.
- Gregoire, F.M., Smas, C.M and Sul H.S. (1998). Understanding adipocytes differentiation. *Physiological Reviews* 78 (3): 81-100.
- Grover, N., Patini, V. (2013). Phytochemical characterization using various solvent extracts and GC-MS analysis of methanolic extract of *Woodfordia fruticosa* (L.) Kurz. Leaves. *International Journal of Pharmacy and Pharmaceutical Sciences* 5 (4): 291-295.
- Grundy SM, Benjamin IJ, Burke GL. (1999). Diabetes and cardiovascular disease: a statement for healthcare professionals from the American Heart Association. *Circulation*; 100: 1134-1146.
- Gupta, R., Walunj, S. S., Tokala, R. K., Parsa, K. V., Singh, S. K., and Pal, M. (2009). Emerging Drug Candidates of Dipeptidyl Peptidase IV (DPP IV) Inhibitor Class for the Treatment of Type 2 Diabetes. *Current Drug Targets* 10: 71-87 71
- Hamaty, M. (2011). Insulin treatment for type 2 diabetes: When to start, which to use. *Journal of Medicine*; 78 (5): 332-342.
- Hamburger, M. and Hostettmann, K. (1991). Bioactivity in plants: the link between phytochemistry and medicine. *Phytochemistry*; 30 (12): 3864-3874.
- Harborne J. B. (2006). *Phytochemical methods: a guide to modern techniques of plant analysis*. India: Springer India.
- Hardie D. G.(2008).Role of AMP-activated protein kinase in the metabolic syndrome and in heart disease. *FEBS Letters*; 582: 81-89.
- Hargus, J.A, Fronczek, F.R., Vicente, M.G., and Smith, K.M. (2007). Mono-(L)-aspartylchlorin-e6. *Photochemistry and Photobiology*, 83(5):1006-1015.
- Harvey, A. L. (2010). Plant natural products in anti-diabetic drug discovery. *Current organic chemistry*; 14 (16), 3.

Hassanein, M., Weidow, B., Koehler, E., Bakane, N., Garbett, S., Shyr, Y., and Quaranta, V. (2011). Development of High-Throughput Quantitative Assays for Glucose Uptake in Cancer Cell Lines. *Molecular Imaging Biology*; 13(5): 840-852.

He, Q., Lv, Y., and Yao, K. (2006). Effects of tea polyphenols on the activities of α -amylase, pepsin, trypsin and lipase. *Food chemistry*; 101: 1178-1182.

Heftmann, E. (1992). *Chromatography: Fundamentals and application of chromatography and related differential migration methods*. (5th ed.) Journal of Chromatography Library; 51A and 51B. Elsevier

Heinrich, M., Barnes, J., Gibbons, S. and Williamson, E.M. (2004). *Fundamentals of Pharmacology and Phytotherapy*. Oxford: Churchill Livingstone.

Hesse U., Ysebaert, D., and de Hemptinne, B. (2001). Role of somatostatin-14 and its analogues in the management of gastrointestinal fistulae: clinical data. *Gut*; 49: iv11-iv20.

Holst, J.J., Gromada, J. (2004). Role of incretin hormones in the regulation of insulin secretion in diabetic and nondiabetic humans. *American Journal of Physiological Endocrinology and Metabolism*; 287: E199-E206.

Hotta, K., Funahashi, T., Bodkin, N. L., Ortmeier, H. K., Arita, Y., Hansen, B. C., and Matsuzawa, Y. (2001). Circulating concentrations of the adipocyte protein adiponectin are decreased in parallel with reduced insulin sensitivity during the progression to Type 2 diabetes in Rhesus monkeys. *Diabetes*; 50: 1127-1133.

Hundal, R., Krssak, M., Dufour, S., Laurent, D., Lebon, V/, Chandramouli, V., Inzucchi, S., Schumann, W., Petersen, K., Landau, B., and Shulman, G. (2000). Mechanism by which metformin reduces glucose production in type 2 diabetes. *Diabetes*; 49(12): 2063–2069.

Hu, W., and Wang, M. (2011). Diarylheotanoid from *Alnushirsuta* Improves Glucose Metabolism via Insulin Signal Transduction in Human Hepatocarcinoma (HepG2) Cells. *Biotechnology and Bioprocess Engineering* 16: 120-126.

Ina, A., Hayashi, K. I., Nozaki, H., and Kamei, Y. (2007). Pheophytin a, a lower molecular weight compound found in the marine brown alga *Sargassum fulvellum*, promotes the differentiation of PC12 cells. *International Journal of Developmental Neuroscience* 25: 63-68.

Inzucchi, S.E. (2002). Oral antihyperglycemic therapy for type 2 diabetes: scientific review. *Jama*; 287: 360-372.

Jelodar Gholamali, A., Maleki, M., Motadayen, M.H., and Sirus, S. (2005). Effect of fenugreek, onion and garlic on blood glucose and histopathology of pancreas of alloxan-induced diabetic rats. *Indian Journal of Medical Sciences*; 59 (2): 64-69.

- Jia, G., Mitra, A.K., Gangahar, D.M., and Agrawal, D.K. (2010). Insulin-like growth factor-1 induces phosphorylation of PI3K-Akt/PKB to potentiate proliferation of smooth muscle cells in human saphenous vein. *Experimental and Molecular Pathology*. 89(1): 20-6.
- Jiang, H., Zhu, H. Wang, J. Fu, B., Lu, Y., Hong, Q., Xie, Y. and Chen, X. (2011). Tissue inhibitor of metalloproteinase-1 counteracts glucolipototoxicity in the pancreatic β -cell line INS-1. *Chinese Medical Journal*; 142(2): 258-261.
- Jo, A., Park J. and Park S.B. (2013). Exploiting the mechanism of cellular glucose uptake to develop an image-based high-throughput screening system in living cells. *The Royal Society of Chemistry* 5-6.
- Jovanovic, L., and Pettitt, D. (2001). Gestational diabetes mellitus. *Jama*; 286, 2516-2518.
- Jung, H.A., Park, J.C., Chung, H.Y., Kim, J., and Choi, J.S. (1999). Antioxidant Flavonoids and Chlorogenic Acid from the Leaves of *Eriobotrya japonica*. *Archives of Pharmacal Research*; 22(2): 213-218.
- Kaneto, H., Katakami, N., Matsuhisa, M., and Matsuoka, T. (2010). Role of Reactive Oxygen Species in the Progression of Type 2 Diabetes and Atherosclerosis. *Mediators of Inflammation*, Article ID 453892, volume 2010, 11 pages.
- Kato, A., Miura, T., and Fukunaga, T. (1995). Effects of steroidal glycosides on blood glucose in normal and diabetic mice. *Biological and Pharmaceutical Bulletin*; 18 (1): 167-8.
- Kavishankar, G.B., Lakshmidhevi, N., Mahadeva Murthy, S., Prakash, H.S., and Niranjana, S.R. (2011). Diabetes and medicinal plants-A review. *International Journal of Pharmaceutical and Biomedical Sciences*; 2(3): 65-80.
- Kendall, D.M., Riddle, M.C., Rosenstock, J., Zhuang, D., Kim, D. D., Fineman, M. S., and Baron, A. D. (2005). Effects of Exenatide (Exendin-4) on Glycemic Control Over 30 Weeks in Patients With Type 2 Diabetes Treated With Metformin and a Sulfonylurea. *Diabetes Care*; 28(5).
- Khan A. H., and Pessin J. E. (2002). Insulin regulation of glucose uptake: a complex interplay of intracellular signalling pathways. *Diabetologia*; 45: 1475-1483.
- Kendall, D. M. (2006). Thiazolidinediones, The case for early use. *Diabetes Care*; 29(1): 154-157.
- Khil, L., Han, S., Kim, S., Chang, T., Jeon, S., So, D., and Moon, C. (1999). Effects of Brazilin on GLUT4 Recruitment in Isolated Rat Epididymal Adipocytes. *Biochemical Pharmacology*; 58: 1705-1712

Kim, C., Newton, K. M., and Knopp, R. H. (2002). Gestational Diabetes and the Incidence of Type 2 Diabetes a systematic review. *Diabetes Care*; 25: 1862-1868.

Kim, W. and Egan, J. M. (2008). The Role of Incretins in Glucose Homeostasis and Diabetes Treatment. *Pharmacology Review*; 60(4): 470-512.

Kim, Y.D., Park, K.G., and Lee, Y.S. (2008). Metformin inhibits hepatic gluconeogenesis through AMP-activated protein kinase-dependent regulation of the orphan nuclear receptor SHP. *Diabetes*; 57(2): 306-14.

Kirpichnikov, D., McFarlane, S.I., and Sowers, J.R. (2002). Metformin: an update. *Annals of Internal Medicine*; 137: 25-33.

Kolterman, O.G., Buse, J.B., Fineman, M.S., Gaines, E., Heintz, S., Bicsak, T.A., Taylor, K., Kim, D., Aisporna, M., Wang, Y., and Baron, A.D. (2003). Synthetic exendin-4 (exenatide) significantly reduces postprandial and fasting plasma glucose in subjects with type 2 diabetes. *The Journal of Clinical Endocrinology and Metabolism*; 88: 3082-3089.

Korytkowski, M., Bell, D., Jacobsen, C., and Suwannasari, R. (2003). A multicenter, randomized, open-label, comparative, two-period crossover trial of preference, efficacy, and safety profiles of a prefilled, disposable pen and conventional vial/syringe for insulin injection in patients with type 1 or 2 diabetes mellitus. *Clinical Therapeutics*; 25 (11): 2836-2848.

Koro, C.M., Bowlin, S.J., Bourgeois, N., and Fedder, D.O. (2004). Glycemic control from 1988 to 2000 among U.S. adults diagnosed with type 2 diabetes. *Diabetes Care*; 27: 17-20.

Krown, K. A., Page, M. T., Nguyen, C., Dietmar, Z., Gutierrez, V., Comstock, K. L., Glembotski, C. C., Quintana, P. J.E., and Sabbadini, R. A. (1996). Tumor Necrosis Factor Alpha-induced Apoptosis in Cardiac Myocytes Involvement of the Sphingolipid Signaling Cascade in Cardiac Cell Death. *The Journal of Clinical Investigation*; 98 (12): 2854-865.

Kulkarni, R. N., Bruning, J. C., Winnay, J. N., Postic, C., Magnuson, M. A., and Kahn, R. (1999). Tissue-Specific knockout of the insulin receptor in pancreatic β -Cells creates an insulin secretory defect similar to that in Type 2 Diabetes. *Cell Press*; 96: 329-339.

Kültür, S. (2007). Medicinal plants used in Kirklareli province (Turkey). *Journal of Endocrinology*; 111: 341-364.

Kunte, H., Schmidt, S., Eliasziw, M., Del Zoppo, G.J., Simard, J.M., Masuhr, F., M., Dirnagl, U. (2007). Sulfonylureas improve outcome in patients with type 2 diabetes and acute ischemic stroke. *Stroke*; 38 (9): 2526-2530.

- Laville, M., and Andreelli, F. (2000). Mécanismes de la prise de poids en cas de normalisation glycémique. *Diabetes & Metabolism*; 26: 42s-45s.
- Lee, M. S., and Kerns, E. H. (1999). LC/MS applications in drug development, *Mass Spectrometry Reviews*; 18: 187-279.
- Lee, S.H., Won, H.S., Khil, L.Y., Moon, C.H., Chung, J.H. and Moon, C.K. (1994). Effects of brazilin on glucose metabolism in epididymal adipocytes from streptozotocin induced diabetic rats. *Journal of Applied Pharmacology*; 2: 65-70.
- Leira, F., Louzao, M.C., Vieites, J.M., Botana, L.M., and Vieytes M.R. (2002). Fluorescent microplate cell assay to measure uptake and metabolism of glucose in normal human lung fibroblasts. *Toxicology in Vitro*; 16: 267-273.
- Liu, G. (2004). Recent advances in protein-tyrosine-phosphatase PTP1B inhibitors for the treatment of type 2 diabetes and obesity. *Drugs of the Future*; 29(12): 1245.
- Liu, I.M., Liou, S.S., Lan, T.W. Hsu, F.L. and Cheng, J.T. (2005). Myricetin as the active principle of *Abelmoshus moschatus* to lower plasma glucose in streptozocin-induced diabetic rats. *Planta Medica* ; 71: 617-621.
- Liu, Y., Jiang, N., Wu, J., Dai, W., and Rosenblum, J.S. (2007). Polo-like kinases inhibited by wortmannin. Labeling site and downstream effects. *Journal of Biology and Chemistry*; 282(4): 2505-11.
- Liu, S., Yang, Y., and Wu, J. (2011). TNF α -induced up-regulation of miR-155 inhibits adipogenesis by down-regulation early adipogenic transcription factors. *Biochemical and Biophysical Research Communications* 414: 618-624.
- Liu, S., Li, D., Huang, B., Chen, Y., Lu, X., and Wang, Y. (2013). Inhibition of pancreatic lipase, α -glucosidase, α -amylase, and hypolipidemic effects of the total flavonoids from *Nelumbo nucifera* leaves. *Journal of Ethnopharmacology*; 149 (1): 263-269.
- Lo Piparo, E., Scheib, H., Frei, N., Williamson, G., Grigorov, M., and Chou, C. J. (2008). Flavonoids for controlling starch digestion: Structural requirements for inhibiting human α -amylase. *Journal of Medicinal Chemistry*; 51: 3555-3561.
- Loots, D.T., Van der Westhuizen, F.H., and Botes, L. (2007). Aloe ferox leaf gel phytochemical content, antioxidant capacity, and possible health benefits. *Journal of Agricultural and Food Chemistry*; 55: 6891-6896.
- Lopes, M. N., Oliveira, A. C. D., Young, M. C. M., and Bolzani, V. D. S. (2004). Flavonoids from *Chiococca braquiata* (Rubiaceae). *Journal of the Brazilian Chemistry Society*; 15(4): 468-471.

Mahmoud, I.I., Marzouk, M.S.S., Moharram, F.A., El-Gindi, M.R., Hassan, A.M.K. (2001). Acylated flavonol glycosides from *Eugenia jambolana* leaves. *Phytochemistry*; 58: 1239-1244.

Mardanyan, S., Sharoyan, S., Antonyan, A., and Zakaryan, N. (2011). Dipeptidyl peptidase IIV and adenosine deaminase inhibition by Armenian plants and antidiabetic drugs. *International Journal of Diabetes and Metabolism*; 19: 69-74.

Maritim, A.C., Sanders R.A., and Watkins J.B. (2003). Diabetes, oxidative stress, and antioxidants. *Journal of Biochemistry and Molecular Toxicology*; 17: 24-39.

Marrero, E. F. (2007). Phytopharmaceuticals as therapeutic tools for veterinary and human therapy: Research on natural health products developed at Censa La Habana, Cuba. Chapter 14.

Mathers, C.D., and Loncar, D. (2006). Projections of global mortality and burden of disease from 2002 to 2030. *PLoS Medicine*; 3: e442.

Matsui, T., Tanaka, T., Tamura, S., Toshima, A., Miyata, Y. and Tanaka, K. (2007). Alpha-glucosidase inhibitory profile of catechins and theaflavins. *Journal of Agricultural and Food Chemistry*; 55: 99-105.

Matsuzawa, Y., Funahashi, T., and Nakamura, T. (1999). Molecular mechanism of metabolic syndrome X: contribution of adipocytokines adipocyte-derived bioactive substances. *Annals of the New York Academy of Sciences*; 892: 146-154.

McAnuff, M. A., Harding, W. W., Omoruyi, F. O., Jacobs, H., Morrison, E. Y., and Asemota, H. N. (2005). Hypoglycemic effects of steroidal saponins isolated from Jamaican bitter yam, *Dioscorea polygonoides*. *Food Chemistry and Toxicology*; 43(11): 1667-72.

Meier, J., Weyhe, D., Michaely, M., Senkal, M., Zumtobel, V., Nauck, M., Holst, J., Schmidt, W., and Gallwitz B. (2004). Intravenous glucagon-like peptide 1 normalizes blood glucose after major surgery in patients with type 2 diabetes. *Critical Care Medicine*; 32 (3): 848-51.

Melchor, G., García, L., Marrero, E. and Lorenzo, L. (1999). Actividad hipoglicémica oral de *Allophylus cominia* L. Sw (palo de caja) en ratas normoglicémicas. *Revista de Salud Animal*; 21:35.

Mentreddy, S. R. (2007). Medicinal plant species with potential antidiabetic properties. *Journal of the Science of Food and Agriculture*; 87 (5): 743-750.

Miller, D. R., Safford, M. M. and Pogach, L. M. (2004). Who Has Diabetes? Best Estimates of Diabetes Prevalence in the Department of Veterans Affairs Based on Computerized Patient Data. *Diabetes Care*; 27(2): b10-b21.

MMP: Merck Manual Professional. (2010). Diabetes Mellitus (DM): Diabetes Mellitus and Disorders of Carbohydrate Metabolism. Merck.com. sec12-ch158-ch158b-1206.

Moon, C.K., Lee, S.H., Chung, J.H., Won, H.S., Kim, J.Y., Khil, L.Y. and Moon, C.H. (1990). Effects of brazilin on glucose metabolism in GLUT4 Recruitment by Brazilin 1711 isolated soleus muscles from streptozotocin induced diabetic rats. *Archives of Pharmaceutical Research*; 13: 359-364,

Mooney, M.H., Fogarty, S., Stevenson, C., Gallagher, A.M., Palit P., Hawley, D.G., Coxon G.D., Waigh, R.D., Tate, R.J., Harvey A.L., and Furman B.L. (2008). Mechanism underlying the metabolic actions of galegine that contribute to weight loss in mice. *British Journal of Pharmacology*; 153: 1669-1677.

Müller HK, Kragballe M, Fjorback AW, Wiborg O (2014) Differential Regulation of the Serotonin Transporter by Vesicle-Associated Membrane Protein 2 in Cells of Neuronal versus Non-Neuronal Origin. *PLoS ONE* 9(5).

Musi, N., Hirshman, M.F., Nygren, J. (2002). Metformin increases AMP-activated protein kinase activity in skeletal muscle of subjects with type 2 diabetes. *Diabetes*; 51(7): 2074-81.

Najafian, M., Ebrahim-Habibi, A., Hezareh, N., Yaghmaei, P., Parivar, K., and Larijani, B. (2011). Trans-chalcone: a novel small molecule inhibitor of mammalian alpha-amylase. *Molecular Biology Reports*; 38: 1617-1620.

Na, M., Oh, W. K., Kim, Y. H., Cai, X. F., Kim, S., Kim, B. Y., and Ahn, J. S. (2006 a). Inhibition of protein tyrosine phosphatase 1B by diterpenoids isolated from *Acanthopanax koreanum*. *Bioorganic and Medicinal Chemistry Letters*; 16: 3061-3064.

Na, M., Jang, J., Njamen, D., Mbafor, J. T., Fomum, Z. T., Kim, B. Y., and Ahn, J. S. (2006 b). Protein tyrosine phosphatase-1B inhibitory activity of isoprenylated flavonoids isolated from *Erythrina mildbraedii*. *Journal of Natural Products*, 69: 1572-1576.

Natarajan, A.T., and Darroudi, F. (1991). Use of human hepatoma cells for in vitro metabolic activation of chemical mutagens/carcinogens. *Mutagenesis*; 6: 399-403.

Nathan, M.D., Buse, J. B., Davidson, M. B., Ferrannini, E., Holman, R. R., Sherwin, R., and Zinman, B. (2009). Medical Management of Hyperglycemia in Type 2 Diabetes: A Consensus Algorithm for the Initiation and Adjustment of Therapy. *Diabetes Care*, 32(1): 193-203.

Nathan, D.M., Cleary, P.A., and Backlund J.Y. (2005). Intensive diabetes treatment and cardiovascular disease in patients with type 1 diabetes. *The New England Journal of Medicine*; 353 (25): 2643-53.

- Nathan, D. M. (2002). Initial management of glycemia in type 2 diabetes mellitus. *The New England Journal of Medicine*; 347: 1342-1349.
- Nickavar, B., Abolhasani, L. and Izadpanah, H. (2008). α -Amylase Inhibitory Activities of Six Salvia Species. *Iranian Journal of Pharmaceutical Research*; 7 (4): 297-303.
- Niki, E., Y. Yoshida, Y. Saito, Y. and Noguchi, N. (2005). Lipid peroxidation: mechanisms, inhibition and biological effects. *Biochemical and Biophysical Research Communications*; 338: 668-676.
- NNS National Nutrition Survey in Japan. (2007). Ministry of Health, Labour and Welfare, Japan, Tokyo Available <http://www.mhlw.go.jp/houdou/2008/12/h1225-5.html>. Accessed 20th September, 2013
- Nomura, M., Takahashi, T., Nagata, N., Tsutsumi, K., Kobayashi, S., Akiba, T., and Miyamoto, K. I. (2008). Inhibitory Mechanisms of Flavonoids on Insulin-Stimulated Glucose Uptake in MC3T3-G2/PA6 Adipose Cells. *Biology and Pharmacology Bulletin*; 31 (7): 1403-1409.
- Ntambi, J.M. and Kim, Y. (2000). Adipocyte differentiation and gene expression. Symposium: Adipocyte function, differentiation and metabolism. *American society for Nutritiona Sciences*. 3122S-3126S.
- Oba, T., Masada, Y., and Tamiaki, H. (1997). Convenient preparation of pheophytin b from plant extract through the C7-Reduced intermediate. *The Chemical Society of Japan*; 70: 1905-1909.
- Oliva Y., Sanchez J., Abad M.J., Bermejo P., Marrero E. (2013). Evaluación del efecto antiinflamatorio de un extracto orgánico de *Allophylus cominia* (L.) Sw.. sobre la actividad de COX-2 y FLA-2s. *Bulletin Latinoamericano y Del Caribe de Plantas Medicinales Y Aromaticas* 12 (2): 150-153.
- Pagán, J.A., and Tanguma, J.T. (2007). Health care affordability and complementary and alternative medicine utilization by adults with diabetes. *Diabetes Care*; 30: 2030-2031.
- Panigrahy, D., Singer, S., and Shen, L.Q. (2002). PPAR gamma ligands inhibit primary tumor growth and metastasis by inhibiting angiogenesis. *Journal of Clinical Investigation*; 110 (7): 923-32.
- Panten, U., Schwanstecher, M., and Schwanstecher, C. (1996). Sulfonylurea receptors and mechanism of sulfonylurea action. *Experimental and Clinical Endocrinology and Diabetes*; 104(1): 1-9.
- Peng, Y., Yuan, J., Liu, F. and Ye, J. (2005). Determination of active components in rosemary by capillary electrophoresis with electrochemical detection. *Journal of Pharmaceutical and Biomedical Analysis*; 39: 431-437.

- Pullela, S. V., Tiwari, A. K., Vanka, U. S., Vummenthula, A., Tatipaka, H. B., Dasari, K. R., and Janaswamy, M. R. (2006). HPLC assisted chemobiological standardization of α -glucosidase-I enzyme inhibitory constituents from Piper longum Linn-An Indian medicinal plant. *Journal of Ethnopharmacology*; 108: 445-449.
- Porte, A., Godoy, R.L.O., Lopes D., Koketsu, M., Gonçalves, S.L. and Torquillo, H.S. (2000). Essential Oil of Rosmarinus officinalis L. (Rosemary) from Rio de Janeiro, Brazil. *Journal Essential Oil Research*; 12: 577-580.
- Porter, A.G. and Janicke, R.U. (1999). Emerging role of caspase-3 in apoptosis (review). *Cell death and differentiation*; 6: 99-104.
- Qayyum, R. and Greene, L. (2011). AHRQ's Comparative Effectiveness Research on Premixed Insulin Analogues for Adults with Type 2 Diabetes: Understanding and Applying the Systematic Review Findings. *Continuing Education*; 17(3): S3-S19.
- Rahimi, R., Nikfar, S., Larijani, B. and Abdollahi, M. (2005). A review of the antioxidants in the management of diabetes and its complications. *Biomedicine and Pharmacotherapy*; 59: 365-373.
- Ramkumar, K.M., Rajaguru, P. and Ananthan, R. (2007). Antimicrobial Properties and Phytochemical Constituents of an Antidiabetic Plant Gymnemamontanum. *Advances in Biological Research*; 1 (1-2): 67-71.
- Ramos, A., Visozo, A., Piloto, J., García, A., Rodríguez, C.A., and Rivero, R.. (2003). Screening of antimutagenicity via antioxidant activity in Cuban medicinal plants. *Journal of Ethnopharmacology*; 87 (2-3): 241-246.
- Risérus, U., Willett, W.C., and Hu, F.B. (2009). Dietary fats and prevention of type 2 diabetes. *Progress in Lipid Research*; 48 (1): 44-51.
- Rodriguez, T.V., Gonzales, J.V., Sanchez, L.M., Perez, M.N., Faz, E.M. Detection and determination of chemical groups in an extract of *Allophylus cominia* (L.). (2005). *Journal of Herbal Pharmacotherapy*; 5(4):31-8.
- Rolla, A. (2008). Pharmacokinetic and pharmacodynamic advantages of insulin analogues and premixed insulin analogues over human insulins: impact on efficacy and safety. *American Journal of Medicine*; 121: S9-S19.
- Rzonca, S.O., Suva, L.J., Gaddy, D., Montague, D.C., and Lecka-Czernick, B. (2004). Bone is a target for the antidiabetic compound rosiglitazone. *Endocrinology*; 145: 401-406.
- Saito, T., Abe, D., and Sekiya, K. (2007). Nobiletin enhances differentiation and lipolysis of 3T3-L1 adipocytes. *Biochemical and Biophysical Research Communications*; 357: 371-376.

Sales, P.M., Souza, P.M., Simeoni, L.A., and Silveira, D. (2012). α -Amylase inhibitors: a review of raw material and isolated compounds from plant source. *Journal of Pharmacy and Pharmaceutical Sciences*; 15(1): 141-83.

Salituro, G.M. and Duresne, C. (1998). Isolation by low pressure column chromatography. In: Cannell, R.J.P. (Ed). *Natural Products Isolation*. Humana Press Inc, Totowa, NJ: 111-140.

Sanchez, J., Young, L., Marrero, E. and Harvey, A. (2014). Antidiabetic effect of aqueous extract and fractions from *Allophylus cominia* (L.) Sw. leaves. *Avances en Diabetología 29* (Special Congress): 108.

Scalbert, A., Manach, C., Morand, C., Remesy, C. and Jimenez, L. (2005). Dietary polyphenols and the prevention of diseases. *Critical Reviews in Food Science and Nutrition*; 45: 287-306.

Sezik, E., Aslan, M., Yesilada, E., and Ito, S. (2005). Hypoglycaemic activity of *Gentiana olivieri* and isolation of the active constituent through bioassay-directed fractionation techniques. *Life Sciences* 76 (11): 1223-1238.

Shamsa, F., Monsef, H., Ghamooshi, R., and Verdian-rizi, M. (2008). Spectrophotometric determination of total alkaloids in some Iranian medicinal plants. *Thai Journal of Pharmaceutical Sciences*; 32: 17-20.

Shivanna, Y., Koteswara, A. R. (2010). Dipeptidyl Peptidase IV inhibitory activity of *Mangifera indica*. *Journal of Natural Products*, 3:76-79.

Sheth, R. A., Josephson, L. and Mahmood, U. (2009). Evaluation and clinically relevant applications of a fluorescent imaging analog to fluorodeoxyglucose positron emission tomography. *Journal of Biomedical Optics*; 14 (6): 014-064.

Sindhu, S. N., Vaibhavi, K., and Anshu, M. (2013). *In vitro* studies on alpha amylase and alpha glucosidase inhibitory activities of selected plant extracts *European Journal of Experimental Biology*, 3(1): 128-132.

Spiller, H.A., and Sawyer, T.S. (2006). Toxicology of oral anti-adipogenic medications. *American Journal of Health System Pharmacy*; 63: 929-938.

Stephens, J. M., Lee, J., and Pilch, P. F. (1997). Tumor Necrosis Factor- α -induced Insulin Resistance in 3T3-L1 Adipocytes is accompanied by a Loss of Insulin Receptor Substrate-1 and GLUT4 Expression without a Loss of Insulin Receptor-mediated Signal Transduction. *The Journal of Biological Chemistry*; 272 (2): 971-976.

Strobel, P., Allard, C., Perez-Acle, T., Calderon, R., Aldunate, R., and Leighton, F. (2005). Myricetin, quercetin and catechin-gallate inhibit glucose uptake in isolated rat adipocytes. *Biochemistry Journal*; 386: 471-478.

Tandon, S. Hydro-distillation and steam distillation from aromatic plants. Available from www.ics.trieste.it/media/136901/df4316.pdf Accessed 10th May, 2013.

Tang, Q. Q. and Lane, M. D. (2012). Adipogenesis: From Stem Cell to Adipocyte. *Annual Review of Biochemistry* 81: 715-736.

Tang L., Wei W., Chen L. and Liu S. (2006). Effects of berberine on diabetes induced by alloxan and a high-fat/high-cholesterol diet in rats. *Journal of Ethnopharmacology*; 108: 109-115.

Tomaz, A.C.A., Nogueira, R.B.S.S., Pinto, D.S., Agra, M.F., Souza, M.F., da-Cunha, E.V.L. (2008). Chemical constituents from *Richardia grandiflora* (Cham. & Schltdl.) Steud. (Rubiaceae). *Brasilian Journal of Pharmacognosy*; 18(1): 47-52.

Turmelle, Y.P., Shikapwashya, O., Tu, S., Hruz, P.W., Yan, Q., and Rudnik, D.A. (2006). Rosiglitazone inhibits mouse liver regeneration. *Federation of American Societies for Experimental Biology Journal*; 20: 2609-2611.

Urquiaga, I. and F. Leighton (2000). Plant polyphenol antioxidants and oxidative stress. *Biological Research*; 33: 55-64.

Valls, J, Véliz, T, Marrero, E, and Lagunas, A. (2000). Evaluación farmacológica de diferentes extractos obtenidos a partir de la especie vegetal *Allophylus cominia* (L.) Sw. *Review Cuban Farmacologica*; 34: 82-3.

Véliz, T. (2001). *Efecto del extracto acuoso de Allophylus cominia* (L.) Sw en modelos roedores in vivo y ex vivo. Tesis para optar por el grado de Master en Farmacología. IFAL. Universidad de La Habana, La Habana, Cuba.

Véliz, T., Marrero, E., and Fernández, O. (2003). Determination of the peripheral glucose consumption in the presence of an *Allophylus cominia* (L.) Sw extract. *Avances en diabetología*; 178-179.

Véliz, T, Valls, J, Sanchez, L.M., Noa, M. and Marrero, E. (2005). Detection and determination of chemical groups in an extract of *Allophylus cominia* (L.). *Journal of Herbal Pharmacotherapy*; 5:31.

Vijayakumar M., Govindarajan R., Rao G.M.M., Rao, C.V., Shirwaikar A., Mehrotra S. and Pushpangadan P. (2006). Action of *Hygrohilaauriculata* against streptozotocin-induced oxidative stress. *Journal of Ethnopharmacology*; 104: 356-361.

Vera, J. C., Reyes, A. M., Velasquez, F. V., Rivas, C. I., Zhang, R. H., Strobel, P., Slebe, J. C., Nunez-Alarcon, J. and Golde, D. W. (2001) Direct inhibition of the hexose transporter GLUT1 by tyrosine kinase inhibitors. *Biochemistry*, 40, 777-790

Vu, H., Pham, N. B., and Quinn, R. J. (2008). Direct Screening of Natural Product Extracts Using Mass Spectrometry. *Journal of Biomolecular Screening*; 13 (4), 265-275.

Waki, H., Yamauchi, T., and Kadowaki, T. (2010). Regulation of differentiation and hypertrophy of adipocytes and adipokine network by PPARgamma. *Nippon Rinsho*; 68 (2): 210-6.

Wang Q., Somwar R., Bilan P. J., Liu Z., Jin J., Woodgett J. R., and Klip A. (1999). Protein Kinase B/Akt Participates in GLUT4 Translocation by Insulin in L6 Myoblasts. *Molecular and Cellular Biology*; 19: 4008-4018.

Wang, L., Xu, M. L., Rasmussen, S. K., and Wang, M. H. (2011). Vomifoliol 9-O- α -arabinofuranosyl (1 \rightarrow 6)- β -D-glucopyranoside from the leaves of *Diospyros Kaki* stimulates the glucose uptake in HepG2 and 3T3-L1 cells. *Carbohydrate Research Journal*; 4: 21.

Warier, P.K. (1995). *Eugenia jambolana* Linn. In: P. K. Warier, V.P.K. Nambiar, C. Ramankutty (eds.). *Indian Medicinal Plants*. Madras; 45.

Watson R. T., Kanzaki M., and Pessin J. E. (2004). Regulated Membrane Trafficking of the Insulin-Responsive Glucose Transporter 4 in Adipocytes. *Endocrinology Review*; 25 (2): 177-204.

Weisburger, J.H. (2002). Lifestyle, health and disease prevention: the underlying mechanisms. *European Journal of Cancer Prevention*; 11: S1-7.

WHO (2005). Preventing chronic diseases: a vital investment: WHO global report. Geneva: World Health Organization.

Wiernsperger, N.F. (2005). Is non-insulin dependent glucose uptake a therapeutic alternative? Part 1: physiology, mechanisms and role of non insulin-dependent glucose uptake in type 2 diabetes. *Diabetes Metabolism*; 31: 415-426.

Wild, S., Roglic, G., Green, A., Sicree, R., King, H. (2004). Global prevalence of diabetes: estimates for the year 2000 and projections for 2030. *Diabetes Care*; 27: 1047-1053.

Williams, D.H. and Fleming, I. (1995). Nuclear magnetic resonance spectra. In: D. H. Williams and I. Fleming (Eds). *Spectroscopic methods in Organic Chemistry*. 5th Edition. New York: Mc Graw-Hill, pp 63-169.

Winkler, M., Stephan, D., Bieger, S., Kühner, P., Wolff, F., and Quast, U. (2007). Testing the Bipartite Model of the Sulfonylurea Receptor Binding Site: Binding of A-, B-, and A _ B-Site Ligands. *The Journal of Pharmacology and Experimental Therapeutics*, JPET; 322:701-708.

Witters, L. A. (2001). The blooming of the French lilac. *Journal of Clinical Investigation*; 108: 1105-1107.

Wolf, A. M., Wolf, D., Rumpold, H., Enrich, B., Tilg, H. (2004). Adiponectin induces the anti-inflammatory cytokines IL-10 and IL-1RA in human leukocytes. *Biochemical and Biophysical Research Communications*; 323(2): 630-635.

Woo, W., LaGasse, J. M., Zhou, Z., Patel, R., Palmer, J. P., Campus, H., and Hagopian, W. A. (2000). Novel high-throughput method for accurate, rapid, and economical measurement of multiple Type 1 diabetes autoantibodies. *Journal of Immunological Methods*; 244: 91-103.

World Health Organization. (2009). Traditional Medicine, Available at <http://www.who.int/mediacentre/factsheets/fs134/en>. Accessed 31st January, 2013

Wucherpfenning K. W., and Eisenbarth, G. S. (2001). Type 1 diabetes. *Nature immunology*, 2 (9): 767-768.

Xu, M-E., Xiao, S-Z., Sun, Y-H., Ou-yang, Y., Guan, C. and Zheng, X-x. (2006). A preadipocyte differentiation assay as a method for screening potential anti-type 1 diabetes drugs from herbal extracts. *Planta Medica* 72 (1): 14-19.

Yach, D., Hawkes, C., Gould, C. L., and Hofman, K. J. (2004). The global burden of chronic diseases, overcoming impediments to prevention and control. *Jama*; 291(21): 2616-2622.

Ye, F., Shen, Z., and Xie, M. (2002). Alpha-glucosidase inhibition from a Chinese medical herb (*Ramulus mori*) in normal and diabetic rats and mice. *Phytomedicine* 9: 161-166.

Yokota, T., Oritani, K., Takahashi, I., Ishikawa, J., Matsuyama, A., Ouchi, N., Kihara, S., Funahashi, T., Tenner, A.J., Tomiyama, Y., and Matsuzawa, Y. (2000). Adiponectin, a new member of the family of soluble defense collagens, negatively regulates the growth of myelomonocytic progenitors and the functions of macrophages. *Blood*; 96: 1723-1732.

Yuhao, L., Wen, S., Prasad-Kota, B., Peng, G., Qian-Li, G., Yamahara, J., and Roufogalis, B.D. (2005). *Punica granatum* flower extract, a potent α -glucosidase inhibitor, improves ostprandial hyperglycemia in Zucker diabetic fatty rats. *Journal of Ethnopharmacology* ; 99: 239-244.

Zhang, J. H., Chung, T. D., and Oldenburg, K. R. (1999). A simple statistical parameter for use in evaluation and validation of high throughput screening assay. *Journal of Biomolecular Screening*; 4: 67-73.

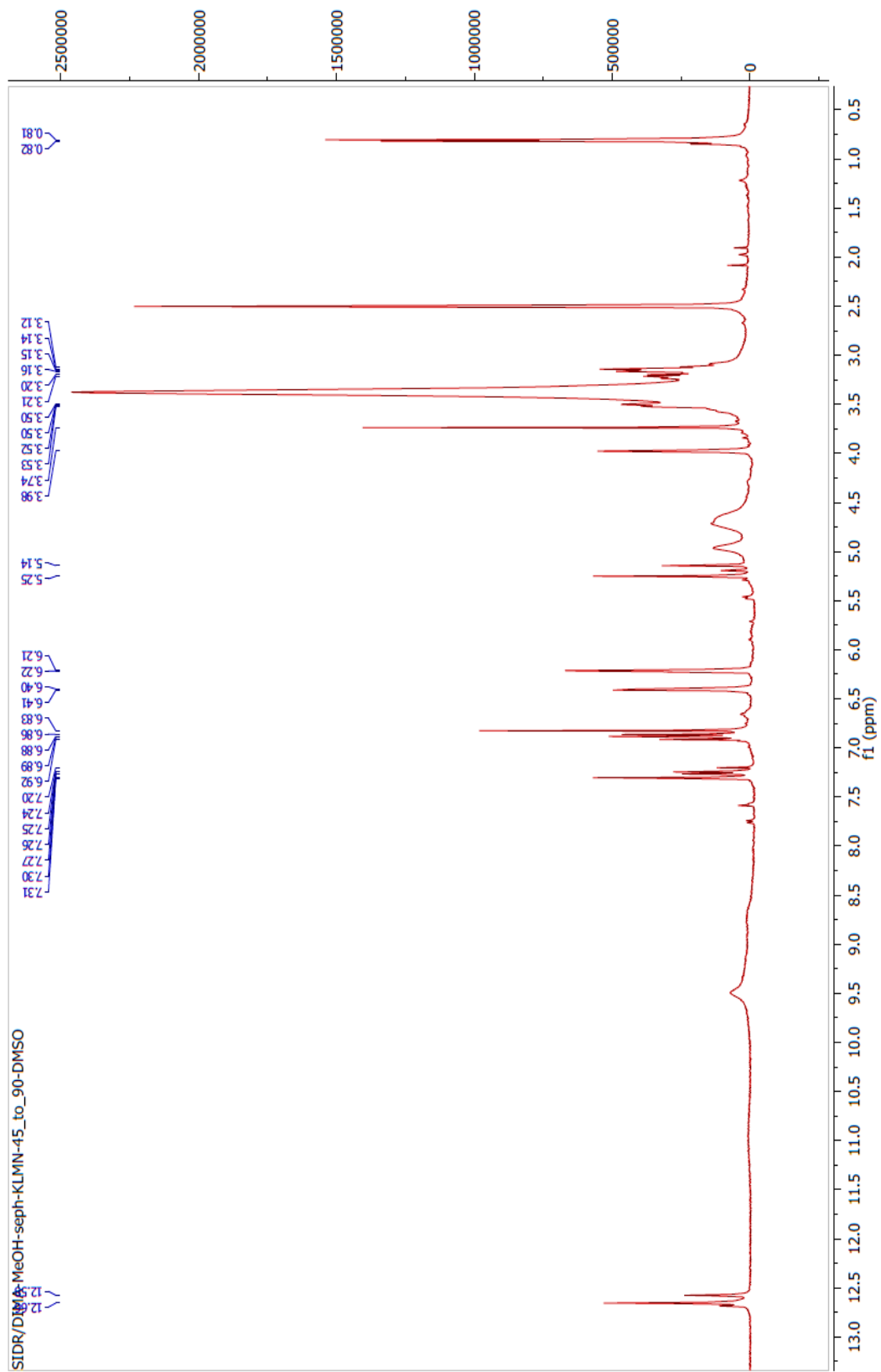
Zhang, J., Shen, Q., Lu, J. C., Li, J. Y., Liu, W. Y., Yang, J. J., and Xiao, K. (2010). Phenolic compounds from the leaves of *Cyclocarya paliurus* (Batal.) Ijinskala and their inhibitory activity against PTP1B. *Food Chemistry*; 119: 1491-1496.

Zhang, W.Y., Lee, J.J., Kim, I.S., Kim, Y., Park, J.S., Myung, C.S. (2010). 7-O-methylaromadendrin stimulates glucose uptake and improves insulin resistance in vitro. *Biological & Pharmaceutical Bulletin*; 33(9): 1494-9.

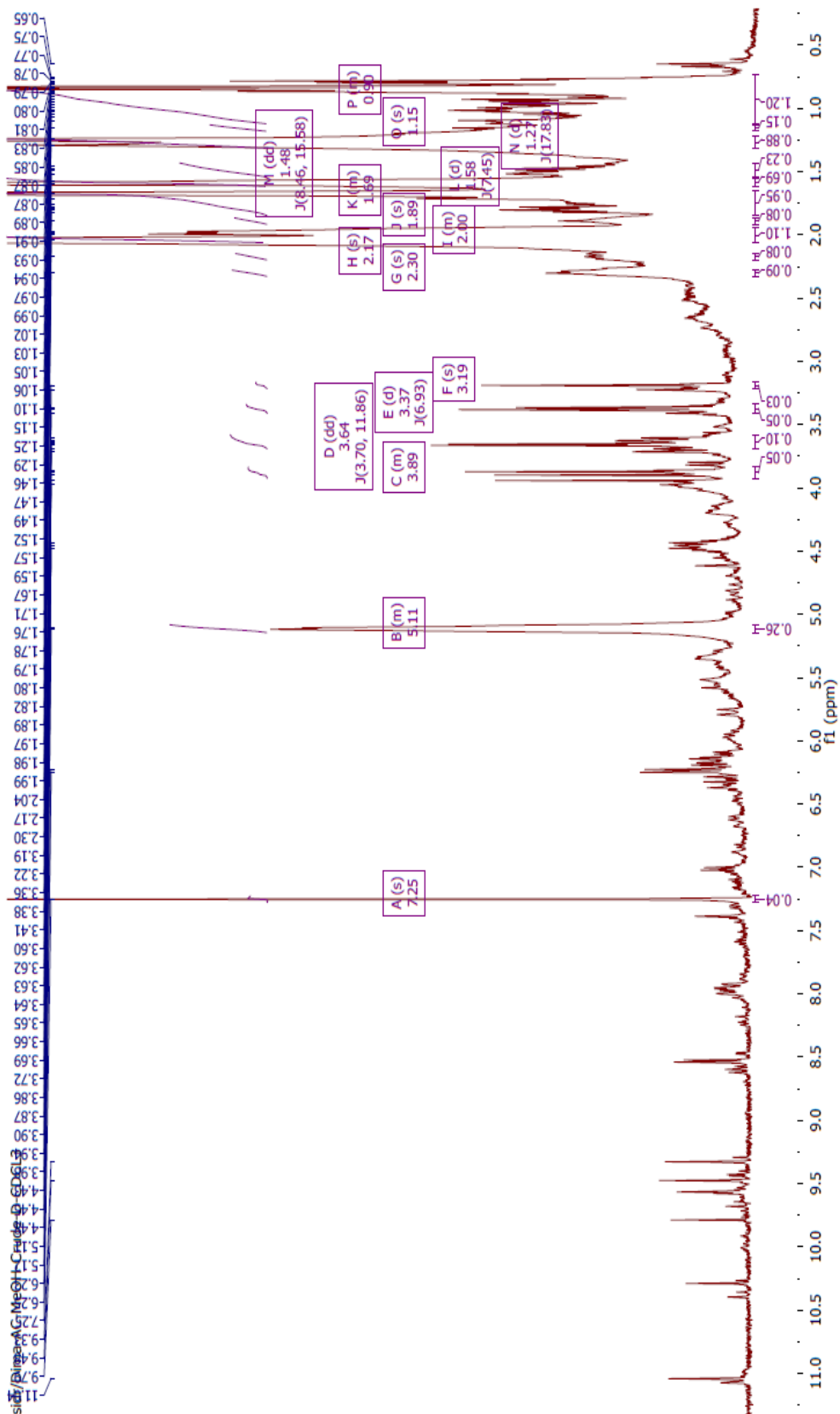
Zhong, L., Furne, J.K., and Levitt, M.D. (2006). An extract of black, green and mulberry teas causes malabsorption of carbohydrate but not of triacylglycerol in healthy volunteers. *American Journal of Clinical Nutrition*; 84: 551-555.

Zhou, G., Myers, R., Li, Y., Chen, Y., Shen, X., Fenyk-Melody, J., Wu, M., Ventre, J., Doebber, T., Fujii, N., Musi, N., Hirshman, M., Goodyear, L., and Moller, D. (2001). Role of AMP-activated protein kinase in mechanism of metformin action. *Journal of Clinical Investigation*; 108(8): 1167-74.

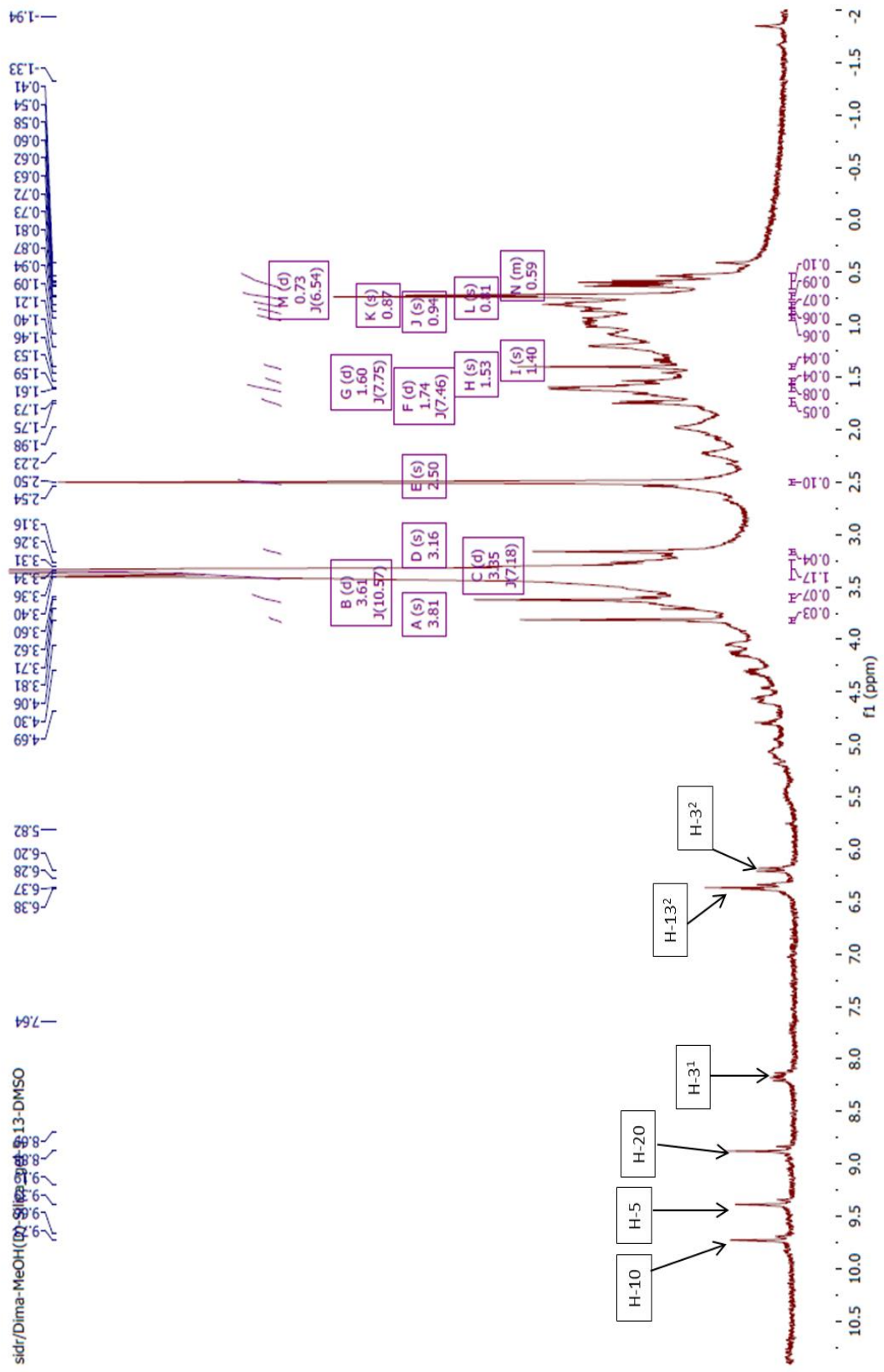
Zou, C., Wang, Y., Shen, Z. (2005). 2-NBDG as a fluorescent indicator for direct glucose uptake measurement. *Journal of Biochemical and Biophysical Methods*; 64: 207-215.



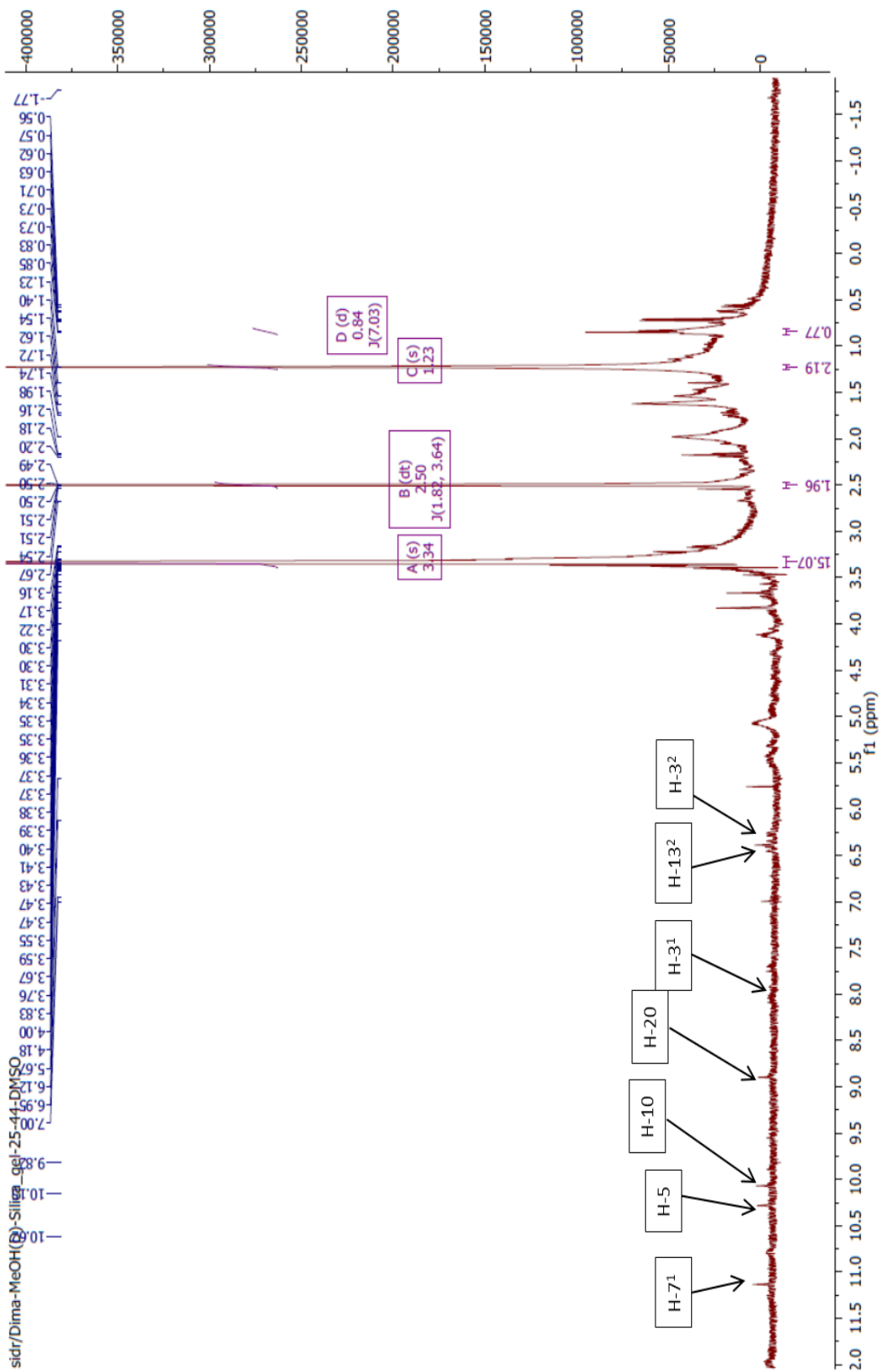
Appendix 1. ^1H NMR spectrum (400 MHz) of the flavonoid mixture from AC-MC-KLMN-91-175 in DMSO-d₆.



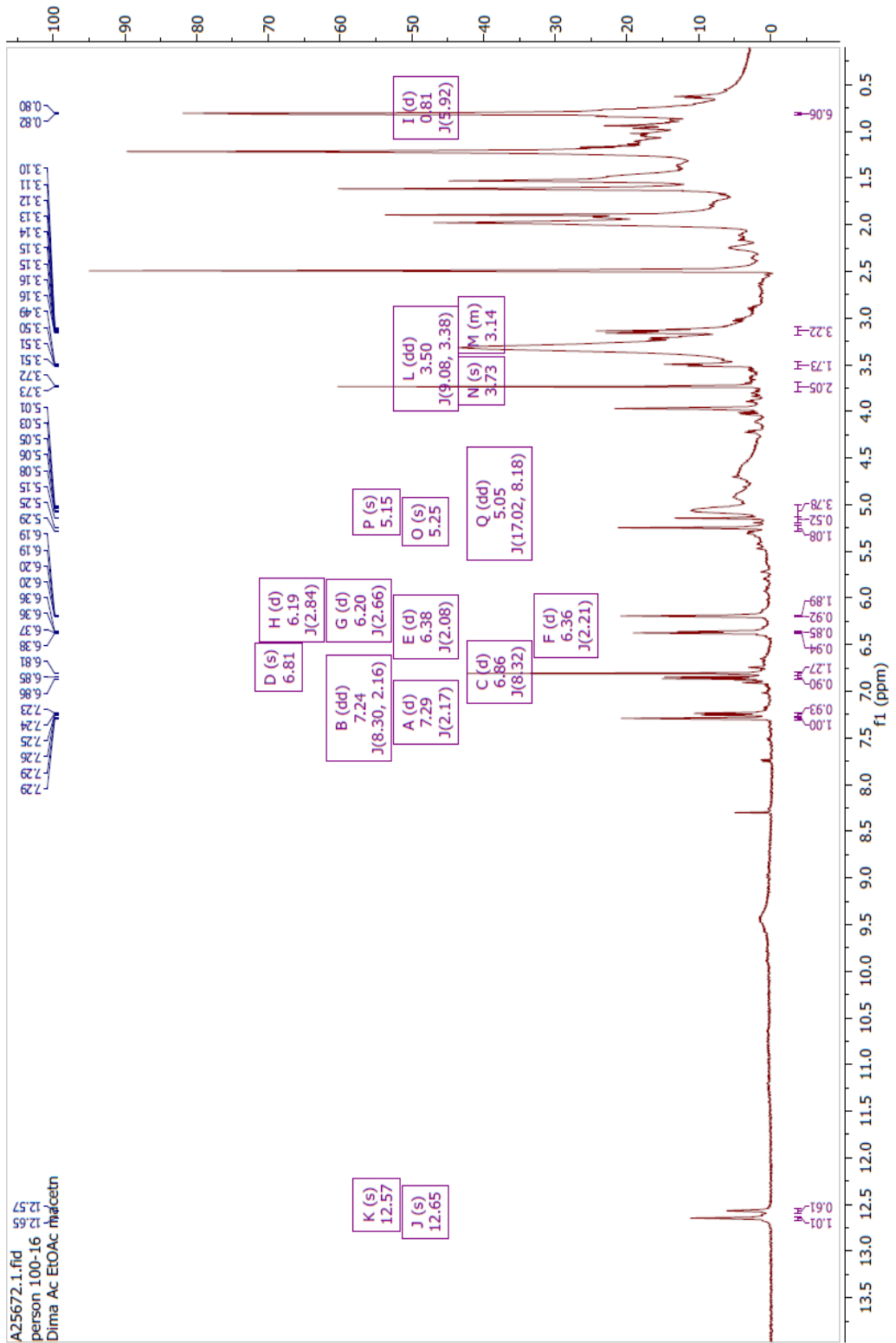
Appendix 2. ¹H NMR spectrum (400 MHz) of MeOH-D (crude) in CDCl₃.



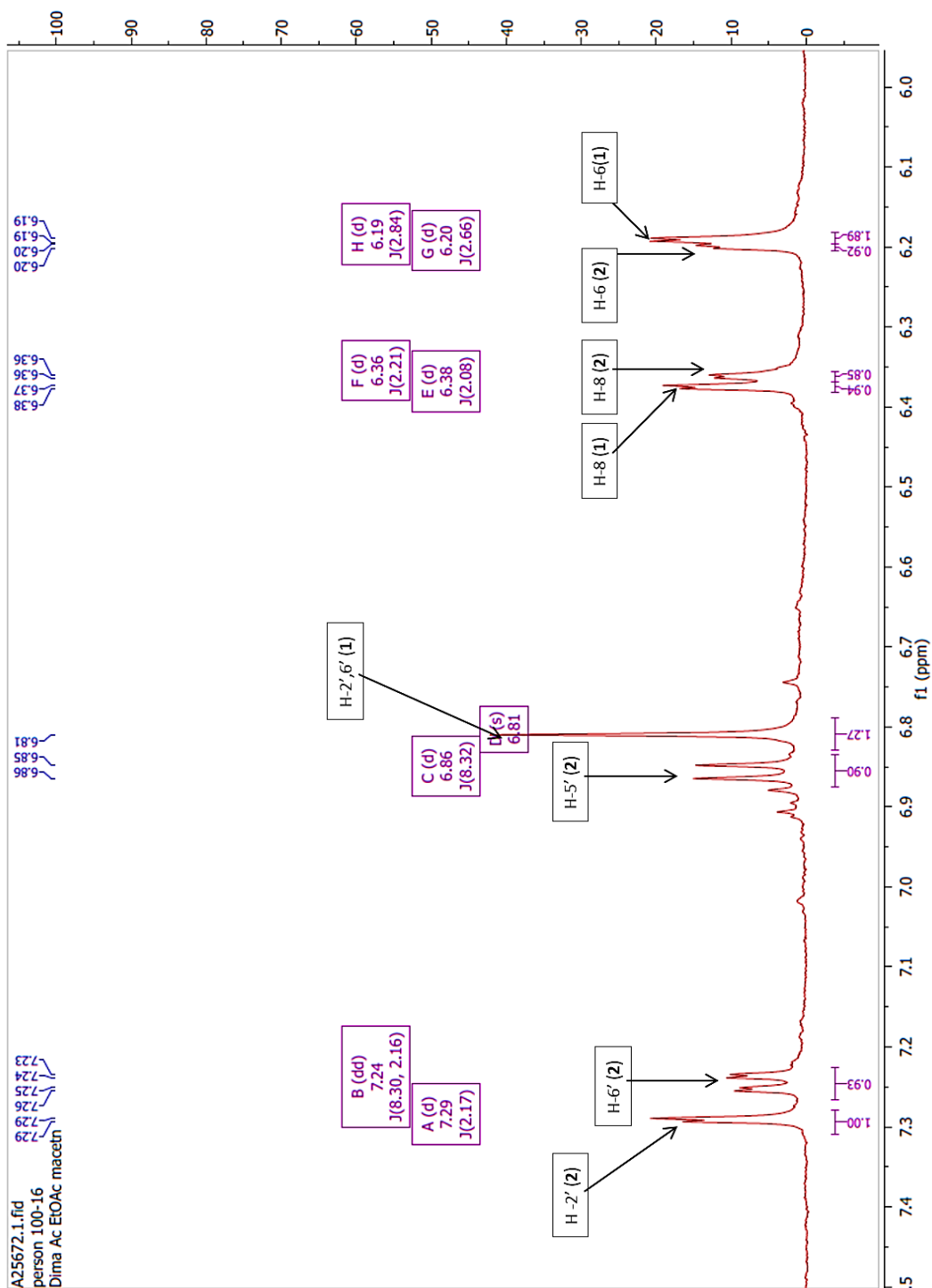
Appendix 3. ¹H NMR spectrum (400 MHz) of pheophytin A (fraction 5-13) in DMSO-d₆.



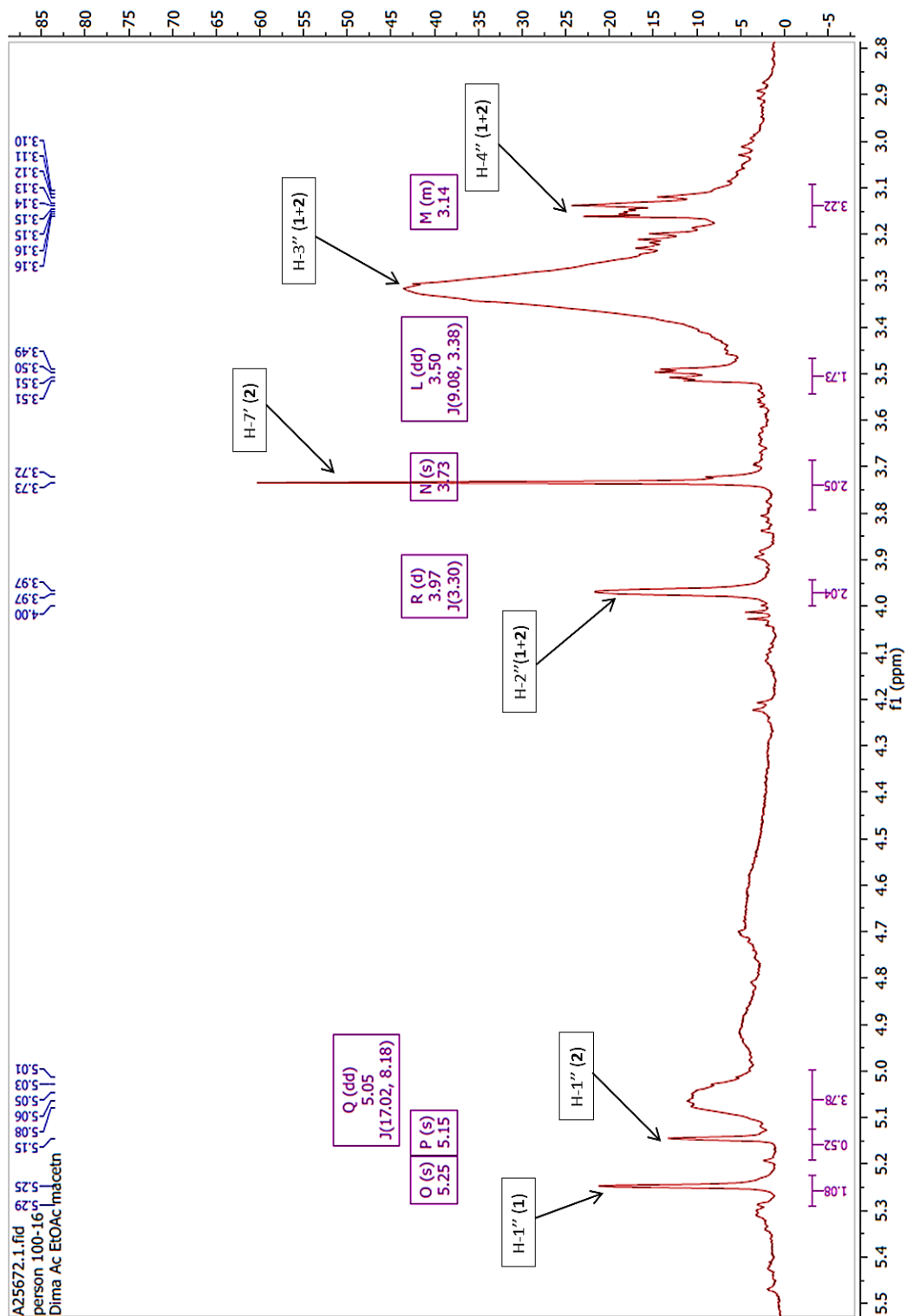
Appendix 4. ^1H NMR spectrum (400 MHz) of pheophytin B (fraction 14-24) in DMSO-d_6 .



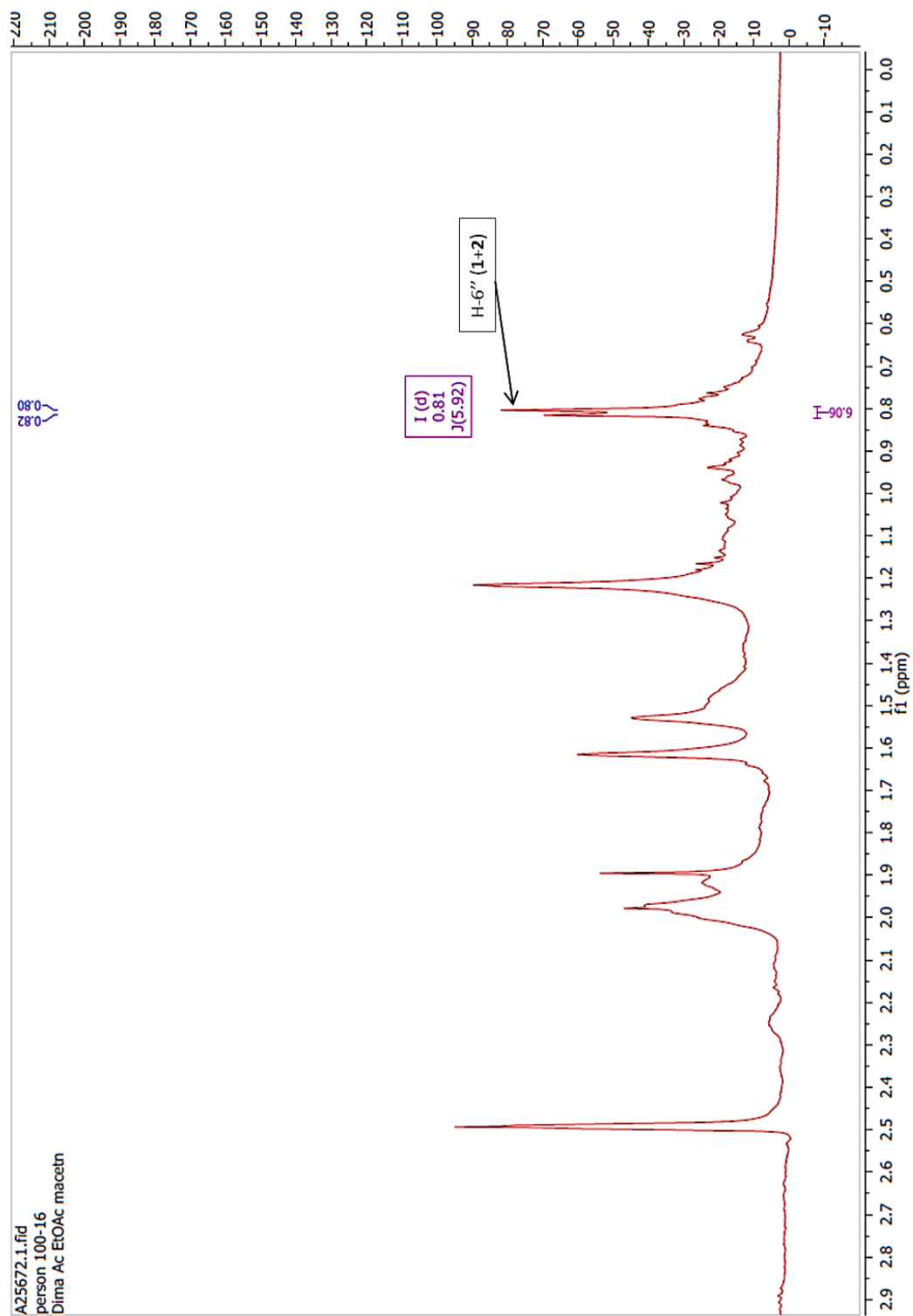
Appendix 5. A. ^1H NMR spectrum (400 MHz) of HEC solid of *A. cominia* in DMSO-d_6 .



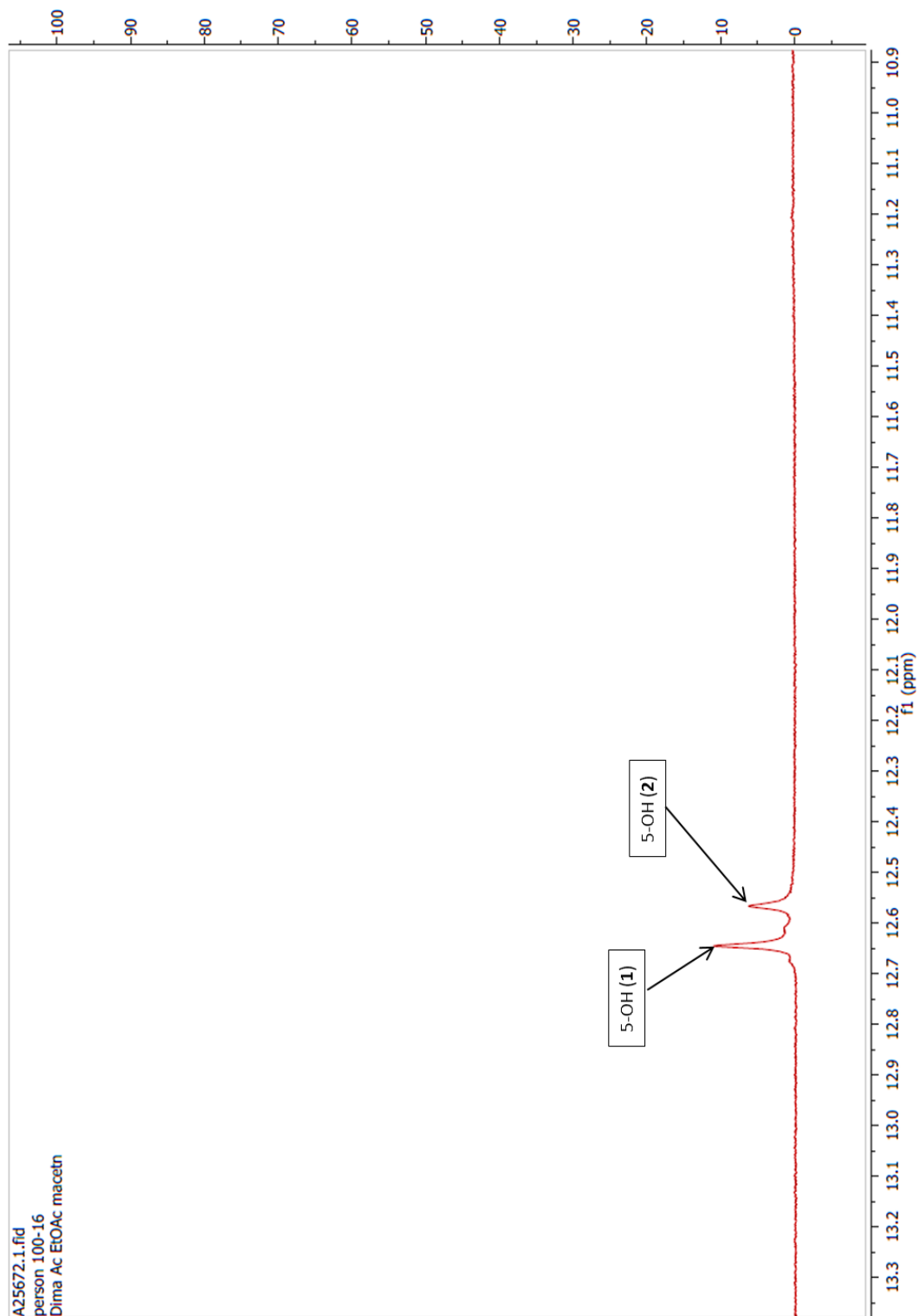
Appendix 5. B. ^1H NMR expanded spectrum for the aromatic region (400 MHz) of HEC solid of *A. cominia* in DMSO- d_6 . (1) is for meansitrin, and (2) is for quercitrin.



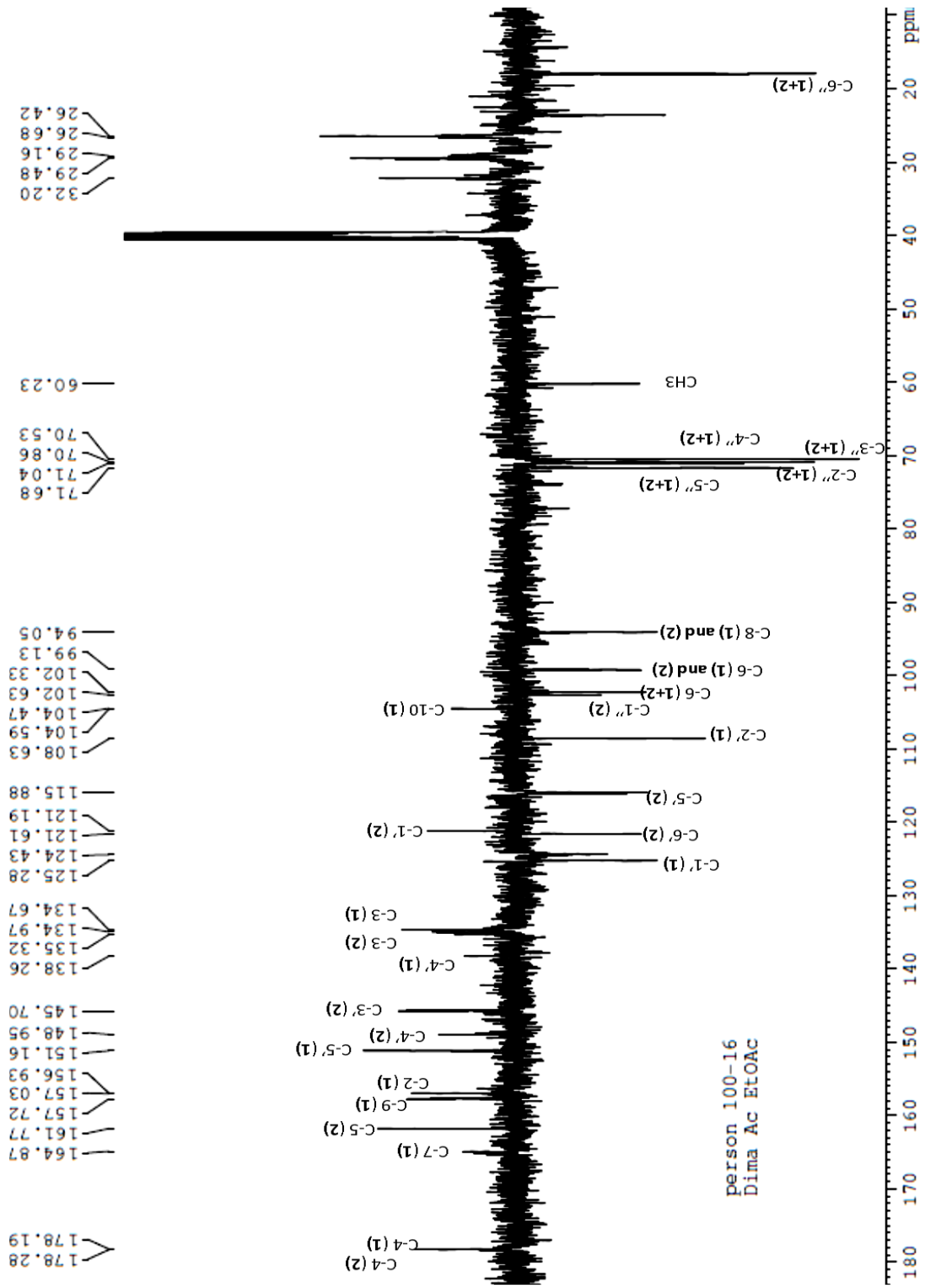
Appendix 5. C. ^1H NMR expanded spectrum for the sugar region (400 MHz) of HEC solid of *A. cominia* in DMSO- d_6 . (1) is for meansitrin, and (2) is for quercitrin.



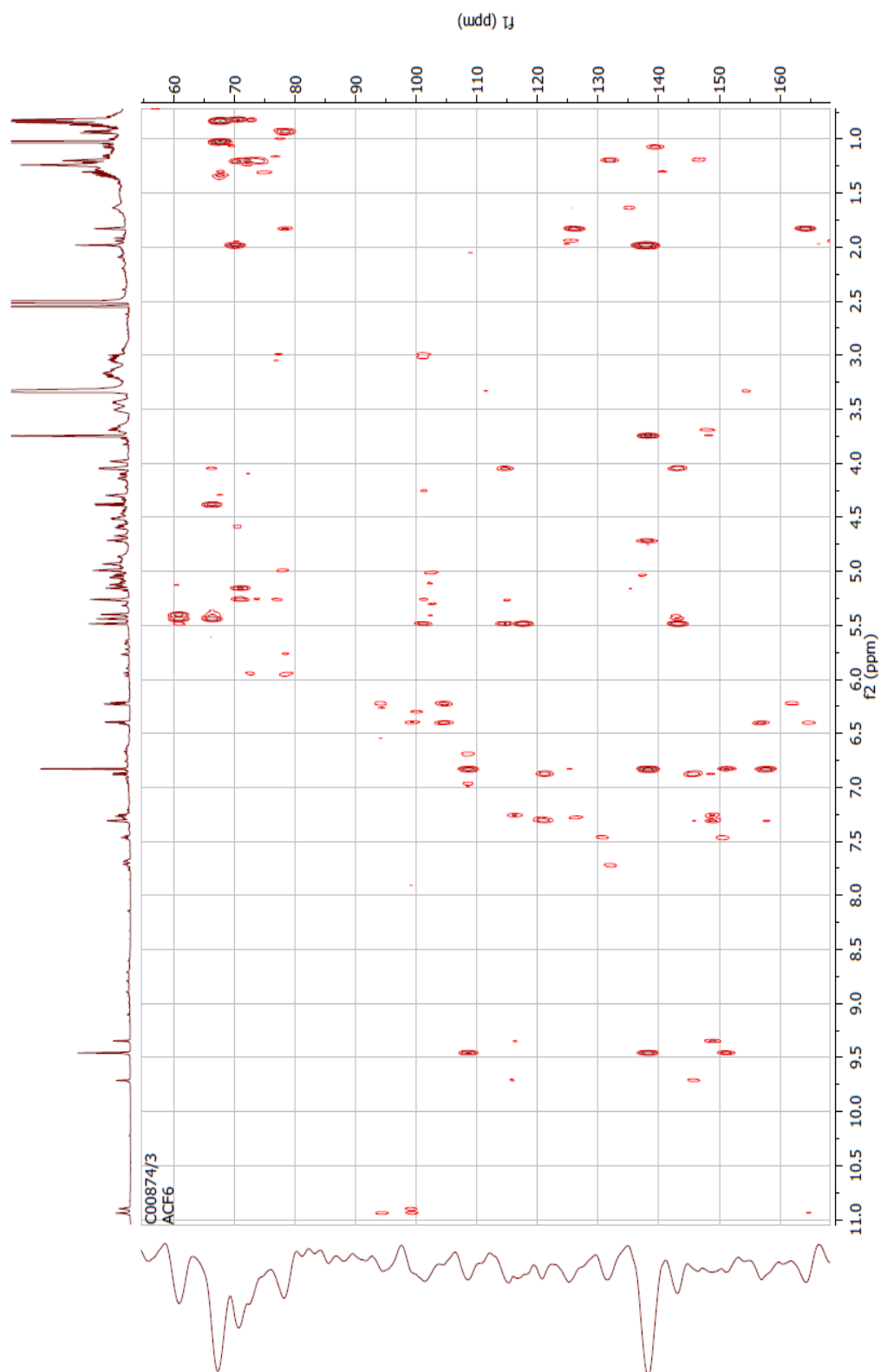
Appendix 5. D. ¹H NMR expanded spectrum for the aliphatic region (400 MHz) of HEC solid of *A. cominia* in DMSO-d₆. (1) is for mearnsitrin, and (2) is for quercitrin.



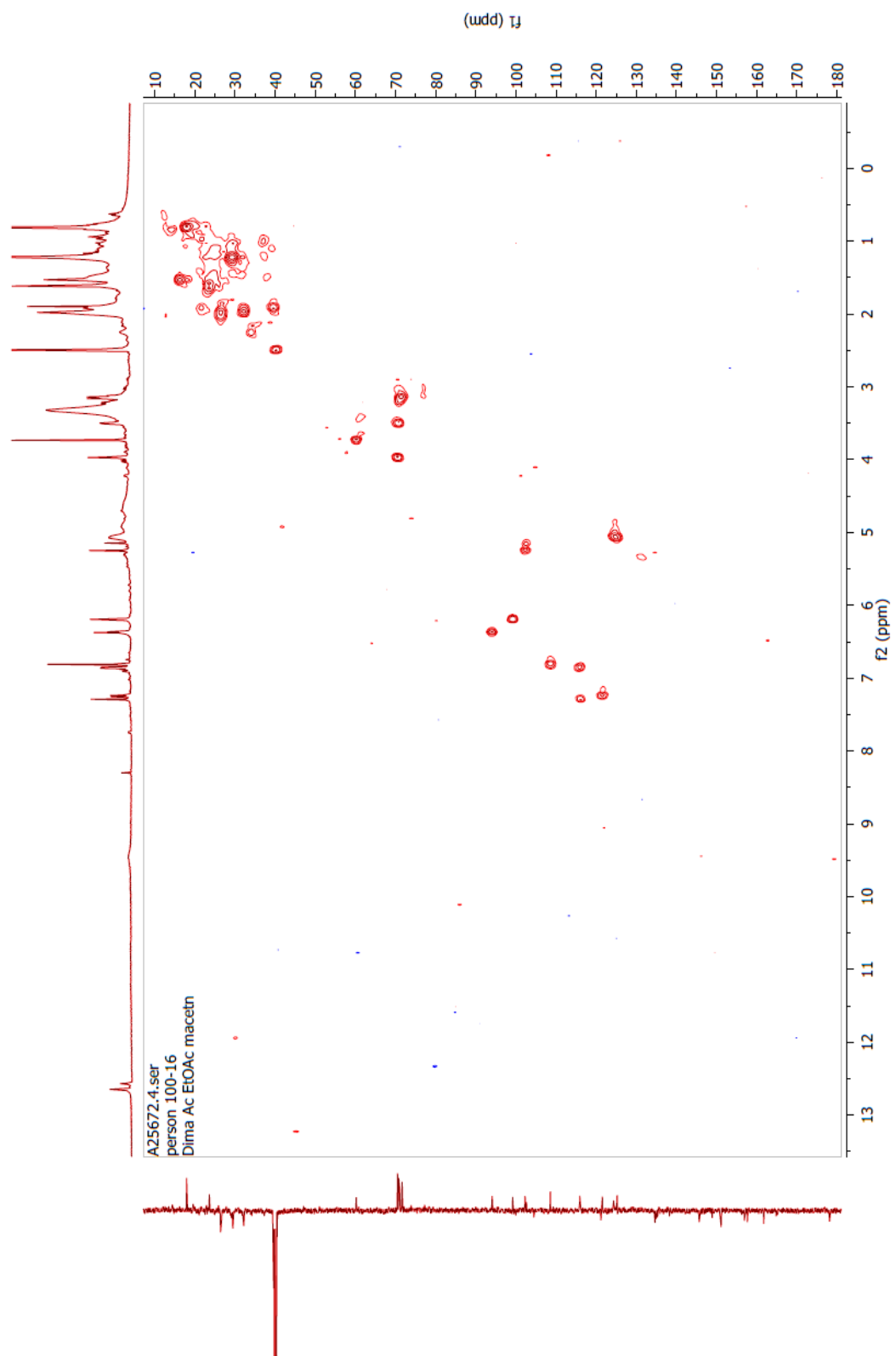
Appendix 5. E. ^1H NMR expanded spectrum for the hydroxyl group (400 MHz) of HEC solid of *A. cominia* in DMSO- d_6 . (1) is for mearnsitrin, and (2) is for quercitrin.



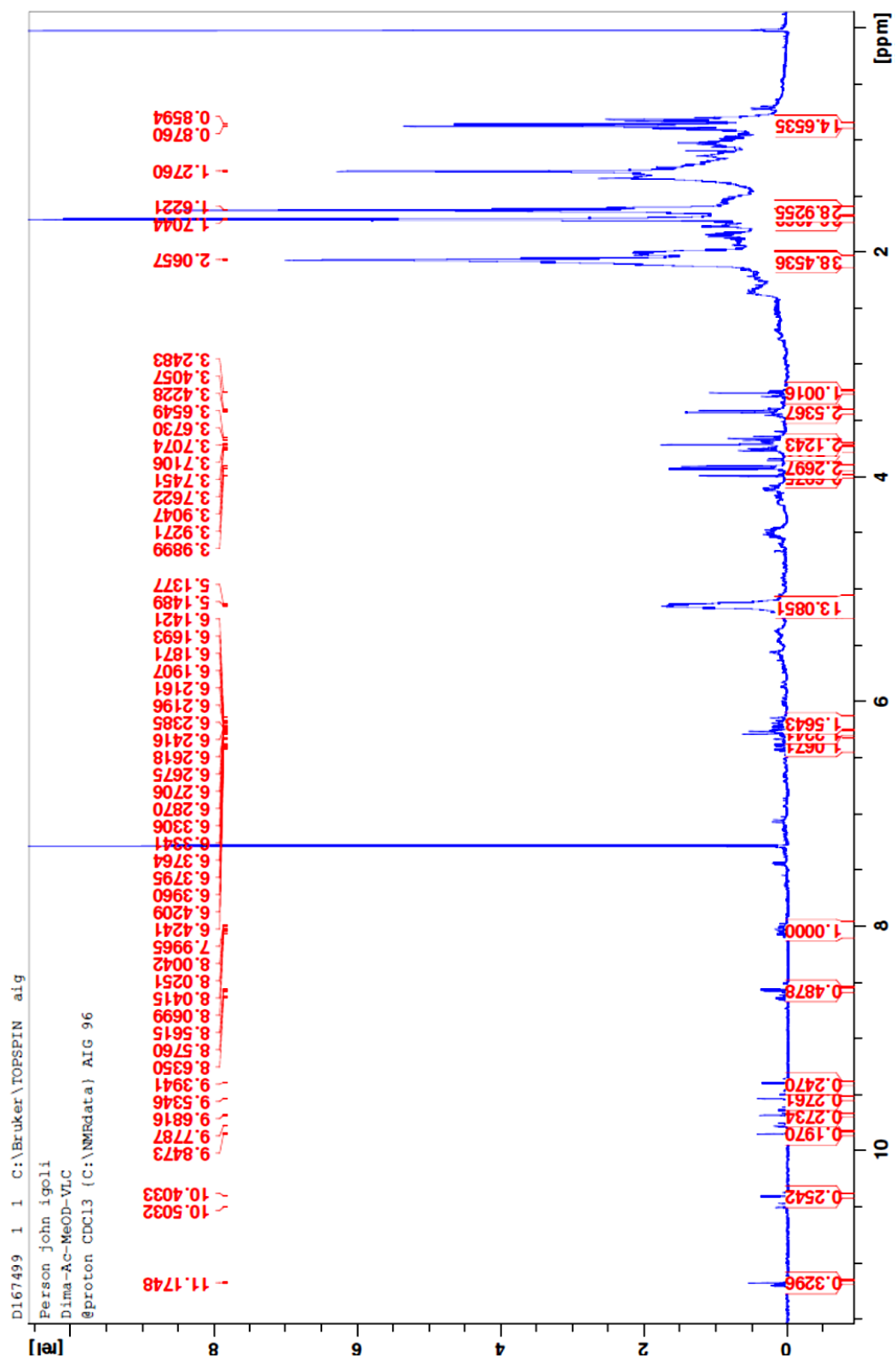
Appendix 6. ^{13}C NMR spectrum (100 MHz) of HEC solid from *A. cominia* in DMSO-d₆. (1) is for mearnsitrin, and (2) is for quercitrin.

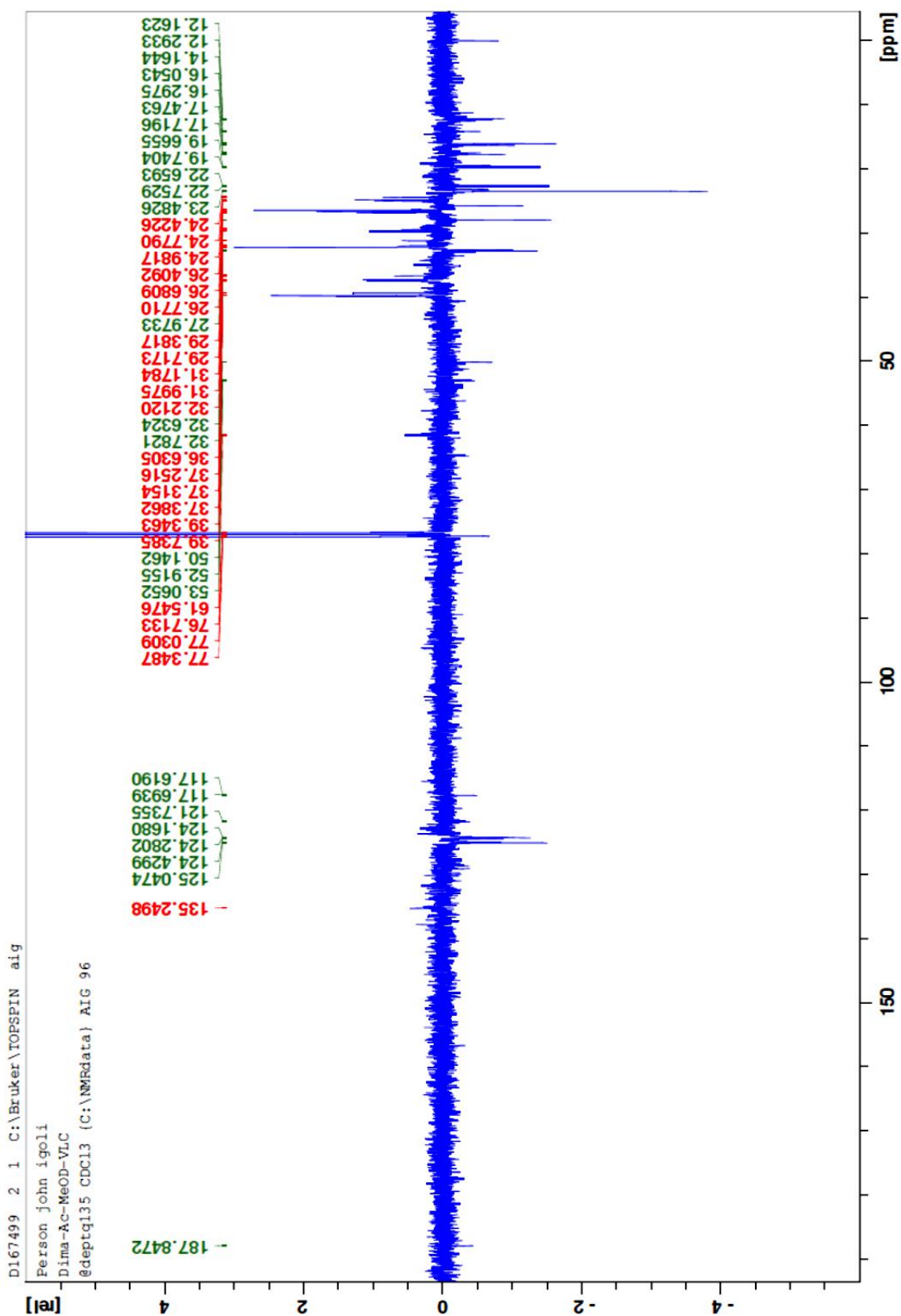


Appendix 7. HMBC spectrum (600 MHz) of HEC solid from *A. cominia* in DMSO-d₆.

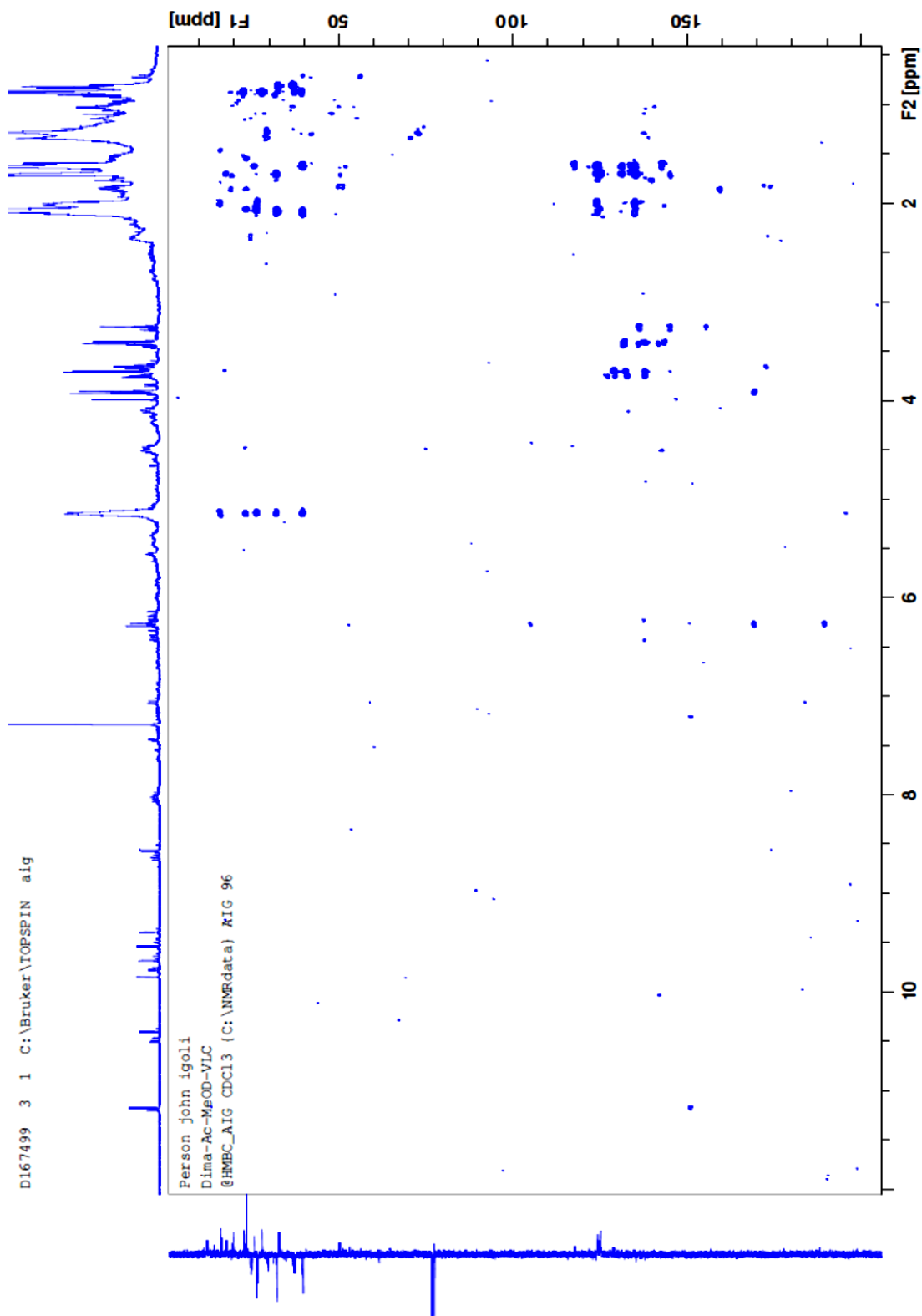


Appendix 8. HSQC spectrum (400 MHz) of HEC solid from *A. cominia* in DMSO-d₆.

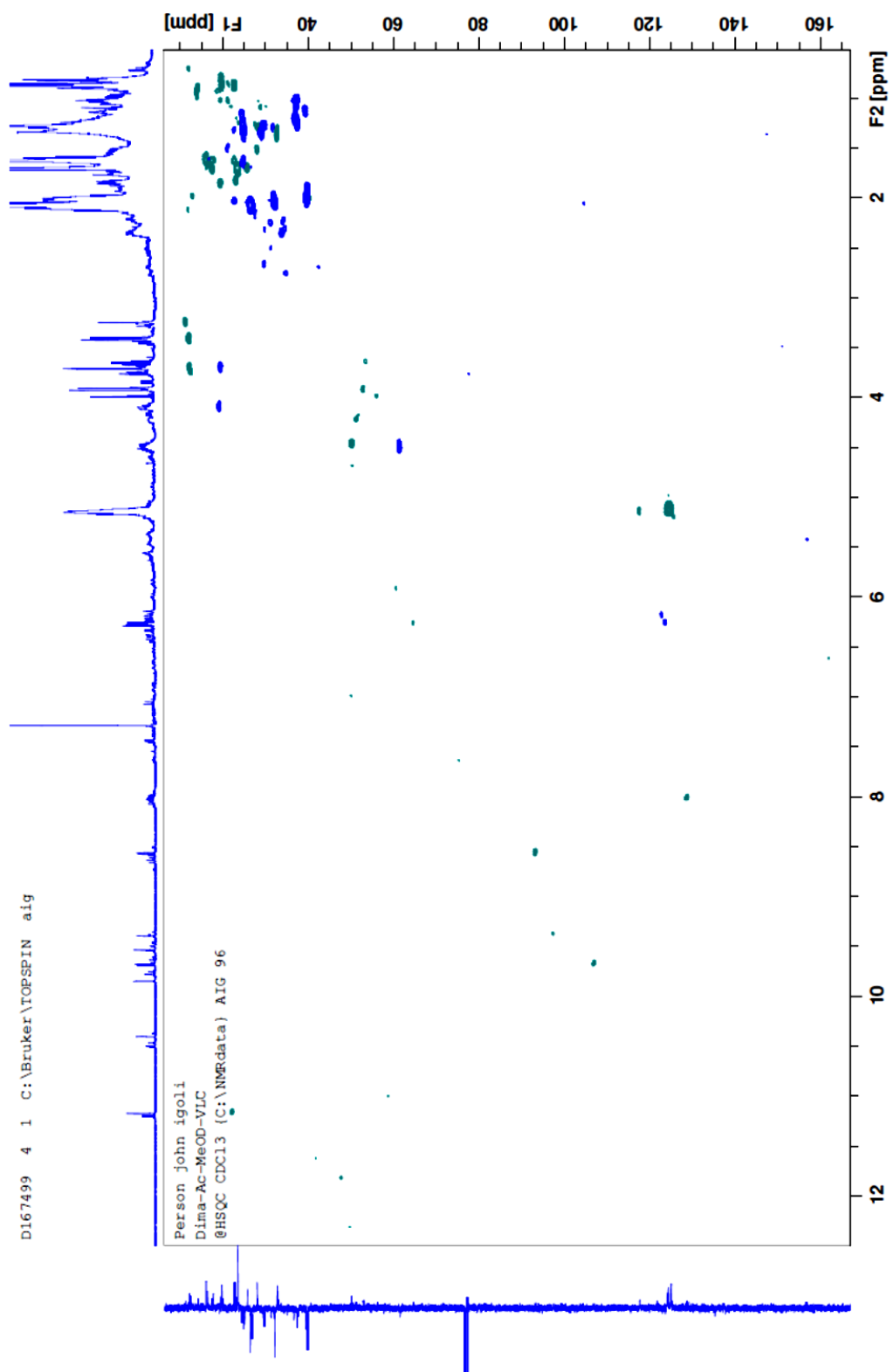




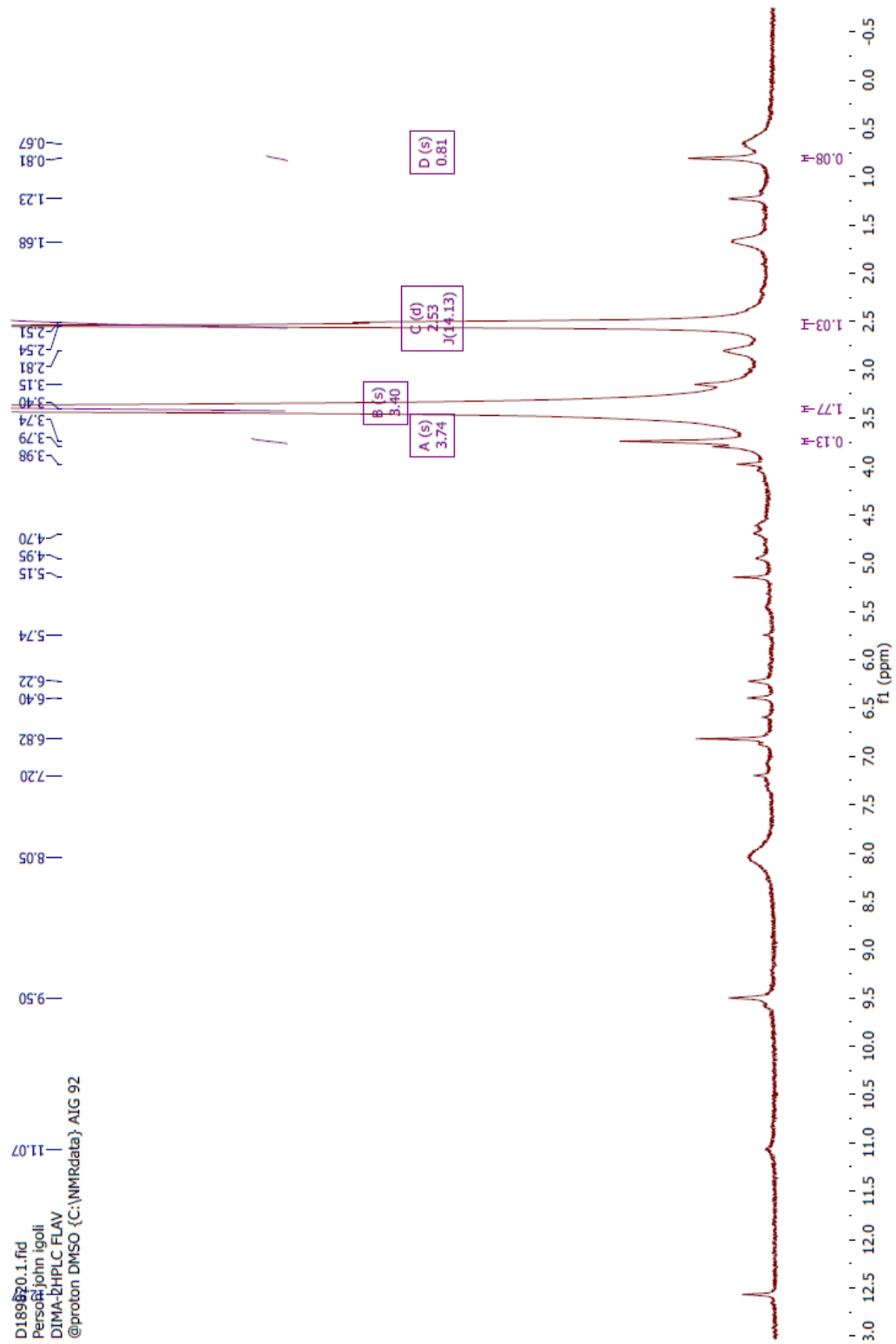
Appendix 10. ^{13}C NMR spectrum (100 MHz) of MeOH-D from *A. cominia* in CDCl_3 .



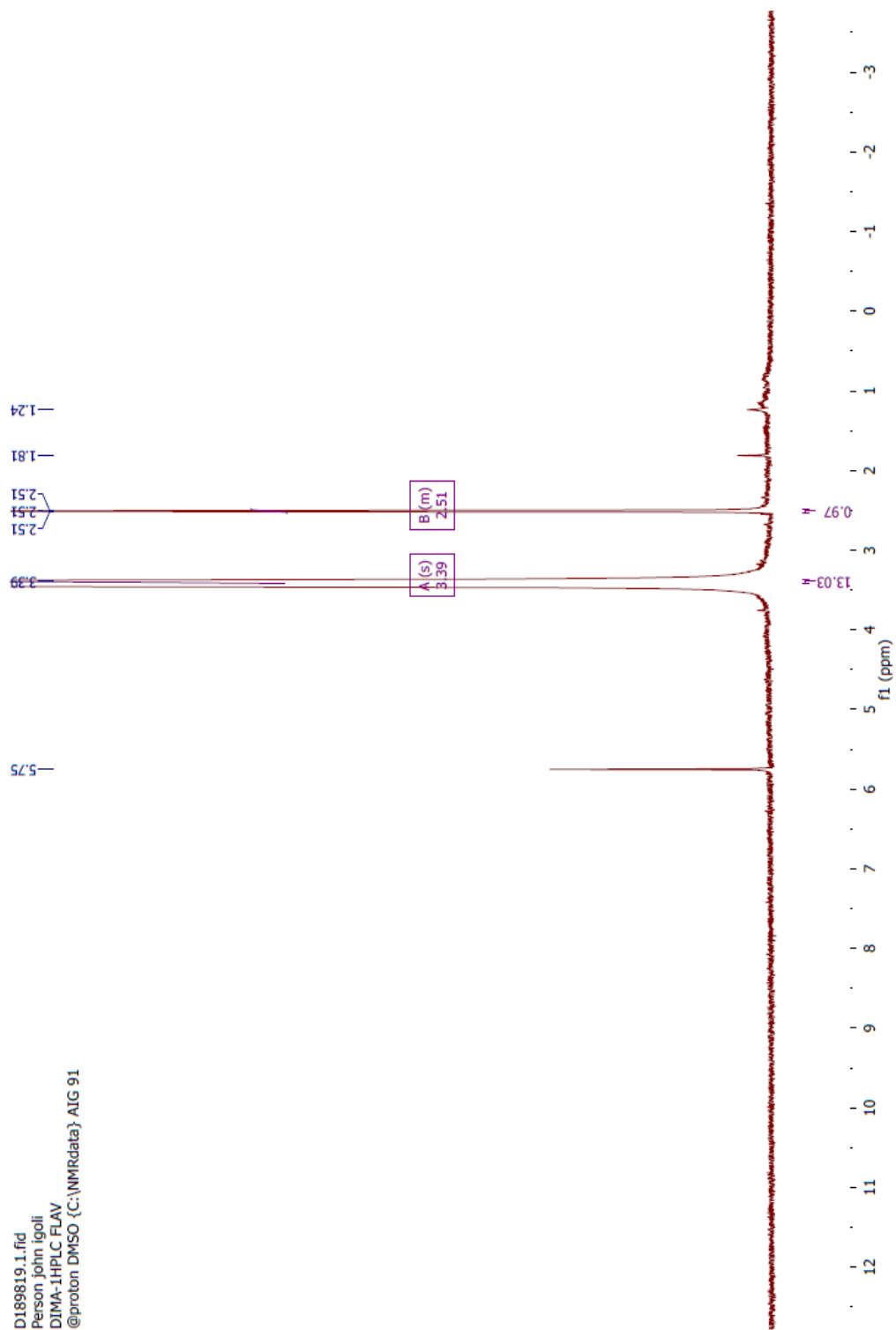
Appendix 11. HMBC NMR spectrum (400 MHz) of MeOH-D from *A. cominia* in CDCl_3 .



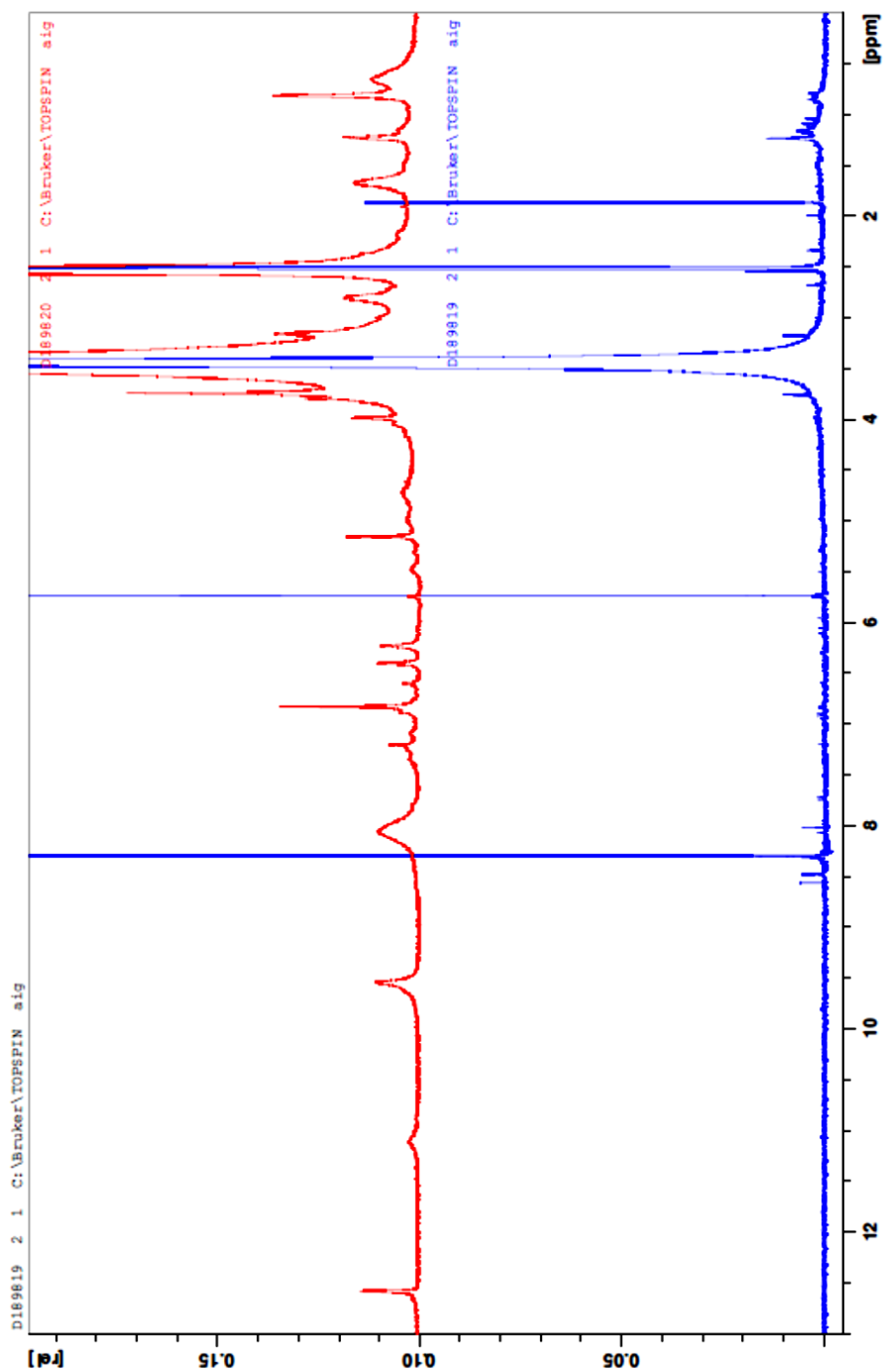
Appendix 12. HSQC NMR spectrum (400 MHz) of MeOH-D from *A. cominia* in CDCl_3 .



Appendix 13. ^1H NMR spectrum (400 MHz) for fraction 2 in DMSO- d_6 . Fraction 2 was separated from the flavonoid mixture by HPLC.



Appendix 14. ^1H NMR spectrum (400 MHz) of fraction 1 in DMSO- d_6 . Fraction 1 was separated from the flavonoid mixture by HPLC.



Appendix 15. Comparison between ^1H NMR spectrum (400 MHz) of fractions 1 and 2. Samples 1 and 2 were separated from the flavonoids mixture by HPLC.

Publication/
Communications

Publication/communications

1. Semaan D., Sanchez J., Marrero E., Young L., Igoli J.O., Gray A.I., Rowan E.G. (2014). Potential anti-diabetisity activities of flavonoids and pheophytins from *Allophylus cominia* (L.) Sw. A poster presentation given at the Diabetes UK conference in ACC, Liverpool.
2. Dima Semaan, Alexander I. Gray, Alan L. Harvey, Janet Sanchez, Evangelina Marrero, John O. Igoli, Louise Young, Carol Clements, Edward G. Rowan. (2013). Finding potential anti-diabetic compounds from *Allophylus cominia* Sw. A poster presentation given at the Cardiovascular conference, Strathclyde University, UK.
3. Ali, S., Igoli, J., Clements, C., Semaan, D., Almazeb, M., Rashid, M-U., Shah, S. Q., Ferro, V., Gray, A.I. & Khan, M.R. (2013). Antidiabetic and antimicrobial activities of fractions and compounds isolated from *Berberis brevissima* Jafri and *Berberis parkeriana* Schneid. *Bangladesh Journal of Pharmacology*; 8(3): 336-342.
4. Semaan D., Rowan E., Gray A.I., Harvey A.L., Sanchez J., Marrero E., Young L., Clements C. (2012). Approaches to finding potential anti-diabetic compounds from *Allophylus cominia*. A poster presentation given at the Annual Symposium at Strathclyde University.
5. Semaan D., Igoli J., Young L., Sanchez J., Marrero E., Furman B.L., Gray A.I., Rowan E.G. (2014). In-vitro anti-diabetic activity of flavonoids and pheophytins from *Allophylus cominia* (Sw) L. *British Journal of Pharmacology* (to be submitted to the journal).